Université de Montréal

Molecular mechanisms for a switch-like mating decision in *Saccharomyces cerevisiae*

par

Mohan Malleshaiah

Département de Biochimie

Programme de Biochimie

Faculté de médecine

Université de Montréal

Thèse présentée à la Faculté des etudes supérieures

en vue de l'obtention du grade de *Philosophiae Doctor (Ph.D)*

en biochimie

April 2011

Université de Montréal

Faculté des etudes supérieures

Cette these intitule:

Molecular mechanisms for a switch-like mating decision in *Saccharomyces cerevisiae*

Présentée par:

Mohan Malleshaiah

a été évaluée par un jury compose des personnes suivantes:

Gerardo Ferbeyre	Président-rapporteur
Stephen Michnick	Directeur de recherché
Daniel Zenklusen	Membre du jury
Tim Elston	Examinateur externe
Sylvain Meloche	Représentant du doyen de la FES

Sommaire

Les changements évolutifs nous instruisent sur les nombreuses innovations permettant à chaque organisme de maximiser ses aptitudes en choisissant le partenaire approprié, telles que les caractéristiques sexuelles secondaires, les patrons comportementaux, les attractifs chimiques et les mécanismes sensoriels y répondant. L'haploïde de la levure *Saccharomyces cerevisiae* distingue son partenaire en interprétant le gradient de la concentration d'une phéromone sécrétée par les partenaires potentiels grâce à un réseau de protéines signalétiques de type kinase activées par la mitose (MAPK). La décision de la liaison sexuelle chez la levure est un événement en "tout–ou-rien", à la manière d'un interrupteur. Les cellules haploïdes choisissent leur partenaire sexuel en fonction de la concentration de phéromones qu'il produit. Seul le partenaire à proximité sécrétant des concentrations de phéromones égales ou supérieures à une concentration critique est retenu. Les faibles signaux de phéromones sont attribués à des partenaires pouvant mener à des accouplements infructueux. Notre compréhension du mécanisme moléculaire contrôlant cet interrupteur de la décision d'accouplement reste encore mince.

Dans le cadre de la présente thèse, je démontre que le mécanisme de décision de la liaison sexuelle provient de la compétition pour le contrôle de l'état de phosphorylation de quatre sites sur la protéine d'échafaudage Ste5, entre la MAPK, Fus3, et la phosphatase, Ptc1. Cette compétition résulte en la dissociation de type « intérupteur » entre Fus3 et Ste5, nécessaire à la prise de décision d'accouplement en "tout-ou-rien". Ainsi, la décision de la liaison sexuelle s'effectue à une étape précoce de la voie de réponse aux phéromones et se produit rapidement, peut-être dans le but de prévenir la perte d'un partenaire potentiel. Nous argumentons que l'architecture du circuit Fus3-Ste5-Ptc1 génère un mécanisme inédit d'ultrasensibilité, ressemblant à "l'ultrasensibilité d'ordre zéro", qui résiste aux variations de concentration de ces protéines. Cette robustesse assure que l'accouplement puisse se produire en dépit de la stochasticité cellulaire ou de variations génétiques entre individus.

Je démontre, par la suite, qu'un évènement précoce en réponse aux signaux extracellulaires recrutant Ste5 à la membrane plasmique est également ultrasensible à l'augmentation de la concentration de phéromones et que cette ultrasensibilité est engendrée par la déphosphorylation de huit phosphosites en N-terminal sur Ste5 par la phosphatase Ptc1 lorsqu'elle est associée à Ste5 *via* la protéine polarisante, Bem1. L'interférence dans ce mécanisme provoque une perte de l'ultrasensibilité et réduit, du même coup, l'amplitude et la fidélité de la voie de réponse aux phéromones à la stimulation. Ces changements se reflètent en une réduction de la fidélité et de la précision de la morphologie attribuable à la réponse d'accouplement. La polarisation dans l'assemblage du complexe protéique à la surface de la membrane plasmique est un thème général persistant dans tous les organismes, de la bactérie à l'humain. Un tel complexe est en mesure d'accroître l'efficacité, la fidélité et la spécificité de la transmission du signal. L'ensemble de nos découvertes démontre que l'ultrasensibilité, la précision et la robustesse de la réponse aux phéromones découlent de la régulation de la phosphorylation stoichiométrique de deux groupes de phosphosites sur Ste5, par la phosphatase Ptc1, un groupe effectuant le recrutement ultrasensible de Ste5 à la membrane et un autre incitant la dissociation et l'activation ultrasensible de la MAPK terminal Fus3. Le rôle modulateur de Ste5 dans la décision de la destinée cellulaire étend le répertoire fonctionnel des protéines d'échafaudage bien au-delà de l'accessoire dans la spécificité et l'efficacité des traitements de l'information. La régulation de la dynamique des caractères signal-réponse à travers une telle régulation modulaire des groupes de phosphosites sur des protéines d'échafaudage combinées à l'assemblage à la membrane peut être un moyen général par lequel la polarisation du destin cellulaire est obtenue. Des mécanismes similaires peuvent contrôler les décisions cellulaires dans les organismes complexes et peuvent être compromis dans des dérèglements cellulaires, tel que le cancer.

Finalement, sur un thème relié, je présente la découverte d'un nouveau mécanisme où le seuil de la concentration de phéromones est contrôlé par une voie sensorielle de nutriments, ajustant, de cette manière, le point prédéterminé dans lequel la quantité et la qualité des nutriments accessibles dans l'environnement déterminent le seuil à partir duquel la levure s'accouple. La sous-unité régulatrice de la kinase à protéine A (PKA),

Bcy1, une composante clé du réseau signalétique du senseur aux nutriments, interagit directement avec la sous-unité α des petites protéines G, Gpa1, le premier effecteur dans le réseau de réponse aux phéromones. L'interaction Bcy1-Gpa1 est accrue lorsque la cellule croit en présence d'un sucre idéal, le glucose, diminuant la concentration seuil auquel la décision d'accouplement est activée. Compromettre l'interaction Bcy1-Gpa1 ou inactiver Bcy1 accroît la concentration seuil nécessaire à une réponse aux phéromones. Nous argumentons qu'en ajustant leur sensibilité, les levures peuvent intégrer le stimulus provenant des phéromones au niveau du glucose extracellulaire, priorisant la décision de survie dans un milieu pauvre ou continuer leur cycle sexuel en choisissant un accouplement.

Mots clés: Évolution, dynamique signalétique, ultrasensibilité, interaction protéine-protéine, décision cellulaire, robustesse, interférence, précision, amplification du signal, etc.

Abstract

Evolution has resulted in numerous innovations that allow organisms to maximize their fitness by choosing particular mating partners, including secondary sexual characteristics, behavioural patterns, chemical attractants and corresponding sensory mechanisms. The haploid yeast *Saccharomyces cerevisiae* selects mating partners by interpreting the concentration gradient of pheromone secreted by potential mates through a network of mitogen-activated protein kinase (MAPK) signaling proteins. The mating decision in yeast is an all-or-none, or switch-like, response that allows cells to make accurate decisions about which among potential partners to mate with and to filter weak pheromone signals, thus avoiding inappropriate commitment to mating by responding only at or above critical concentrations when a mate is sufficiently close. The molecular mechanisms that govern the switch-like mating decision are poorly understood.

In this thesis I demonstrate that the switching mechanism arises from competition between the MAPK Fus3 and a phosphatase Ptc1 for control of the phosphorylation state of four sites on the scaffold protein Ste5. This competition results in a switch-like dissociation of Fus3 from Ste5 that is necessary to generate the switch-like mating response. Thus, the decision to mate is made at an early stage in the pheromone pathway and occurs rapidly, perhaps to prevent the loss of the potential mate to competitors. We argue that the architecture of the Fus3–Ste5–Ptc1 circuit generates a novel ultrasensitivity mechanism that resembles "zero-order ultrasensitivity", which is robust to variations in the concentrations of these proteins. This robustness helps assure that mating can occur despite stochastic or genetic variation between individuals.

I then demonstrate that during the mating response, an early event of Ste5 recruitment to plasma membrane is ultrasensitive and that it is generated by dephosphorylation of eight N-terminal phosphosites on Ste5 by the phosphatase Ptc1 when associated with Ste5 *via* the polarization protein Bem1. Interference with this mechanism results in loss of ultrasensitivity and reduced amplitude and therefore fidelity

of the pheromone signaling response. These changes are reflected in reduced fidelity and accuracy of the morphogenic mating response. Polarized assembly of signaling protein complexes at the plasma membrane surface is a general theme recapitulated in all organisms from bacteria to humans. Such complexes can increase the efficiency, fidelity and specificity of signal transduction. Together with our previous findings, our results demonstrate that ultrasensitivity, accuracy and robustness of the pheromone response occurs through regulation of the stoichiometry of phosphorylation of two clusters of phosphosites on Ste5, by Ptc1, one cluster mediating ultrasensitive recruitment of Ste5 to the membrane and the other, ultrasensitive dissociation and activation of the terminal MAP kinase Fus3. The role of Ste5 as a direct modulator of a cell-fate decision expands the functional repertoire of scaffold proteins beyond providing specificity and efficiency of information processing. Regulation of dynamic signal-response characteristics through such modular regulation of clusters of phosphosites may be a general means by which cell fate decisions are achieved. Similar mechanisms may govern cellular decisions in higher organisms and be disrupted in cancer.

Finally, in a related theme, I present the discovery of a novel mechanisms by which the threshold of pheromone response is controlled by a nutrient-sensing pathway, thus adjusting the set-point at which the quantity and quality of nutrients available in the environment set the threshold of pheromone at which yeast will mate. The regulatory subunit of protein kinase A (PKA), Bcy1, a key component of a nutrient sensing signaling network, directly interacts with the α subunit of G-protein, Gpa1, the primary effector of the pheromone signaling network. The Bcy1-Gpa1 interaction is enhanced when cells are grown in their ideal carbon source glucose, lowering the threshold concentration at which the mating response is activated. Disruption of Bcy1-Gpa1 interaction or Bcy1 deletion increased the threshold concentration for the mating response. We argue that by adjusting their sensitivity, yeast can integrate pheromone stimulus with glucose levels and prioritize decisions to survive in a nutrient-starved environment or to continue their sexual cycle by mating.

Key words: Evolution, Signalling dynamics, ultrasensitivity, protein-protein interaction, cellular decision, robustness, cross-talk, accuracy, signal amplification, etc.

Table of Contents

List of Tables

List of Figures

Chapter I

Chapter II

Supplementary figures

Chapter III

Supplementary figures

Chapter IV

Supplementary figures

Chapter V

Abbreviations

MAPK	Mitogen activated protein kinase
MAPKK	Mitogen activated protein kinase kinase
MAPKKK	Mitogen activated protein kinase kinase kinase
MAPKKKK	Mitogen activated protein kinase kinase kinase kinase
GPCR	G protein coupled receptor
PKA	Protein kinase A
CDK	Cyclin dependent kinase
Cln	Cyclin
GEF	Guanine exchange factor
GAP	GTPase accelerating factor
HOG	High osmolarity glycerol
ROS	Reactive oxygen species
GTP	Guanosine triphosphate
GDP	Guanosine diphosphate
ATP	Adenosine triphosphate
AMP	Adenosine monophosphate
cAMP	3’5’- adenosine monophosphate
K	Kinase
[K]	Kinase concentration
P	Phosphatase
[P]	Phosphatase concentration
[S]	Stimulus concentration
n_H	Hill coefficient
EC_{50}	Half maximal concentration
ORF	open reading frame
DNA	Deoxy ribonucleic acid
RNA	Ribonucleic acid
E. coli	*Escherichia coli*

S. cerevisiae	*Saccharomyces cerevisiae*
LB	Liquid broth
YPD	Yeast extract Peptone Dextrose
SD	Synthetic depleted
SC	Synthetic complete
LFM	Low fluorescent medium
DIC	Differential interference contrast
DTT	Dithiotreitol
ECL	Enhanced Chemoluminiscence
EDTA	Ethylenediaminotetraaceticacid
^{0}C	Grade Celsius
HEPES	4-(2-hydroxyethyl)-1-piperazineethane sulfonic acid
Kb	Kilo bases
K Da	Kilo Dalton
pH	Potential of Hydrogen
TBS	Tris-buffered saline
PBS	Phosphate-buffered saline
Tris	Trishydroxymethylaminomethane
TBST	Tris-buffered saline tween
SDS	Sodium dodecyl sulfate
Rpm	rounds per minute
PCR	Polymerase chain reaction
OD	Optical density
PAGE	Polyacrylamide gel electrophoresis
ml	milliliter
µl	microliter
mg	milligram
µg	microgram
mM	milli molar
nM	nano molar
µM	micro molar

Amino acid codes

Amino acid	Three letter code	One letter code
Alanine	ala	A
Arginine	arg	R
Asparagine	asn	N
Aspartic acid	asp	D
Cystiene	cys	C
Glutamic acid	glu	E
Glutamine	gln	Q
Glycine	gly	G
Histidine	his	H
Isoleucine	ile	I
Leucine	leu	L
Lysine	lys	K
Methionine	met	M
Phenylalanine	phe	F
Proline	pro	P
Serine	ser	S
Threonine	thr	T
Tryptophan	try	W
Tyrosine	tyr	Y
Valine	val	V

Acknowledgements

Without the constant support, guidance, motivation and encouragement of all the people around me, achieving this thesis would have been impossible. So, I use this space to convey my gratitude and thank you note to all those who have directly or indirectly were with me through this important journey!

First of all, I would like to thank my parents, brother and sister, who although kept asking me (almost every time we spoke!) as to when am I completing my thesis, they showed their tremendous patience, trust and love for me. Even though they have no clue about the nature of my research, but since they live in harmony with nature, they understand it's something very basic, important and worth pursuing. They have been and will be my constant source of inspiration.

My colleagues at University of Montreal and collaborators who were at McGill University are invaluable in terms of their guidance, support and contributions towards my PhD thesis and life. I am indebted to the energetic and talented, present and past members of the Michnick lab who are just awesome. As colleagues and as friends, they have taught me anywhere from running an experiment to learn more about science, religion, philosophy, music, cultures and many more through their unique way of thinking and stimulating discussions. Thanks to the post-docs (Eduard Stefan, Emmanuel Levy, Durga Sivanesan, Emmanuelle Tchekanda, Eugene Kanshin, Livia Otte, Emily Manderson, Luz Carrillo, Christian Landry and many more) for taking good care of the poor PhD students!; the PhD students (Po Hien, Vincent Messier, Louis-Philippe, Francois-Xavier Campbell -Valois, Alexis, Diala, etc.) for sharing the similar ups and downs of PhD life and the new kid Arturo Papaluca for enchanting us to believe in only the real deal whether it is science or music! Special thanks to Jean-Francois Paradis and Jacqueline Moreno for being good friends and their excellent help with almost every other thing in the lab.

Very special thanks to Vahid Shahrezaei and Prof. Peter Swain for not just being great collaborators but also for their guidance and sharing their stimulating ideas. I am also grateful to Prof. Jackie Vogel, Prof. Wendell Lim and Prof. Peter Pryciak for kindly providing us plasmids and yeast strains; my PhD committee members – Prof. Pascal Chatrand, Prof. Normand Brisson and Prof. Franz Lang, who have carefully followed and guided my thesis progress; the thesis committee – Prof. Tim Elston, Prof. Gerardo Ferbeyre and Prof. Daniel Zenklusen, for reviewing my thesis, their comments and discussions. I thank Prof. Luc DesGroseillers for guiding through the thesis procedural aspects. I also extend my thanks to the administration staff, especially Sylvie Beauchemin for her tremendous help.

Most importantly, I would like to express my sincere gratitude and appreciation to my research supervisor, Prof. Stephen Michnick. He has been very instrumental in my success in addition to his mentorship, encouragement, patience and guidance. Among many, I am particularly indebted to him for inculcating a sense of direction for not just my thesis but for doing science in general and his encouragement to conduct independent research. Apart from science, I am also thankful to him for providing me with a learning opportunity over the past six years. My learning in his lab will never be forgotten or surpassed.

Friends, they are the pillars of life! I am eternally grateful to all my near and far friends for their love, support and for being with me through this journey. I like to thank all my friends who have directly or indirectly inspired and motivated me. In particular, I would like to extend my special thanks to Lakshmi Suvarnan, Soumya Krishnamurthy, Danis Lalan, Venkatesh Prasanna, Pavani Mocharla, Eduard Stefan, Vahid Shahrezaei, Mathieu Vernier, Mark Andrew Smith, Amélie Forget, Frank Gallardo, Manas Paliwal and many others.

Dedication

To

my simple yet grateful and loving parents,

brother and sister!

INTRODUCTION

Chapter I: Introduction

Living cells have evolved to constantly monitor their environments, tune their activity and respond to changes in both their external and internal conditions. Single celled organisms such as bacteria and yeast, sense changing conditions such as nutrients availability, osmolar stress, fluctuations in temperature, presence of chemicals such as pheromones and respond by either synthesizing the required nutrients or chemicals or by executing adaptive gene transcription and biochemical programs that optimizes their survival under particular circumstances. Motile organisms have evolved to sense the concentration gradients in their surroundings and respond by migrating up the gradient, for example to seek more nutrients or migrate away from the gradient in order to avoid the harmful substances. In higher organisms, the hormones stimulate cellular energy metabolism and growth factors induce cell proliferation through their division. In addition, individual metazoan cells must communicate and respond to other cells in the organism. Plants cells, in response to different ratios of hormones (Auxins and Cytokines) respond by differentiating into different types of cells such as a root or a shoot cell. Plants also precisely adapt to changing conditions such as temperature, water and nutrient availability to optimize their survival. Thus, unicellular and multicellular organisms alike have evolved to sense the external stimuli, elicit and integrate their specific responses in a remarkable way that allows them to adapt to ever-changing and sometimes extreme conditions.

Such cellular responses must be carefully and precisely orchestrated to generate the specific biological response often at the right time and place. Loss in precision of response often leads to unfavorable outcomes or even challenges the survival of the cells. For example; cells, from unicellular bacteria, yeast, of plants to metazoans have to maintain a turgor pressure that balances the intracellular osmolarity with that of extracellular conditions. When the surrounding environment becomes hypo or hyper osmotic, and if the cells fail to respond by adjusting their internal osmotic conditions in tune with the environment, they are either flooded with water or loose it and shrink

respectively, either of which would risk their survival. If cells fail to sense concentration gradients of nutrients or pheromones, they risk death or ability to reproduce. In metazoans, if cells lose their ability to respond to carcinogens they could enter an unfavorable and uncontrolled proliferation state that would result in cancers. In embryo development, where a single zygotic cell progressively divides and differentiates into different lineages that go on to develop into different organs of the fetus is a complex process. These differentiation steps are also highly sensitive to various stimuli. The precision of cellular response to proliferation or differentiation inducing factors is thus crucial during embryonic development. Here, the loss of cells ability to respond precisely to specific stimuli could result in a deformed fetus that could lead to congenital diseases or death. **Hence, cellular responses and thus adaptation to changing environments are essential to the survival and propagation of species (Darwin 1859; Darwin 1871).**

1.1 Signal Transduction

For a long time now, discovering, understanding and unraveling the molecular mechanisms that underlie diverse cellular responses to stimuli in nature have been and continues to be a major goal of biologists. The process of recognizing a 'stimulus' (a molecule or a change in extracellular environments), transforming the recognized stimulus into an intracellular chemical 'signal' and processing of this signal through molecular processes within the cell in order to generate a 'response' is called "signal transduction" (**Figure 1**). Although the term is commonly used in physics and electronics (for example; a microphone transduces sound waves into electrical signals), it made its first appearance in biological literature in 1979 (Springer, Goy et al. 1979). The first biological description of 'transferring the extracellular information into internal signals' was given by Martin Rodbell in 1980, when he summarized his work on hormone G-protein coupled receptors which eventually resulted in him being awarded with the Nobel prize in 1994 (Rodbell 1980). Rodbell's description of signal transduction triggered its widespread use reflecting discoveries of a wide variety of signal transducing mechanisms

in diverse organisms. It all began with discoveries of extracellular ligands such as hormones, neurotransmitters, growth factors and cytokines as the first messengers, followed by discoveries of receptors and effector proteins that the first messengers bind to and activate. 3',5'-cyclic AMP (cAMP) was discovered earlier and described as a second messenger whose intracellular synthesis reflects the extracellular ligand signal being transduced (Berthet, Rall et al. 1957). This followed the discovery of Adenylyl cyclase, the enzyme that catalyzes the synthesis of cAMP from ATP.

Post-translational covalent modification of proteins has been amply demonstrated to be among the most common means of intracellular signal transduction (Deribe, Pawson et al. 2010). The most common post-translational modification observed during signal transduction –phosphorylation, was first described by Eugene P. Kennedy (Burnett and Kennedy 1954). Krebs, Graves and Fischer first demonstrated that the enzyme phosphorylase kinase was switched from inactive to active states by phosphorylaton (Fischer and Krebs 1955; Krebs, Graves et al. 1959; Fischer 2009). Decades of research have led to the discovery of a variety of signal processing or post-translational modifying enzymes and proteins including the kinases, phosphatases, proteases, ubiquitinases, scaffolds, adaptors, transcription factors, methylases, acetylases and many others (Deribe, Pawson et al. 2010). Often the proteins involved in processing specific stimuli organize and co-ordinate with each other in the form of a 'signal transduction pathway' that help cells to maintain the specificity and efficiency of signaling (**Figure 1**).

As we understand today, eliciting a specific response to a variety of stimuli requires a remarkable array of sophisticated signal detection and processing systems within the cells. Most of these signal processing systems consists of networks of proteins (Pawson 1995). These networks of signaling proteins transmit the extracellular ligand information from the cell membrane to co-ordinate an appropriate set of responses. Thus, understanding signaling has proved to be the key to describe how living systems manage the information that brings about higher-level biological phenomenon such as proliferation or differentiation decisions (Nurse 2008).

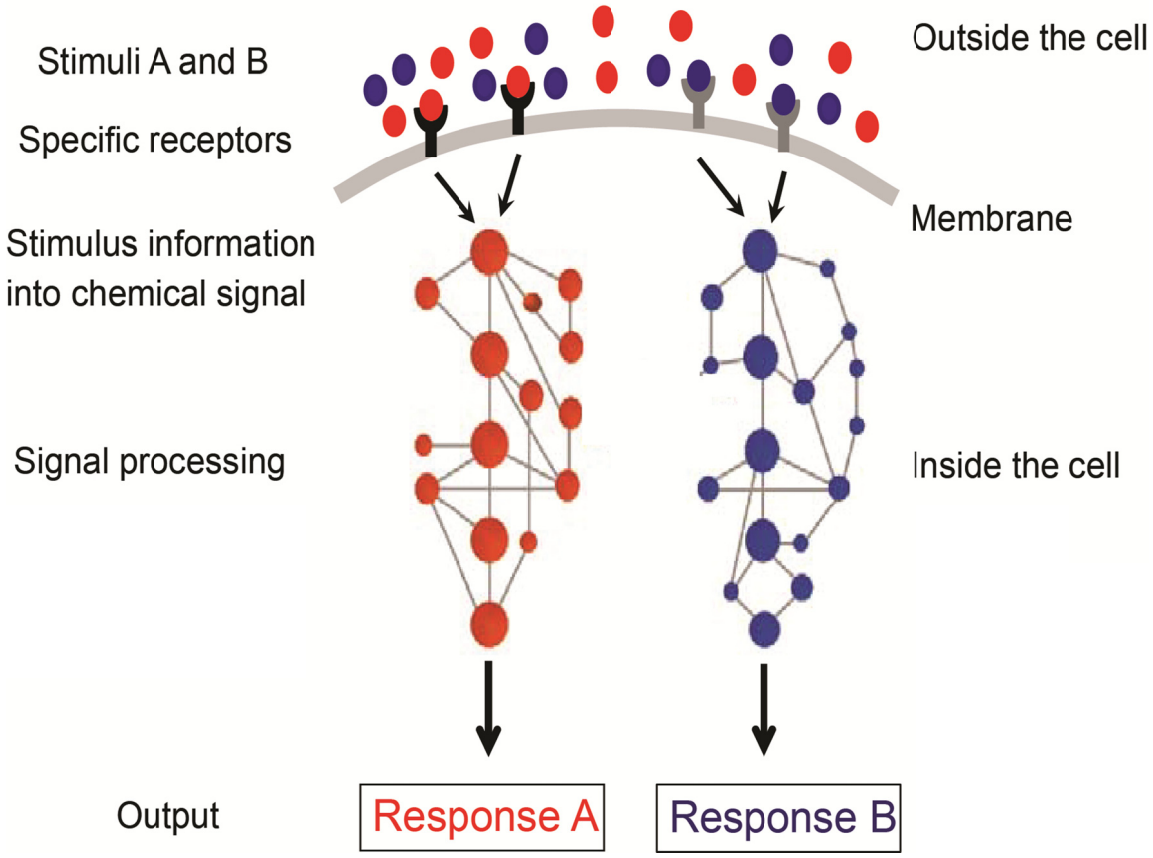

Figure 1. A general schematic for cell signaling.
Stimuli (red and blue circles) or changes in the extracellular environment are sensed at the membrane normally by specific receptors. The stimuli information is converted into intracellular chemical signal which is then processed by a specific network of proteins (red and blue networks) resulting in a stimulus specific response. Source: adapted from (Campbell-Valois and Michnick 2005).

For example, the switch in yeast from budding (proliferation) to shmooing (differentiation) decision in the presence of pheromone stimulus is regulated by the mitogen activated protein kinase signal transduction network that senses the extracellular pheromone, processes the information and elicits a specific response (Elion 2000).

1.2 Mitogen activated protein kinase (MAPK) pathways

The MAPK signaling module is a highly conserved signaling pathway that influences a variety of cellular processes either directly or indirectly through gene expression, including metabolism, cell division, cell morphology and cell growth and proliferation. Each MAPK pathway contains a highly conserved three tiered kinase cascade comprising a MAP kinase kinase kinase (MAPKKK), a MAP kinase kinase (MAPKK) and the MAPK proteins (Qi and Elion 2005) (**Figure 2**). Each kinase of the cascade acts sequentially to phosphorylate and activate its downstream partner. Frequently, a MAPKKK kinase (MAPKKKK) activates the MAPKKK and is linked to the plasma membrane – for example Ste20, of yeast. MAPKKKs phosphorylate and activate MAPKK which activates MAPKs. MAPKKs and MAPKs are activated by dual phosphorylation of tyrosine and threonine residues within their activation loop of the catalytic domain and phosphorylate their targets on serine and threonine residues within a consensus PT/SP motif (Payne, Rossomando et al. 1991; Robbins, Zhen et al. 1993; Chen, Gibson et al. 2001). Often, the MAPK cascade proteins are bound to scaffold proteins. Scaffolds regulate MAPK signaling in several ways, in principle acting to insulate signaling molecules from being activated by parallel signals, increasing the efficiency of signaling by organizing them together and through interactions of the scaffold with other proteins, organizing the MAPK module to specific regions of the cell (Burack and Shaw 2000; Elion 2001; Mishra, Socolich et al. 2007). MAPK activity is usually down regulated by dual specificity MAPK phosphatases (MKPs), tyrosine phosphatases and serine/threonine phosphatases (Keyse 2000). These phosphatases maintain a continuous basal repression of MAPKs which might create a threshold for

MAPKs activation levels. Signaling complexes of MAPK module components exhibit temporal and spatial dynamics. In addition to their localization to numerous sub cellular structures, active MAPKs translocate from the cytoplasm to the nucleus to phosphorylate nuclear targets often to activate target gene expression.

1.3 Yeast as a model system

The unicellular budding yeast *Saccharomyces cerevisiae* is among the most studied and well understood eukaryotic model organisms (Botstein and Fink 1988; Botstein, Chervitz et al. 1997). The genome and proteome of yeast is best understood and various genetic and biochemical tools have been designed to manipulate practically any gene in their genome. In addition, it has evolved to elicit specific biological responses to variety of stimuli in their surroundings. These features make the yeast a "prototypical example" for the study of signaling response outputs (**Figures 1 & 3**). Some of the extensively studied yeast stimulus responses include the following: In response to mating pheromone secreted by the opposite mating partner, haploid yeast undergo growth arrest, polarize towards each other and fuse to form a diploid cell (Qi and Elion 2005). When the carbon or nitrogen nutrient sources are limiting in the surroundings, yeast cells exhibit filamentous or pseudohyphal growth, thus increasing the surface area per cell so they can absorb more nutrients. If they encounter high osmotic conditions, cells undergo temporary growth arrest and induce the synthesis of intracellular osmolyte glycerol in order to maintain the cellular turgor pressure. In situations where there is acute deprivation of nutrients, diploid yeast cells stop growth, undergo immediate meiosis, halt metabolism and transform into spores until the nutrient conditions are restored. Yeast cells also commit themselves to self-death through apoptosis under extreme stress conditions such as high salt, sugar, pheromone, acetic acid or when reactive oxygen species (ROS) are synthesized within the cells (Carmona-Gutierrez, Eisenberg et al. 2010). Each stimulus response is driven by a typical signal transduction machinery that involves sensing the changes in extracellular environment or the ligands at the membrane

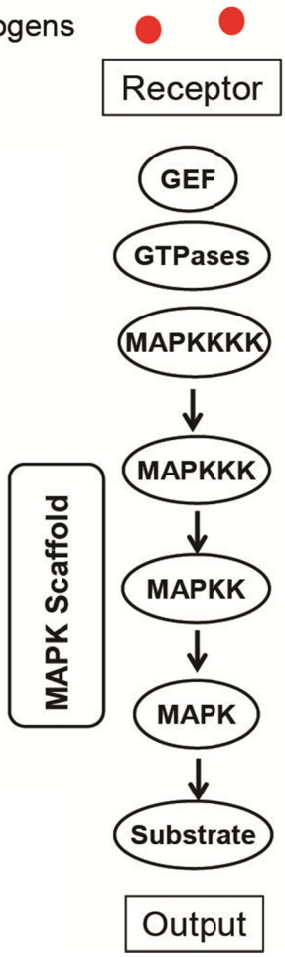

Figure 2. Classical MAPK pathway components.
The mitogens or stimuli are sensed by the receptors. Through the actions of Guanine nucleotide exchange factor (GEF) and the Guanine tri-phosphatases (GTPase), the extracellular information is converted into chemical signal often in the form of phosphorylations. Mitogen activated protein kinase (MAPK) pathways consist of core cascade of three kinases; MAPK kinase kinase (MAPKKK), MAPK kinase (MAPKK) and MAPK that sequentially phosphorylate to activate the next kinase. Often the pathways also consist of MAPKKK kinase (MAPKKKK) that activate MAPKKK. The core cascade kinases are often assembled on the scaffold proteins. Activated MAPK phosphorylate their various substrates towards eliciting stimulus specific response.

by specific receptors, transducing the extracellular information into intracellular signal through receptor associated proteins such as trimeric G-proteins, and signal processing circuits for controlling amplitude, fidelity adaptations to stimuli and cross-talk between signaling pathways (Pawson 1995; Dueber, Yeh et al. 2004; Artyukhin, Wu et al. 2009; Ma, Trusina et al. 2009). In addition, nearly 31% of the potential protein-encoding genes of yeast (open reading frames, or ORFs), have homologs among the mammalian protein sequences (Botstein, Chervitz et al. 1997). Several signaling proteins such as MAPK cascade proteins, Rho GTPases, Proteins kinase A (PKA), Ras, G-proteins and Cyclin dependent kinase (CDK) are highly conserved from yeast to metazoans (Kataoka, Powers et al. 1985; Hartwell 2004; Qi and Elion 2005; Tamaki 2007; Perez and Rincon 2010). In mammals the proliferation, differentiation and disease states such as cancer are often found to be associated with the regulation of these conserved proteins and their pathways (Hirosumi, Tuncman et al. 2002; Hartwell 2004; Lawrence, Jivan et al. 2008). These features make budding yeast an ideal system of choice to study and understand the dynamics of signal transduction through protein interaction networks and their influence on the stimulus-response of cellular decisions.

1.4 Yeast MAP kinase pathways and their response outputs

The yeast genome encodes several MAPKs each of which is attributed to a distinct signal transduction pathway that induces a specific stimulus response (Elion, Qi et al. 2005; Qi and Elion 2005). One of these, (Fus3) mediates cellular response to peptide pheromones secreted by opposite mating partners. Another (Kss1) allows adaptation of cells to nutrient limiting conditions. A third (Hog1) is necessary to maintain cell survival under hyper-osmotic conditions. When a yeast cell encounters stress that could damage its cell wall, a fourth MAPK (Slt2/Mpk1) is attributed to maintain and restore its integrity. A fifth MAPK (Smk1) is known to regulate spore wall assembly during meiosis and sporulation, a developmental response of *MAT***a**/*MAT*α diploid cells to acute nutrient deprivation (**Figure 4**).

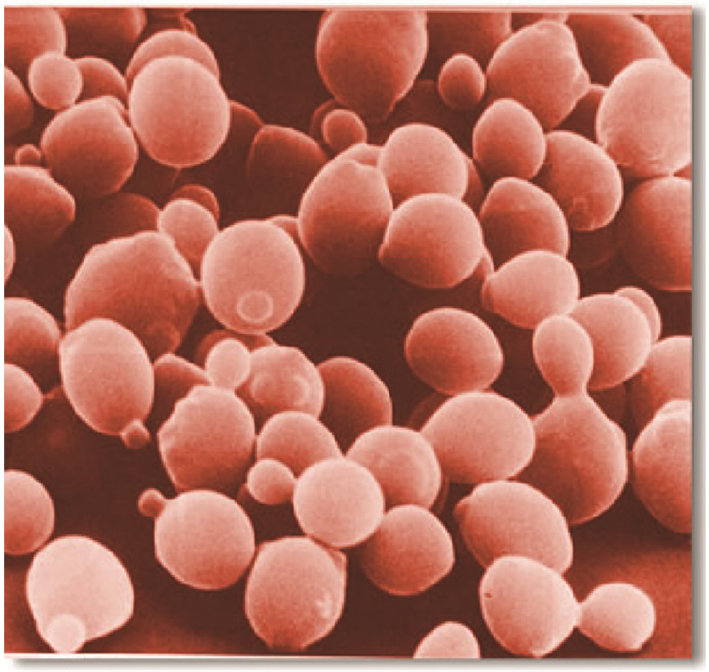

Figure 3. Budding yeast (*Saccharomyces cerevisiae*) as a model system.
The extensive understanding and the availability of genetic, biochemical and *in-vivo* quantitative experimental methods makes budding yeast a favorite choice of model system to understand the stimulus-response behaviors and their dynamics. Source: *http://sustainabledesignupdate.com/?p=932*

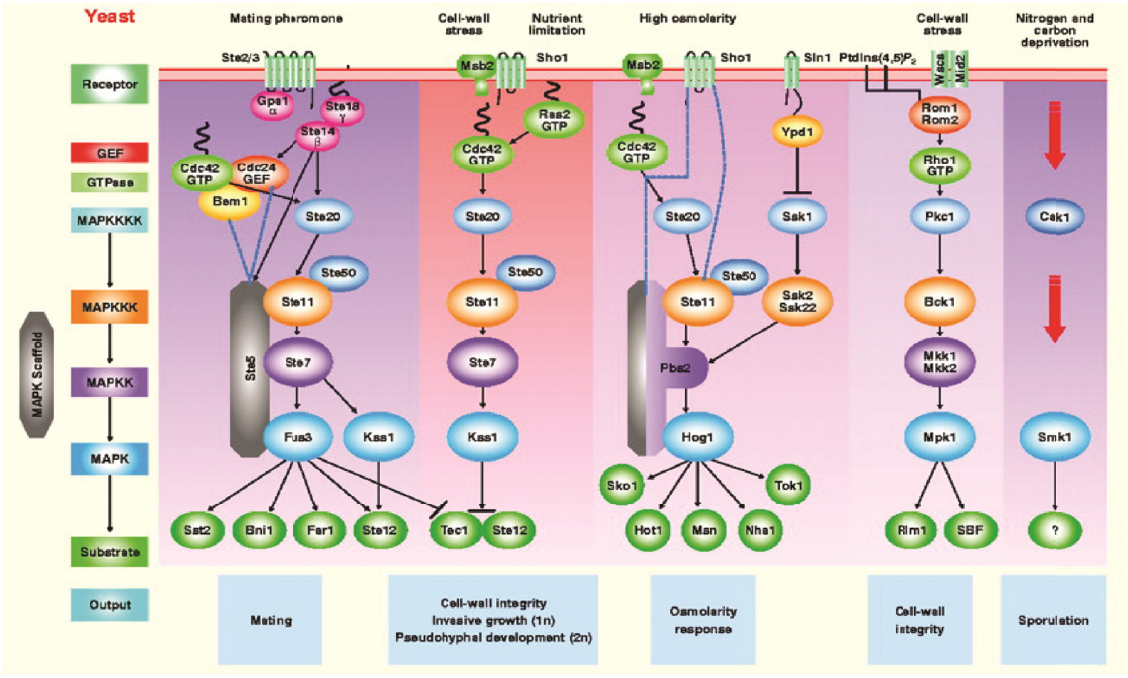

Figure 4.Various MAPK pathways in yeast.
MAPK signalling networks that sense and elicit specific response are shown. Mating MAPK pathway sense the presence of mating pheromone and mediates mating; filamentous pathway allow cells to survive on nutrient starvation; osmolar pathway help cells adapt to high osmolar conditions; cell wall integrity pathway allow cells to survive cell wall stress and under extreme conditions the sporulation pathway permits yeast survival by inducing spore formation. Source: (Qi and Elion 2005).

1.4.1 Pheromone response pathway

Like the gametes of multicellular organisms, the two haploid forms of *S. cerevisiae* '*MAT***a**' and '*MAT*α' can mate by undergoing cellular and nuclear fusion to generate a diploid cell type - *MAT***a**/*MAT***α.** Mating is the end result of a complex series of changes in cellular physiology that are all initiated in response to peptide pheromones secreted by the haploid cells. The *MAT***a** and *MAT*α cells recognize the presence of opposite mating partners in their vicinity and respond by sensing the pheromone (α-factor and a-factor respectively) secreted. Sensing of the pheromone at the membrane by specific receptors activate the cascade of signaling events through 'pheromone or mating signaling pathway' that results in the differentiation of cells towards each other followed by the fusion of haploid cells to form a diploid (**Figure 5**). The pheromone pathway results in activation of the Fus3 MAP kinase that is essential for the mating response (Farley, Satterberg et al. 1999; Elion 2000).

Haploid yeast cells choose their mating partner among potential mates, those cells that secrete the highest concentration of the pheromone (Jackson and Hartwell 1990; Jackson and Hartwell 1990). Thus, they must sense the concentration gradient of pheromone to differentiate into states that allow both the finding and selection of a suitable mate (Jackson and Hartwell 1990; Erdman and Snyder 2001; Paliwal, Iglesias et al. 2007). Since two haploid cells must be within a certain distance to undergo fusion, the mating response should occur only at concentrations of pheromone that imply partner cells are close enough for mating to be successful. Cells must therefore have evolved sensory mechanisms that sharply discriminate between low and high concentrations of pheromone. They must not respond to weak signals of pheromone to avoid an inappropriate commitment to mating.

Depending on the local concentration of pheromone, a haploid yeast cell responds by differentiating into several morphological states (**Figure 6**). At no or very low concentrations, cells divide by axial budding. At higher concentrations, they differentiate into a bipolar budding state in which the daughter cells are generated in the direction of

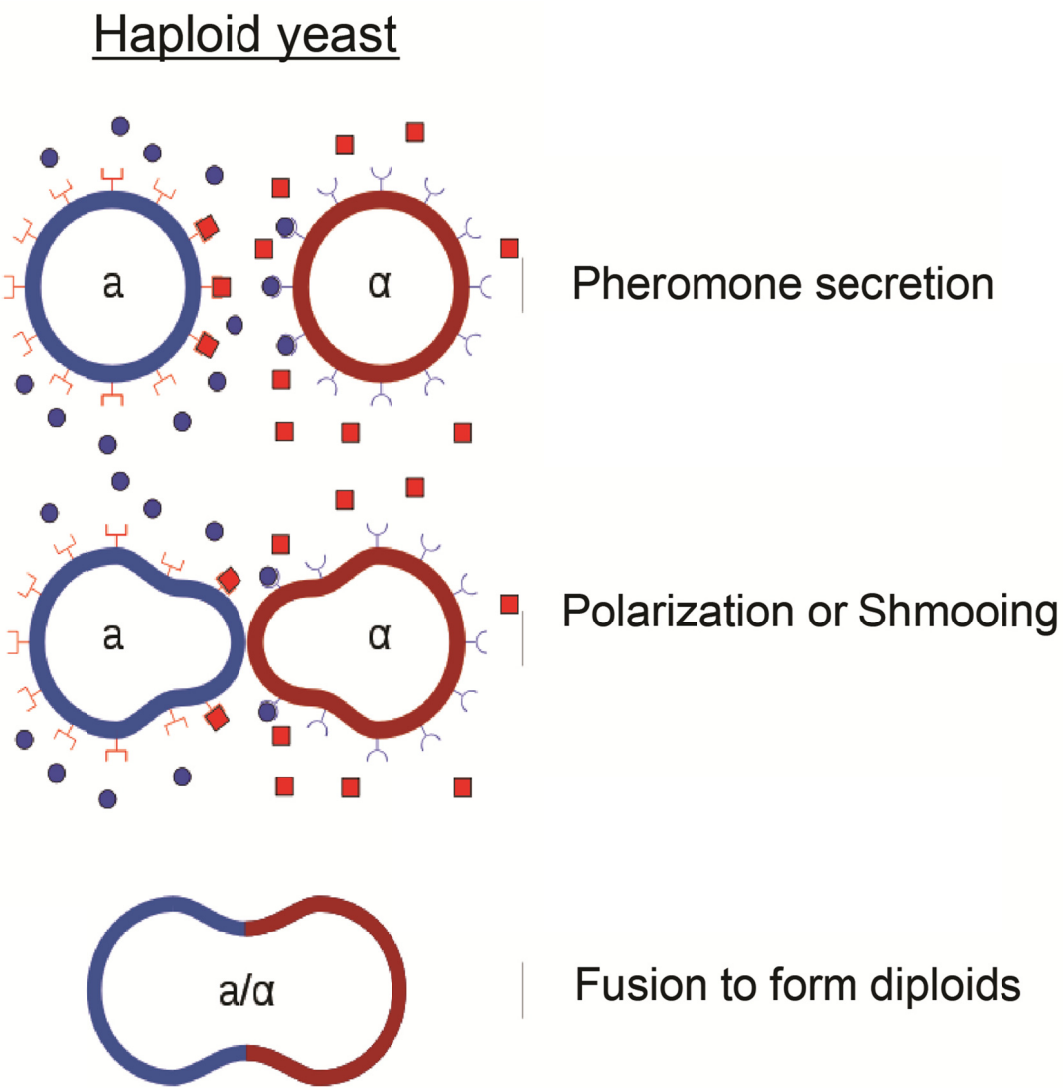

Figure 5.Cartoon showing three stages of yeast mating response.
In the first stage, haploid yeast secrete pheromones (a and α cells secrete a and α factor pheromones respectively) and sense the pheromone secreted by opposite mating type. In second stage they polarize towards each other – also termed as shmooing. In the final stage of response, the two cells make contact and fuse to form a diploid cell.

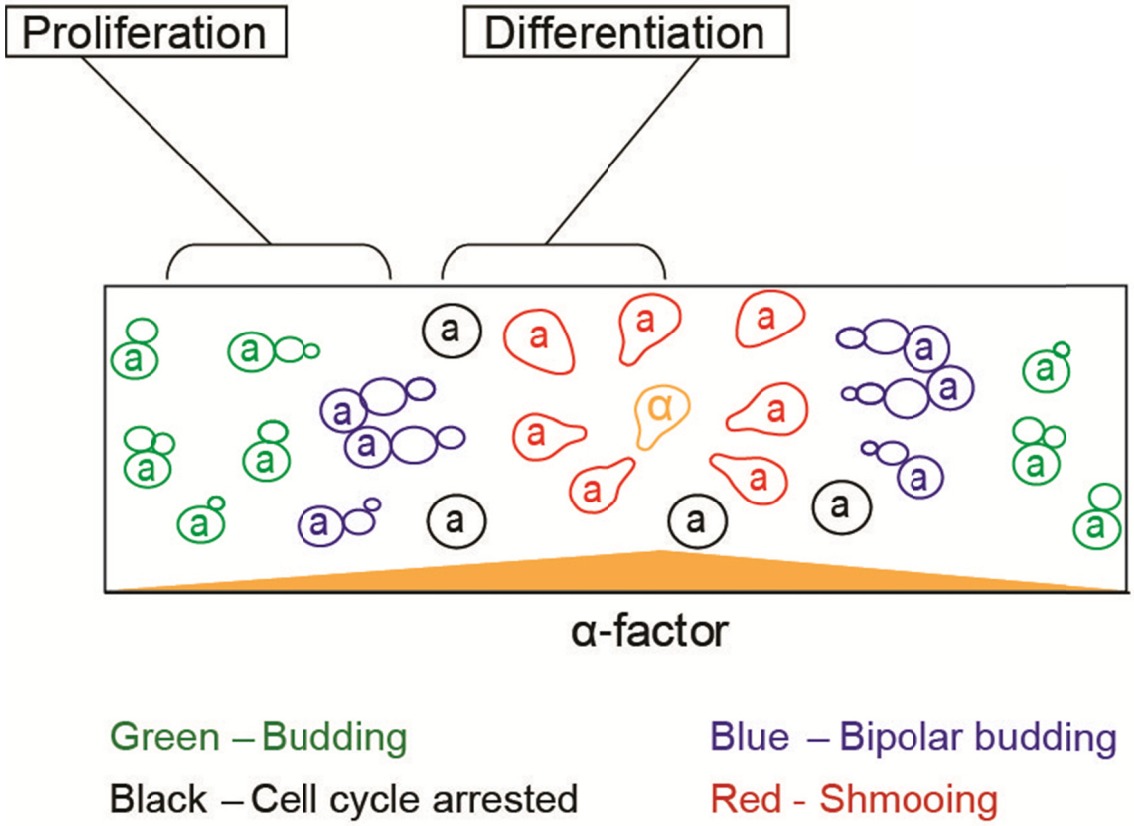

Figure 6.Cartoon depicting the multiple phenotypes observed in an increasing pheromone concentration gradient.
While the budding and bipolar budding reflect the proliferation, cell cycle arrest and shmooing phenotypes resemble differentiation behaviours observed in metazoans. Phenotypes are color coded; budding – green, bipolar budding – blue, cell cycle arrested – black and shmooing – red.

increasing pheromone concentration (Erdman and Snyder 2001). At yet higher concentrations, cells undergo cell cycle arrest and stop dividing. Finally, at a critical concentration the majority of cells differentiate into shmoos ("shmooing"), a pre-fusion state in which two cells of opposite mating type are close enough to fuse (Cross, Hartwell et al. 1988). At any given concentration of pheromone, cells with different phenotypes can also co-exist (Erdman and Snyder 2001; Paliwal, Iglesias et al. 2007; Hao, Nayak et al. 2008).

1.4.2 Filamentous growth pathway

In environments containing sufficient nutrients, *S. cerevisiae* cells are round and proliferate by budding. Under these conditions, a haploid mother cell always buds off new daughter cells adjacent to a previous bud site (axial budding pattern); a diploid mother cell buds off new daughters at opposite to the previous bud site (bipolar budding pattern) (Madden and Snyder 1998). In environments where nutrients are limiting, the haploid cells undergo morphological changes and become elongated and proliferate in a bipolar budding pattern forming a chain of cells which is also referred to as pseudohyphal or filamentous growth. Filamentous growth is mostly driven in parallel by the activation of Kss1 MAPK and protein kinase A (PKA) signaling pathways (Palecek, Parikh et al. 2002) (**Figure 4**).

1.4.3 High osmolarity / glycerol pathway

Cell viability is threatened when the solute concentrations in the extracellular environments is increased which causes a decrease in intracellular turgor pressure. Yeast cells adapt to such extreme osmotic conditions by increasing the internal osmolyte concentration by synthesizing glycerol. This adaptation is commonly referred to as the high osmolarity glycerol (HOG) response (Brewster, de Valoir et al. 1993; Qi and Elion 2005). High osmotic conditions activate the osmolar MAP kinase signaling pathway (**Figure 4**). Survival under hyperosmotic conditions via the HOG pathway requires

activation of the Hog1 MAPK, whose functional ortholog in mammalian cells is the p38 family of stress-activated MAPKs (SAPKs) (Han, Lee et al. 1994). During osmolar response, yeast cells slow down proliferation and exhibit growth arrest until the environment reaches normal osmotic conditions.

1.4.4 Cell wall integrity pathway

Cell walls provide the structural support and protection to cells. They also act as a filtering system. A major function of the cell wall is to act as a pressure vessel, preventing over-expansion to maintain the integrity of the cell structure and shape. The yeast cell wall structure and function are stressed by different extracellular conditions including hypotonic medium, treatment of cells with glucanases (e.g Zymolyase), exposure to chitin-binding agents (e.g. Calcofluor white and Congo red), oxidative stress, depolarization of the actin cytoskeleton and pheromone-induced morphogenesis. (Harrison, Zyla et al. 2004; Levin 2005). These stress conditions activate the cell wall integrity MAPK pathway that results in the activation of MAP kinase Slt2/Mpk1 (**Figure 4**). The final response leads to increased synthesis of cell wall material for the repair or extension of the cell wall.

1.4.5 Spore wall assembly pathway

When *MAT***a**/*MAT*α diploid cells encounter a condition where both a fermentable carbon source and an additional essential nutrient (nitrogen, phosphorus, or sulfur) are deprived, they switch from proliferating to meiosis resulting in the formation of haploid spores (Freese, Chu et al. 1982). When the nutrients are restored, the haploid spores are able to germinate and switch back to proliferative state (Neiman 2005). The sporulation process involves the activation of sporulation MAP kinase pathway (Qi and Elion 2005) (**Figure 4**). Although not completely understood, the activation of the MAP kinase Smk1 seems to be essential for proper spore formation (Huang, Doherty et al. 2005).

Of all the five MAPK signaling pathways in yeast, the mating pathway is perhaps the most well-characterized and is known to exhibit very specific responses to a very specific stimulus. The details of the mating MAPK pathway components and the biochemical steps of signal transduction are discussed below.

1.5 Yeast mating signaling pathway

The pheromone signaling pathway is a description of the steps through which pheromone binds to their specific plasma membrane receptors, activates a receptor coupled heterotrimeric G-protein and passes signal to a MAP kinase cascade through their activation which in turn results in the phosphorylation and activation of proteins that control transcription, cell polarity, cytoskeletal structure and the cell cycle (**Figures 5 & 6**). These changes in cell physiology and structure are required for the cell fusion to result in diploid cells (*MAT***a**/*MAT*α). Polarized cell growth (or shmooing) is required to ensure that the two cells grow towards each other and to form the contact site of cell fusion. Induction of transcription is required to produce new proteins essential for the physiological changes, e.g. proteins that mediate cell adhesion and fusion, while cell cycle arrest is necessary to synchronize the two mating partners to be at the same cell cycle stage (Elion 2000; Bardwell 2005). The information flow through pheromone signaling pathway can be best understood as a temporal ordering of the signaling processes as outlined below (**Figure 7**).

1.5.1 Receptor activation and G-protein cycle

In *MAT***a** cells, the *α*-factor pheromone secreted by *MAT**α*** cells binds to the receptor Ste2. The intracellular domains of the receptors are coupled to the G-protein (Conklin and Bourne 1993). The G-protein is a heterotrimer and consists of the subunits G*α* (Gpa1), G*β* (Ste4) and G*γ* (Ste18). G*β* and G*γ* act as the heterodimer G*βγ* (Hirschman, De Zutter et al. 1997). G*α* interacts with G*βγ* to form a heterotrimer (Ford, Skiba et al.

1998) and full coupling to the receptor requires all three subunits of the heterotrimer (Blumer and Thorner 1990). Pheromone binding induces activation of receptor by exchange of GDP for GTP on Gα which, results in release of G$\beta\gamma$ (Conklin and Bourne 1993). The dissociation of G$\alpha\beta\gamma$ heterotrimer into Gα and G$\beta\gamma$ is essential to activate the pathway and relay the exterior pheromone information into intracellular effectors (**Figure 7**). A GTPase accelerating protein (GAP) Sst2 enhances the hydrolysis of Gα-GTP to Gα-GDP, allowing Gα to reassociate with G$\beta\gamma$ to re-form a heterotrimeric G$\alpha\beta\gamma$. The activity of Sst2 is further dependent on active levels of the MAP kinase Fus3. Reformation of heterotrimer prevents further signal transmission to intracellular effectors (Dohlman and Thorner 1997; Lan, Zhong et al. 2000), thus restraining the cellular response to pheromone (**Figure 7**). Gα subunit in its hydrolyzed state thus acts as a negative regulator of G$\beta\gamma$ during pheromone response. By cycling through its dissociated and associated state the heterotrimeric G-protein can thus effectively control the extent of signal transmission from exterior to interior of the cell.

1.5.2 The downstream intracellular effectors of Gβγ

The free G$\beta\gamma$ heterodimer interacts with a number of intracellular proteins including Cdc24, Cdc42, Ste20 and the scaffold protein Ste5. Of the G$\beta\gamma$ heterodimer, 'β' subunit interacts with other proteins while the 'γ' subunit tethers the heterodimer to the plasma membrane *via* dual lipid modification (Manahan, Patnana et al. 2000). Cdc24 is a member of the ubiquitous class of small G-protein regulators that are critical for the cell growth in all eukaryotes. Cdc24 also acts as a guanine exchange factor (GEF) for Cdc42, a highly conserved Rho GTPase. Cdc42 acts as a molecular switch, ON, in the GTP-bound state and OFF in the GDP bound state to trigger downstream signaling as well as morphology related events including polarization (**Figures 4 & 7**). The binding of G$\beta\gamma$ with Cdc24 and Cdc42 is essential for polarized growth (shmooing) towards the pheromone source. In addition, G$\beta\gamma$ interaction with the scaffold proteins Ste5, Far1 and other proteins like Ste20 and Bem1 is necessary to relay the extracellular pheromone information to the downstream MAP kinase cascade proteins (Butty, Pryciak et al. 1998; Nern and Arkowitz 1999; Elion 2000). Cdc42 binds to Ste20, a p21-activated protein

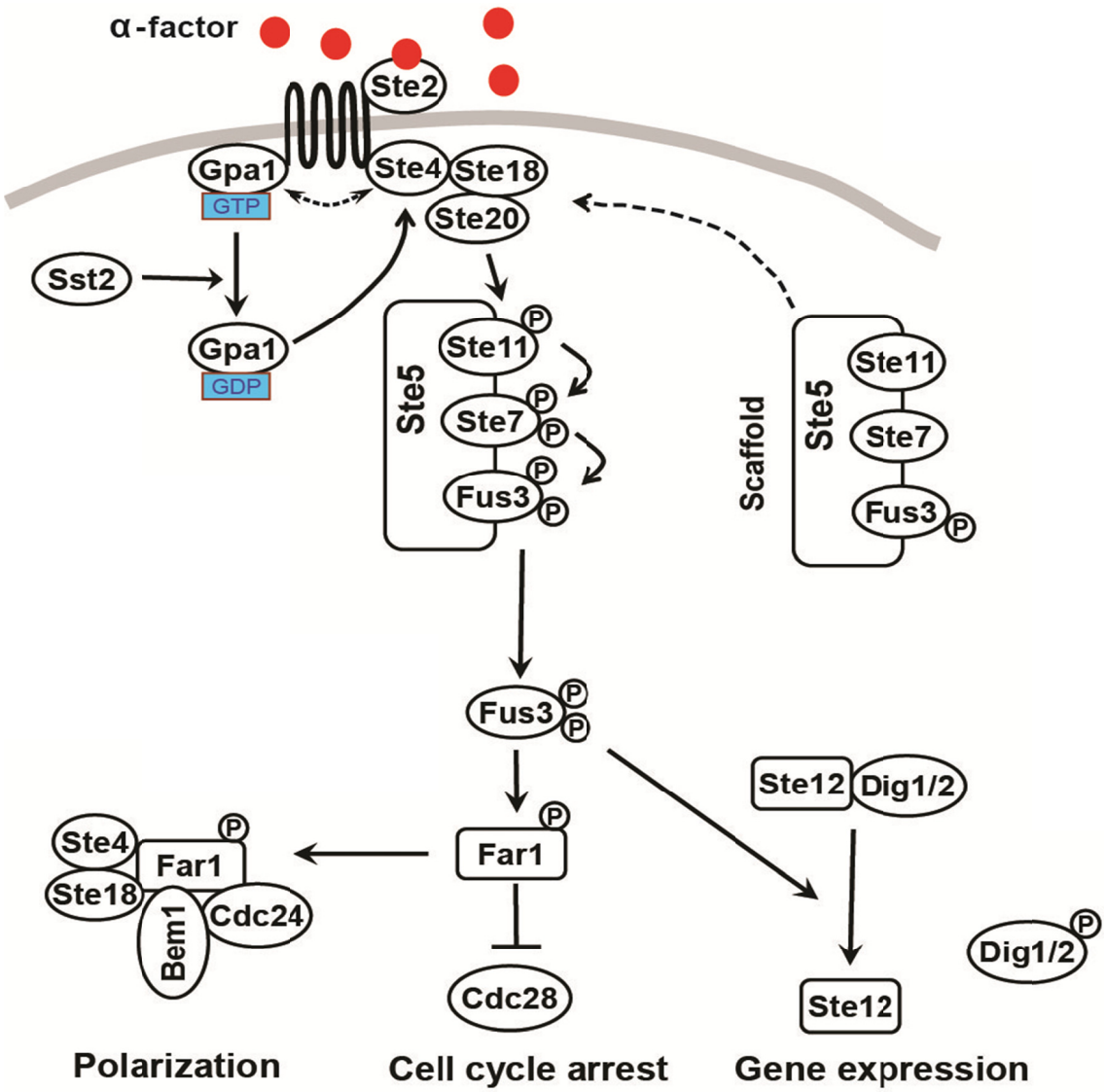

Figure 7. Mating MAPK signalling network showing key components involved in various modules of signalling.
Activation of receptor coupled G-protein and its cycling; Ste5 scaffold and the MAP kinase cascade complex and its translocation; Fus3 activation and its substrates; gene expression induction, cell cycle arrest and polarization complex components.

(Bardwell, Cook et al.) kinase that also acts as a MAPKKKK in the mating pathway (Leeuw, Wu et al. 1998; Song, Chen et al. 2001). This multiprotein complex is anchored to the plasma membrane and accumulated in the polarization tips in stimulated cells (Zhao, Leung et al. 1995). Through its binding to the G$\beta\gamma$ heterodimer, the scaffold protein Ste5 is also tethered to the plasma membrane (Inouye, Dhillon et al. 1997; Pryciak and Huntress 1998) (**Figure 7**). By localizing Ste5 (and its bound MAPK cascade proteins) at the plasma membrane, Ste11 – MAPKKK of the cascade is brought into proximity with the membrane-associated Ste20 (MAPKKKK) (Pryciak and Huntress 1998). Cdc42-GTP induces auto-phosphorylation and activation of Ste20, which initiates the activation of MAP kinase cascade proteins by phosphorylating and activating Ste11 (Whiteway, Wu et al. 1995; van Drogen, O'Rourke et al. 2000; Dan, Watanabe et al. 2001). This step is pheromone dependent and essential for signal transmission to the Ste11.

1.5.3 The Ste5 scaffold and the MAP kinase cascade complex

The pheromone signaling network consists of a highly conserved core MAP kinase cascade proteins Ste11, Ste7 and Fus3 assembled on the scaffold protein, Ste5, forming a multiprotein complex. Ste5 scaffold has specific binding or docking regions for each of these MAP kinase cascade proteins. The formation of this complex is independent of the pheromone stimulus (Yablonski, Marbach et al. 1996; Inouye, Dhillon et al. 1997). Interactions among Ste5, Ste11, Ste7 and Fus3 do not require signaling from either G-protein or Ste20; the multiprotein complex also exists in cells that are not exposed to pheromone (Marcus, Polverino et al. 1994) (**Figure 7**). Ste5 seems to be crucial to maintain the signal and substrate specificity by preventing crosstalk between different yeast MAP kinase pathways, especially provided Ste11 and Ste7 are also involved with filamentous and osmolar signaling. Similar to other known scaffolds, Ste5 is essential to co-localize the proteins in specific areas of the cell - bringing them in close proximity to each other (Burack and Shaw 2000), prevent the influence of negative regulators (e.g., phosphatase) on the bound kinases, and suppresses auto-inhibitory conformations of the kinases (especially Ste11) (van Drogen, O'Rourke et al. 2000). Ste5 binding to Ste11 in

the presence of pheromone is known to facilitate Ste11 activation (Elion 2001). Ste7 interacts with Ste5 through its C-terminal kinase domain (Choi, Satterberg et al. 1994; Marcus, Polverino et al. 1994; Printen and Sprague 1994). In its inactive form Fus3 establishes a stable association with Ste5 (Choi, Satterberg et al. 1994; Kranz, Satterberg et al. 1994; Marcus, Polverino et al. 1994; Printen and Sprague 1994).

In the absence of pheromone, Ste11 remains associated with Ste5 and auto-inhibits itself. Phosphorylation by the upstream kinase- Ste20 and binding to Ste5 in the presence of pheromone are essential for Ste11 activation (Elion 2001). Active Ste11 phosphorylates two highly conserved residues in the activation loop of the MAPKK Ste7 in order to activate it (Neiman and Herskowitz 1994). Through its N-terminus, Ste7 interacts with Fus3 (Bardwell and Thorner 1996). Fus3 is the terminal MAP kinase (MAPK) in the cascade of the pheromone pathway. Ste7 activates Fus3 by phosphorylating the threonine and tyrosine residues in its activating loop (Bardwell and Thorner 1996) (**Figure 7**). Fus3 shows some similarities to Kss1, another MAP kinase activated by Ste7 during pheromone response. Although Kss1 can complement the function of Fus3 in its absence, it is mostly involved in the invasive growth-inducing pathway (Madhani and Fink 1998; Breitkreutz and Tyers 2002). Intrinsically, Fus3 is a poor but Kss1 is an excellent substrate for Ste7. In the presence of pheromone, the mating MAPK Fus3 activation is selectively favored by the Ste5 scaffold protein which is essential for Fus3 activation. A domain of Ste5 catalytically unlocks Fus3 thus selectively increasing its phosphorylation by Ste7. The same domain has no effect on the Ste7 mediated Kss1 phosphorylation (Good, Tang et al. 2009). Active Fus3 is also known to feedback phosphorylate Ste5, Ste7 and Ste11. Active Fus3 rapidly dissociates from Ste5 while the scaffold protein itself remains bound at the plasma membrane, forming a platform which allows activation of many Fus3 molecules (**Figure 7 & 10**). This mechanism might lead to an amplification of the signal in the form of Fus3 activation. The magnitude of this amplification still remains unknown (van Drogen and Peter 2001). Several phosphatases such as; tyrosine phosphatases Ptp2, Ptp3 and a dual specificity phosphatase Msg5 are known to deactivate Fus3 by dephosphorylating the threonine and tyrosine on its activation loop (Zhan, Deschenes et al. 1997).

1.5.4 Active Fus3 and its substrates

Fus3 acts as a key kinase by phosphorylating many substrates to initiate several physiological changes required for the mating response (**Figure 7**). It does so by phosphorylating and regulating the function of various nuclear and cytoplasmic proteins (Dohlman 2002): Sst2 - necessary for G-protein cycling, Ste5 - the scaffold protein for the MAPK cascade (Kranz, Satterberg et al. 1994), Ste11 and Ste7 – upstream MAPK cascade kinases (Bardwell and Thorner 1996), Far1 - required for morphological changes and for cell cycle arrest (Peter, Gartner et al. 1993), Ste12 - involved in the transcriptional activation of mating genes (Metodiev, Matheos et al. 2002), Dig1/Rst1 and Dig2/Rst2 - necessary for transcriptional inhibition of Ste12 (Tedford, Kim et al. 1997) and others.

1.5.5 Transcriptional activation by Fus3

Ste12 is a transcriptional factor that activates the expression of mating genes in response to pheromone (Pi, Chien et al. 1997). In the absence of pheromone, Ste12 is inhibited by direct binding of its repressors Dig1/Rst1 and Dig2/Rst2 at its regulatory domain. Hence the mating genes are in the 'off' state. In the presence of pheromone, active Fus3 phosphorylates the repressors, which then dissociate from Ste12 thus relieving the inhibition of Ste12 (Tedford, Kim et al. 1997; Bardwell, Cook et al. 1998) (**Figure 7**). This allows the transcription of mating genes which include the signaling proteins of the pheromone pathway itself, proteins essential to morphological transformation and enzymes that degrade the cell wall to facilitate cell fusion to form diploids. Transcription of a pheromone endo-peptidase Bar1 is also important to regulating pheromone response Bar1 is secreted to the extracellular environment where it cleaves the α-factor pheromone between leucine 6 and lysine 7 yielding inactive pheromone fragments (Ciejek and Thorner 1979; Ballensiefen and Schmitt 1997). This reduces the effective concentration of pheromones in the environment and helps cells recover from pheromone induced growth arrest (Ciejek and Thorner 1979). This regulation constitutes one negative feedback loop in the pheromone response pathway. Bar1 protease mediated degradation of pheromone may play another important role in

refining and aligning the pheromone gradient in the direction of the nearest partner to increase accuracy in polarization and thus mating efficiency (Barkai, Rose et al. 1998).

1.5.6 Cell cycle arrest

Pheromone induces growth arrest at the G1 phase in order to synchronize both 'a' and 'α' cells to be in the same state and cell cycle stage. Growth arrest at G1 phase is essential for the mating response and is mediated by Far1 protein. Far1 is commonly referred to as a Cyclin dependent kinase (CDK) inhibitor. In the presence of pheromone, it is actively translocated from nucleus to cytoplasm and the polarizing region. Far1 is bifunctional; cytosolic Far1 is involved in polarized growth (Butty, Pryciak et al. 1998; Nern and Arkowitz 1999) while the nuclear Far1 controls the cell cycle. In the absence of pheromone, Far1 is degraded in the nucleus in an ubiquitin and proteasome-dependent manner. This degradation is cell cycle-dependent; Far1 is stable only in the G1 phase of the cell cycle and during the other stages it is rapidly degraded (Henchoz, Chi et al. 1997). The CDK complexes formed of Cdc28 (kinase) and Cln (G1 cyclins: Cln1, Cln3 and especially Cln2) phosphorylate Far1, which primes it to be recognized by the ubiquitination system for degradation (Peter, Gartner et al. 1993; Henchoz, Chi et al. 1997). In the presence of pheromone, Far1 levels increase by two mechanisms: Ste12 dependent increase in expression of Far1 (Chang and Herskowitz 1990; Oehlen, McKinney et al. 1996) and active Fus3-dependent phosphorylation and stabilization (**Figure 7**). Fus3 phosphorylates Far1 on two phosphorylation sites that prevent it from being degraded by the ubiquitination system (Peter, Gartner et al. 1993; Tyers and Futcher 1993; Oehlen, McKinney et al. 1996; Breitkreutz, Boucher et al. 2001; Breitkreutz and Tyers 2002). Stabilized Far1 in turn inhibits Cdc28 – Cln complex activity, which leads to arrest of the cell cycle in the G1 phase (Peter, Gartner et al. 1993; Gartner, Jeoung et al. 1998).

1.5.7 Polarization

Haploid yeast cells sense the direction of pheromone secreted by their mating partner and undergo polarized growth, forming a projection often referred to as a 'shmoo' towards the source of pheromone (Arkowitz 1999) (Chant 1999). Shmoo formation is a complex process that involves the actin cytoskeleton, polarization and signalling proteins, plasma membrane and cell wall along the axis defined by the pheromone source (Leberer, Thomas et al. 1997; Arkowitz 1999). Pheromone activated Fus3 controls the polarization by inducing the expression of a variety of genes required for morphogenesis, including components of the protein kinase C pathway that regulates cell wall remodelling (Farley, Satterberg et al. 1999; Roberts, Nelson et al. 2000).

Polarization takes place at a localized landmarks on a cell and consist of pheromone receptor and its activated G-protein subunits (i.e. Gβγ) bound to effectors involved in morphogenesis (Arkowitz 1999; Nern and Arkowitz 2000). The activated Gβγ subunit, in addition to recruiting the Ste5 scaffold and the MAP kinase signalling complex, also recruits a multiprotein complex of polarity establishment proteins that includes Far1, Cdc24, Cdc42 and Bem1 (Butty, Pryciak et al. 1998; Nern and Arkowitz 1998; Nern and Arkowitz 1999). Far1 is thought to act as a polarity scaffold protein as it binds the polarization proteins Cdc24, Cdc42, Bem1 and links them to Gβγ (Butty, Pryciak et al. 1998; Nern and Arkowitz 1999) (**Figure 7**). Far1 is also shown to control the access of Cdc24 to the sites of polarization by being able to sequester it in nucleus in the absence of pheromone signal (Ayscough and Drubin 1998; Nern and Arkowitz 2000; Shimada, Gulli et al. 2000).

1.6 Complexes through docking interactions

Signaling proteins are rich in protein interaction modular domains. Interaction domains can control activity and substrate specificity of enzymes, can target proteins to a specific sub cellular location and provide a means for posttranslational modifications

(Pawson and Scott 1997; Pawson and Nash 2003). Domains also provide means to form multiprotein signaling complexes (as in scaffold and adaptor proteins). By being linked to one another by scaffolds, signaling proteins are able to process stimulus information efficiently. The flexibility and combinatory nature of signal transduction proteins allow them to be more evolvable to forge new functional links and corresponding phenotypes (Pawson and Scott 1997; Bhattacharyya, Remenyi et al. 2006; Peisajovich, Garbarino et al. 2010).

As a result of recent advances in mechanistic, quantitative and structural studies as well as the sequencing of multiple eukaryotic genomes, our understanding of signaling proteins has dramatically increased. Signaling pathways consist of enzymes that catalyze reactions such as phosphorylation, dephosphorylation and nucleotide exchange. Signaling enzymes exhibit precise input-output control behaviors. While the input control for a signaling enzyme determines how, when and by what they are activated, the output control determines what downstream partners these enzymes act upon. Such input-output connectivities of signal transduction enzymes are largely organized in a modular nature (Pawson and Nash 2003). In addition to their core catalytic function, signaling proteins (e.g. kinases) often contain multiple independently folding domains. Since these domains have often evolved to be independent of the core catalytic function of their enzymes, they mediate their direct interactions with other signaling proteins, to facilitate the functional connectivity and thus form a network of signaling enzymes (**Figure 8**). Three basic modular mechanisms have been recently well described to form connectivity among signaling proteins: the use of peripheral docking sites, modular interaction domains and scaffolding or adapter proteins (Bhattacharyya, Remenyi et al. 2006). Each of these mechanisms can be used to select functional upstream and downstream partners as well as, in many cases, to allosterically regulate catalytic activity of a protein.

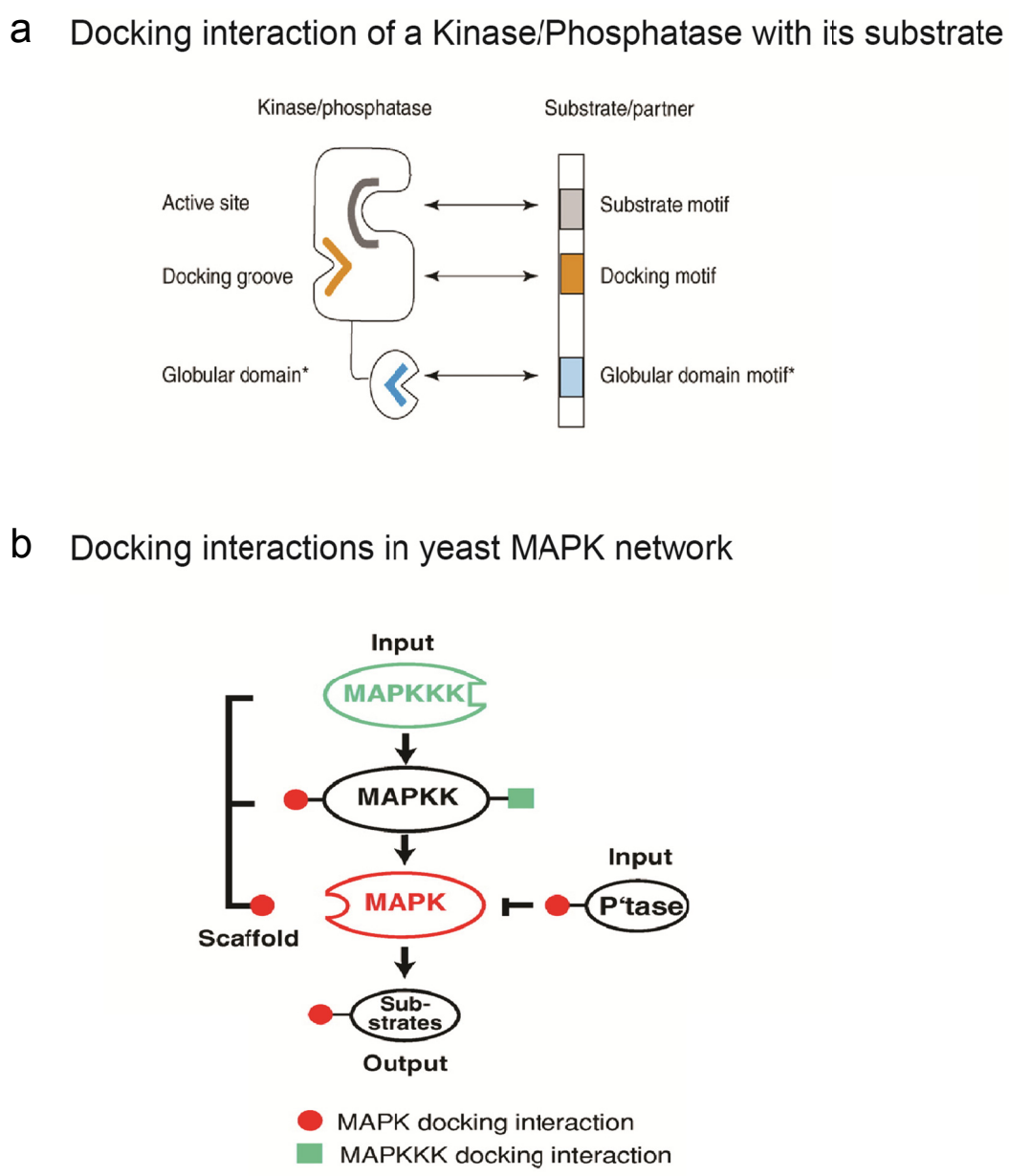

Figure 8. Schematics to depict docking motif interactions of a kinase or phosphatase with its substrate.
(a) and in yeast MAP kinase signalling network (b). Kinases and phosphatases often have of docking groove that recognizes and bind a docking motif on their substrates (orange in 'a'), which is independent of the enzyme active site interaction with its substrate motif (gray in 'a'). Source: (Remenyi, Good et al. 2005; Bhattacharyya, Remenyi et al. 2006).

1.6.1 Docking sites mediate signaling networks through protein – protein interactions

Recent studies, in contrast to traditional belief that enzyme-substrate specificity is controlled by the stereo chemical complementarity at the active site (like that of lock and key hypothesis), have shown that the surface binding sites that are independent of the catalytic site also determine their specificity. Signaling enzymes are often found to have a surface distinct from their active site, referred to as a 'docking domain or site' through which they recognize and bind to 'docking motif'- short peptide sequence present on their substrates (Holland and Cooper 1999; Biondi and Nebreda 2003; Remenyi, Good et al. 2005). On substrates, this docking motif is distinct from the actual phosphoacceptor site (**Figure 8a**). Docking interactions play an important role in mediating substrate or partner recognition. The importance of docking motifs in partner recognition is well understood with the kinases that are often found to have docking motifs and also form the majority of signaling components. For example, Serine (Ser)/threonine (Thr) kinases use docking motif interactions as a common mechanism to specifically interact with their substrates and regulators (Holland and Cooper 1999; Biondi and Nebreda 2003; Remenyi, Good et al. 2005). Enzyme-substrate encounters are increased through the surface recognition of docking interactions in addition to the catalytic site alone. Since the docking interaction and the catalytic active site are functionally separated from each other, the docking interactions can increase the efficiency and specificity of 'input – output' function of an 'enzyme – substrate' complex in a signaling network.

Several Ser/Thr kinase families have been found to contain docking motifs (Sharrocks, Yang et al. 2000; Tanoue, Adachi et al. 2000). For example; the docking site (or groove) on the MAPKs recognize a well-characterized docking motif, referred to as the d-box (Jacobs, Glossip et al. 1999) on their substrates. Specific mutations in either the docking motif of the substrates or the docking groove of the MAPKs is known to disrupt the enzyme-substrate interaction and the signal transmission from MAPKs to their substrates (Kusari, Molina et al. 2004; Remenyi, Good et al. 2005; Grewal, Molina et al. 2006). Many MAPKs including the mammalian MAPKs p38, c-Jun N-terminal kinase

(JNK), extracellular signal regulated kinase (ERK), and the yeast MAPKs Fus3 and Kss1 in *Saccharomyces cerevisiae* and Spc1 in *Schizosaccharomyces pombe* (Bardwell and Thorner 1996; Jacobs, Glossip et al. 1999; Tanoue, Adachi et al. 2000; Tanoue, Maeda et al. 2001; Nguyen, Ikner et al. 2002; Ho, Bardwell et al. 2003; Kusari, Molina et al. 2004) are found to have a conserved d-box docking motif interacting groove on their surface. Docking grooves have also been identified in several other families of kinases (Biondi and Nebreda 2003). Studies with MAPK pathways have revealed the importance and versatility of docking interactions in forming specific network connections through protein-protein interactions (**Figure 8b**). MAPK specific docking motifs are found in several types of MAPK interacting partners; substrates (such as transcription factors), in upstream kinases (MAPKKs), downregulatory phosphatases, their scaffolds, adaptors and other regulatory partners (Tanoue, Adachi et al. 2000; Bardwell, Flatauer et al. 2001; Ho, Bardwell et al. 2003; Kusari, Molina et al. 2004; Remenyi, Good et al. 2005) (**Figure 8b**).

In addition to recognizing the docking motifs, the docking grooves on kinases have also evolved to exhibit sequence preference in their recognition there by distinguishing the docking motifs of multiple substrates (Remenyi, Good et al. 2005) (Barsyte-Lovejoy, Galanis et al. 2002). In this way, even though an enzyme might have multiple substrates, it can selectively and specifically bind to the docking motif of an appropriate substrate under a given condition. This property further increases the specificity of kinase – substrate interactions in signaling networks. For example; the yeast homologous kinases, Fus3 and Kss1 act as functional MAPKs in the mating and invasive growth pathways respectively. Both of these MAPKs have docking grooves that equally allow them to recognize docking motifs on their common interacting partners, such as the MAPKK Ste7 (Bardwell, Cook et al. 1996; Remenyi, Good et al. 2005). However, they have evolved some degree of discrimination in recognizing the pathway specific substrates: Fus3 binds the docking motif from the mating pathway effector Far1 more tightly than does Kss1 (Remenyi, Good et al. 2005), explaining its specific selectivity towards this substrate (Breitkreutz, Boucher et al. 2001).

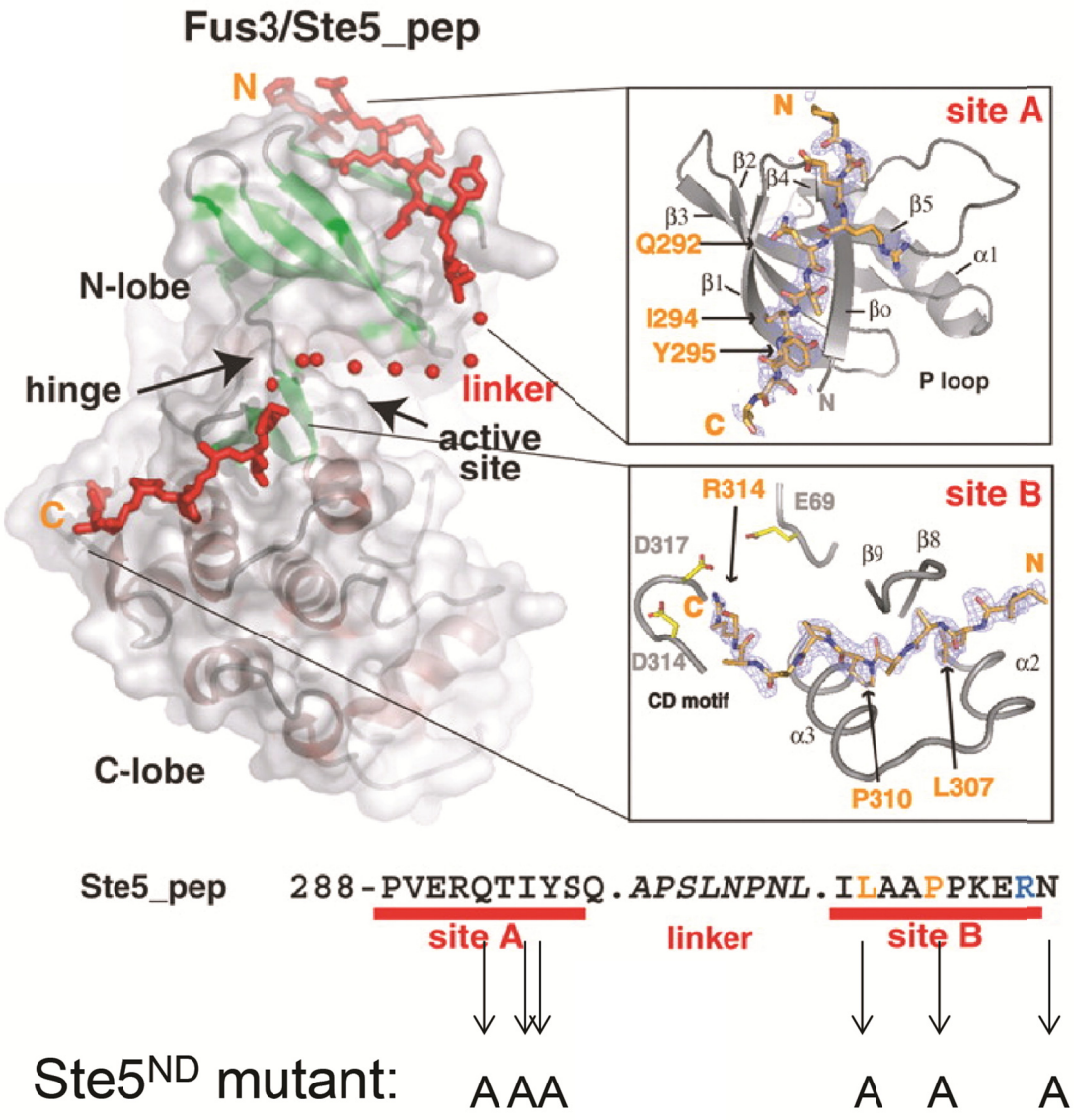

Figure 9. Co-crystal structure visualizing the docking interaction of Fus3 with Ste5. Ste5 docking motif (sequence shown at the bottom) binds Fus3 at two sites separated by a linker. Site A binds to the N-terminal lobe of Fus3 and site B to its C-terminal lobe. The bottom panel also indicates the specific amino acids of Ste5 docking motif that are mutated to Alanine (A) in order to generate the Ste5ND mutant that disrupts the docking interaction of Fus3 with Ste5. Source: (Bhattacharyya, Remenyi et al. 2006).

Thus, even related kinases have evolved slightly different docking grooves, allowing them to have distinct specificities towards their substrates, which in turn influence the information transmission through a signaling pathway. This flexibility of forming new connections through docking interactions increases the chances of evolvability of new functional circuits within signaling networks.

Apart from increasing the likelihood of enzyme – substrate encounter and specificity of protein interactions in some cases, docking interactions have also been shown to regulate the kinase function of the enzyme directly (Chang, Xu et al. 2002; Bhattacharyya, Remenyi et al. 2006). For example; the mating pheromone MAPK Fus3 binds to the scaffold protein Ste5 by recognizing it's docking motif that is partly similar to the docking motif present on its other substrate Far1 (**Figure 9**). This binding of Fus3 with its docking peptide on the scaffold Ste5 allosterically induces auto-phosphorylation on one of its activation loop phosphorylation sites making it partially active. The partially active Fus3 in turn feedback phosphorylates Ste5 at a phosphorylation site located closer to the docking peptide. Functionally, this auto-phosphorylation of Fus3 and feedback phosphorylation of Ste5 further inhibits the mating response output.

1.7 Protein translocation dynamics

Following cell-surface receptor activation, the process of converting extracellular information into a meaningful intracellular signal and eliciting a response output often involves re-organization of the signal-transducing proteins within the cell and its compartments. For efficient processing of signal, proteins are translocated to specific regions where their function is important. For example; upon activation of a signaling pathway, signaling proteins, which are otherwise cytosolic or nuclear are recruited to the membrane for efficient signal transduction. The theme of regulated translocation of signaling proteins to membrane is universal to all organisms - from bacteria to mammals (Widmann, Gibson et al. 1999; Elion 2000; Zhang and Klessig 2001; Laub and Goulian 2007; Lemmon and Schlessinger 2010). During the yeast mating response, proteins

involved in signaling, polarization, cell adhesion and fusion are localized to the mating projection (shmoo) at the membrane (**Figure 10a**).

The subcellular dynamic localization of several components of the mating signal transduction pathway has been examined to understand how the mating signal is transduced from the plasma membrane to the nucleus. A very important step in activation of the mating signaling is the plasma membrane recruitment (to the pheromone activated Gβγ dimer) of Ste5 scaffold protein along with the MAPK cascade kinases (Pryciak and Huntress 1998; Mahanty, Wang et al. 1999; van Drogen, Stucke et al. 2001; Winters, Lamson et al. 2005). In the absence of pheromone, Ste5 is observed to be largely localized to the nucleus (**Figure 10a**). Nuclear localization promotes G1-CDK dependent, ubiquitin mediated proteasomal degradation of Ste5 (Garrenton, Braunwarth et al. 2009). This mechanism helps to maintain minimal levels of Ste5 and thus prevent spurious stimulus-independent activation of signaling (Garrenton, Braunwarth et al. 2009). Ste5 recruits the core MAPK cascade proteins (Ste11, Ste7 and Fus3) through its unique binding sites (Choi, Satterberg et al. 1994; Kranz, Satterberg et al. 1994; Marcus, Polverino et al. 1994). This multiprotein complex is formed even in the absence of pheromone stimulus.

In response to pheromone, Ste5 is redistributed to the cytoplasm and a fraction of it accumulates at the tips of mating projections colocalizing with activated receptors and Gβγ (Pryciak and Huntress 1998; Mahanty, Wang et al. 1999). Nuclear export of Ste5 is mediated by the exportin Msn5/Ste21 (Mahanty, Wang et al. 1999). The translocation of Ste5 and its associated MAPK cascade proteins to membrane is facilitated by the actin cytoskeleton (Qi and Elion 2005). Membrane recruitment of Ste5 serves critical functions in activating the mating pathway; it facilitates Ste11 activation by its membrane-localized activator, Ste20 (Pryciak and Huntress 1998; van Drogen, O'Rourke et al. 2000), it ‘amplifies’ signal transmission from active Ste11 through the rest of the MAP kinase cascade (Lamson, Takahashi et al. 2006), it connects signaling with polarization and cell cycle control components to coordinate the overall mating response.

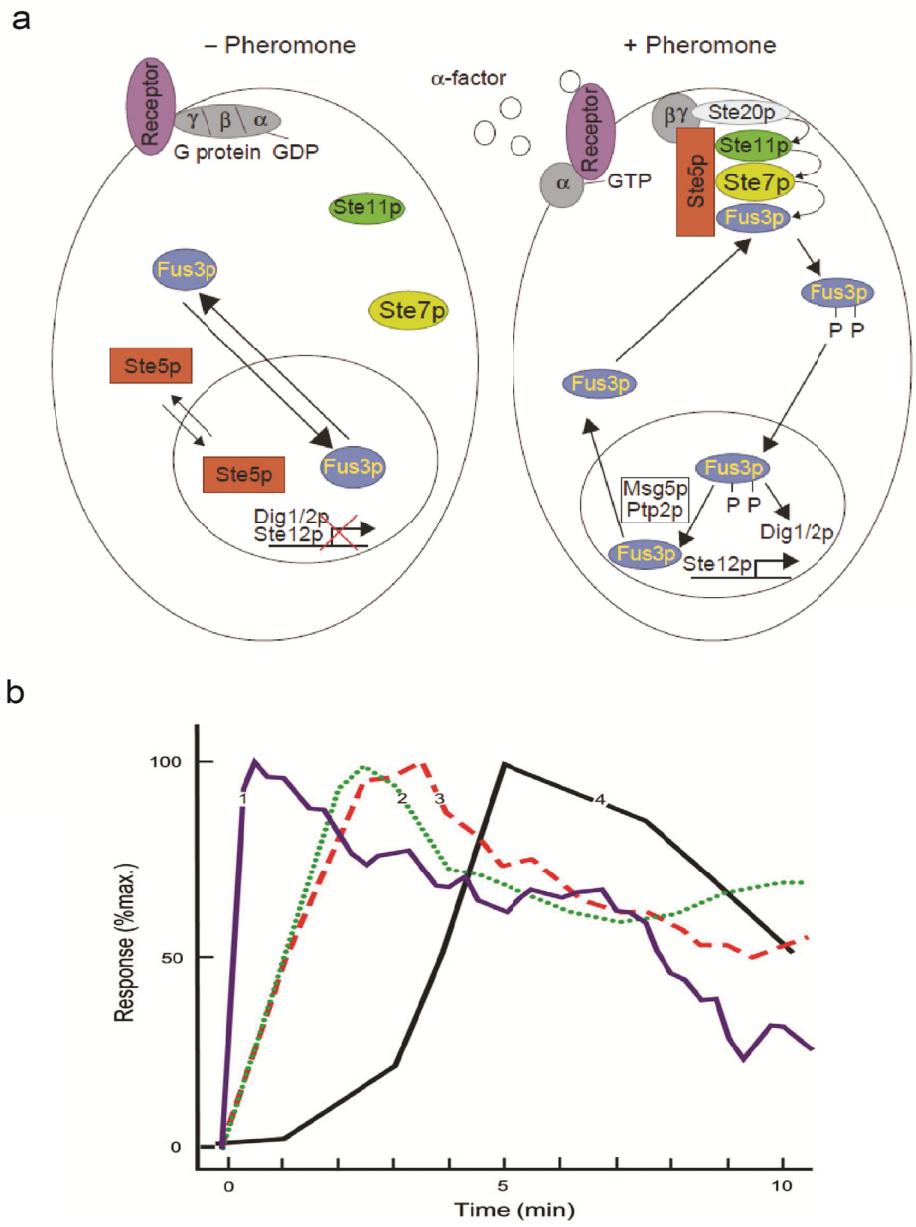

Figure 10. Pheromone induced translocation (a) and temporal (b) signalling dynamics during mating response.
In the absence of pheromone Ste5 and Fus3 shuttle between nucleus and cytosol (left in 'a'). Pheromone induces rapid translocation of Ste5 and its associated kinases to the membrane (right in 'a' and curve 1 in 'b'). Fus3 is rapidly activated (curve 2 in 'b') which dissociates from Ste5 and translocates to nucleus (right in 'a'). Inactive and dephosphorylated Fus3 cycles back to signalling complex at the membrane. In 'b': 1 - Ste5 recruitment to membrane, 2 - Fus3 phosphorylation, 3 -De-suppression of Ste12, 4 - Fus1 mRNA transcript. Source: (van Drogen, Stucke et al. 2001; Brent 2009).

Although biding of Ste5 to Gβγ is essential to trigger signaling, it is not sufficient for the Ste5 recruitment. Recently it has been discovered that Ste5 also directly binds to plasma membrane through a basic 'PM' (plasma membrane binding) domain and 'PH' (plectstrin-homology) domains (Winters, Lamson et al. 2005; Garrenton, Young et al. 2006; Strickfaden, Winters et al. 2007). PM domain is a short basic amino acids rich amphipathic a helix that binds acidic phospholipid membranes (Winters, Lamson et al. 2005). In addition, the PM domain is flanked by multiple (eight) CDK phosphorylation sites, the phosphorylation of which prevents Ste5 membrane interaction (Strickfaden, Winters et al. 2007) in absence of pheromone stimulus. The mechanism proposed involves the 'electrostatic repulsion' between the multiple negatively charged phosphates (due to G1 CDK mediated phosphorylations) and the acidic phospholipids of inner membrane (Strickfaden, Winters et al. 2007). The PH domain binds to membrane phosphoinositides such as phosphatidylinositol 4,5-*bis*phosphate [PtdIns (4,5)P_2] that are localized to the shmoo tip during mating response (Garrenton, Young et al. 2006; Garrenton, Stefan et al. 2010). The Ste5 membrane interaction with phospholipids through PM and PH domains are not required for its Gβγ binding, but together are essential to the full function of Ste5 (Winters, Lamson et al. 2005; Garrenton, Young et al. 2006; Strickfaden, Winters et al. 2007).

Ste11 is found throughout the cytoplasm both in the absence and presence of pheromone (Ferrigno, Posas et al. 1998). Ste11 activator Ste20 is detected at the tips of buds in the absence of pheromone and in mating projections in its presence (Peter, Neiman et al. 1996; Leberer 1997). Ste7 is found in the cytosol in the absence of pheromone and at the shmoo tips in its presence. The MAPK Fus3 is found in the nucleus in the presence or absence of pheromones (Choi, Kranz et al. 1999). Nuclear translocation of MAP kinases (for example; Hog1, ERK1/2, etc) has been shown to correlate with their activation. Nuclear accumulation of MAPKs in response to extracellular signals can be regulated at multiple levels, including increased nuclear import or decreased nuclear export, as well as release from cytoplasmic-anchoring proteins such as the scaffold proteins. The MAPK Fus3 and its scaffold Ste5 constitutively shuttle between the

cytoplasm and the nucleus and these translocation are not regulated by pheromone (van Drogen, Stucke et al. 2001) (**Figure 10a**). In the presence of pheromone both proteins are rapidly recruited to the mating projection tip where, activated Fus3 rapidly dissociates from Ste5 and is imported into the nucleus (**Figure 10b**). Within the nucleus, active Fus3 induces *STE12*-dependent gene transcription and cell cycle arrest by phosphorylating the Dig proteins and Far1 respectively (Elion 2000) (**Figure 10b**).

It has also been proposed that in addition to improving the specificity and speed of signal transmission, regulated translocation of signaling proteins to membrane can generate ultrasensitivity in signaling that could control the nature of a system's response behavior - turn a graded stimulus into a switch-like response outputs (Ferrell 1998; Serber and Ferrell 2007). Different types of response outputs to varying stimulus concentrations and the properties of their underlying circuits are further discussed below.

1.8 Input-output response types

Traditionally, the response outputs of signal transduction pathways were measured as an average readout of a population of cells, which normally consisted of anywhere from hundreds to millions of cells. Although such measurements provided meaningful qualitative interpretations, the quantitative details and response dynamics were observed. In addition, such measurements made it difficult to understand how an individual cell integrates signaling information in order to elicit its response and most important, how individual cells respond to a stimulus by choosing between several potential responses (Elowitz, Levine et al. 2002; Rosenfeld, Young et al. 2005; Batchelor, Loewer et al. 2009). More recently, with the improvement of quantitative measurement techniques such as microscopy in parallel with the application of computer simulations has made it possible to understand signal processing dynamics of individual cells. New methods have also made it possible to generate quantitative response profiles over a full spectrum of stimulus concentrations (dose-response) and temporal response profiles. This has allowed

researchers to describe different types of response outputs that cells employ as individuals as well as in their population (Lahav, Rosenfeld et al. 2004; Nachman, Regev et al. 2007; Locke and Elowitz 2009). For example; measuring the average dose-dependent activation of the MAPK in *Xenopus oocyte* cells over many cells (population) indicated a continuous increase in phosphorylation. However, the same measurements in single cells showed that activation of MAPK is an all or none response in which simply the proportion of cells with fully activated MAPK increase as a function of stimulus (Ferrell and Machleder 1998). In another example, the average measurement of p53 levels in mammalian cells lead researchers to believe there was no change in its levels. In contrary, the time dependent quantitative measurements of single cells indicated that p53 levels are dynamic and vary from cell to cell (Batchelor, Loewer et al. 2009).

Cells can generate different types of response outputs to a continuously variable stimulus (**Figure 11**). For example, with an increasing chemical stimulus concentration (dose-response), a biological response could be any of three basic types:

1. **Michaelian (or graded) response;** resembles the Michaelis-Menton enzymatic hyperbolic curve where, the initial response is high but reaches a plateau with increasing stimulus (**Figure 11a**) (Ferrell 1996; Huang and Ferrell 1996; Ferrell 1998; Ferrell and Machleder 1998).

2. **All-or-none (or switch-like) response;** a response type that resembles positively cooperative enzyme kinetics where the response increases as a positive exponent of the stimulus concentration. The result is that the dynamic range of response is narrower than that of a graded response. With larger exponents or Hill number (>2) responses resemble switches and are referred to as "switch-like" or "ultrasensitive" responses (**Figure 11b**).

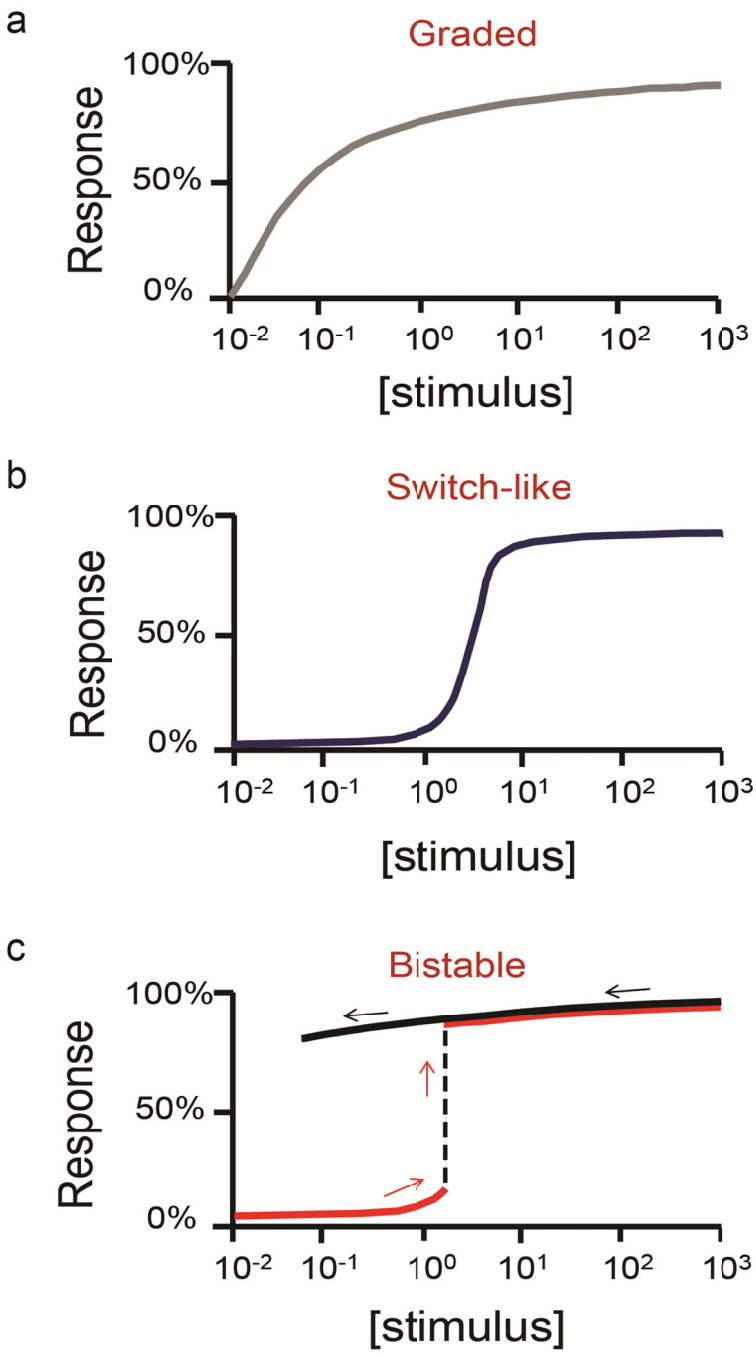

Figure 11. Different types of stimulus/response behaviors.
Graded (a), switch-like (b) and bistable (c) response curve types.

While an 81-fold increase in stimulus is required to drive a graded stimulus/response from 10% to 90% maximal response, ultrasensitive or switch-like responses require less than 81-fold stimulus increase (Goldbeter and Koshland 1981; Goldbeter and Koshland 1982; Koshland, Goldbeter et al. 1982; Ferrell 1996; Huang and Ferrell 1996).

3. **Bistable response;** When the stimulus-response exhibits two distinguishable stable states within a population, such as responding and non-responding states simultaneously, it is referred to as bistability (Ferrell 2002; Veening, Smits et al. 2008). In bistable systems, the range of stimulus concentration required to switch (or flip) the stimulus/response from its minimum to maximum is indistinguishable (Ferrell 1998; Ferrell and Xiong 2001; Ferrell 2002) (**Figure 11c**). Thus, the Hill coefficient is effectively infinite in bistable stimulus/ responses. Due to their discontinued and stable states from minimal to maximum, bistable responses are irreversible or often exhibit hysteresis or memory; a process wherein, the response remains in two distinct stable states even after removing the stimulus (Ferrell 1998; Ferrell 2002). Bistability has been invoked as a basic mechanism for irreversible cellular differentiation and cell cycle transitions. (Ferrell and Xiong 2001; Dubnau and Losick 2006; Veening, Smits et al. 2008; Yao, Lee et al. 2008).

1.9 Sources of ultrasensitivity

Ultrasensitivity can be generated by various mechanisms. Some of the earliest mechanisms that could give rise to ultrasensitivity were proposed by Goldbeter and Koshland in the 1980's, which included the 'Zero-order ultrasensitivity', 'multistep ultrasensitivity' and their combinations (Goldbeter and Koshland 1981; Goldbeter and Koshland 1982; Koshland, Goldbeter et al. 1982; Goldbeter and Koshland 1984).

Proposed mechanisms include;

1. Zero-order ultrasensitivity
2. Multistep ultrasensitivity or multistep sensitivity amplification
3. Inhibitor ultrasensitivity
4. Positive or double negative feedback loops

Switch-like responses could be achieved through one of the above mechanisms or even from a combination of them.

1.9.1 Zero-order ultrasensitivity

When a substrate is acted upon by two enzymes of opposing function (for example; a kinase and a phosphatase phosphorylating and de-phosphorylating respectively the same phosphorylation sites on a substrate) and if one enzyme is near saturation (activity is independent of substrate concentration), the level of modified substrate is very sensitive to a change in concentration of the other enzyme (Goldbeter and Koshland 1981; Goldbeter and Koshland 1982; Ferrell 1996). Even a small increase in the levels of the non-saturated enzyme will cause a large change in the net modified substrate, resulting in an ultrasensitive response (**Figure 12**). Zero-order ultrasensitivity was first experimentally (*in-vitro*) demonstrated with the cyclic interconversion of phosphorylase *a* (active form) and phosphorylase *b* (inactive form) catalyzed by the enzymes phosphorylase *b* kinase which phosphorylates its substrate (phosphorylase *b*) and phosphorylase *a* phosphatase which removes the phosphate its substrate (phosphorylase *a*) (Meinke and Edstrom 1991). Recently zero-order ultrasensitivity was suggested to regulate the threshold generation in order to create separate developmental domains in the *Drosophila embryo* (Melen, Levy et al. 2005). It was proposed that a zero-order mechanism translated graded MAPK activation into an all-or-none transition in the levels of Yan protein which is required to create boundary between developmental domains in the embryo. Yan phosphorylation by the MAPK results in its degradation. The cyclic network of Yan phosphorylation by the MAPK and its dephosphorylation by a yet unknown phosphatase was proposed to generate a sharp all-or-none threshold for the Yan levels (Melen, Levy et al. 2005).

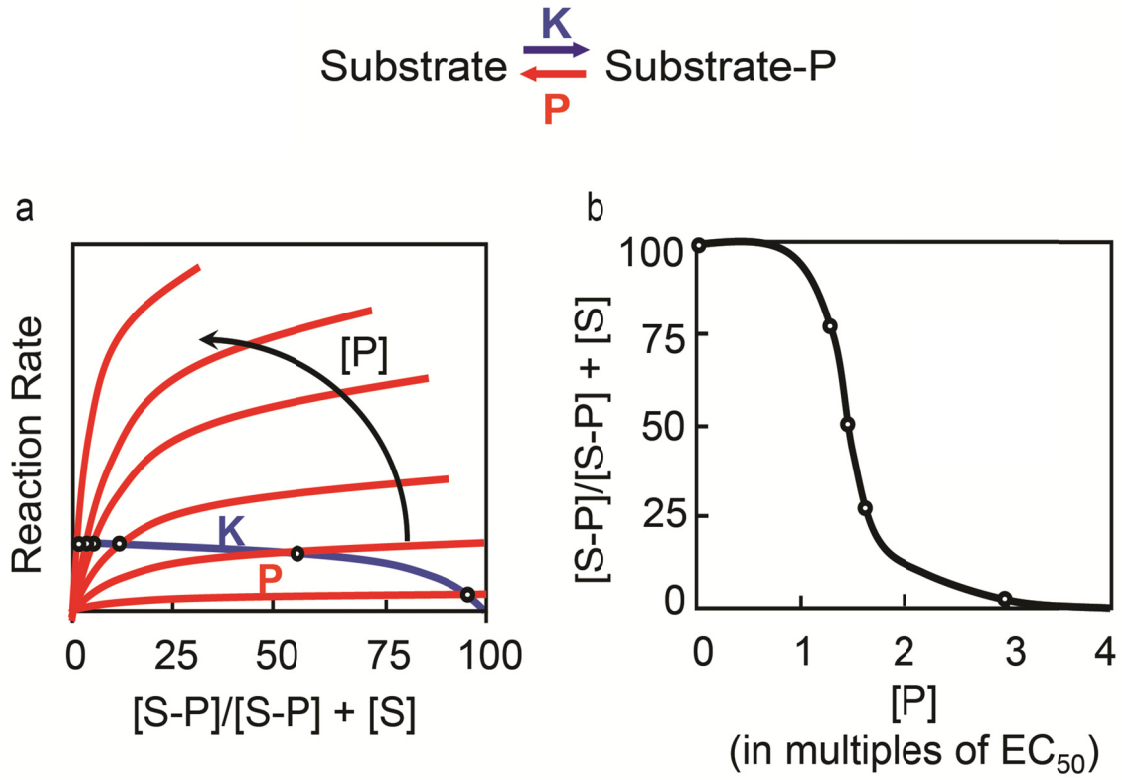

Figure 12. Graphical representation of zero-order ultrasensitivity.
In a simple circuit with a substrate being modified by two enzymes of opposing function, for example, phosphorylated by a kinase (K) and de-phosphorylated by a phosphatase (P). (a) Reaction rates/net phosphorylated substrate with a constant Kinase but increasing phosphatase concentrations ([P]). Circles at the intersection of kinase and phosphatase kinetics curve indicate the steady-state level in substrate phosphorylation. (b) Steady-state substrate phosphorylation states from 'a' *vs* the increase in phosphatase concentration. The plot shows a huge change in the net substrate phosphorylation for a very small change in phosphatase concentration when both the enzymes are operating under zero-order condition. Source: (Goldbeter and Koshland 1981; Ferrell 1996).

1.9.2 Multistep ultrasensitivity

Goldbeter and Koshland also discussed the presence of multistep inputs through a cascade as a mechanism to generate ultrasensitivity (Goldbeter and Koshland 1984; Ferrell 1996; Huang and Ferrell 1996). Multistep being the source of ultrasensitivity was first observed in the effective appearance of cAMP in 5 different steps of the glycogen synthesis cascade, revealed in the classic studies of Krebs, Fisher, Cohen and others (Krebs and Fischer 1956). Signal transduction pathways consist of cascades with multistep enzyme modifications, thus raising potentials to generate ultrasensitive responses. The first experimental and theoretical description of ultrasensitivity in a highly conserved MAP kinase signaling cascade was provided by the studies of James Ferrell in the 1990s (Ferrell 1996; Huang and Ferrell 1996; Ferrell and Machleder 1998). In *Xenopus oocytes*, the activation of the MAP kinase Erk2 was observed to be cooperative with a Hill coefficient of 4 or 5 (Ferrell 1996; Huang and Ferrell 1996). A variation of the multistep ultrasensitivity, termed two-collision (or distributive mechanism) dual phosphorylation reactions are attributed in part to generate the ultrasensitivity in ERK2 (MAPK) activation by its upstream kinase (MAPKK) (Ferrell 1996; Huang and Ferrell 1996). In the distributive multistep process, the MAPKK phosphorylates one of the two sites on MAPK with a first collision, dissociates and the second site is phosphorylated with their second collision step. This second-order rate dependence translates into an ultrasensitive stimulus/response curve since the rate of conversion of single phosphorylated MAPK to doubly phosphorylated MAPK will increase as the square of the stimulus concentration (Ferrell 1996).

1.9.3 Inhibitor ultrasensitivity

In an ultrasensitive stimulus/response, the initial response is suppressed until a certain threshold stimulus concentration after which the response reaches maximum within a narrow range of stimulus concentration (Ferrell 1996). In the case of zero-order ultrasensitivity, such suppression is brought about by the action of an opposing enzyme. Similar suppression can also be brought about by the presence of a stoichiometric

inhibitor which soaks up some activity of the enzyme. One such example is the activation of Cyclin dependent kinases (CDK) during the cell cycle progression, the activity of which are controlled by the stoichiometric inhibitors (Ferrell 1996; Drapkin, Lu et al. 2009).

1.9.4 Positive or double negative feedback loops

The presence of a positive feedback or a double negative feedback loops in a signalling pathway can generate an ultrasensitive response (Ferrell 2002). If one step in a pathway is ultrasensitivity, the addition of a positive or double negative feedback further reduces the range of stimulus concentration thus sharpening the ultrasensitivity even to an extent that the responsive state becomes a separate and discontinued state, often referred to as 'Bistability'. Bistability produces two discontinuous states of a stimulus/response system. It could also create an irreversible state. Although most biochemical reactions and stimulus-responses are reversible, in certain cases, as that of cellular differentiation, the biological transitions are irreversible (Ferrell 2002). Similarly, cell cycle transitions from one phase to another are also irreversible. Such irreversible cellular response decisions are attributed to the presence of a positive feedback loop that generates bistability (Ferrell 2002). Bistability does not guarantee irreversibility of a stimulus/response but will always exhibit some degree of hysteresis or resistance to revert to the other state (Ferrell 2002; Angeli, Ferrell et al. 2004). But, if the feedback in the bistability is sufficiently strong, then the system might exhibit true irreversibility and might stay in one state indefinitely. Some of the examples for systems that exhibit bistability include; the Mos-mitogen activated p42 MAPK cascade in *Xenopus oocytes* where it controls the all-or-none type of oocyte maturation (Ferrell and Machleder 1998; Ferrell 2002). Bistability in p42 cascade is generated through a positive feedback (active p42 MAPK stimulates the accumulation of its upstream activator, the Mos oncoprotein) in combination with the inherent ultrasensitivity of p42 activation (from the two collision distributive dual phosphorylation by the upstream kinase-MAPKK). Budding yeast cells commit to a new division cycle at the G1-S transition step in a bistable manner. This bistability and its irreversibility is created by a transcriptional positive feedback wherein G1 cyclins Cln1,2 activate their

own expression by inactivating Whi5, a repressor of SBF/MBF complex (Charvin, Oikonomou et al. 2010). A similar bistable switch is observed in mammalian cells at the G1-S transition of the cell cycle (Yao, Lee et al. 2008). Another bistable system from the oocytes is the activation of a c-Jun amino-terminal kinase (JNK) MAP kinase which is also embedded in a positive feedback loop in addition to the inherent switch-like activation of JNK in response to progesterone or hyperosmolar sorbitol stimuli (Ferrell 2002).

Thus, generally through competition and positive or negative feedbacks between component enzymes, circuits of signaling protein networks can precisely control the input – output stimulus/response(Goldbeter and Koshland 1981; Ferrell 1999; Ferrell and Xiong 2001; Tyson, Chen et al. 2003; Angeli, Ferrell et al. 2004; Brandman, Ferrell et al. 2005; Serber and Ferrell 2007; Tsai, Choi et al. 2008). By doing so, these circuits can produce different types of cellular responses such as graded, switch-like, bistable or oscillatory outputs in response to specific stimuli (**Figure 11**). For instance switching behavior is required for spatially defined differentiation of cells in response to morphogens. Switch-like, bistable and oscillatory circuits have also been shown to control accurate timing of cell cycle transitions (Nash, Tang et al. 2001; Holt, Krutchinsky et al. 2008; Skotheim, Di Talia et al. 2008; Yao, Lee et al. 2008; Charvin, Oikonomou et al. 2010).

1.10 Unknowns of the yeast mating response

Yeast mating response has been one of the most well-studied stimulus/response systems. It has been signal transduction researchers favorite system of choice mainly due to the feasibility of experiments and extensive understanding of this relatively simple model. Decades of research on the yeast mating response has identified almost all the components involved in this signaling pathway (Elion 2000; Bardwell 2005). Extensive genetic and physical interactions studies have helped to identify the components and map them as a pathway in the order of information processing. Although mating response is

one of the most studied pathways, little is understood about its dynamics. Even though the components and their interactions within the pathway are mapped, their *in-vivo* dynamics and its significance to the response outputs are still not well understood. The advent of new quantitative, single cell experiments and mathematical modeling methods are beginning to reveal the mysteries of this signaling pathway (Maeder, Hink et al. 2007; McClean, Mody et al. 2007; Paliwal, Iglesias et al. 2007; Slaughter, Schwartz et al. 2007; Yu, Pesce et al. 2008). Despite these advances, many questions remain to be answered about how information is transferred through the pheromone response MAPK pathway, including: 1), what is the dynamics of protein-protein interactions that mediate the transfer of chemical signals from one protein to another during signaling?; 2), how do cells interpret and integrate the spatio-temporal gradients of the pheromone secreted by the opposite mating partner both as single cells and in a population?; 3), what are the types of response outputs generated to varying pheromone concentrations?; 4), what is the evolutionary significance of such responses? Furthermore, scaffold proteins are common in signaling pathways and are believed to tether the appropriate signaling components together for efficient signal transduction. Scaffolds are generally considered to maximize signaling efficiency and specificity by passively increasing the local concentration of signaling proteins (Pawson and Scott 1997; Burack and Shaw 2000; Pawson and Nash 2003). In mating response, although Ste5 scaffold is essential, its active role in signal processing is not well understood. For instance; how does it bring about signal amplification and specificity in the MAPK cascade? In other words, how does it regulate the input-output stimulus/response behaviors of the mating system? Recently the Ste5 scaffold was paradoxically shown to inhibit the mating response (Bhattacharyya, Remenyi et al. 2006). Why does a molecule, purportedly serving the role of increasing signaling efficiency, in fact seem to decrease it? Does it actively participate in any way to regulate the mating stimulus/response types? Because of the void in dynamics and with a possibility of addressing some of the above exciting questions, my doctoral thesis goals became to study the *in-vivo* signaling dynamics of yeast mating MAP kinase signaling and to understand the regulatory circuits that determine the cellular response outputs to pheromone.

1.11 Our approach

Understanding protein–protein interactions have become a crucial component of efforts to define gene function, the information flow and organization of biochemical networks and the actions of perturbations or stimuli on these networks. Among various methods to study protein-protein interactions, the protein-fragment complementation assay (PCA) is a method that allows insights beyond the static representations towards understanding the *in-vivo* dynamics of protein interaction networks.

In the PCA strategy *in-vivo* protein–protein interactions are measured by fusing each of the proteins of interest to two fragments of a 'reporter' protein that has been rationally dissected into two fragments using protein-engineering strategies (Johnsson and Varshavsky 1994; Pelletier and Michnick 1997; Pelletier, Campbell-Valois et al. 1998; Michnick, Remy et al. 2000) (**Figure 13**). If the two proteins of interest bind to each other, the reporter protein fragments are brought into proximity, which allows them to fold together into the native three-dimensional structure and reconstitutes its activity. PCAs have been created with a variety of reporter proteins which provides for different types of readouts depending on the desired application. PCAs have been developed based on a number of reporter proteins, including murine dihydrofolate reductase (DHFR) (Pelletier and Michnick 1997; Pelletier, Campbell-Valois et al. 1998; Remy and Michnick 1999; Remy, Wilson et al. 1999; Remy and Michnick 2001), glycinamide ribonucleotide transformylase (Michnick, Remy et al. 2000), aminoglycoside kinase (Michnick, Remy et al. 2000), hygromycin B kinase (Michnick, Remy et al. 2000), TEM1 β-lactamase (Galarneau, Primeau et al. 2002; Spotts, Dolmetsch et al. 2002; Wehrman, Kleaveland et al. 2002), green fluorescent protein (GFP) (Ghosh, Hamilton et al. 2000) and its variants (Hu, Chinenov et al. 2002; Remy and Michnick 2004; Remy and Michnick 2004; Manderson, Malleshaiah et al. 2008), firefly (Luker 2004), Renilla (Kaihara, Kawai et al. 2003; Paulmurugan and Gambhir 2003; Stefan, Aquin et al. 2007) and Gaussia luciferases (Remy and Michnick 2006).

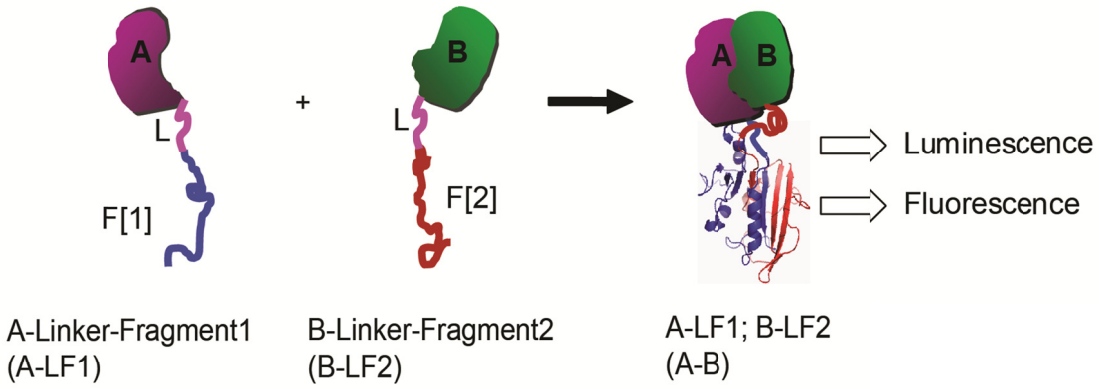

Luminescence : human Renilla Luciferase (Rluc) PCA
- highly sensitive
- Reversible
- Dynamic

Fluorescence : Yeast Enhanced Yellow Fluorescent Protein (Venus) PCA
- precise localization of protein complexes
- non-reversible
- trap transient interactions

Figure 13. Schematic of Protein fragment complementation assay (PCA) strategy.
A reporter enzyme is rationally dissected into two fragments and each fragment is fused to each of the two proteins of interest (ex. A and B) separated by a flexible 10 amino acids linker. When two proteins interact the fragments re-fold into functional enzyme, the activity of which can be directly measured as a readout for protein-protein interactions. The bottom text indicates the unique features of two PCAs based on *Renilla luciferase* enzyme and *yeast enhanced Yellow fluorescent protein* (Venus).

We were interested in understanding the *in-vivo* dynamics within a protein interaction network and its significance to the input-output stimulus/response behaviors. We employed yeast mating response as a prototypical example for our study. Because of the powerful genetic, biochemical and cell biological techniques that can be applied to yeast, studying their signaling dynamics and cellular response decisions should provide insights into the mechanisms by which other eukaryotic cells generate various responses to environmental signals. To this end we utilized multidisciplinary approaches including but not limited to genetic, biochemical, *in-vivo* and *in-vitro* assays to study protein-protein interaction dynamics. We used microscopic methods to visualize protein interactions within living cells and to carry out single cell analysis of cellular decision responses. In order to gain quantitative and mechanistic understanding of the signal processing we resorted to computational modeling in combination with the experimental methods.

1.12 Overview of the findings

Our attempts to understand signaling dynamics lead to novel discoveries in the signaling transduction mechanisms of yeast mating response (Chapters II, III and IV). We discovered a central mechanism in the mating signaling that is a variant of 'zero-order ultrasensitivity' first proposed by Goldbeter and Koshland that precisely controls the stimulus response outputs (Chapter II). We observed that in response to pheromone yeast cells exhibit a switch-like mating decision and that this stimulus/response behavior is generated early in the signaling through a simple competition between a kinase (Fus3) and a phosphatase (Ptc1) for the multiple phosphorylation sites of their substrate (Ste5). This switch-like response allows cells to ignore spurious pheromone concentrations and respond only at meaningful concentrations where the mating is most likely to be successful. In the process, we also established a very active role, otherwise thought to have a passive function, for the scaffold protein Ste5 directly regulating the switch-like mating decision. The findings also lead us to understand the unique mechanisms that the signal transduction pathways have evolved to amplify the initial signal in order to filter

out weak or noisy signals (Chapter III). This initial priming of the signal is essential to maintain the physiologically relevant sensitivity to pheromone concentrations and to produce the sufficient amplitude of response. Finally, we also came to understand that yeast cells can integrate multiple stimuli through cross-talk of different signaling networks that allow them to prioritize their responses by controlling their sensitivities (Chapter IV). A part of the results and the insights obtained from these studies are published in a peer reviewed journal (Chapter II). The rest of the findings are submitted (Chapters III and IV). The overall study is sub-divided into three sections as discussed below in the order of their publication.

RESULTS

Chapter II: The scaffold protein Ste5 directly controls a switch-like mating decision in yeast

Mohan K. Malleshaiah[1*], Vahid Shahrezaei[3*], Peter S. Swain[4, 5, †] and Stephen W. Michnick[1, 2, †]. ***Nature,*** 2010 May 6; 465(7294):101-5. Epub 2010 Apr 18.

In the following article that was published in the journal *Nature*, we have systematically elucidated the molecular mechanism that underlies a 'switch-like' mating response decision in yeast. We demonstrate that switch-like behavior is controlled by a simple catalytic circuit composed of the kinase Fus3, phosphatase Ptc1 and their mutual substrate, the scaffold protein Ste5. Then by performing specific mutations of Ste5 phosphosites that are targeted by Fus3 and Ptc1, we demonstrate that the correct functioning of the circuit is essential to generate and maintain a robust switch-like mating response. A mathematical model based on ordinary differential equations and including only the three molecules produce behavior that resembles classic zero-order ultrasensitivity and predicts robust, switch like behavior. A robust response is required to assure that mating occurs in spite of variations in protein levels among individuals and it occurs over approximately an order of magnitude in concentration of proteins, typical for general variations observed for most proteins in yeast.

Author contributions

Mohan Malleshaiah	Designed and performed experiments. Analyzed both experimental and mathematical modeling results. Extensively wrote the manuscript.
Vahid Shahrezaei	Performed mathematical modeling and mainly analyzed its results. Wrote the manuscript.
Peter Swain	Analyzed mainly mathematical modeling results. Wrote the manuscript.
Stephen Michnick	Planning and general supervision. Wrote the manuscript.

The scaffold protein Ste5 directly controls a switch-like mating decision in yeast

Mohan K. Malleshaiah[1*], Vahid Shahrezaei[3*], Peter S. Swain[4, 5, †] and Stephen W. Michnick[1, 2, †]. ***Nature,*** 2010 May 6; 465(7294):101-5. Epub 2010 Apr 18.

One-sentence summary: Multiple phosphorylations of the scaffold protein Ste5 mediate a switch-like morphological response to mating pheromone in *S. cerevisiae* through a mechanism involving a novel and robust form of ultrasensitivity driven by competition between the kinase Fus3 and the phosphatase Ptc1 for four phosphosites of Ste5.

[1]Département de Biochimie
[2]Centre Robert-Cedergren, Bio-Informatique et Génomique
Université de Montréal
C.P. 6128, Succursale centre-ville
Montréal, Québec H3C 3J7, Canada

[3]Department of Mathematics
Imperial College London
South Kensington Campus
London SW7 2AZ, UK

[4]Department of Physiology
McGill University
3655 Promenade Sir William Osler
Montréal, Québec H3G 1Y6, Canada

[5]Centre for Systems Biology at Edinburgh
University of Edinburgh
Edinburgh EH9 3JD
Scotland, UK

* These authors contributed equally to this work.
† Authors for correspondence

2.1 Abstract

Evolution has resulted in numerous innovations that allow organisms to maximize their fitness by choosing particular mating partners, including secondary sexual characteristics, behavioral patterns, chemical attractants, and corresponding sensory mechanisms (Darwin 1871). The haploid yeast *Saccharomyces cerevisiae* select their mating partners by interpreting the concentration gradient of pheromone secreted by potential mates through a network of Mitogen Activated Protein (MAP) kinase signaling proteins (Jackson and Hartwell 1990; Elion 2000). The mating decision in yeast is an all-or-none, or switch-like, response that allows cells to filter weak pheromone signals, thus avoiding inappropriate commitment to mating by responding only at or above critical concentrations when a mate is sufficiently close (Paliwal, Iglesias et al. 2007). The molecular mechanisms that govern the switch-like mating decision are poorly understood. Here, we show that the switching mechanism arises from a competition between the MAP kinase Fus3 and a phosphatase Ptc1 for control of the phosphorylation state of four sites on the scaffold protein Ste5. This competition results in a switch-like dissociation of Fus3 from Ste5 that is necessary to generate the switch-like mating response. Thus, the decision to mate is made at an early stage in the pheromone pathway and occurs rapidly, perhaps to prevent the loss of the potential mate to competitors. We argue that the architecture of the Fus3-Ste5-Ptc1 circuit generates a novel ultrasensitivity mechanism, which is robust to variations in the concentrations of these proteins. This robustness helps assure that mating can occur despite stochastic or genetic variation between individuals. The role of Ste5 as a direct modulator of a cell-fate decision expands the functional repertoire of scaffold proteins beyond providing specificity and efficiency of information processing (Pawson and Scott 1997; Burack and Shaw 2000). Similar mechanisms may govern cellular decisions in higher organisms and be disrupted in cancer.

Key words: Evolution, Mate selection, Scaffold, Ultrasensitivity, Zero-order competition, Signaling dynamics, etc.

2.2 Introduction and results

The two haploid forms of *S. cerevisiae* '*MAT***a**' and '*MAT*α' secrete a-factor and α-factor pheromones respectively, which bind to pheromone-specific receptors and activate a canonical MAP kinase cascade (Fig. 1a). Cells respond by differentiating into several morphological states depending on the local concentration of pheromone. At a critical concentration, the majority differentiates into shmoos; a pre-fusion state in which two cells of opposite mating type become close enough to form diploid cells (Erdman and Snyder 2001; Paliwal, Iglesias et al. 2007; Hao, Nayak et al. 2008) (Fig. 1a-b and Supplementary Fig. 2). At any concentration of pheromone, different morphological phenotypes co-exist, but shmooing is an all-or-none response (Paliwal, Iglesias et al. 2007) (Fig. 1b and Supplementary Fig. 3). It is not known how switch-like shmooing is generated, but activation of the MAP kinase Fus3 is switch-like, suggesting that the switch is generated upstream or in the MAPK cascade (Hao, Nayak et al. 2008) (Supplementary Fig. 4).

Disrupting the interaction between Fus3 and Ste5 using a $Ste5^{ND}$ mutant surprisingly relieves an inhibition of the mating response (Bhattacharyya, Remenyi et al. 2006) and is sufficient to destroy switch-like shmooing (Fig.1c). Hence, we reasoned that the switch could be generated by modulating this interaction. $Ste5^{ND}$ has a disrupted 'Fus3 docking motif' (FDM) preventing its binding to Fus3 (Bhattacharyya, Remenyi et al. 2006). With $Ste5^{ND}$, the activation of Fus3 becomes graded and, fitting a Hill function to data of Fig. 1b-c, we observe a Hill coefficient of ≈ 9 for *wildtype versus* 1 for $Ste5^{ND}$ (Supplementary Figs. 3 & 4). The Fus3 homologue Kss1 does not contribute to switch-like shmooing (Hao, Nayak et al. 2008) (Supplementary Figs. 4, 5 & 6).

Direct measurement of the steady-state levels of the Fus3-Ste5 complex showed a switch-like dissociation of the complex over the same range of α-factor concentrations for which shmooing occurred (Hill coefficient of 6; EC_{50} of 0.15 μM) (Figs. 2a and 1b).

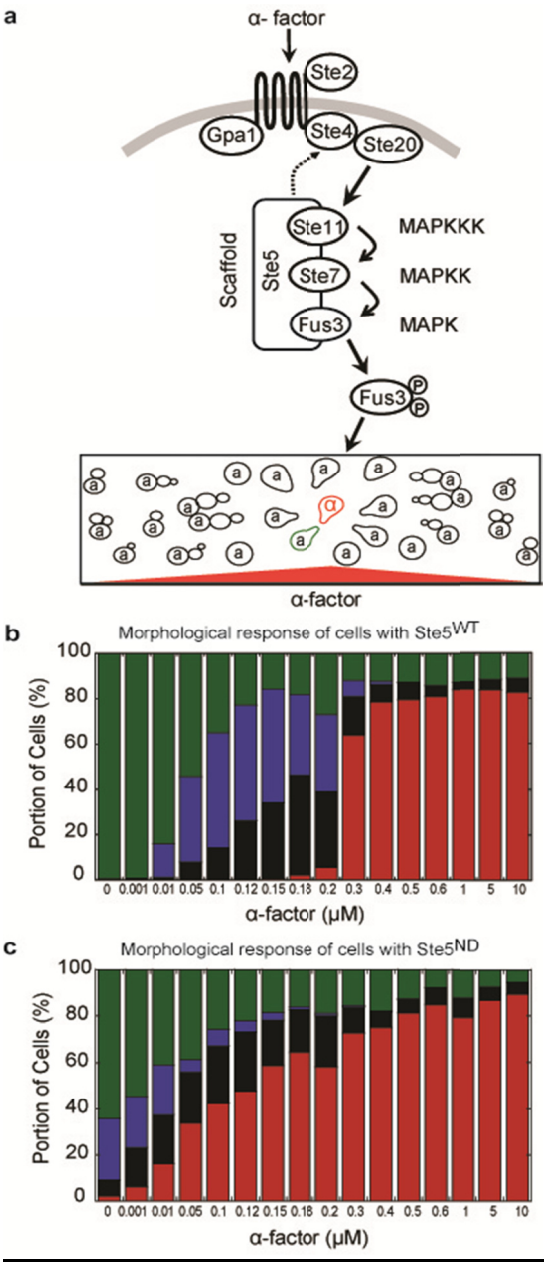

Figure 1. Switch-like shmooing in yeast requires the Fus3-Ste5 interaction.
(a) In *MAT*a cells, α-factor pheromone activates a MAPK cascade that generates phosphorylated, active Fus3, which dissociates from Ste5 and phosphorylates downstream targets to mediate mating. Lower panel: A *MATα* cell (red) secretes α-factor. Surrounding *MAT*a cells display different morphologies determined by the α-factor concentration sensed. The *MAT*a cell sensing a critical concentration of α-factor (green) "shmoos" and mates with the *MATα* cell. The fraction of different morphologies observed in *MAT*a *ste5*Δ cells expressing either *wildtype* Ste5 ($Ste5^{WT}$) (b) or $Ste5^{ND}$ mutant (c). Morphologies: axial (green) or bipolar (blue) budding, arrested (black) and shmooing (red).

We measured the levels of the Fus3-Ste5 complex using a Protein-fragment Complementation Assay (PCA) based on *Renilla reniformis* (Rluc) luciferase as a reporter that detects interactions among proteins expressed endogenously without significantly altering their binding kinetics (Stefan, Aquin et al. 2007) (Supplementary Fig. 7; see Supplementary Information). The Hill coefficient for our PCA results (≈ 6) is smaller than that of the single cell response (≈ 9; Supplementary Fig. 3), partly because the assay measures an average over a population of cells (Ferrell and Machleder 1998). For the $Ste5^{ND}$ strain, we observed a weak, although not zero, signal for all concentrations of α-factor. The switch-like decision also occurs rapidly: the steady-state level of the Fus3-Ste5 complex is invariant after 2 minutes of treatment with pheromone (Supplementary Figs. 8 and 18).

How is the dissociation of the Fus3-Ste5 complex modulated? Dephosphorylation of T287, a substrate of Ste5-bound Fus3, partially relieves inhibition of the mating response (Bhattacharyya, Remenyi et al. 2006). We hypothesized that full relief and dissociation of the Fus3-Ste5 complex could require dephosphorylation of other sites. On Ste5, we identified three potential MAPK phosphorylation sites within a peptide (Ste5_pep2; residues 214-334) that binds to Fus3 with the same affinity as Ste5 and contains T287 (Bhattacharyya, Remenyi et al. 2006) (Fig. 2b). In an *in vitro* kinase assay, Ste5 peptides (Ste5_pep2) in which all but one of the putative phosphosites were mutated to a non-phosphorylatable form were phosphorylated by Fus3 (Supplementary Fig. 9). Further, the switch-like dissociation of Fus3 from Ste5 requires the kinase activity of Fus3 (Fig. 2a) as the Fus3-Ste5 complex is independent of α-factor with kinase-dead Fus3 (K42R).

The steady-state levels of the Fus3-Ste5 complex are linearly proportional to the number of phosphosites on Ste5. We systematically mutated each phosphosite on Ste5 to be non-phosphorylatable (Ser to Ala and Thr to Val) individually (-1PS) and as combinations of two (-2PS), three (-3PS) and all four sites (-4PS). We then measured the Fus3-Ste5 complex using Rluc PCA in cells either not treated or treated with α-factor (1 μM) (Fig. 2c and Supplementary Fig. 10b). Our results demonstrate that α-factor can

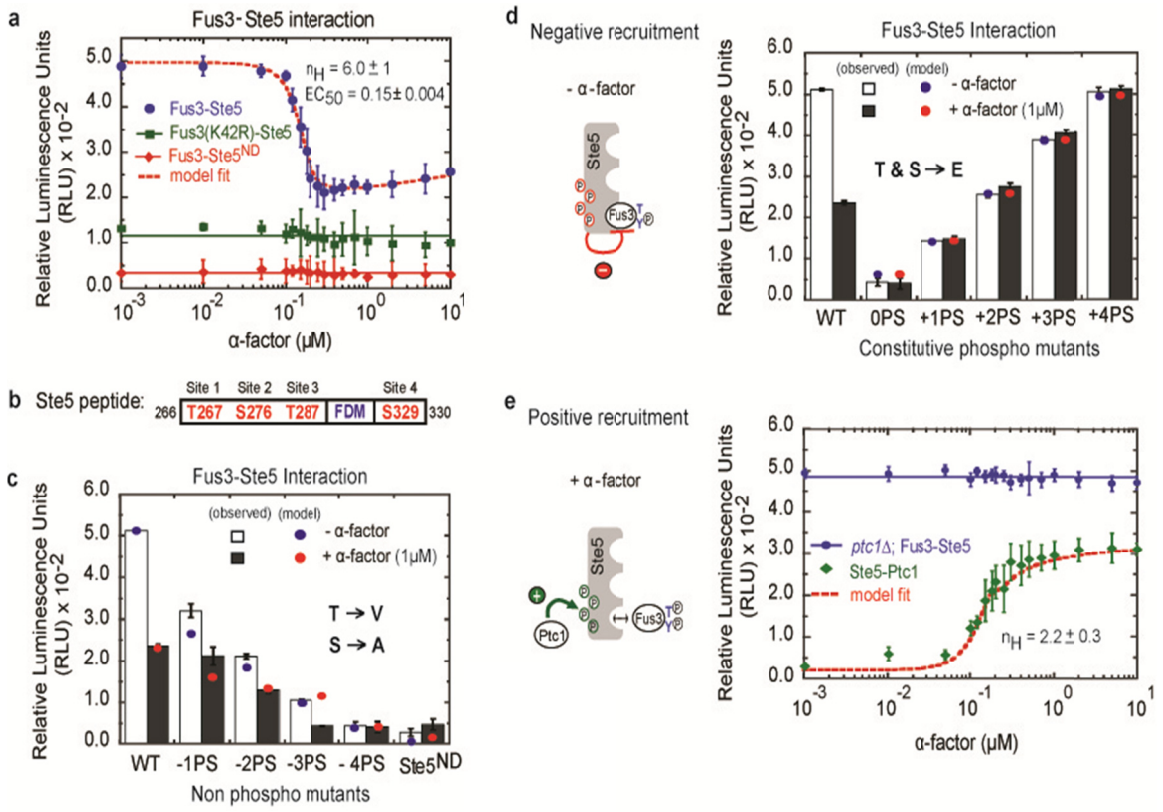

Figure 2. Levels of the Fus3-Ste5 complex are determined by the Ste5 phosphorylation state.

(a) Steady-state levels of Fus3-Ste5, Fus3-Ste5ND and kinase-dead Fus3 (K42R)-Ste5 *versus* α-factor. Model fit: dashed line. (b) Ste5 peptide (residues 226-230) with four MAPK phosphorylation sites. (c) Levels of Fus3-Ste5 complex with non-phosphorylatable phosphosites on Ste5. WT: *wildtype* Ste5. Red and blue circles: model predictions. (d) As in (c), for pseudo-phosphorylated Ste5. Red and blue circles: model fits. (e) Fus3-Ste5 (*ptc1*Δ cells) and Ste5-Ptc1 (*wildtype* cells) interactions *versus* α-factor. Dashed red line: model fit. Hill coefficient (n_H), EC_{50} and their errors were calculated from fits to a Hill equation. Error bars are s.e.m. (n=3).

Induce a change in the steady-state levels of Fus3-Ste5 complex if any individual site on Ste5 can be phosphorylated and that complete mutation of all sites (-4PS) is equivalent to $Ste5^{ND}$. Dephosphorylation of all four sites is therefore sufficient to disrupt the Fus3-Ste5 complex and result in full activation of Fus3 (Supplementary Fig. 10c). Pseudo-phosphorylation of the four sites (Ser or Thr to Glu mutations) as individuals (+1PS), combinations of two (+2PS), three (+3PS) and all four sites (+4PS) in 0PS (or -4PS) protein suggests that Fus3 dissociates from Ste5 and becomes fully active only when all four sites are dephosphorylated (Fig. 2d and Supplementary Figs. 11 & 12). If there is at least one pseudo-phosphorylation of Ste5, Fus3 is never fully activated and is unaffected by α-factor (Supplementary Fig. 11c). Our phosphosite mutants did not affect the expression or cellular localization of Ste5 (Supplementary Figs. 13 & 14).

We next postulated that Ste5 must be dephosphorylated by a phosphatase whose activity at Ste5 is α-factor dependent. We identified a serine/threonine phosphatase Ptc1 that is essential for shmooing (Supplementary Fig. 15). Ptc1's interaction with Ste5 is α-factor-dependent and the levels of the Fus3-Ste5 complex are independent of α-factor in a *ptc1Δ* strain (Fig. 2e). Deletion of Ptc1 substantially prevents shmooing and reduces activation of Fus3, while its over-expression enhances both (Supplementary Fig. 15b-c). Ptc1 acts neither indirectly through the MAPK Hog1, a known substrate (Warmka, Hanneman et al. 2001; McClean, Mody et al. 2007), nor directly through Fus3 (Supplementary Figs. 16 & 17).

Our results suggest that α-factor induces recruitment of Ptc1 to Ste5, dephosphorylation of Ste5, and the consequent dissociation of the Fus3-Ste5 complex within the same time-frame (Fig. 2e and Supplementary Fig. 18). I*n vitro,* Ptc1 was found to compete with Fus3 for the Ste5 phosphosites (Supplementary Fig. 19). Recruitment of Ptc1 occurs through a 4-residue motif (amino acids 277 to 280) on Ste5, within the same region as the phosphosites, that when mutated to alanine ($Ste5^{AAAA}$) prevents association of Ptc1 to Ste5 and, while not affecting Fus3-Ste5 binding, does prevent the dissociation of the Fus3-Ste5 complex with a concomitant loss of shmooing (Supplementary Figs. 20 & 21). In our phosphosite mutants of Ste5, changes in levels of the Fus3-Ste5 complex

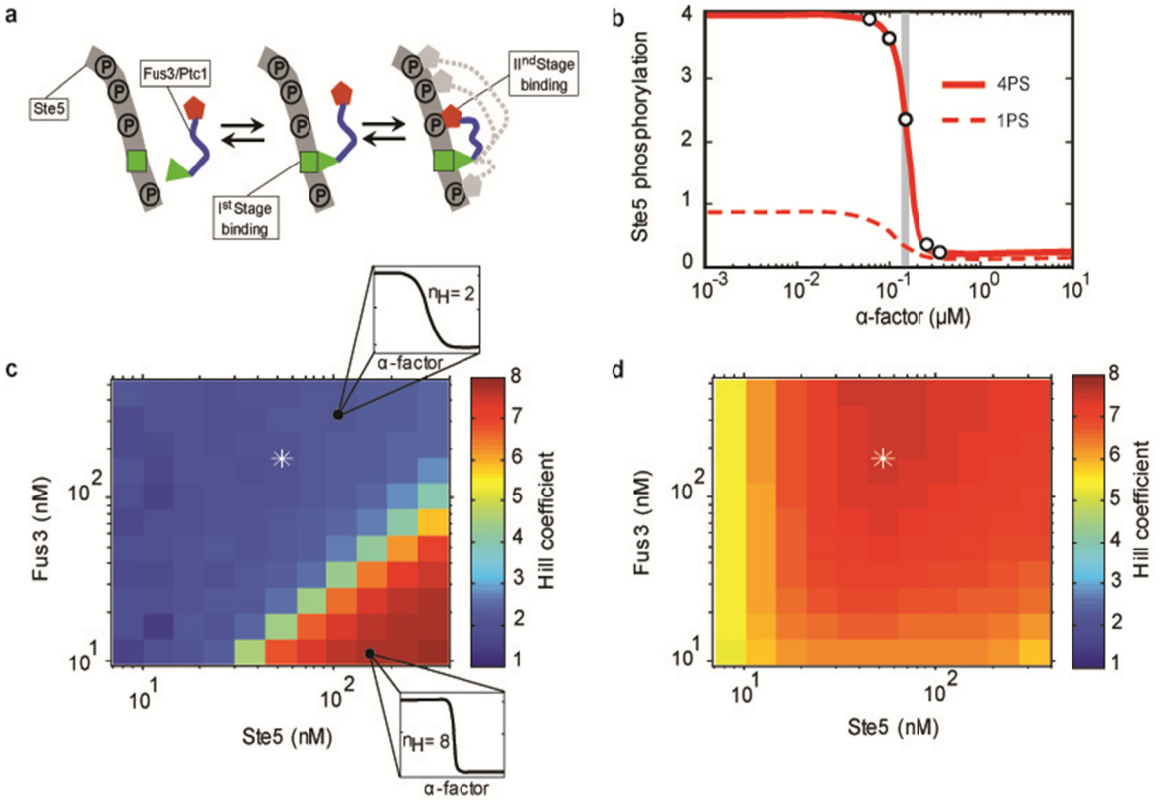

Figure 3. A novel form of ultrasensitivity explains the switch-like mating decision.
(a) Two-stage binding: Fus3 or Ptc1 first bind to their Ste5 docking sites (green) and then bind to individual phosphosites (red and gray enzyme domains). (b) Steady-state Ste5 phosphorylation (open circles) *versus* α-factor for Ste5 with four (solid) or one (dashed) phosphosites. Grey bar: threshold concentration of α-factor. (c) Predicted Hill coefficients for classic zero-order ultrasensitivity determined from Ste5 phosphorylation during α-factor doses-responses at fixed concentrations of Fus3 and Ste5 (insets).
Asterisk: physiological Fus3 and Ste5 concentrations. (d) As in (c) for full two-stage binding plus steric hinderance model of Supplementary Fig. 23b.

and the shmooing response were insensitive to either the presence or absence of Ptc1 (Supplementary Fig. 22).

To understand how recruitment of Ptc1 to Ste5 (with a Hill coefficient ≈ 2; Fig. 2e) and a change in the phosphorylation state of Ste5 generates a switch-like decrease in the levels of the Fus3-Ste5 complex (Hill coefficient > 6; Fig. 2a), we examined potential mechanisms by mathematical modeling with a reduced system of differential equations, including only Ste5, Ptc1, and Fus3 (Fig. 3).

Switching could be partially explained by 'steric hindrance': the competition between Fus3 and Ptc1 for the phosphorylation of the four phosphosites on Ste5 (Salazar and Hofer 2007). The linear relationship between the degree of Ste5 phosphorylation and its affinity for Fus3 (Fig. 2c-d) implies that the capacity of Fus3 to compete with Ptc1 is reduced as Ptc1 is recruited to Ste5. Consequently, the rate of dephosphorylation increases ultrasensitively with increasing concentrations of pheromone. However, the sharpness of the switch generated is not compatible with our data.

We propose a robust zero-order ultrasensitivity mechanism based on a novel 'two-stage' binding of Fus3 and Ptc1 to Ste5 that can generate sufficient switching when coupled to steric hindrance. In our model, the enzymes are locally saturated, or at `zero-order', because both Fus3 (Bhattacharyya, Remenyi et al. 2006) and Ptc1 must first bind to separate docking motifs on Ste5 and only then can bind to and catalyze transformations of the phosphosites (Fig. 3a & Supplementary Fig. 23). This two-stage binding causes the competition between Fus3 and Ptc1 to be mostly insensitive to their cytosolic concentrations: locally, at each Ste5, the enzymes are saturated because the ratio of the substrate (the phosphosites) to the enzymes can be 4:1 (Fig. 3a). With both enzymes working near saturation, the level of phosphorylated Ste5 is very sensitive to a change in concentration of either enzyme (Goldbeter and Koshland 1981; Ferrell 1996). When the concentration of pheromone reaches a threshold, a small increase in the levels of recruited Ptc1 will cause a large increase in unphosphorylated Ste5 because Fus3 is locally saturated and unable to compete with Ptc1, which is itself working near its

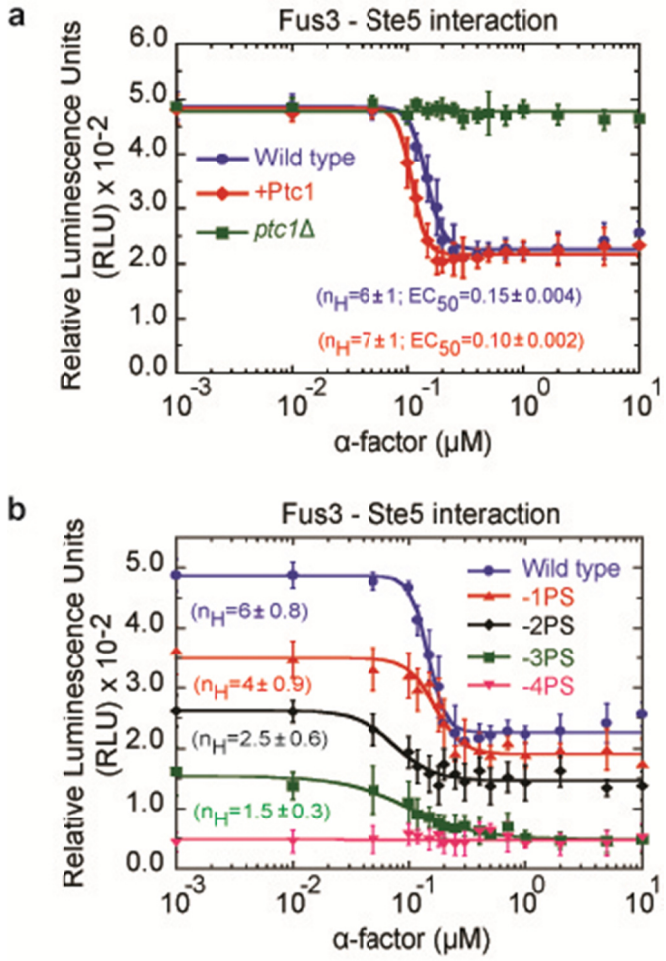

Figure 4. Experimental validations of model predictions.
(a) Changes in the steady-state levels of the Fus3-Ste5 complex with various Ptc1 concentration *in vivo*: *wildtype* (WT), knockout (*ptc1Δ*) and over-expression (+Ptc1).
(b) *In vivo* analysis of the steady-state levels of Fus3-Ste5 complex as a function of α-factor using single (-1PS: AbCD), double (-2PS: abCD), triple (-3PS: Abcd) or quadruple (-4PS: abcd) non-phosphorylatable mutants of Ste5. The Hill coefficient (n_H), EC_{50} and their errors are calculated from fits of the data to a Hill function (solid lines). Error bars are s.e.m. (n=3).

maximum rate (Supplementary Fig. 24). Consequently, there is a sharp, ultrasensitive drop in the level of Ste5's phosphorylation (Fig. 3b), reducing the affinity of Fus3 to Ste5 (Fig. 2c-d), and Fus3 undergoes a switch-like dissociation (Fig. 2a).

Our model predicts that the observed ultrasensitivity is generated by multi-site phosphorylation, two-stage binding, and steric hinderance. We examined each in turn. First, if there is only one phosphosite on Ste5, the enzymes are not locally saturated at each Ste5 (Supplementary Fig. 25a), and there is little steric hindrance of Ptc1 because Fus3 binds weakly to Ste5 (Fig. 2c). Consequently, the sharpness of the switch is reduced (Fig. 3b). Second, eliminating two-stage binding of Ptc1 and Fus3 to Ste5 can give classic zero-order ultrasensitivity (Goldbeter and Koshland 1981), but only at non-physiological concentrations of Ste5 (Fig. 3c). Finally, two-stage binding or steric hindrance alone will give a Hill coefficient of 4 to 5 (Supplementary Fig. 25b-c), but if we include both we obtain the high Hill coefficients consistent with our data at physiological and a wide range of Fus3 and Ste5 concentrations (Fig. 3d, Supplementary Fig. 26).

Consistent with the predictions of our model, we confirmed that the sharpness of the switch is robust to changes in the concentration of Ptc1 for both the binding of Fus3 to Ste5 and the fraction of cells that shmoo and that the sharpness of the Fus3-Ste5 interaction and the shmoo response is controlled by the number of active phosphosites (Fig. 4 and Supplementary Figs. 26 & 27).

We can speculate how the phosphorylation-dependent change in affinity of Ste5 for Fus3 occurs: either the negative charge of the phosphate groups on Ste5 or a known conformation change in a domain of Ste5 directly affects the binding of Fus3 (Nash, Tang et al. 2001; Serber and Ferrell 2007; Strickfaden, Winters et al. 2007; Good, Tang et al. 2009). Further, we need to understand how α-factor mediated binding of Ptc1 to the phosphosites on Ste5 is enhanced. Two possibilities are that upon its membrane recruitment, Ste5 undergoes conformation changes that increase the accessibility of the phosphosites to Ptc1 or simply that the local concentration of Ptc1 at Ste5 increases at the membrane (Elion 2000; Strickfaden, Winters et al. 2007). Finally, why are individual

cells with $Ste5^{ND}$ always found in one of the four morphological states? It is possible that there are other switches downstream of the Fus3-Ste5 switch, with thresholds that vary stochastically across a population of cells. Such variation is only revealed by the graded activation of Fus3 generated by $Ste5^{ND}$. While specific switching mechanisms are unknown, there is a precedent for feedback generating ultrasensitive and bistable responses (Peter and Herskowitz 1994; Paliwal, Iglesias et al. 2007; Strickfaden, Winters et al. 2007).

Multiple phosphorylation sites are common (Cohen 2000; Holmberg, Tran et al. 2002). As well as generating ultrasensitivity in cascades of enzymes (Ferrell and Machleder 1998), potentially allowing proofreading of substrates (Swain and Siggia 2002), and determining binding specificity(Nash, Tang et al. 2001; Lenz and Swain 2006), our results provide another function: generating robust, switch-like cellular decisions. Scaffold proteins are found in many eukaryotic signaling pathways, and scaffolded MAPKs are central to diseases including cancers, inflammatory disease, obesity, and diabetes (Hirosumi, Tuncman et al. 2002; Lawrence, Jivan et al. 2008). If similar mechanisms to the one we have discovered occur in mammalian signaling, they could prove to be important targets for therapeutic intervention.

2.3 Methods summary

Plasmid constructions, cloning and gene manipulations were performed using standard methods. The mathematical model was constructed using the *Facile* network compiler with a rule-based modeling scheme to generate a description of the model as a set of differential equations(Siso-Nadal, Ollivier et al. 2007). The model was integrated in Matlab (Mathworks, Nattick, Massachusetts) and parameters were fit using an efficient Markov chain Monte Carlo method(H. Haario 2006). Detailed experimental, modelling and simulation methods are described in Supplementary Information.

2.4 References

Bhattacharyya, R. P., A. Remenyi, et al. (2006). The Ste5 scaffold allosterically modulates signaling output of the yeast mating pathway. *Science* **311**(5762): 822-826.

Burack, W. R. and A. S. Shaw (2000). Signal transduction: hanging on a scaffold. *Curr Opin Cell Biol* **12**(2): 211-216.

Cohen, P. (2000). The regulation of protein function by multisite phosphorylation--a 25 year update. *Trends Biochem Sci* **25**(12): 596-601.

Darwin, C. (1871). The Descent of Man and Selection in Relation to Sex. London, John Murray.

Elion, E. A. (2000). Pheromone response, mating and cell biology. *Curr Opin Microbiol* **3**(6): 573-581.

Erdman, S. and M. Snyder (2001). A filamentous growth response mediated by the yeast mating pathway. *Genetics* **159**(3): 919-928.

Ferrell, J. E., Jr. (1996). Tripping the switch fantastic: how a protein kinase cascade can convert graded inputs into switch-like outputs. *Trends Biochem Sci* **21**(12): 460-466.

Ferrell, J. E., Jr. and E. M. Machleder (1998). The biochemical basis of an all-or-none cell fate switch in Xenopus oocytes. *Science* **280**(5365): 895-898.

Goldbeter, A. and D. E. Koshland, Jr. (1981). An amplified sensitivity arising from covalent modification in biological systems. *Proc Natl Acad Sci U S A* **78**(11): 6840-6844.

Good, M., G. Tang, et al. (2009). The Ste5 scaffold directs mating signaling by catalytically unlocking the Fus3 MAP kinase for activation. *Cell* **136**(6): 1085-1097.

H. Haario, M. L., A. Mira & E.Saksman. (2006). DRAM: Efficient adaptive MCMC. *Stat Comput* **16**: 339–354.

Hao, N., S. Nayak, et al. (2008). Regulation of cell signaling dynamics by the protein kinase-scaffold Ste5. *Mol Cell* **30**(5): 649-656.

Hirosumi, J., G. Tuncman, et al. (2002). A central role for JNK in obesity and insulin resistance. *Nature* **420**(6913): 333-336.

Holmberg, C. I., S. E. Tran, et al. (2002). Multisite phosphorylation provides sophisticated regulation of transcription factors. *Trends Biochem Sci* **27**(12): 619-627.

Jackson, C. L. and L. H. Hartwell (1990). Courtship in S. cerevisiae: both cell types choose mating partners by responding to the strongest pheromone signal. *Cell* **63**(5): 1039-1051.

Lawrence, M. C., A. Jivan, et al. (2008). The roles of MAPKs in disease. *Cell Res* **18**(4): 436-442.

Lenz, P. and P. S. Swain (2006). An entropic mechanism to generate highly cooperative and specific binding from protein phosphorylations. *Curr Biol* **16**(21): 2150-2155.

McClean, M. N., A. Mody, et al. (2007). Cross-talk and decision making in MAP kinase pathways. *Nat Genet* **39**(3): 409-414.

Nash, P., X. Tang, et al. (2001). Multisite phosphorylation of a CDK inhibitor sets a threshold for the onset of DNA replication. *Nature* **414**(6863): 514-521.

Paliwal, S., P. A. Iglesias, et al. (2007). MAPK-mediated bimodal gene expression and adaptive gradient sensing in yeast. *Nature* **446**(7131): 46-51.

Pawson, T. and J. D. Scott (1997). Signaling through scaffold, anchoring, and adaptor proteins. *Science* **278**(5346): 2075-2080.

Peter, M. and I. Herskowitz (1994). Direct inhibition of the yeast cyclin-dependent kinase Cdc28-Cln by Far1. *Science* **265**(5176): 1228-1231.

Salazar, C. and T. Hofer (2007). Versatile regulation of multisite protein phosphorylation by the order of phosphate processing and protein-protein interactions. *FEBS J* **274**(4): 1046-1061.

Serber, Z. and J. E. Ferrell, Jr. (2007). Tuning bulk electrostatics to regulate protein function. *Cell* **128**(3): 441-444.

Siso-Nadal, F., J. F. Ollivier, et al. (2007). Facile: a command-line network compiler for systems biology. *BMC Syst Biol* **1**: 36.

Stefan, E., S. Aquin, et al. (2007). Quantification of dynamic protein complexes using Renilla luciferase fragment complementation applied to protein kinase A activities in vivo. *Proc Natl Acad Sci U S A* **104**(43): 16916-16921.

Strickfaden, S. C., M. J. Winters, et al. (2007). A mechanism for cell-cycle regulation of MAP kinase signaling in a yeast differentiation pathway. *Cell* **128**(3): 519-531.

Swain, P. S. and E. D. Siggia (2002). The role of proofreading in signal transduction specificity. *Biophys J* **82**(6): 2928-2933.

van Drogen, F., V. M. Stucke, et al. (2001). MAP kinase dynamics in response to pheromones in budding yeast. *Nat Cell Biol* **3**(12): 1051-1059.

Warmka, J., J. Hanneman, et al. (2001). Ptc1, a type 2C Ser/Thr phosphatase, inactivates the HOG pathway by dephosphorylating the mitogen-activated protein kinase Hog1. *Mol Cell Biol* **21**(1): 51-60.

Supplementary Information is linked to the online version of the paper at www.nature.com/nature.

Acknowledgements The authors would like to thank James Ferrell Jr., Wendell Lim, Madan Babu, Edi Stefan, Christian Laundry, François-Xavier Campbell-Valois and Emmanuel Levy for useful comments on the manuscript; Wendell Lim and Jackie Vogel for providing plasmids and yeast strains. This work was supported by grants from the CIHR (MOP-GMX-152556) and a Canada Research Chair in Integrative Genomics to S.W.M. P.S.S. was supported by a Canada Research Chair in Systems Biology and currently holds a Scottish Universities Life Sciences Alliance Professorship also in Systems Biology.

Author contributions MKM and SWM planned and designed experiments; MKM performed experiments; VS and PSS planned and VS performed the mathematical modelling; MKM, SWM, VS, and PSS analyzed the results; MKM, VS, PSS and SWM wrote the manuscript.

Author Information The authors declare no competing financial interests. Correspondence should be addressed to either S.W.M. or P.S.S. Requests for materials should be addressed to S.W.M.

2.5 Supplementary Figures

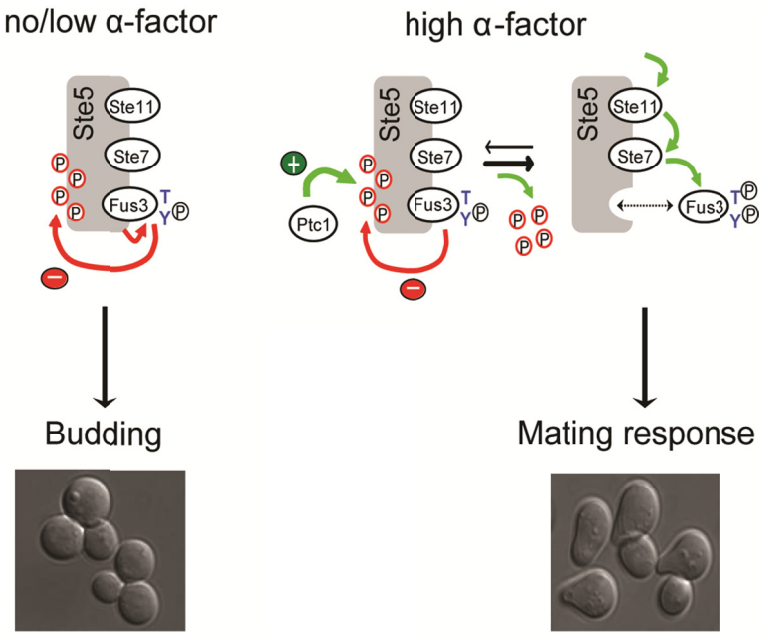

Supplementary figure 1. Schematic for the direct control of mating decision by the Ste5 scaffold.
Although essential for mating, Fus3 through binding to Ste5 is initially inhibitory. Multisite phosphorylation of Ste5 by partially active Fus3 increases the association of Fus3 with Ste5. In the absence of a mate or when two potential mates are far from each other, these phosphorylations of Ste5 prevent release and full activation of Fus3 and hence shmooing. High α-factor concentrations indicating the presence of a suitable mate induces dephosphorylation of Ste5 and allows Fus3 to become fully activated and induce shmooing and eventually mating.

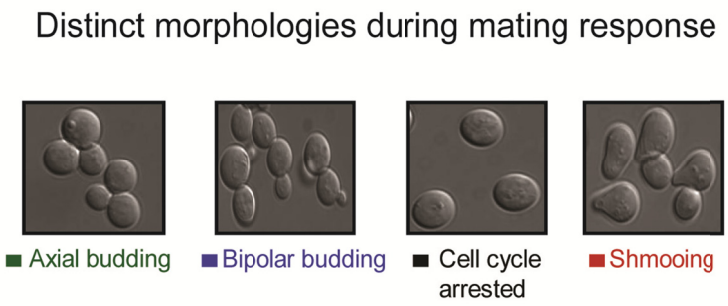

Supplementary figure 2. Different morphological phenotypes observed during yeast mating response.
Axial budding, bipolar budding, cell cycle arrested and shmooing.

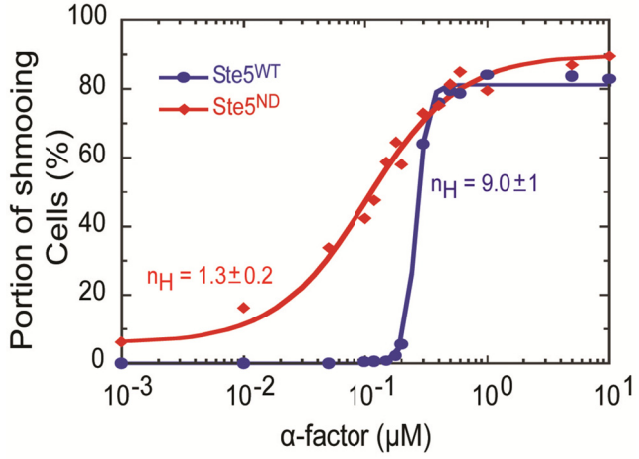

Supplementary figure 3. Fus3 interaction with Ste5 is essential for the switch-like shmooing response.
α-factor-dependent changes in the fraction of shmooing cells in *ste5*Δ strain expressing either $Ste5^{WT}$ (blue circles) or $Ste5^{ND}$ (red diamonds). Assuming the final shmooing response is driven by underlying molecular events, the data for shmooing cells from Figure 1b & c were fit to a Hill function. The Hill coefficients were calculated from the fit.

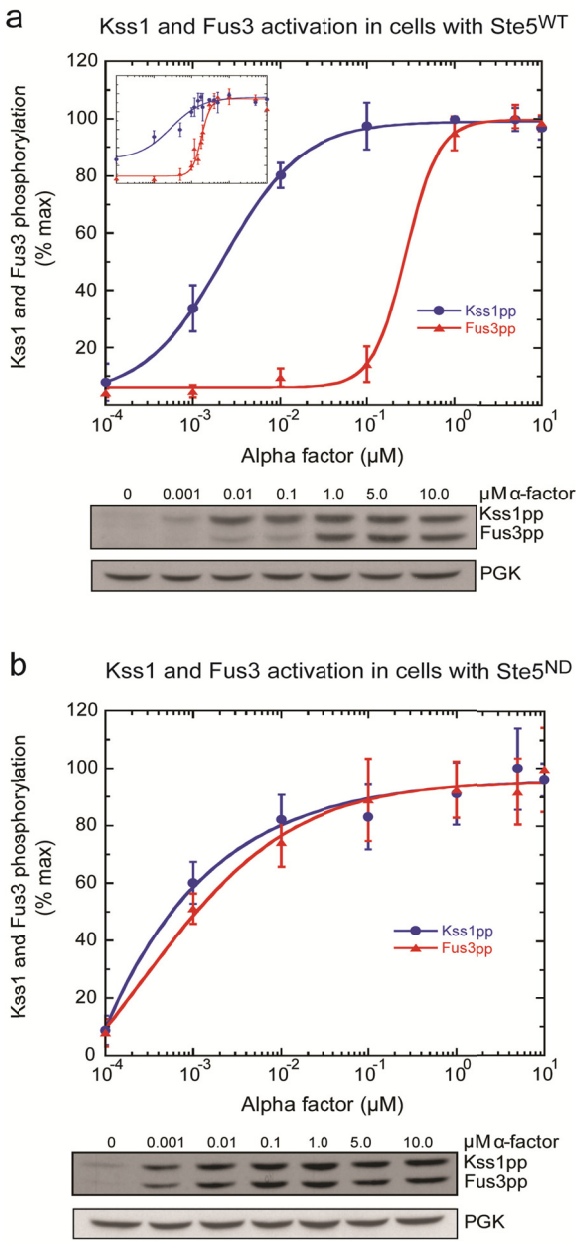

Supplementary figure 4. MAP kinase Kss1 and Fus3 activation levels during mating response.

The activation levels of MAPKs (Fus3 and Kss1) measured in *ste5*Δ cells expressing $Ste5^{WT}$ (a) and $Ste5^{ND}$ (b) after stimulating with the indicated concentration of α-factor. Fully active MAPK levels (dually phosphorylated) were detected by western blotting using anti-phospho MAPK antibody. Inset curves in (a) shows similar activation profiles for Fus3 and Kss1 when measured with many more concentrations in the dynamic range of response. Error bars indicate the standard errors of the mean from three experiments. Phosphoglycerate kinase (PGK) expression level was used as loading controls.

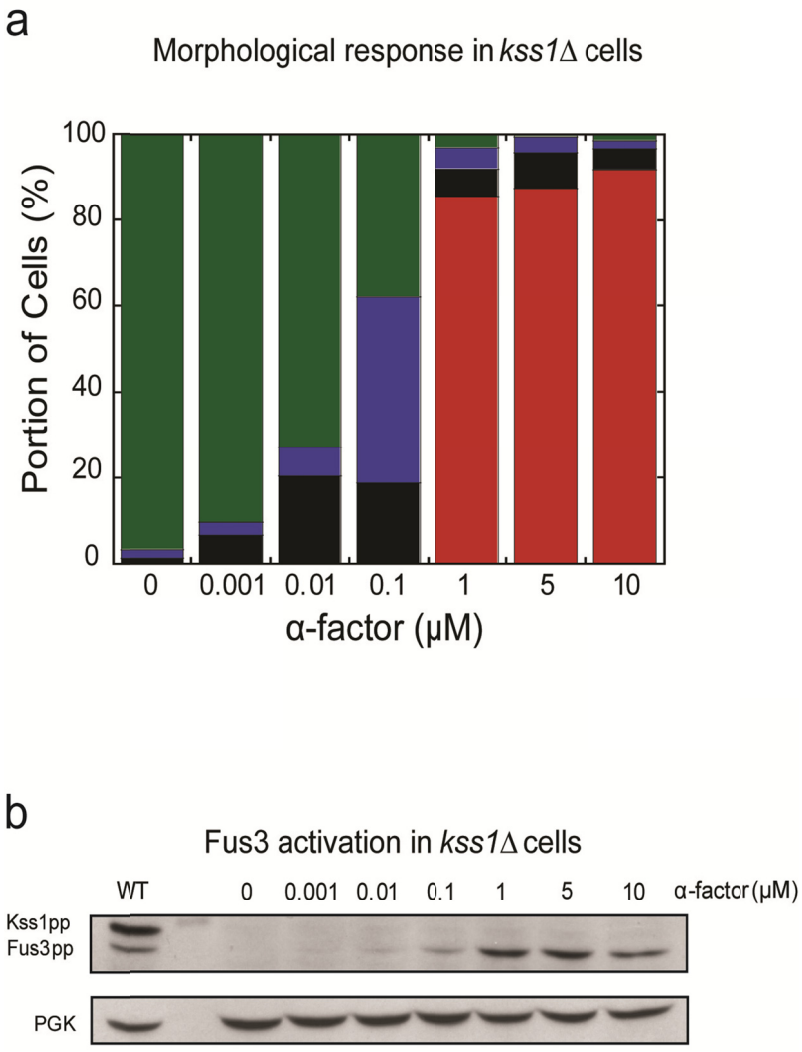

Supplementary figure 5. Mating response in *kss1*Δ cells.
(a) Mating response in *kss1*Δ cells. In a dose response to α-factor, cells lacking Kss1 respond similar to wild type cells with no detectable difference in shmooing ability.
(b) Active Fus3pp levels detected by Western blotting using anti-phospho MAPK antibody. Kss1 does not interfere with the switch-like activation of Fus3pp in an α-factor dose response.

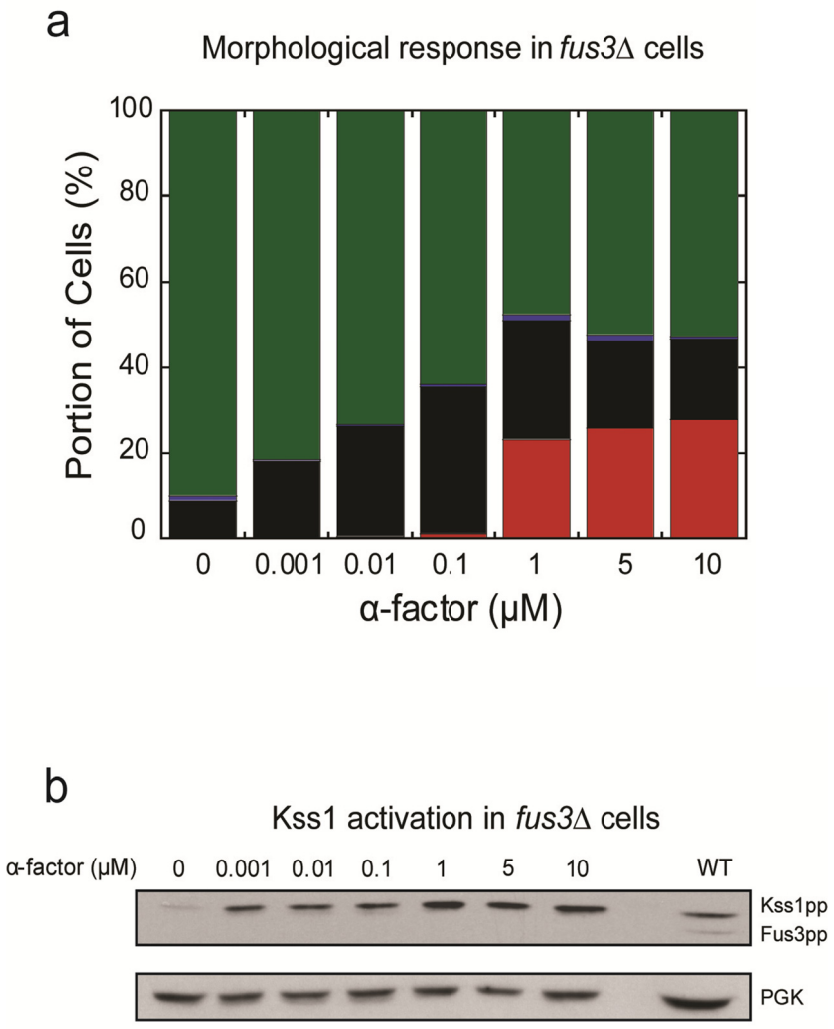

Supplementary figure 6. Mating response in *fus3*Δ cells.
(a) Mating response in *fus3*Δ cells. In a dose response to α-factor, cells lacking Fus3 have a severely diminished shmooing ability. Bipolar budding is lost and very minimal shmooing was observed. The homologue of Fus3 MAPK, Kss1, which is also activated during the pheromone response, partially compensates for the role of Fus3.
(b) Active Kss1pp levels detected by Western blotting using anti-phospho MAPK antibody. Kss1pp exhibits a linear rather than a switch-like activation. Thus, Fus3 is essential for the mating response along with the switch-like differentiation of shmooing cells.

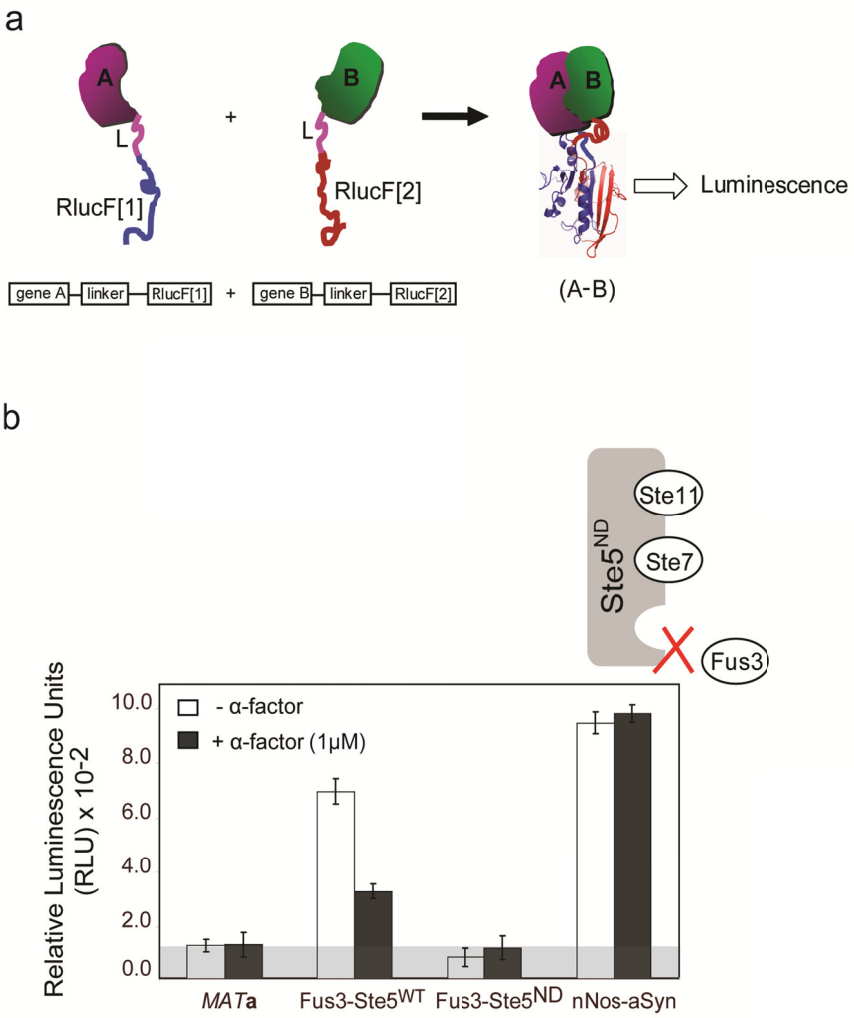

Supplementary figure 7. Renilla luciferase PCA (Rluc PCA) to measure the dynamics of protein-protein interactions.

(a) Schematic model with hypothetical proteins to show the PCA strategy. PCA fragments F[1] and F[2] (in this study Rluc F[1] and Rluc F[2]) are fused to the C-terminus of the proteins of interest A and B respectively and preceded by a 10 amino acid flexible linker $((GGGGS)_2)$. Only when the two proteins interact do the fragments of the PCA reporter (e. g. Renilla luciferase) fold into a fully functional enzyme. The activity of the functional enzyme is measured as the readout for a direct protein-protein interaction between A and B. For Rluc PCA, bioluminescence is measured using a luminometer as a function of protein-protein interaction.

(b) Specificity of Rluc PCA for the Fus3 and Ste5 interaction. Using Rluc PCA, a specific interaction between Fus3 and Ste5 can be measured along with its dynamics under α-factor treated conditions. With a mutant of Ste5 ($Ste5^{ND}$) that is known to disrupt its interaction with Fus3, the PCA signal reduces to background. Two PDZ domains that are known to form heterodimers (nNOS and aSyn) are used as a positive control for Rluc PCA and as a negative control for the dynamics induced as a function of α-factor.

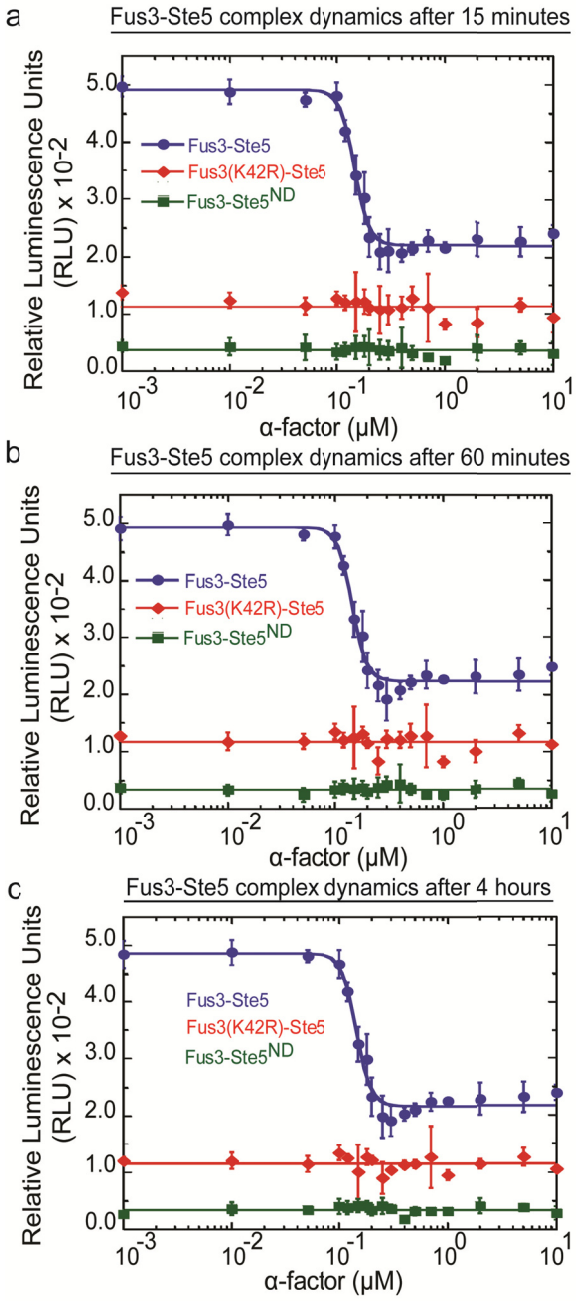

Supplementary figure 8. Steady state levels of the Fus3-Ste5 complex at different time points during the mating response.
The steady-state levels of the Fus3-Ste5 complex at 15 minutes (a), 60 minutes (b) and 4 hours (c) after treatment with the indicated concentration of α-factor in a dose response. Errors indicate the standard error of the mean from three experiments.

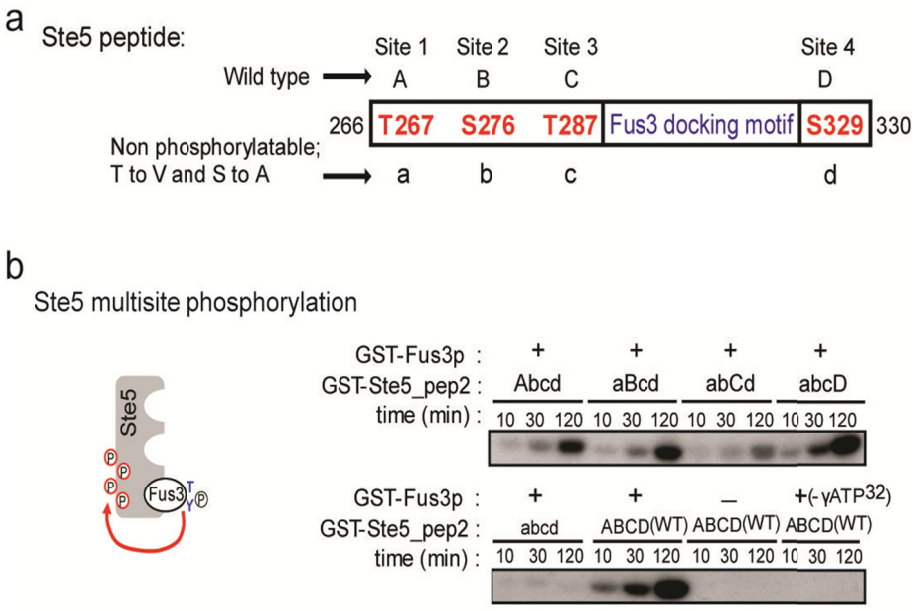

Supplementary figure 9. Partially active Fus3 phosphorylates all four Ste5 phosphosites in an *in-vitro* kinase assay.

(a) A map of the Ste5 peptide (residues 266 to 330) showing the four MAPK phosphorylation sites and their mutations. Phosphosites 1, 2, 3 and 4 are *wildtype* (A, B, C, or D) or non-phosphorylatable mutants (a, b, c, or d) with either threonine (T) to valine (V) or serine (S) to alanine (A).

(b) Schematic: Ste5-bound, partially activated Fus3 phosphorylates all four phosphosites. Autoradiography of phosphorylation on individual phosphosites of Ste5 using the indicated form of GST-Ste5_pep2 (residues 214 to 334) in the presence or absence of GST-Fus3p and γ^{32}P-ATP.

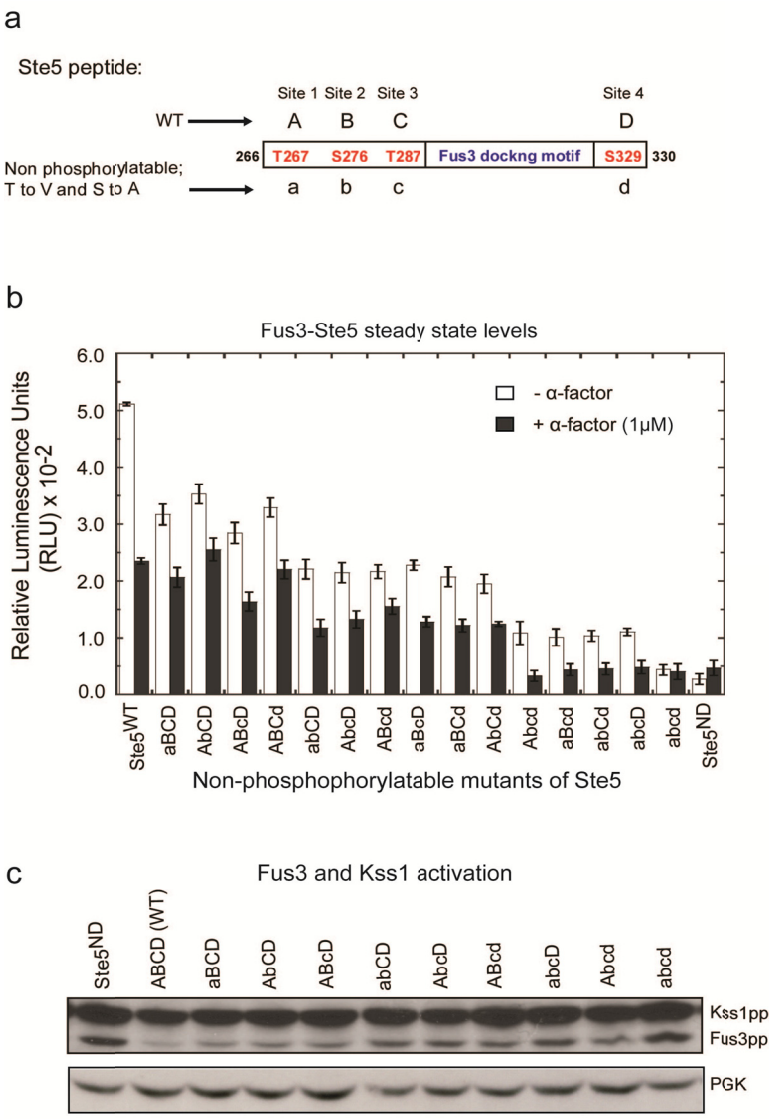

Supplementary figure 10. Non-phospho mutants of Ste5 and their effect on the Fus3-Ste5 steady-state.

(a) A map of a Ste5 peptide (residues 266 to 330) showing the location of the consensus MAPK phosphorylation site (S/T-P) mutations. Phosphosites 1, 2, 3 and 4 are labeled as follows: wild type (WT): Capital A, B, C and D; non-phosphorylatable form: small a, b, c and d. To generate these mutations all threonines (T) were mutated to valine (V) and serines (S) to alanine (A).

(b) The effect of non-phosphorylatable mutations, either singly or in combinations of two, three or all four sites on the steady-state levels of the Fus3-Ste5 complex under non-treated and α-factor treated conditions.

(c) The activity levels of the MAPKs Fus3 and Kss1 detected by Western blotting with the non-phosphorylatable mutants. Fus3 activation increase with an increase in the number of non-phosphorylatable sites while there is no change in the activation of Kss1. Cells were treated with 1 μM of α-factor for 15 minutes.

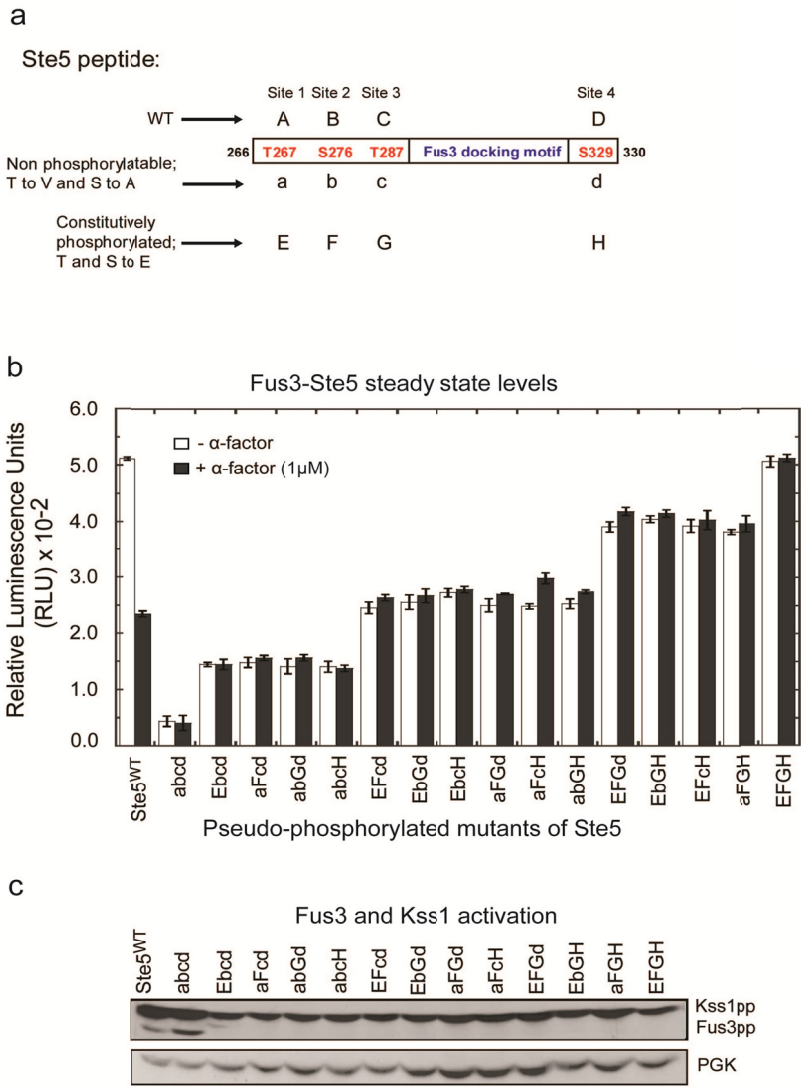

Supplementary figure 11. Constitutively active phosphosite mutants of Ste5 and their effect on the steady-state levels of the Fus3-Ste5 complex.

(a) A map of a Ste5 peptide showing the location of the consensus MAPK phosphorylation site (S/T-P) mutations. Phosphosites 1, 2, 3 and 4 are labeled as follows: wild type (WT): capital A, B, C and D; non-phosphorylatable form: small a, b, c and d; constitutively phosphorylated form: capital E, F, G and H. To generate constitutively active phosphosites both threonines and serines were mutated to glutamic acid (E).

(b) The effect of constitutively phosphorylated mutations, either singly or in combinations of two, three or all four sites on the steady-state levels of the Fus3-Ste5 complex under non-treated and α-factor treated conditions.

(c) The activation levels of the MAPKs Fus3 and Kss1 detected by Western blotting with the indicated pseudo-phosphorylation mutants. Fus3 activation is completely prevented if there is a single pseudo-phosphorylated site. While there is no change in the activation levels of Kss1.

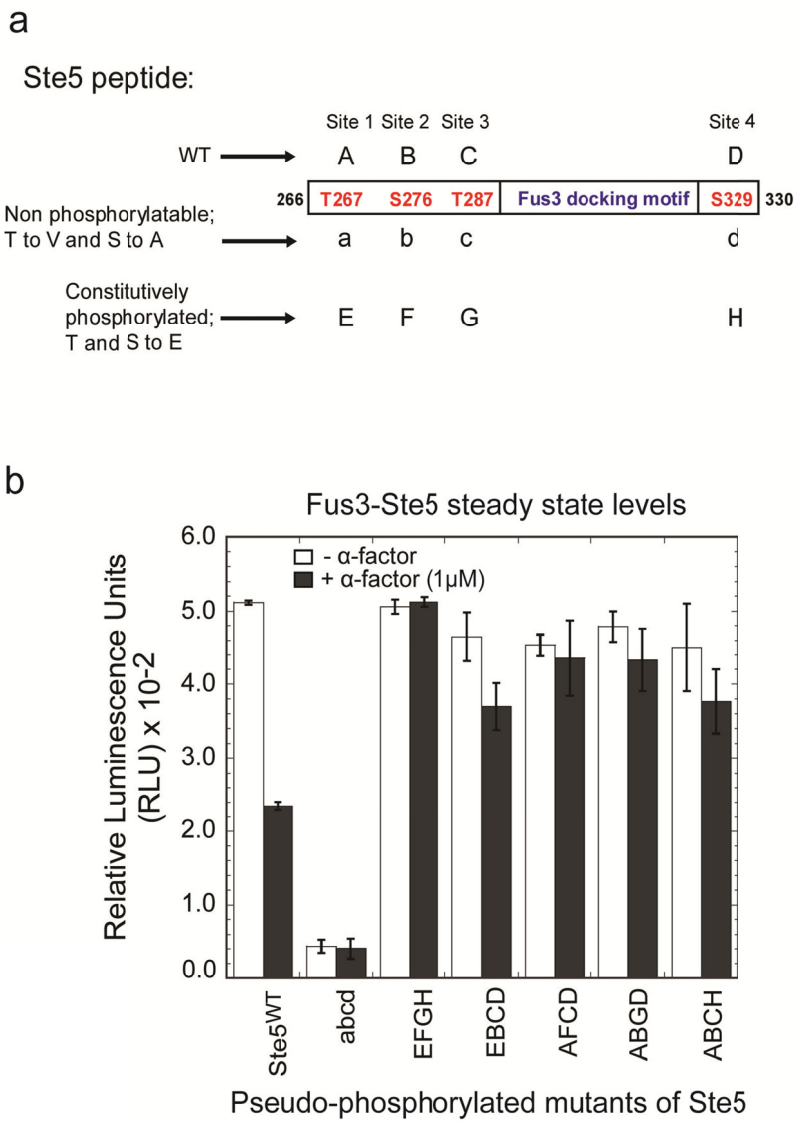

Supplementary figure 12. Constitutively active phosphosite mutants of Ste5 on single sites and their effect on the steady-state levels of the Fus3-Ste5 complex.
(a) A map of a Ste5 peptide showing the location of the consensus MAPK phosphorylation site (S/T-P) mutations.
(b) The effect of the constitutively pseudo-phosphorylated mutations at single sites on Ste5 on the steady-state levels of the Fus3-Ste5 complex under non-treated and α-factor treated conditions.

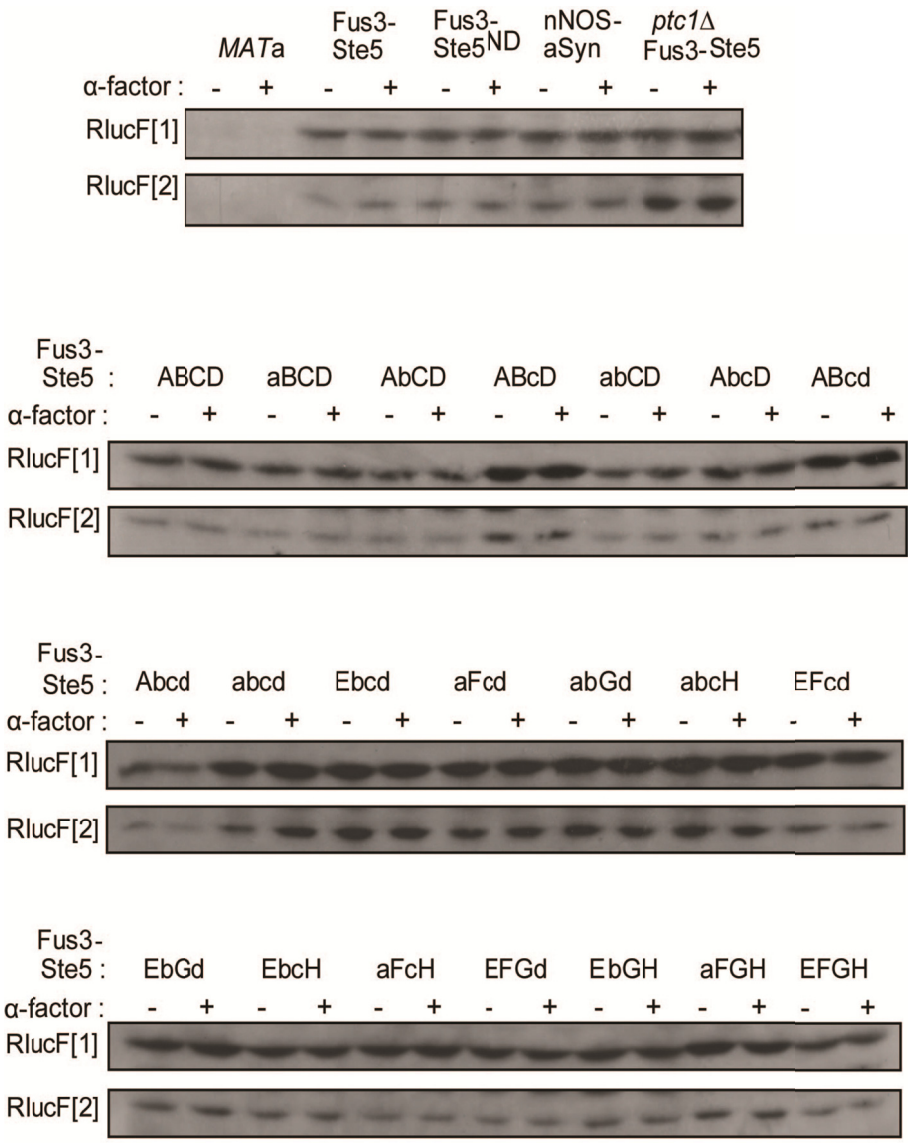

Supplementary figure 13. Protein expression of genes fused with Rluc PCA fragments.

Normal expression levels of genes fused with Rluc fragments including the variants of Ste5 were checked using the specific antibodies for Rluc F[1] and Rluc F[2]. Expression levels were checked without and with α-factor treatment (1 μM) as indicated. As seen, the fusion of Rluc fragments does not interfere with the normal expression levels of the genes modified in the study.

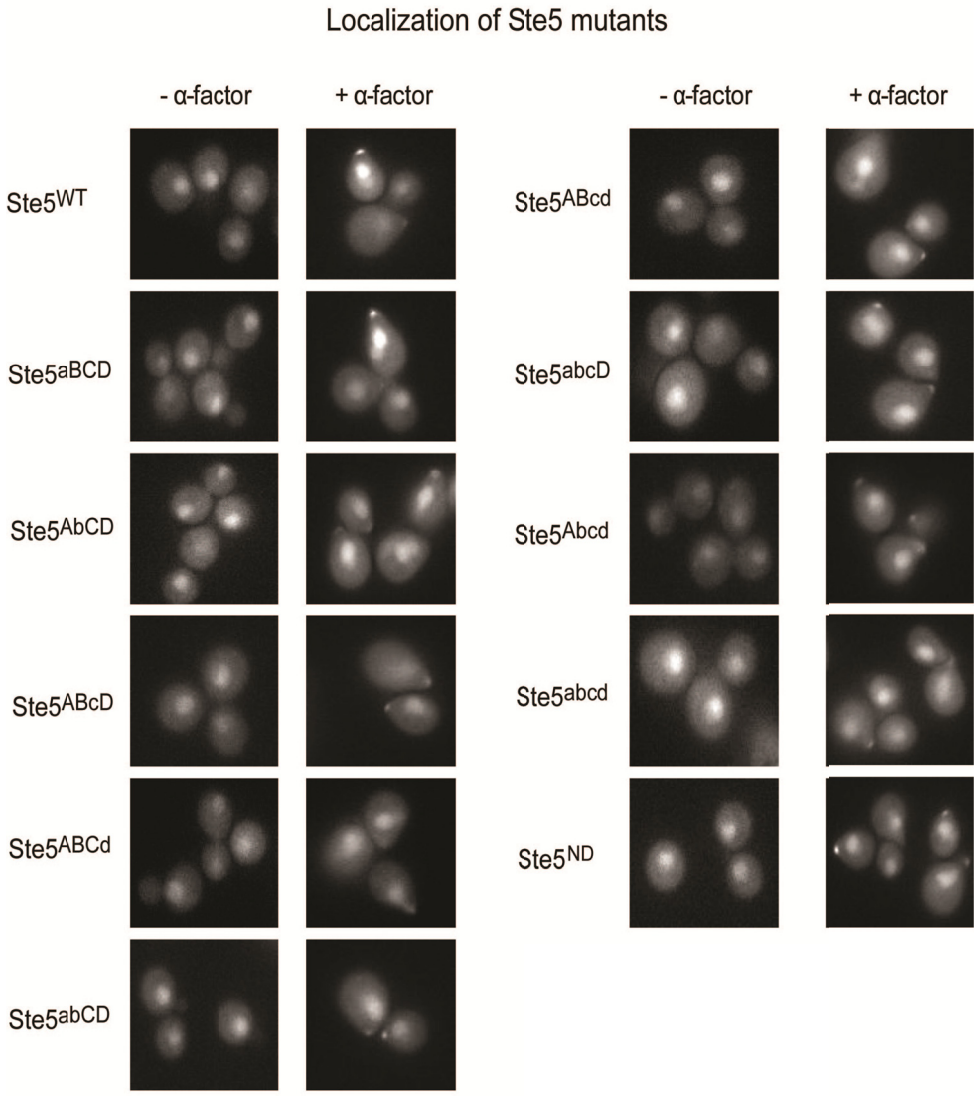

Supplementary figure 14. Cellular location of the variants of Ste5 with phosphosite mutations.

Fluorescence microscopy images showing the location of the indicated form of Ste5 under non-treated and α-factor treated (1μM) conditions. Consistent with previously work, variants of Ste5 are predominantly in the nucleus in the absence of stimulus and localize to 'shmoo tip' in the presence of α-factor. Thus, the phosphosite mutations do not seem to affect the normal localization and expression of Ste5, but selectively regulate its interaction with Fus3.

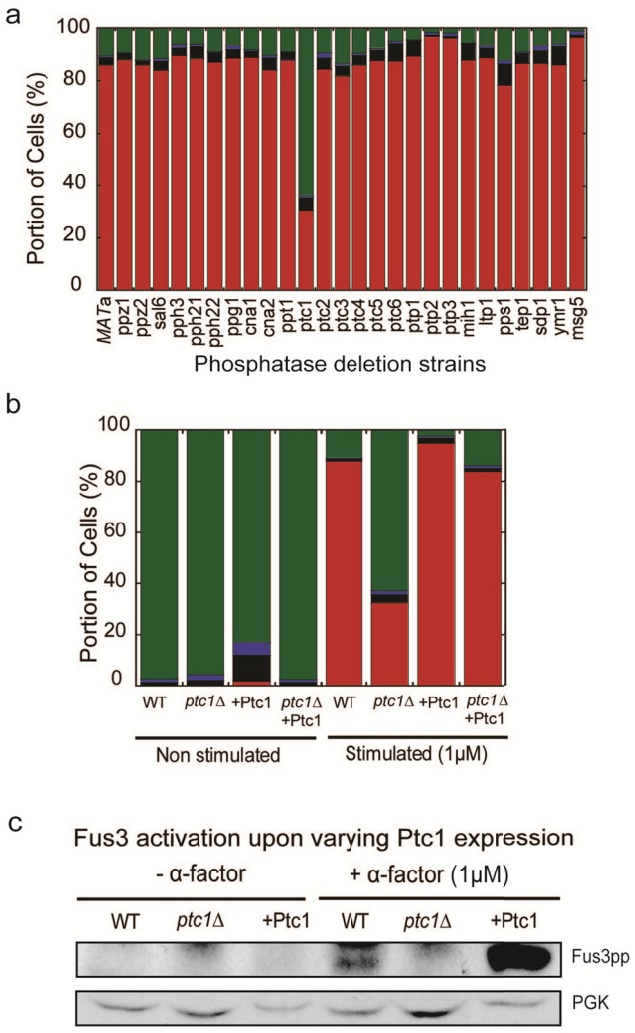

Supplementary figure 15. Serine/threonine phosphatase Ptc1 is required for the mating response.

(a) Morphological responses in a collection of *MAT***a** strains deleted individually for one of the 26 phosphatase genes in yeast in comparison to *wildtype* (*MAT***a**) cells.

(b) The fraction of cells with different phenotypes in strains with *wildtype* (WT), knockout (*ptc1*Δ), over-expression of Ptc1 (+Ptc1) and *ptc1*Δ with plasmid-borne Ptc1 (*ptc1*Δ + Ptc1). In +Ptc1 and *ptc1*Δ + Ptc1 strains, Ptc1 was constitutively expressed from a plasmid under the control of the *ADH* promoter. Cells were stimulated with 1 μM α-factor for 3 to 4 hours. Phenotypes are color-coded: axial budding (green), bipolar budding (blue), cell cycle arrested (black) and shmooing (red).

(c) Fus3pp levels detected using anti-phospho MAPK antibody in cells lacking Ptc1 (*ptc1*Δ) and over-expressing Ptc1 (+*PTC1*) in comparison to wild type (WT) *MAT***a** under non-treated and α-factor treated conditions. To over-express Ptc1, it was expressed constitutively under the ADH promoter from a plasmid (pMM60). The absence of Ptc1 reduced the activation of Fus3 and its over-expression substantially increased the levels of active Fus3.

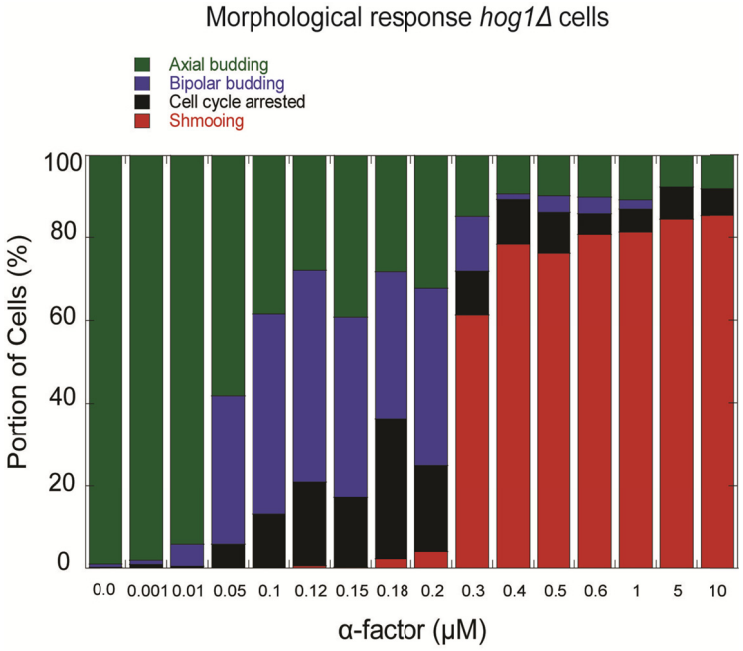

Supplementary figure 16. The shmooing response is insensitive to the deletion of Hog1.

Histograms showing the portion of different morphologies observed with increasing concentrations of α-factor in *hog1Δ* cells. Results show that the response with *hog1Δ* cells is identical to *wild type* cells (Figure 1b). Although the fraction of bipolar budding and cell cycle arrested cells are slightly reduced, the switch-like dose response of shmoo formation to pheromone is insensitive to the deletion of Hog1.

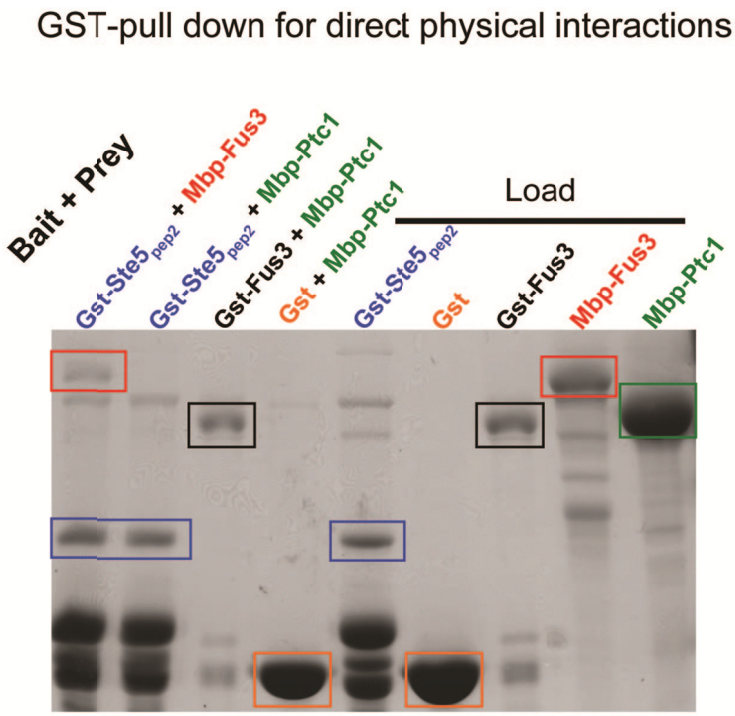

Supplementary figure 17. A physical interaction of Ptc1 with Fus3 and Ste5.
In vitro binding experiment using GST-pull down to test for the interaction of Ptc1 with Fus3 and Ste5_pep2 (Ste5). The indicated proteins are used as bait or prey in the GST-pull downs. Bands in color coded boxes correspond to the respective color coded proteins while the rest of the bands are mostly degradation products or contaminants during purifications. The known interaction of Fus3 with Ste5_pep2 is detected (lane 1). In agreement with its α-factor stimulus dependent recruitment and its interaction with the phosphosites on Ste5 (Figure 2f and Supplementary Figure 16), Ptc1 is observed not to interact with non-phosphorylated Ste5_pep2 (lane 2). Ptc1 was also found to not interact with Fus3 (lane 3). GST alone was used as negative control (lane 4). Lanes 5 to 9 indicate the loadings.

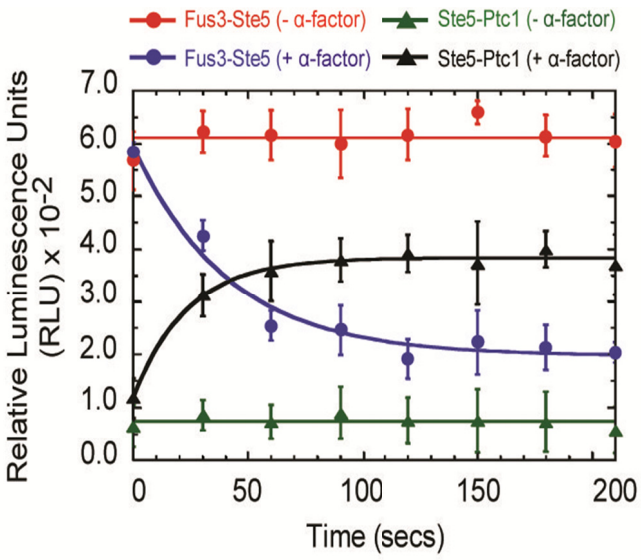

Supplementary figure 18. Fus3 dissociates from Ste5 simultaneous to the association of Ptc1 with Ste5.

Real-time kinetics for the Fus3-Ste5 and Ste5-Ptc1 interactions using Rluc PCA. Data were fit to a single exponential giving effective rates of $0.04s^{-1}$ for Ste5-Ptc1 (R^2=0.99) and $0.02s^{-1}$ for Fus3-Ste5 (R^2=0.97).

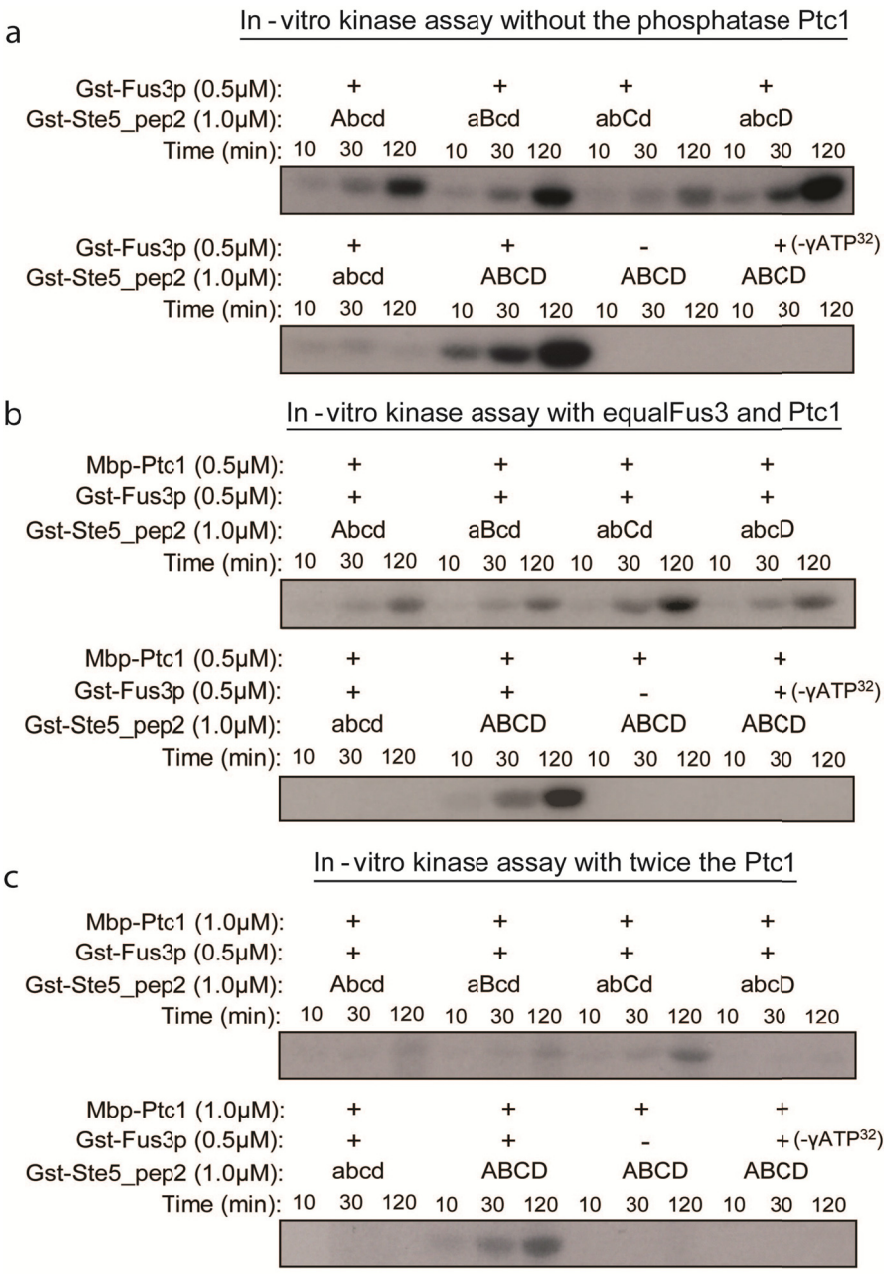

Supplementary figure 19. Ptc1 is capable of dephosphorylating the Ste5 phosphosites by competing with Fus3.
Blots from an *in vitro* kinase assay without the phosphatase Ptc1 (a), with equal Fus3 and Ptc1 (b) and with twice the amount of Ptc1 to Fus3 (c). Phosphorylation levels decrease with an increase in Ptc1 concentration. In conclusion, Ptc1 can interact with and dephosphorylate the phosphosites on Ste5 in the presence of the kinase Fus3.

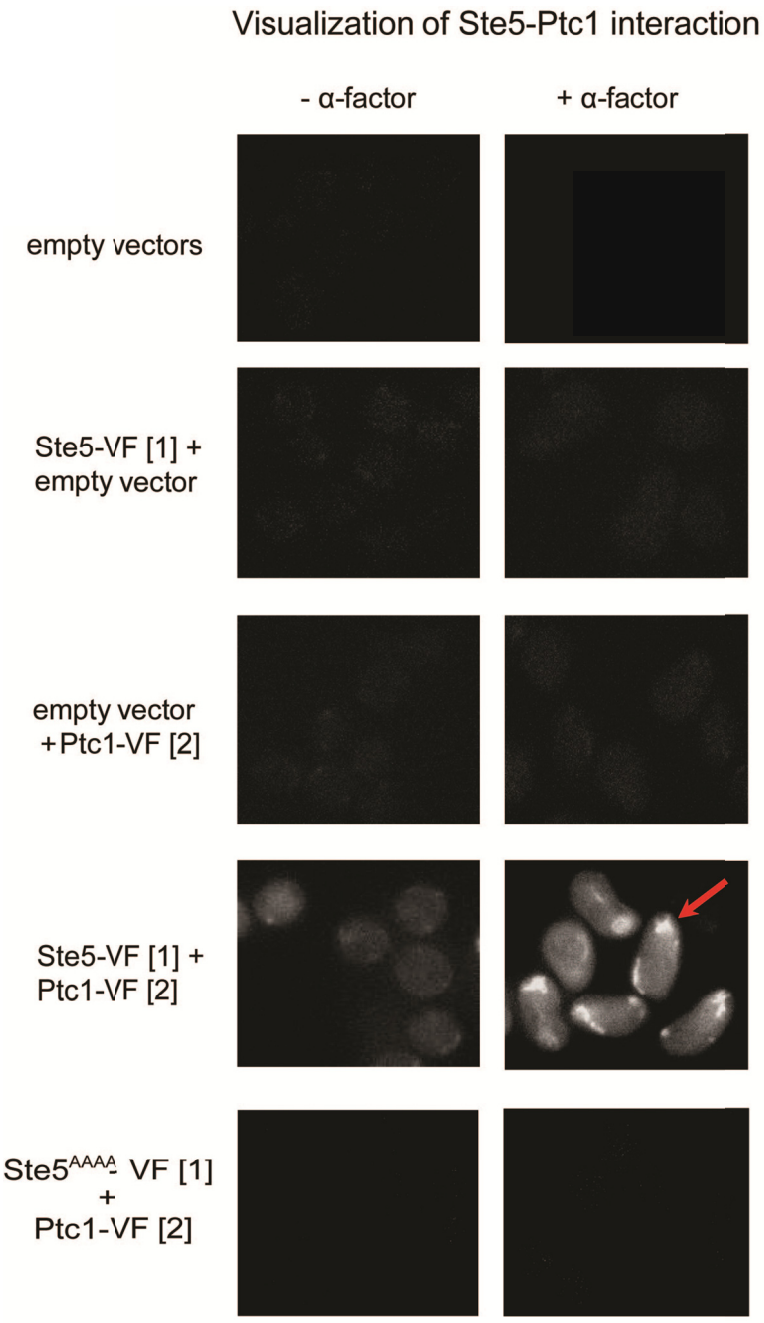

Supplementary figure 20. Detection of Ste5-Ptc1 interaction using Venus PCA.
Detection of the Ste5-Ptc1 interaction and visualization of its cellular location. No detectable signal was observed with the fragments alone. While there is minimal interaction when both proteins fused to fragments are present in the absence of α-factor, significant signal was observed in the presence of α-factor. The signal also localized to the region of polarization (arrow). The lower panel indicates the results with the Ste5 mutant ($Ste5^{AAAA}$; amino acids 277 to 280 mutated to alanine). These results indicate that Ptc1 is recruited to Ste5 at the shmooing region in α-factor dependent manner.

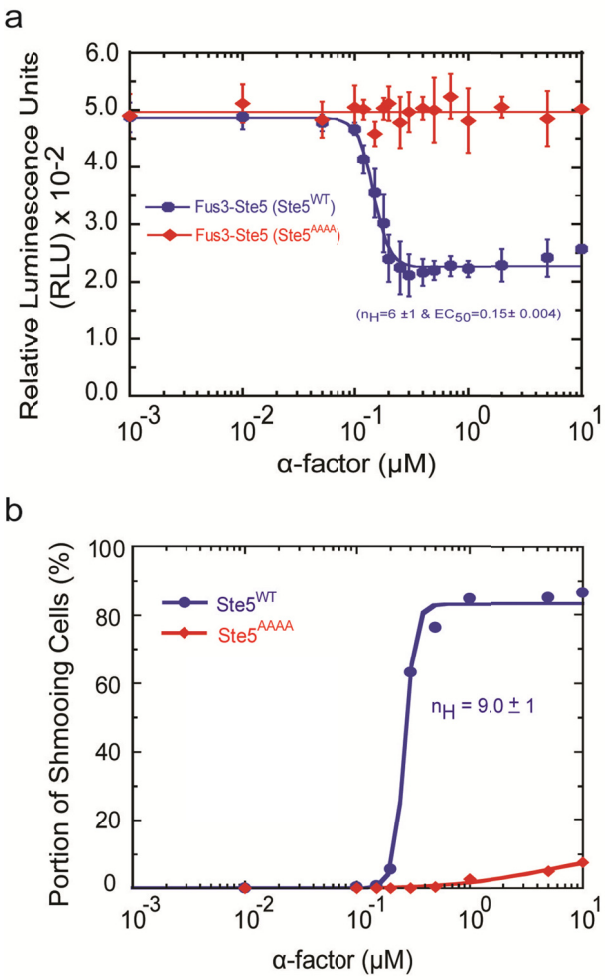

Supplementary figure 21. The steady-state levels of the Fus3-Ste5 complex and shmooing in *ste5Δ* cells with the Ste5^{AAAA} mutant in comparison to Ste5^{WT}.
(a) The Ste5 mutant (Ste5^{AAAA}; amino acids 277 to 280 mutated to alanine) that disrupts the recruitment of Ptc1 to the phosphosites on Ste5 does not interfere with the binding of Fus3 to Ste5, but prevents the Fus3-Ste5 complex from achieving low levels at steady-state. **(b)** The fraction of shmooing cells in *wildtype* cells with Ste5^{WT} or with the Ste5 mutant (Ste5^{AAAA}).

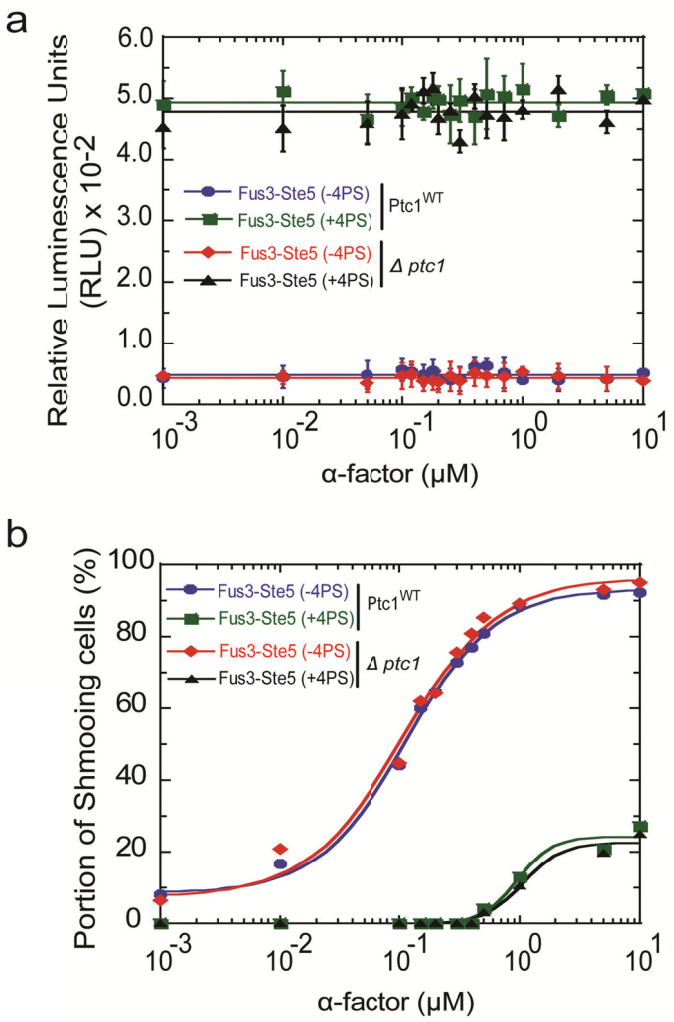

Supplementary figure 22. The effect of varying the phosphatase Ptc1 on the responses for the phosphosite mutants.

(a) and (b) Changes in the steady-state levels of the Fus3-Ste5 complex and shmooing in cells with Ste5 mutants where all phosphorylation sites of Fus3 have been replaced by alanine (-4PS; non-phosphorylatable) or by glutamic acid (+4PS; pseudo-phosphorylated) in the presence ($Ptc1^{WT}$) and absence (*ptc1*Δ) of Ptc1.

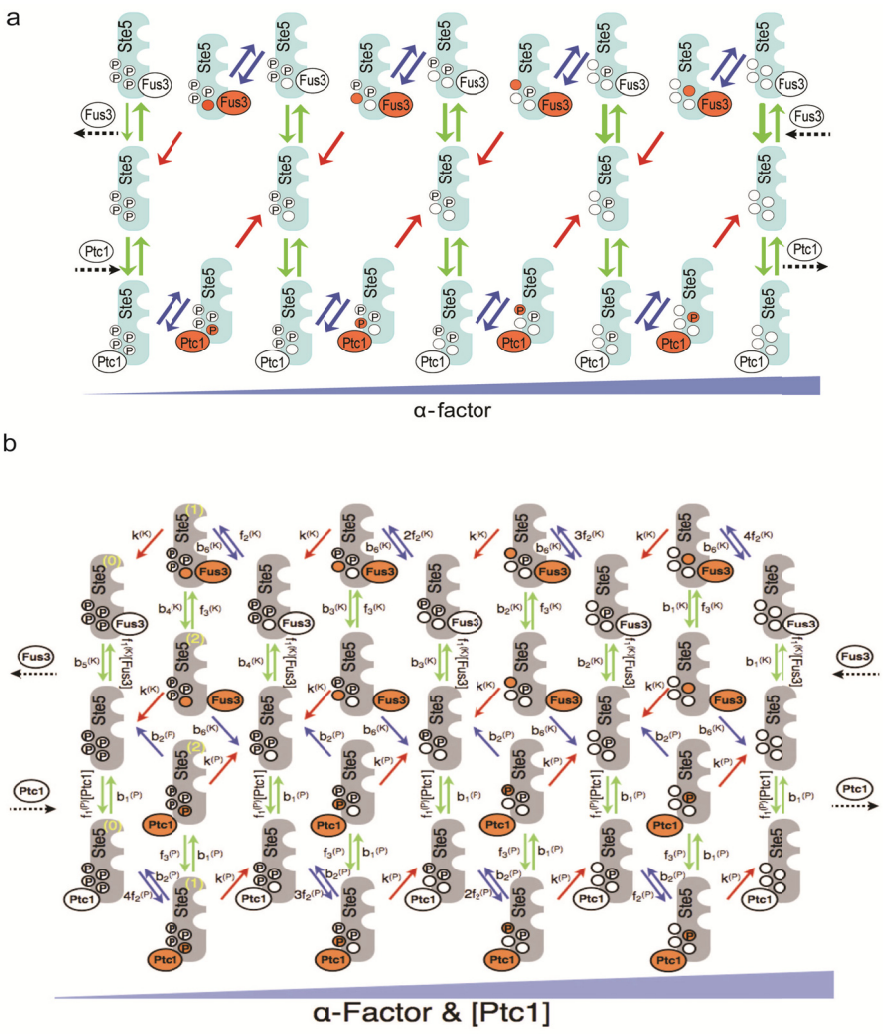

Supplementary figure 23. Illustration of two versions of the computational model
(a) A model of the switch-like dissociation of the Fus3-Ste5 complex that includes two-stage binding and exhibits zero-order ultrasensitivity. Green arrows; Fus3/Ptc1 binding at their docking site. Blue arrows and white complexes: enzyme–phosphosite binding. Red arrows and orange complexes; catalytic conversion of a phosphosite. Increasing width of green arrows indicate increasing rate of Fus3 dissociation as Ste5 is less phosphorylated. Data were fit to an equivalent but slightly more complex version of this model as shown in (b). (b) A general model of Ptc1, Ste5, and Fus3 circuit with two-stage binding that exhibits zero-order ultrasensitivity. We assume that Ste5 has 4 identical phosphosites and that both Fus3 and Ptc1 need to bind Ste5 at a docking site (green arrows) before they can engage in Michaelis-Menton enzymatic reactions with the phosphosites (blue and red arrows). Enzymes interacting with the phosphosites are highlighted in orange. This model is slightly more general than the model presented in (a). Here we assume enzymes can dissociate from the docking motif while bound to the phosphosites. The numbers (0), (1) and (2) specify three types of enzyme-substrate complexes (see Supplementary Information text). All the kinetic rates are given in Supplementary Table 3.

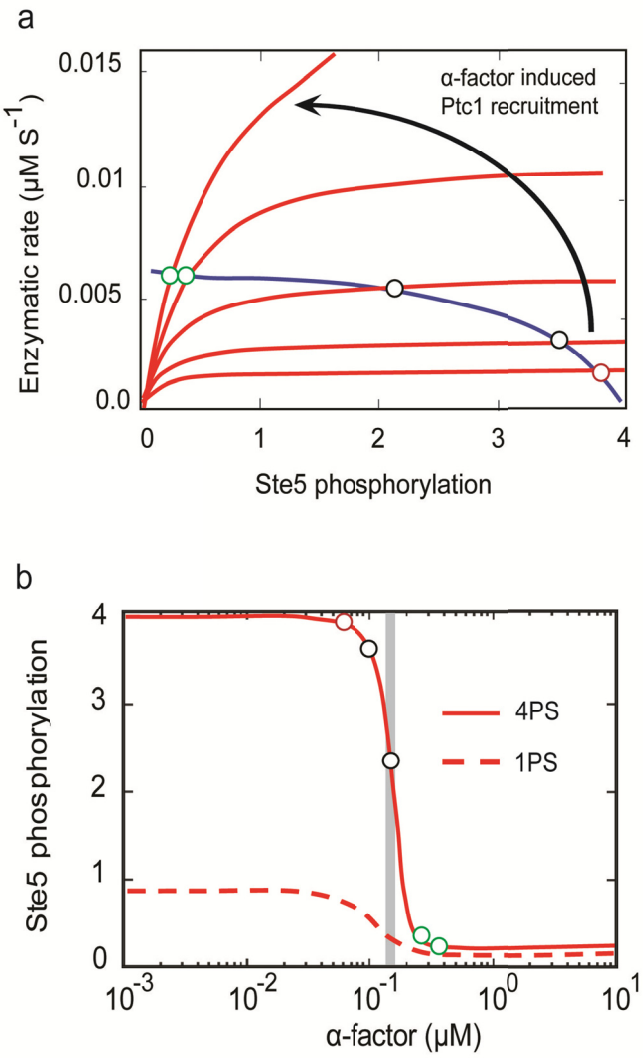

Supplementary figure 24. Zero-order enzymatic rates explain the switch-like drop in Ste5 phosphorylation level with an increase of local Ptc1 concentration.
(a) Predicted enzymatic rates as a function of the average number of phosphorylated phosphosites on Ste5. The activity curve for Fus3 at its endogenous concentration (blue) is shown with 5 activity curves for Ptc1 (red) at increasing concentrations of α-factor (arrow). Points of intersection of the Fus3 and Ptc1 activity curves (open circles) determine the mean steady-state phosphorylation of Ste5, which goes from complete phosphorylation (red) to complete de-phosphorylation (green).
(b) Mean steady-state number of phosphorylated phosphosites on Ste5 (from 3c) *versus* α-factor concentration. We show Ste5 with four (solid line) or one (dashed line) phosphosites. At the threshold concentration of α-factor (grey bar), sufficient Ptc1 is bound to Ste5 to saturate the activity of Fus3 and drive the mean phosphorylation of the phosphosites towards zero (Supplementary Figure 25a). These simulations are done using the model of Supplementary Figure 23b with the fitted parameters.

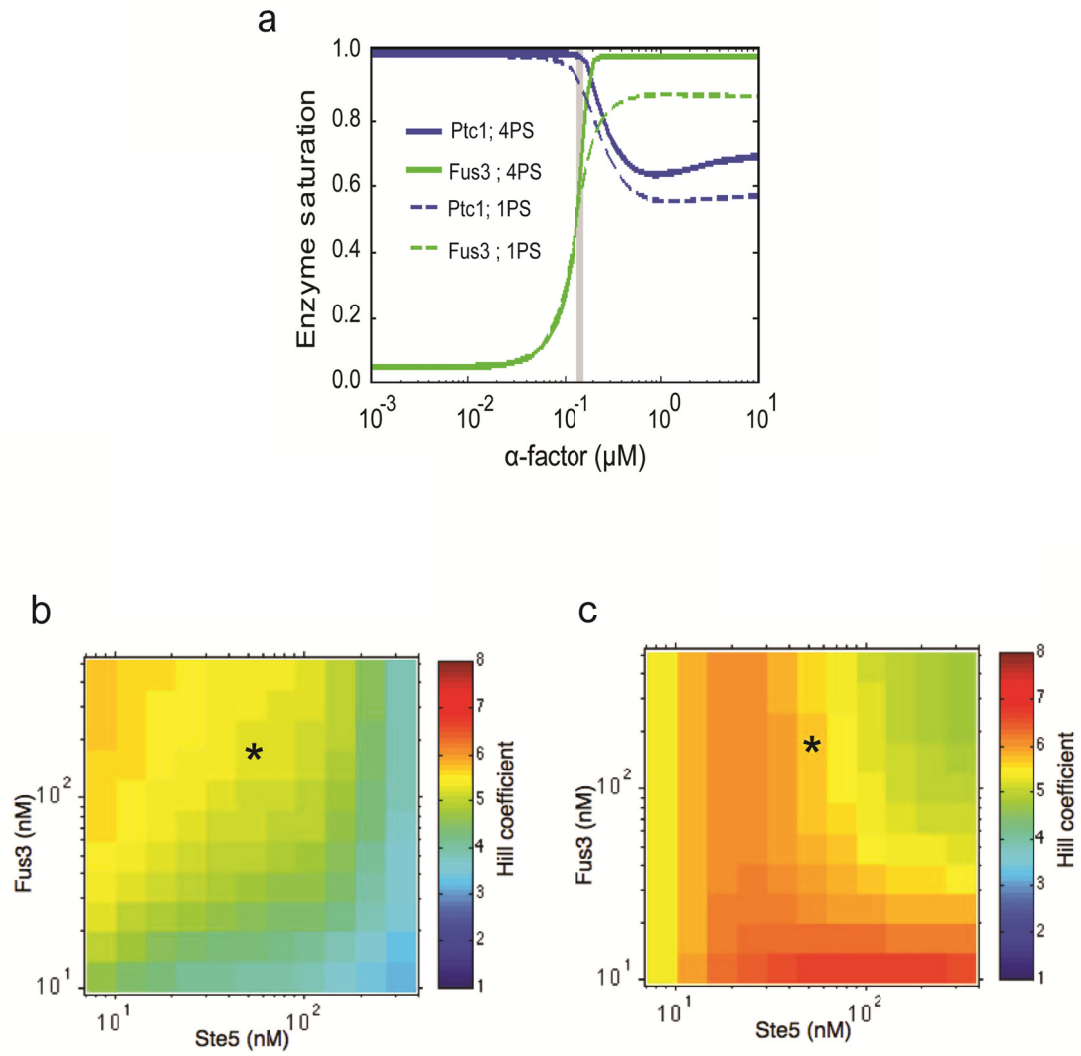

Supplementary figure 25. Predictions for enzyme saturation, robustness of steric hinderance and zero-order mechanisms.

(a) Enzyme (Fus3 and Ptc1) saturation (the ratio of bound to phosphosites to free enzyme) as a function α-factor concentration for Ste5 with either four phosphosites (4PS; solid lines) or a single site (1PS; dashed lines) predicted using the full model of Supplementary Figure 23b. Grey bar specifies the threshold concentration of α-factor.

(b) and (c) Heat maps of the Hill coefficients obtained for two modifications of the model. Each pixel represents the value of the Hill coefficient determined from a dose response of α-factor at given concentrations of Fus3 and Ste5. (b) A one-stage model based on the model of supplementary Figure 23b with parameters that allow only steric hinderance. (c) A two-stage model based on the model of Supplementary Figure 23b with parameters that allow only zero-order ultrasensitivity.

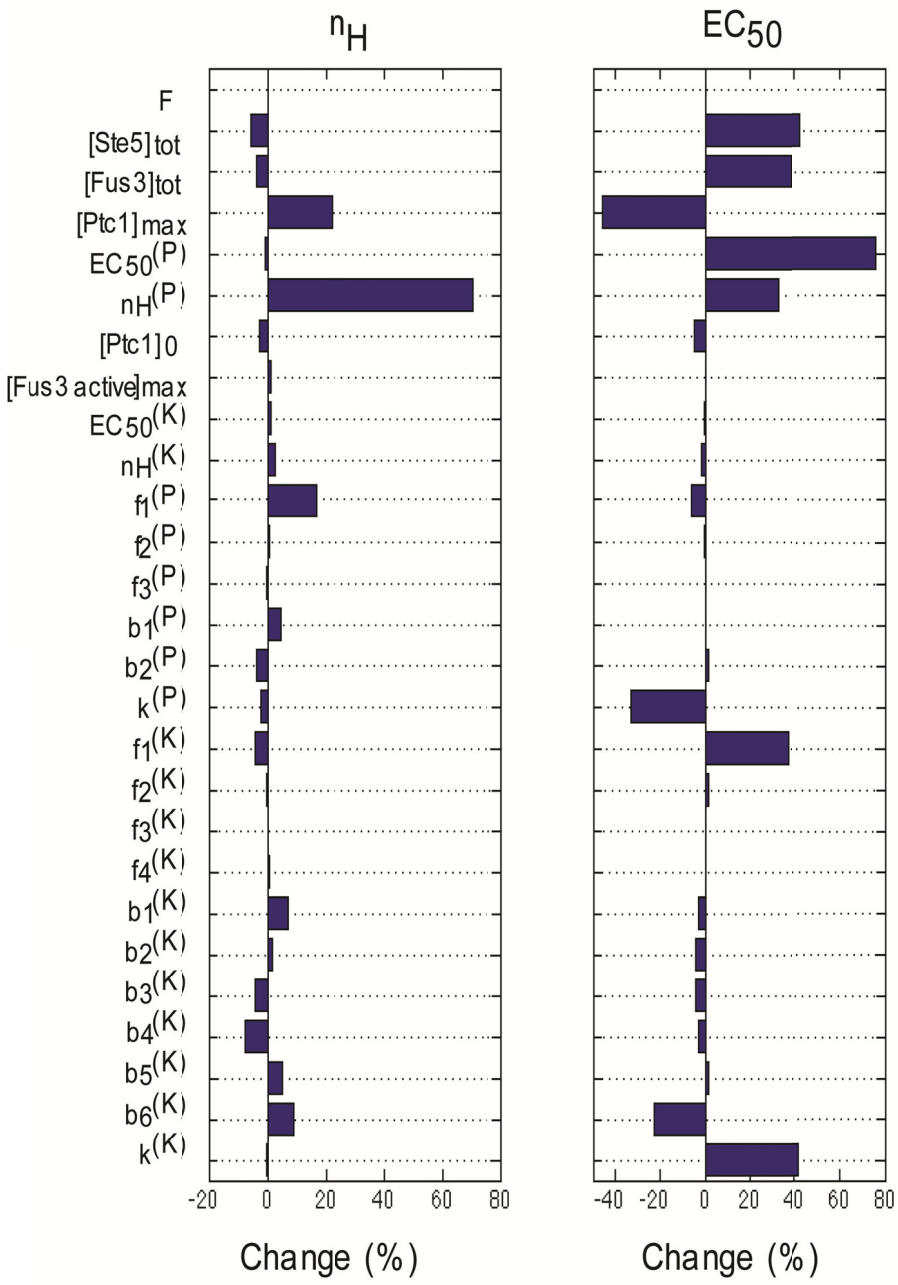

Supplementary figure 26. Sensitivity analysis of the model.
Sensitivity of the n_H and EC_{50} for a switch-like change in phosphorylation of Ste5 to variations in the model parameters. The mean absolute percentage change in the Hill coefficient (n_H) and EC_{50} is shown as each parameter is either multiplied or divided by 2. A negative change denotes a decrease and a positive change an increase in n_H and EC_{50} as the parameter increased.

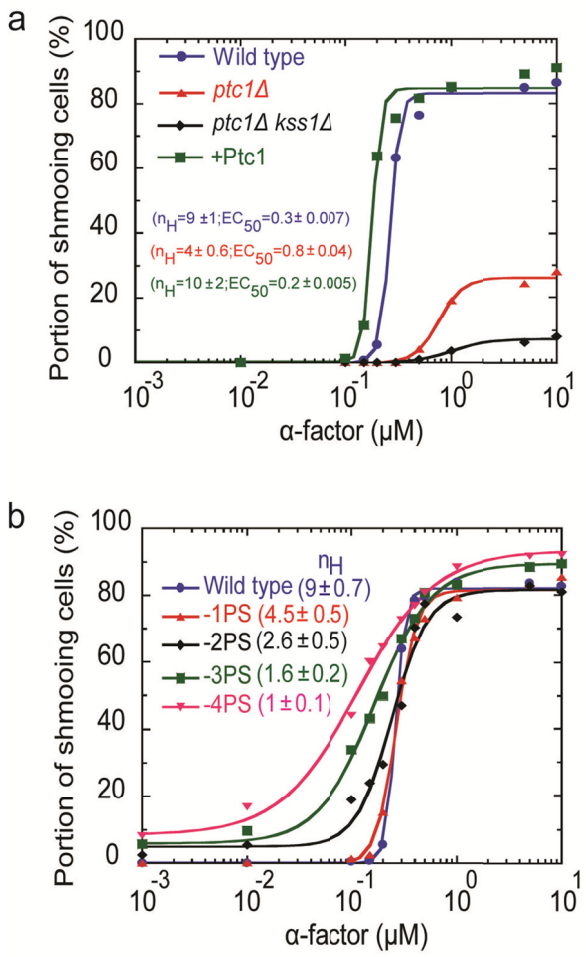

Supplementary figure 27. Experimental validations of robust zero-order ultrasensitivity model predictions.

Changes in the fraction of shmooing cells (a), upon varying the Ptc1 concentration *in-vivo*. We used *wildtype* (WT), Ptc1 knockout (*ptc1Δ*) and a strain over-expressing Ptc1 (+Ptc1). A double deletion of *ptc1Δ kss1Δ* abolished the shmooing observed with *ptc1Δ* alone. Analysis of switching of the shmooing (b) as a function of α-factor using single (-1PS: AbCD), double (-2PS: abCD), triple (-3PS: Abcd) or quadruple (-4PS: abcd) non-phosphorylatable mutants of Ste5. The Hill coefficient, EC_{50} and their errors are calculated from fits of the data to a Hill function (solid lines).

Chapter III: Ultrasensitive membrane recruitment of Ste5 scaffold is essential for fidelity and accuracy of yeast mating decisions

Mohan K. Malleshaiah[1] and Stephen W. Michnick[1, 2, †]

In our continued efforts to understand the switch-like mating response and its mechanisms, in the following article we describe another novel mechanism that might be more general to signalling across species from bacteria to metazoans. We first describe a novel adaptor protein that is essential to bring Ptc1 and Ste5 in close proximity. Then we elucidate the mechanism behind the ultrasensitivity in Ptc1-Ste5 complexes with a revelation that this process primes the mating signalling, which is essential to generate and maintain the fidelity and accuracy of switch-like cellular response to pheromone concentration gradients. The following article has been submitted at the journal *Nature*.

Author contributions

Mohan Malleshaiah	Designed and performed experiments. Analyzed results and wrote the manuscript.
Stephen Michnick	General supervision. Analyzed Results and wrote the manuscript.

Ultrasensitive membrane recruitment of Ste5 scaffold is essential for fidelity and accuracy of yeast mating decisions

Mohan K. Malleshaiah[1] and Stephen W. Michnick[1, 2, †]

One sentence summary: Multiple phosphorylation sites at the N-terminal membrane binding region of Ste5 regulate its ultrasensitive recruitment which in-turn primes the downstream MAP kinase signalling to achieve the right sensitivity and amplitude in mating response.

[1]Département de Biochimie
[2]Centre Robert-Cedergren, Bio-Informatique et Génomique
Université de Montréal
C.P. 6128, Succursale centre-ville
Montréal, Québec H3C 3J7
Canada

† Authors for correspondence

3.1 Abstract

Polarized assembly of protein complexes at the plasma membrane surface is a general phenomenon, which serves to increase the efficiency, fidelity and specificity of signal transduction (Ferrell 1998; Kholodenko, Hoek et al. 2000; Kolch 2000; Kholodenko 2006). In the budding yeast *Saccharomyces cerevisiae*, an early event in response to detection of extracellular signals that drive cell fate decisions is recruitment of MAP kinase signalling modules to the plasma membrane *via* interactions of scaffold proteins. The Ste5 scaffold regulates the mating response to pheromone secreted by the nearby opposite mating partner (Elion 2000; Kolch 2000; Wellbrock, Karasarides et al. 2004). Here we show that recruitment of Ste5 to membrane is ultrasensitive with increasing pheromone signal and that ultrasensitivity is generated by dephosphorylation of eight N-terminal phosphosites on Ste5 by the phosphatase Ptc1 when associated with Ste5 *via* the polarization protein Bem1. Interference with this mechanism results in loss of ultrasensitivity and reduced amplitude and therefore fidelity of response of the pheromone signalling pathway to stimulation. These changes are reflected in reduced fidelity and accuracy of the morphogenic mating response. Together with our previous findings, our results demonstrate that ultrasensitivity, fidelity, accuracy and robustness of the pheromone response occurs through regulation of the stoichiometry of phosphorylation of two clusters of phosphosites on Ste5, by Ptc1, one cluster mediating ultrasensitive recruitment of Ste5 to the membrane and the other, ultrasensitive dissociation and activation of the terminal MAP kinase Fus3 (Malleshaiah, Shahrezaei et al. 2010). Regulation of dynamic signal-response characteristics through such modular regulation of clusters of phosphosites on scaffold proteins, combined with membrane assembly may be a general means by which polarized cell fate decisions are achieved.

Key words: Accuracy, signalling dynamics, pre-amplification, ultrasensitivity, scaffolds, etc.

3.2 Introduction and results

Regulated translocation of signalling proteins to plasma membrane in response to extracellular signals is universal theme observed in all organisms - from bacteria to mammals (Elion 2000; Laub and Goulian 2007; Grecco, Schmick et al. 2011) (Widmann, Gibson et al. 1999; Zhang and Klessig 2001; Lemmon and Schlessinger 2010). Recruitment of scaffold or anchoring proteins to membrane can organize protein complexes, sometimes composing an entire signalling cascade, at the membrane. It has been proposed that in addition to improving the specificity and efficiency of signal transmission, regulated translocation of signalling proteins to membrane can generate ultrasensitivity in signalling that could be necessary to generating an accurate response, particularly if conflicting or alternative signals may arise from distinct sources. For example a decision to polarize in one direction or the other may need to be made when there are subtle differences in signal intensity arising from different sources (Ferrell 1998; Serber and Ferrell 2007).

Haploid budding yeast *S. cerevisiae,* polarize in response to pheromone secreted by a potential mating partner. The two haploid forms of *S. cerevisiae*, *MAT**a*** and *MAT*α, secrete **a**- and α-factor pheromones respectively, which bind to pheromone-specific receptors and activate a canonical MAPK cascade (Fig. 1a). Individual cells detect their mating partners by interpreting the spatial concentration gradient of the pheromone (Jackson and Hartwell 1990; Paliwal, Iglesias et al. 2007). Although cells respond by differentiating into several morphological states and at any concentration of pheromone, different phenotypes co-exist, shmooing (mating polarization) is a deterministic switch-like response (Erdman and Snyder 2001; Paliwal, Iglesias et al. 2007; Hao, Nayak et al. 2008; Malleshaiah, Shahrezaei et al. 2010) (Fig 1a-c). We recently demonstrated that the switching mechanism that results in the shmoo response arises from competition between the MAPK Fus3 and a phosphatase Ptc1 for control of the phosphorylation state of four sites on the mating scaffold protein Ste5 (Malleshaiah, Shahrezaei et al. 2010). This competition results in a switch-like dissociation of Fus3 from Ste5 that is necessary to

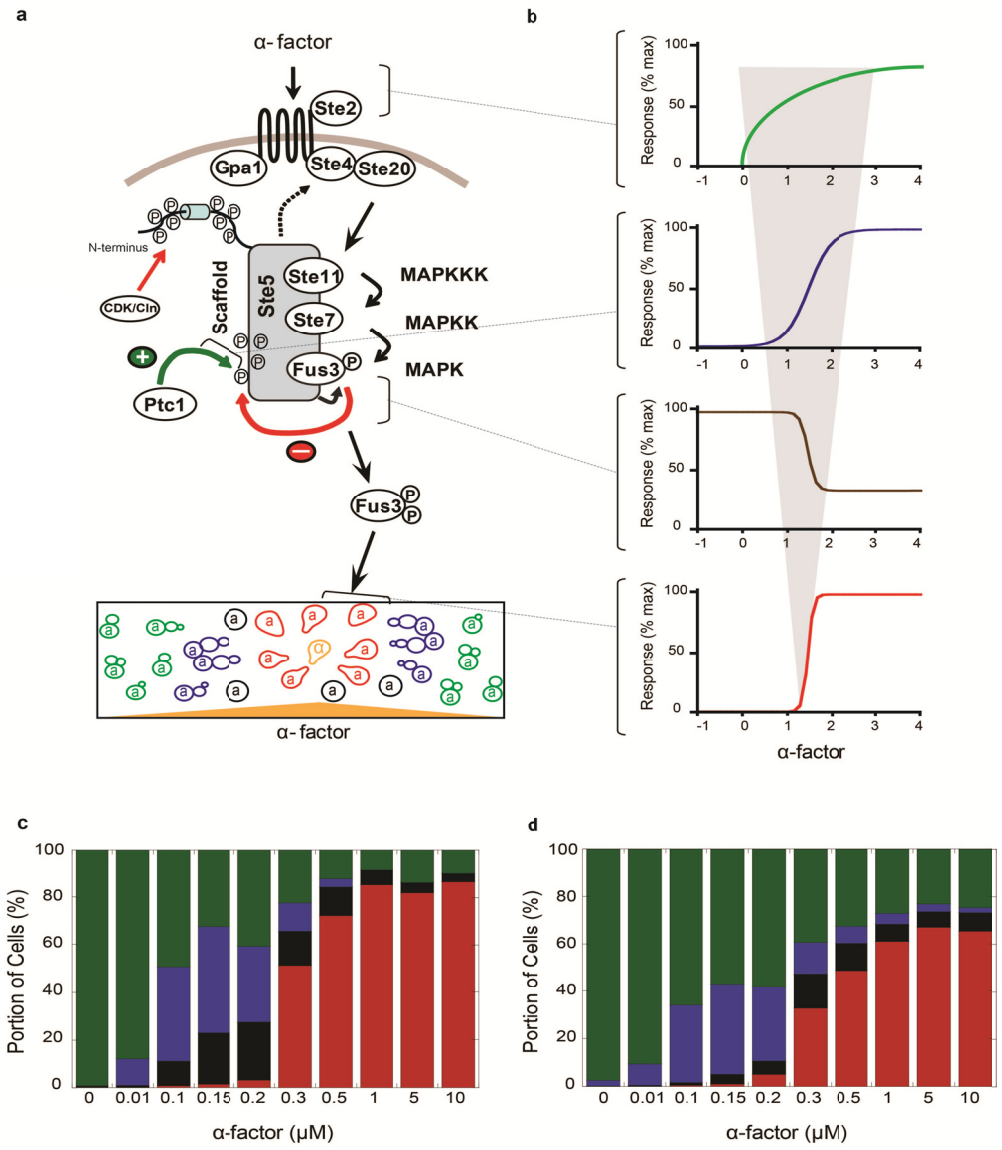

Figure 1. Priming of yeast mating response through pre-amplification step. (a) Schematic of the yeast mating signalling switch in *MAT*a cells, regulating the switch-like shmooing. In the absence of pheromone, Ste5 is phosphorylated at four sites adjacent to or within a Fus3 docking motif (phosphorylated by auto activated Fus3) and eight phosphosites surrounding a basic plasma membrane binding (PM) domain (phosphorylated by the cyclin dependent kinase Cdc28 (CDK)). Pheromone (α-factor) binding to its receptor results in recruitment of Ptc1 to Ste5 and its competition with Fus3 for proximal four phosphosites results in ultrasensitive dissociation/activation of Fus3 and switch-like differentiation of cells to shmoos. Lowe panel – different pheromone-induced morphological states of *MAT*a cells in response to α-factor gradient generated by the *MAT*α cell. Green – axial budding, Blue – bipolar budding, Black – cell cycle arrested and Red – shmooing. (b) Stimulus/response profiles for indicated steps in the pheromone pathway response show progressive sharpening of ultrasensitive response. Morphological states of cells with $Ste5^{WT}$ (c) and $Ste5^{8E}$ (d) in response to α-factor. Different states are color coded as in (a).

generate the switch-like mating response (Fig 1a-b). Thus, the decision to mate is made at an early stage in the pheromone pathway and occurs rapidly, perhaps to prevent the loss of the potential mate to competitors.

Furthermore, the ultrasensitivity we observed results from a series of separate ultrasensitive steps, in which the graded initial response of pheromone receptor binding and trimeric G-protein activation is converted to an ultrasensitive recruitment of the phosphatase Ptc1 to Ste5 ($n_H \approx 2$) followed by the Ptc1-Fus3 competition for phosphorylation of four phosphosites on Ste5 ($n_H \approx 7$) (Malleshaiah, Shahrezaei et al. 2010) (Fig. 1a-b). The hierarchical dynamics results in sharpening of the dynamic range of signal response from Michaelian sensitivity (range of signal over which response goes from 10 % to 90 %) of 80 % change of signal to 15% , and finally to 5% (Ferrell 1998). The initial ultrasensitive step, recruitment of Ptc1 to Ste5, is interesting because it immediately follows the initial effector response, corresponding to recruitment of the MAPK module to the plasma membrane and association with a protein complex that links pheromone signalling to actin cytoskeletal organization involved in shmoo and bud formation. This initial assembly occurs *via* interactions of the Ste5 scaffold with the activated G-protein beta-gamma complex, and phospholipids *via* a plasma membrane binding peptide and PH domain (Whiteway, Wu et al. 1995; Feng, Song et al. 1998; Pryciak and Huntress 1998; Garrenton, Young et al. 2006; Strickfaden, Winters et al. 2007). This initial "pre-amplification" of pheromone signal may be an adaptation that helps cells to distinguish subtle differences in pheromone concentration gradient arising from competing potential mates while the more ultrasensitive downstream switch and rapid response prevents errors in mate selection by preventing responses to spurious fluctuations in pheromone concentration (Fig 1a-b).

The molecular mechanism by which Ptc1 is recruited to Ste5 is not known nor how ultrasensitivity at this step occurs. However, a clue to its origins could be found in the discovery of a mechanism that participates in the recruitment of Ste5 to plasma membrane, whereby the binding of an N-terminal basic peptide plasma membrane-

binding motif (PM) is modulated by phosphorylation of eight sites around the PM by the cyclin-dependent kinase Cdc28 (Fig. 1a) (Serber and Ferrell 2007; Strickfaden, Winters et al. 2007). Indeed, we observe that Ser/Thr to Ala mutations of these eight sites in Ste5 results in both reduction in number of cells that shmoo and of ultrasensitivity of the shmoo response (Fig. 1c-d). Here we demonstrate that ultrasensitivity of Ptc1 recruitment is the result of ultrasensitive recruitment of Ste5 to a signal initiation and polarization complex. Further, it is Ptc1 itself that dephosphorylates the Ste5 phosphosites thus generating ultrasensitive recruitment of Ste5 to plasma membrane *via* the PM.

We first asked how Ptc1 is recruited to the Ste5. Our reasoning was as follows. In our previous work we showed that Ptc1 is recruited to Ste5 as a function of pheromone stimulation, but found no evidence of a direct physical interaction (Malleshaiah, Shahrezaei et al. 2010). In a homologous MAPK pathway that mediates yeast response to extracellular osmolar stress, Ptc1 is recruited to the scaffold protein Pbs2 through constitutive interaction with an adaptor protein Nbp2 (Mapes and Ota 2004). Nbp2 binds to Pbs2 by recognising the SH3 domain interaction motif (SIM) through its second SH3 domain (SH3-2) and to Ptc1 through its N-terminal region, thus bringing Ptc1 into proximity with Pbs2 and its bound osmolar MAPK Hog1. Thus Nbp2 was a candidate to act as an adapter, linking Ptc1 to Ste5. However, an equally likely candidate could be the scaffold protein Bem1, which also harbours two SH3 domains and interacts with Ste5 and enhances the pheromone MAPK Fus3 activation. Together, Bem1, Ste5 and its associated MAPK cascade are known to localize and form a multiprotein complex at the shmooing tip that links signalling machinery to actin remodelling complexes implicated in polarization of shmoos (van Drogen, Stucke et al. 2001). Indeed, deletion of Nbp2 did not, but of Bem1 did abolish pheromone response (Supplementary Fig. 1).

We thus set out to test whether Bem1 acts as an adapter for recruitment of Ptc1 to Ste5. We utilized the same sensitive Renilla Luciferase based protein-fragment complementation assay (Rluc PCA) that we reported early could be used to detect the

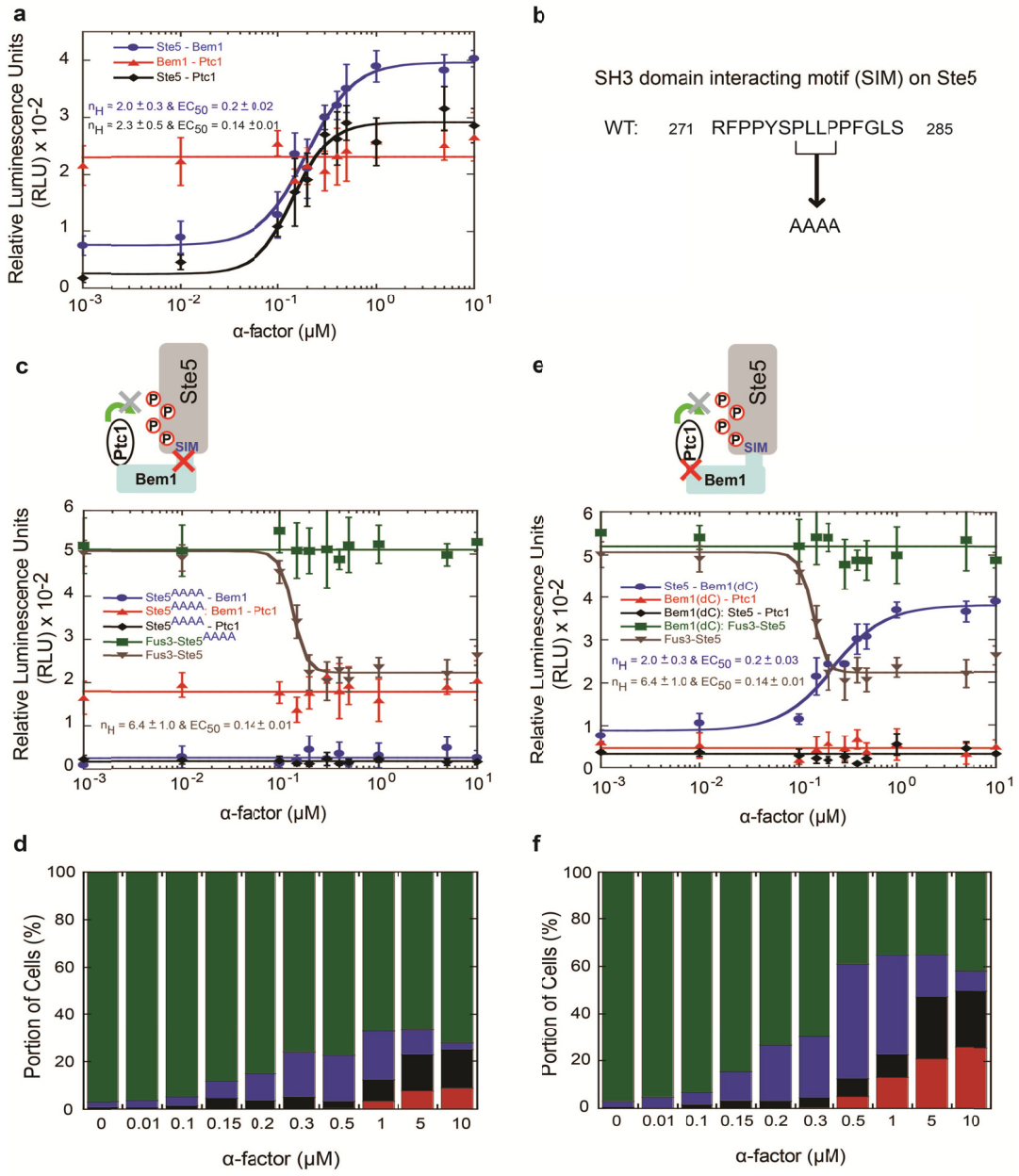

Figure 2. Bem1 acts as an adaptor protein between Ptc1 and Ste5.
(a) α-factor dose-responses for Ste5-Bem1, Bem1-Ptc1, Ste5-Ptc1 and Fus3-Ste5 interactions. (b) Ste5 amino acid sequence (residues 271 to 285) of consensus SH3-2 domain interaction motif (SIM) and its mutation. α-factor dose-responses for $Ste5^{AAAA}$-Bem1, Bem1-Ptc1, $Ste5^{AAAA}$-Ptc1 and Fus3-$Ste5^{AAAA}$ interactions in comparison to Fus3-$Ste5^{WT}$ (c) and for morphological states in *ste5Δ* strain with $Ste5^{AAAA}$ mutant (d). α-factor dose-responses for Ste5- Bem1(dC), Bem1(dC)-Ptc1, Ste5-Ptc1 and Fus3-Ste5 interactions (e) for morphological states in *bem1Δ* strain with *bem1*(dC) mutant (f). Bem1(dC) has amino acids from 417 to 467 deleted. Where indicated, $Ste5^{WT}$ is replaced with $Ste5^{AAAA}$ in *ste5Δ* cells and $Bem1^{WT}$ is replaced with Bem1(dC) in *bem1Δ* cells. Data in (a), (c) and (e) were fit to standard Hill function. Errors indicate standard error of the mean (n=3).

dynamics of pheromone response protein interaction dynamics in living cells (Stefan, Aquin et al. 2007; Malleshaiah, Shahrezaei et al. 2010). In all cases, Rluc reporter fragment coding DNA sequences were introduced directly into the genome of *MAT***a** Ste5 knockout (*STE5*Δ) cells 3' to the coding sequences of proteins of interest, with the exception of Ste5, which was expressed off of a centromeric single-copy plasmid under control of its natural promoter as reported earlier (Malleshaiah, Shahrezaei et al. 2010). Bem1 interacted with both Ste5 and Ptc1 though while the Ptc1-Bem1 interaction is constitutive, the Bem1-Ste5 interaction was ultrasensitive, mirroring precisely the same pheromone induced dynamics (Hill number $n_H \approx 2$) we previously reported for the Ptc1-Ste5 interaction (Fig. 2a). Since Bem1 is plasma membrane-bound, our results suggest that Ptc1 is constitutively associated with Bem1, and that Ptc1 and Bem1 association with Ste5 follow membrane recruitment of Ste5 following pheromone signalling. These results were supported by imaging of the complexes using an enhanced yellow fluorescent protein (Venus) based PCA (Manderson, Malleshaiah et al. 2008; Malleshaiah, Shahrezaei et al. 2010). Both Bem1 and Nbp2 were found to interact with Ptc1 while only Bem1 interacted with Ste5 (Supplementary Fig. 2). In addition, Bem1 complexes with Ptc1 and Ste5 showed polarized fluorescence in the presence of pheromone while Nbp2-Ptc1 complexes remained cytosolic.

We next precisely identified the sites of direct interaction of Bem1 with Ste5 and Ptc1. It is known that Bem1 interacts with Ste5 and that Bem1 facilitates the activation of Fus3 during mating response (Lyons, Mahanty et al. 1996). We reasoned that analogous to the Npb1-Pbs2 complex, Bem1 could interact with Ste5 through one of its two SH3 domains. We identified a SH3 interaction motif (SIM) consensus sequence on Ste5 to which the Bem1 SH3-2 domain that resembled the Pbs2 SIM through which the Npb1 SH3 interacts with it (Fig. 2b). Mutating the C-terminal 'PxxP' SH3 consensus binding motif to 'AAAA' disrupted both the Bem1-Ste5 and Ptc1-Ste5 interactions, but the Bem1-Ptc1 interaction remained intact (Fig. 2c). As we previously demonstrated, Ptc1 recruitment to Ste5 is required to dephosphorylate four phosphosites which in turn results in an ultrasensitive pheromone-dependent dissociation of the MAP kinase Fus3 from Ste5(Malleshaiah, Shahrezaei et al. 2010). Thus, we would predict that disruption of the

Bem1-Ste5 interaction should prevent Ptc1 recruitment and thus Fus3-Ste5 dissociation. As predicted, for $Ste5^{WT}$, the Fus3-Ste5 complex dissociates in response to pheromone, but not for the $Ste5^{AAAA}$ mutant (Fig. 2c). The disruption of these interactions was also confirmed with the Venus PCA (Supplementary fig 3). Finally, the loss of pheromone-dependent Fus3-Ste5 dissociation was reflected in a loss of the normal shmoo formation, with residual shmooing due to activation of the complementary Fus3 homologue Kss1 (Farley, Satterberg et al. 1999) (Fig. 2d).

Next, we dissected Bem1 and Ptc1 to identify the region of their interaction. Since Bem1 consists of two SH3 domains and Ptc1 has a 'PxxP' motif at its N-terminus, we first tested whether Bem1 binds to Ptc1at this SIM. Mutating the Ptc1 SIM to AAAA did not disrupt Bem1-Ptc1 interaction and did not have any effect on the mating response indicating that Bem1 utilizes a different mechanism to bind to Ptc1 (Supplementary Figs. 4 and 1). We then deleted different regions of Bem1 and tested their interaction with Ptc1 as well as mating response (Supplementary Figs. 5 and 6). Both interaction and response were disrupted when a domain consisting of residues 417 to 467 ($Bem1^{\Delta 417-467}$) was deleted (Fig. 2e-f and Supplementary Figs.5 and 6). The $Bem1^{\Delta 417-467}$ mutation resulted in disruption of the Bem1-Ptc1 and Ste5-Ptc1 interactions, but Ste5-Bem1 pheromone dependence was not affected (Fig. 2e). However, pheromone-dependent dissociation of the Ste5-Fus3 complex was lost, as would be predicted if Ptc1 is not recruited to and therefore does not dephosphorylate Ste5.

Finally, the $Bem1^{\Delta 417-467}$ disrupted the pheromone shmoo response (Fig. 2f). Thus Bem1 acts as a specific adapter protein, constitutively associated with Ptc1 in the absence of pheromone. Bem1 organizes proteins into a complex that controls actin cytoskeleton involved in bud polarization, but on pheromone stimulus, Ste5 is recruited to the membrane and becomes coupled to this polarization machinery *via* it's interaction with Bem1 (Madden and Snyder 1998; van Drogen, Stucke et al. 2001; Brent 2009).

Having established that Bem1 acts as an adapter for recruiting Ptc1 to Ste5 at the plasma membrane, we next tested the hypothesis that Ptc1 regulates ultrasensitivity of

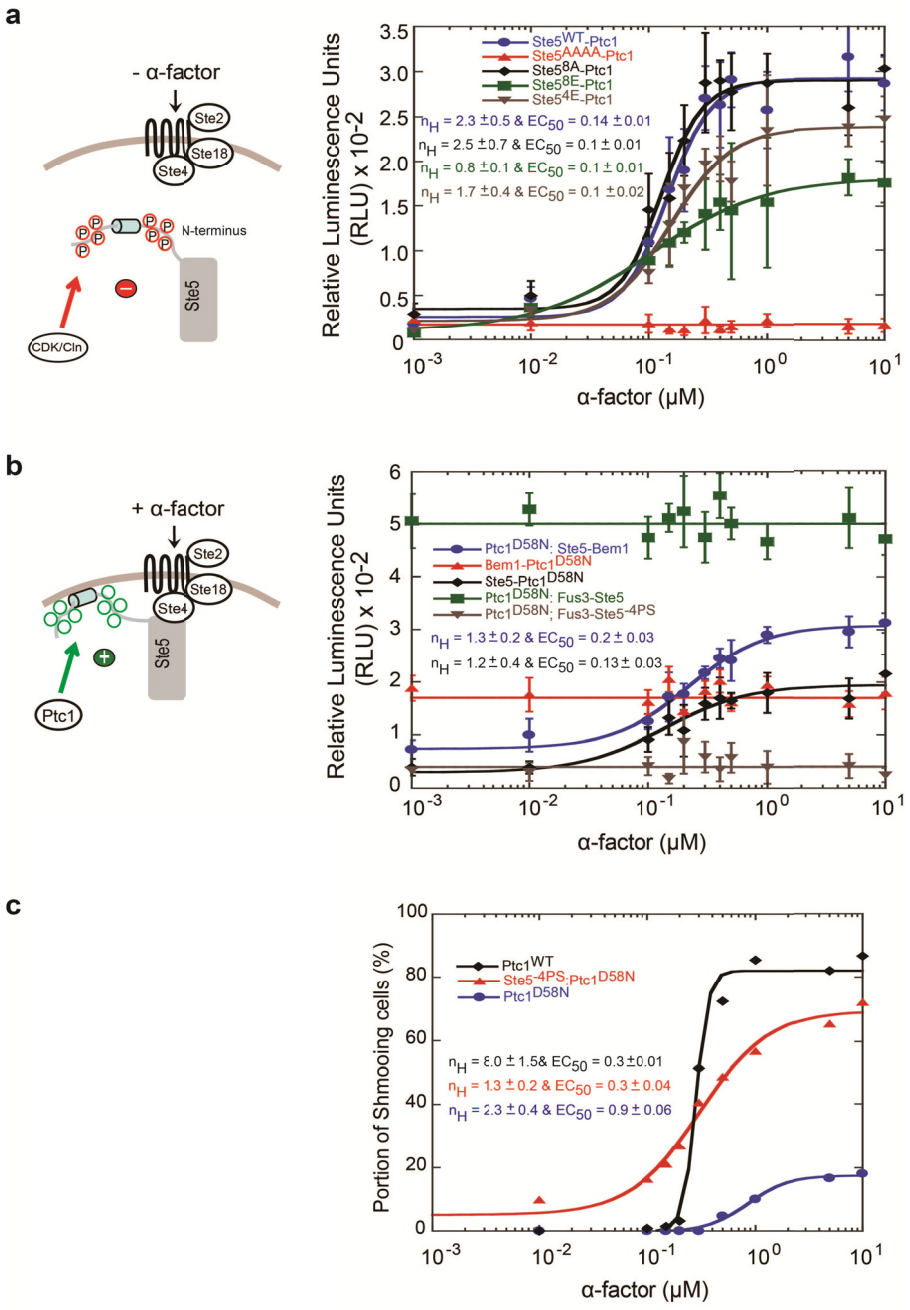

Figure 3. Ste5 membrane recruitment through its N-term phosphosites regulate the ultrasensitive Ste5-Ptc1 interaction.

α-factor dose-responses for Ste5-Ptc1 interaction in cells with $Ste5^{WT}$ or its indicated mutant (a) and for indicated pairs of interactions in cells where $Ptc1^{WT}$ is replaced with catalytically inactive $Ptc1^{D58N}$ (b). Proportion of shmooing cells with inactive Ptc1 mutants in comparison to wild type (c). $Ste5^{-4PS}$ - Ste5 with the phosphosites at FDM (T267, S276, T287 and S329) mutated to Alanine. $Ptc1^{D58N}$ – Catalytically inactive form of Ptc1. Data were fit to standard Hill function. Errors indicate standard error of the mean (n=3).

Ste5 recruitment to the plasma membrane by dephosphorylating eight cyclin-dependent-kinase phosphosites, previously identified N-terminal Ste5 phosphosites (Winters, Lamson et al. 2005) (Serber and Ferrell 2007; Strickfaden, Winters et al. 2007). As we observed, Ser or Thr to Ala mutations of these sites reduced both the quantity and ultrasensitivity of the shmoo response to pheromone (Fig. 1d). We utilized mutants of the Ste5 N-terminal phosphosites to investigate their potential role in ultrasensitive recruitment of Ste5. When all eight phosphosites were mutated to non-phosphorylatable Ala (8A), did not affect the ultrasensitivity of pheromone-induced Ptc1 recruitment to Ste5 (Fig. 3a). However, pseudophosphorylation mutants (Ser or Thre to Glu; 8E), reduced the relative amplitude of pheromone induced Ptc1-Ste5 recruitment by 50 % and shifted the dynamic response from ultrasensitive to graded ($n_H \approx 2.3$ *vs* 0.8). Pseudophosphorylation mutants of four of the phosphosites resulted in intermediate amplitude and ultrasensitivity.

To determine whether Ptc1 catalytic activity is necessary to ultrasensitive assembly of Ste5 at the membrane and recruitment to Bem1 we created a catalytically inactive mutant of Ptc1 (D58N)(Warmka, Hanneman et al. 2001). Both Ste5-Ptc1^{D58N} and Ste5-Bem1 interactions were now graded ($n_H \approx 1$) but as expected, the Ptc1^{D58N}-Bem1 interaction was unchanged (Fig. 3b). As predicted in our previous study, the Ptc1^{D58N} resulted in complete loss of pheromone-dependence of the Fus3-Ste5 dissociation since this requires dephosphorylation of four other Ptc1-dependent phosphosites and mutation of these sites to non-phosphorylatable (McLaughlin and Aderem) residues (Ste5^{-4PS}) results in complete dissociation of the Ste5-Fus3 complex, independent of pheromone or Ptc1 activity (Fig. 3b)(Malleshaiah, Shahrezaei et al. 2010). Further, Ptc1^{D58N} mimicked the deletion of *Ptc1* in reducing disrupting the pheromone-dependent shmoo response (Fig. 3c). Finally, we examined the effects of the 8A, 8E and 4E Ste5 mutants on both the Ste5-Fus3 interaction and shmoo response (Fig 4a-b and supplementary fig 7). The 8A mutant had no effect but the 8E mutant reduced the relative amplitude of the Fus3-Ste5 interaction dissociation by 50% in response to pheromone and ultrasensitivity from $n_H \approx$ 6.5 to 4.2 (Fig 4a) and consistent with these changes, the shmoo response amplitude

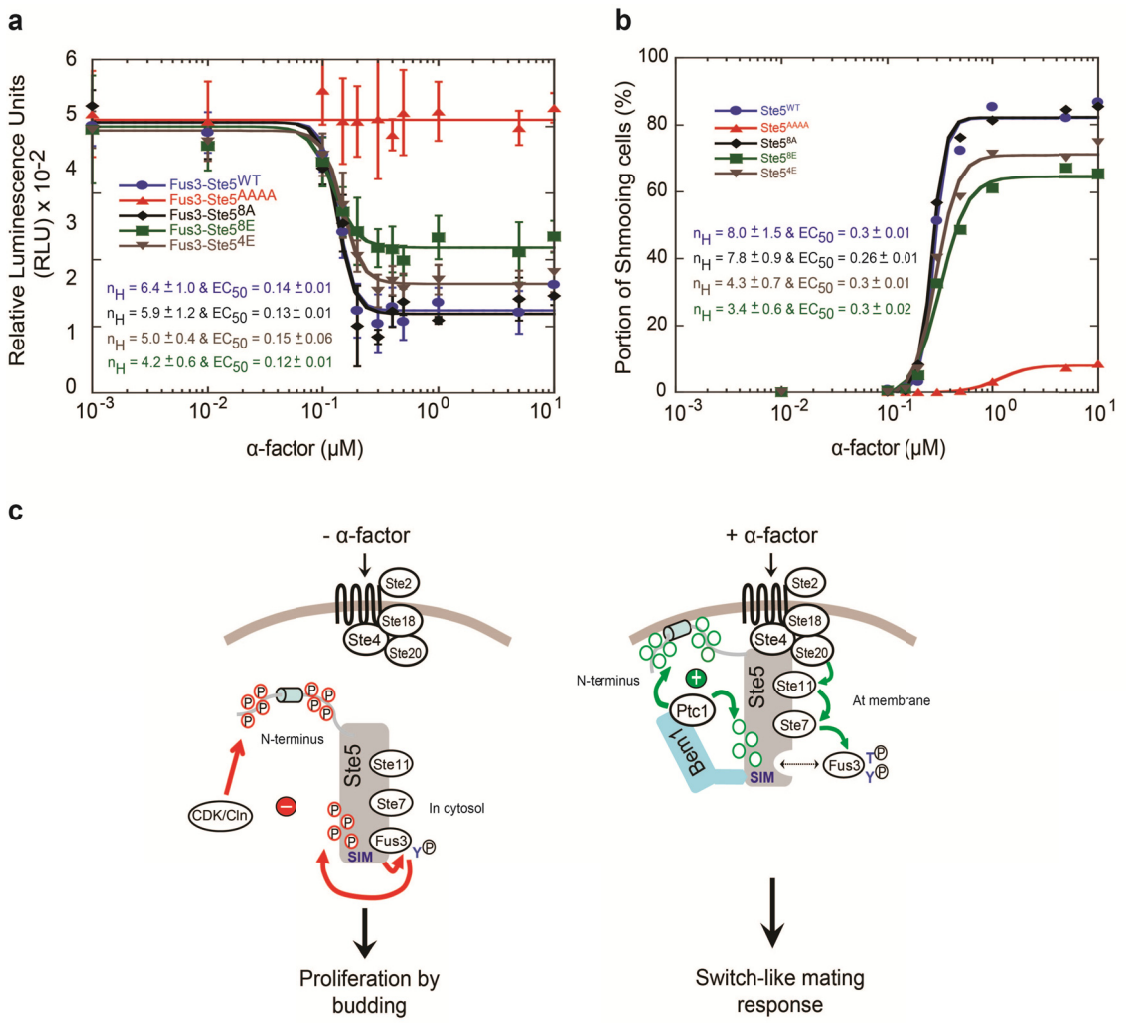

Figure 4. Initial priming regulates the overall ultrasensitivity and amplitude of mating response.

(a) α-factor dose-responses for Fus3-Ste5 interaction in cells with $Ste5^{WT}$ or its indicated mutant. (b) Proportion of shmooing cells with indicated Ste5 mutants in comparison to $Ste5^{WT}$ cells. $Ste5^{8A}$ and $Ste5^{8E}$; Ste5 with N-term phosphosites (T4, S11, T29, S43, S69, S71, S81 and T102) mutated to Alanine (A) and Glutamate (E) respectively. $Ste5^{4E}$ – Ste5 with N-term phosphosites (S11, S43, S71 and T102) mutated to Glutamate (E). Data were fit to standard Hill function. Errors indicate standard error of the mean (n=3). (c) Schematic of the yeast mating signalling switch in *MAT***a** cells, regulating the switch-like shmooing. In the absence of pheromone, Ste5 is phosphorylated at two separate clusters of multiple sites. Pheromone (α-factor) binding to its receptor results in Ste5 membrane recruitment increases its local access to Bem1 associated Ptc1, which dephosphorylates the PM proximal phosphosites, resulting in ultrasensitive ($n_H \approx 2$) enhancement of membrane association of Ste5. Ptc1 equally competes with Fus3 for proximal four phosphosites resulting in ultrasensitive ($n_H \approx 6$) dissociation/activation of Fus3 and switch-like differentiation of cells to shmoos.

was reduced and ultrasensitivity also reduced from $n_H \approx 7.5$ to 3.4 (Fig 4b). The 4E mutant produced an intermediate effect in both cases. These results are completely consistent with and imply that the changes in Fus3-Ste5 interaction and the shmoo response are dependent on changes in Ste5-Bem1 interaction and Ptc1 recruitment caused by the 8E and 4E mutations of Ste5.

Our results are consistent with a simple model for ultrasensitive recruitment of Ste5 to the membrane, in which initially, following pheromone stimulation, Ste5 is recruited to the beta-gamma complex of the activated trimeric G-protein complex, an interaction essential to activation of the MAPK cascade (Feng, Song et al. 1998). This interaction and that of a Ste5 PH domain with phosphoinositide lipids is reflected in the graded recruitment of Ptc1 to Ste5 in the 8E mutant (Garrenton, Young et al. 2006)(Fig. 3a). Following this initial step, we propose that Ptc1 dephosphorylates the eight phosphosites, permitting the Ste5 basic phospholipid binding motif to bind to the membrane (Serber and Ferrell 2007; Strickfaden, Winters et al. 2007)(Figs. 3a and 4c). A mathematical model predicts ultrasensitivity for this interaction based purely on bulk electrostatics created by phosphorylation and membrane-cytosol partitioning of the Ste5 (McLaughlin and Aderem 1995; Serber and Ferrell 2007).

Stimulus dependent membrane recruitment of signalling proteins, often mediated through scaffold and adaptors can create ‘nanoclusters’ – a non-random and selective concentration of signalling proteins on the plasma membrane surface (Murakoshi, Iino et al. 2004; Hancock and Parton 2005; Plowman and Hancock 2005; Plowman, Muncke et al. 2005). Such clusters can also operate as ‘switches’ by converting a graded stimulus switch-like responses (Tian, Harding et al. 2007). The modular nature of signalling proteins permit their recombination, rewiring and even build a new and novel signalling complexes to obtain a preferable response output (Bashor, Horwitz et al. 2010; Lim 2010). Together with our previous findings, our results demonstrate ultrasensitivity, fidelity accuracy and robustness of the pheromone response occurs through regulation of the stoichiometry of phosphorylation of two clusters of phosphosites on Ste5, the by Ptc1, one cluster mediating ultrasensitive recruitment of Ste5 to the membrane and the other,

ultrasensitive dissociation and activation of the terminal MAP kinase Fus3 (Malleshaiah, Shahrezaei et al. 2010). Regulation of dynamic signal-response characteristics through such modular regulation of clusters of phosphosites on scaffold proteins combined membrane assembly may be a general means by which polarized cell fate decisions are achieved.

3.3 References

Bashor, C. J., A. A. Horwitz, et al. (2010). Rewiring cells: synthetic biology as a tool to interrogate the organizational principles of living systems. *Annual review of biophysics* **39**: 515-537.

Brent, R. (2009). Cell signaling: what is the signal and what information does it carry? *FEBS letters* **583**(24): 4019-4024.

Elion, E. A. (2000). Pheromone response, mating and cell biology. *Curr Opin Microbiol* **3**(6): 573-581.

Erdman, S. and M. Snyder (2001). A filamentous growth response mediated by the yeast mating pathway. *Genetics* **159**(3): 919-928.

Farley, F. W., B. Satterberg, et al. (1999). Relative dependence of different outputs of the Saccharomyces cerevisiae pheromone response pathway on the MAP kinase Fus3p. *Genetics* **151**(4): 1425-1444.

Feng, Y., L. Y. Song, et al. (1998). Functional binding between G[beta] and the LIM domain of Ste5 is required to activate the MEKK Ste11. *Curr. Biol.* **8**: 267-278.

Ferrell, J. E., Jr. (1998). How regulated protein translocation can produce switch-like responses. *Trends in biochemical sciences* **23**(12): 461-465.

Garrenton, L. S., S. L. Young, et al. (2006). Function of the MAPK scaffold protein, Ste5, requires a cryptic PH domain. *Genes & Development* **20**(14): 1946-1958.

Grecco, H. E., M. Schmick, et al. (2011). Signaling from the living plasma membrane. *Cell* **144**(6): 897-909.

Hancock, J. F. and R. G. Parton (2005). Ras plasma membrane signalling platforms. *The Biochemical journal* **389**(Pt 1): 1-11.

Hao, N., S. Nayak, et al. (2008). Regulation of cell signaling dynamics by the protein kinase-scaffold Ste5. *Mol Cell* **30**(5): 649-656.

Jackson, C. L. and L. H. Hartwell (1990). Courtship in S. cerevisiae: both cell types choose mating partners by responding to the strongest pheromone signal. *Cell* **63**(5): 1039-1051.

Kholodenko, B. N. (2006). Cell-signalling dynamics in time and space. *Nature reviews. Molecular cell biology* **7**(3): 165-176.

Kholodenko, B. N., J. B. Hoek, et al. (2000). Why cytoplasmic signalling proteins should be recruited to cell membranes. *Trends in cell biology* **10**(5): 173-178.

Kolch, W. (2000). Meaningful relationships: the regulation of the Ras/Raf/MEK/ERK pathway by protein interactions. *The Biochemical journal* **351 Pt 2**: 289-305.

Laub, M. T. and M. Goulian (2007). Specificity in two-component signal transduction pathways. *Annual review of genetics* **41**: 121-145.

Lemmon, M. A. and J. Schlessinger (2010). Cell signaling by receptor tyrosine kinases. *Cell* **141**(7): 1117-1134.

Lim, W. A. (2010). Designing customized cell signalling circuits. *Nature reviews. Molecular cell biology* **11**(6): 393-403.

Lyons, D. M., S. K. Mahanty, et al. (1996). The SH3-domain protein Bem1 coordinates mitogen-activated protein kinase cascade activation with cell cycle control in Saccharomyces cerevisiae. *Molecular and cellular biology* **16**(8): 4095-4106.

Madden, K. and M. Snyder (1998). Cell polarity and morphogenesis in budding yeast. *Annual review of microbiology* **52**: 687-744.

Malleshaiah, M. K., V. Shahrezaei, et al. (2010). The scaffold protein Ste5 directly controls a switch-like mating decision in yeast. *Nature* **465**(7294): 101-105.

Manderson, E. N., M. Malleshaiah, et al. (2008). A novel genetic screen implicates Elm1 in the inactivation of the yeast transcription factor SBF. *PloS one* **3**(1): e1500.

Mapes, J. and I. M. Ota (2004). Nbp2 targets the Ptc1-type 2C Ser/Thr phosphatase to the HOG MAPK pathway. *The EMBO journal* **23**(2): 302-311.

McLaughlin, S. and A. Aderem (1995). The myristoyl-electrostatic switch: a modulator of reversible protein-membrane interactions. *Trends in biochemical sciences* **20**(7): 272-276.

Murakoshi, H., R. Iino, et al. (2004). Single-molecule imaging analysis of Ras activation in living cells. *Proceedings of the National Academy of Sciences of the United States of America* **101**(19): 7317-7322.

Paliwal, S., P. A. Iglesias, et al. (2007). MAPK-mediated bimodal gene expression and adaptive gradient sensing in yeast. *Nature* **446**(7131): 46-51.

Plowman, S. J. and J. F. Hancock (2005). Ras signaling from plasma membrane and endomembrane microdomains. *Biochimica et biophysica acta* **1746**(3): 274-283.

Plowman, S. J., C. Muncke, et al. (2005). H-ras, K-ras, and inner plasma membrane raft proteins operate in nanoclusters with differential dependence on the actin cytoskeleton. *Proceedings of the National Academy of Sciences of the United States of America* **102**(43): 15500-15505.

Pryciak, P. M. and F. A. Huntress (1998). Membrane recruitment of the kinase cascade scaffold protein Ste5 by the Gβγ complex underlies activation of the yeast pheromone response pathway. *Genes & Development* **12**(17): 2684-2697.

Serber, Z. and J. E. Ferrell, Jr. (2007). Tuning bulk electrostatics to regulate protein function. *Cell* **128**(3): 441-444.

Stefan, E., S. Aquin, et al. (2007). Quantification of dynamic protein complexes using Renilla luciferase fragment complementation applied to protein kinase A activities in vivo. *Proc Natl Acad Sci U S A* **104**(43): 16916-16921.

Strickfaden, S. C., M. J. Winters, et al. (2007). A mechanism for cell-cycle regulation of MAP kinase signaling in a yeast differentiation pathway. *Cell* **128**(3): 519-531.

Tian, T., A. Harding, et al. (2007). Plasma membrane nanoswitches generate high-fidelity Ras signal transduction. *Nature cell biology* **9**(8): 905-914.

van Drogen, F., V. M. Stucke, et al. (2001). MAP kinase dynamics in response to pheromones in budding yeast. *Nat Cell Biol* **3**(12): 1051-1059.

Warmka, J., J. Hanneman, et al. (2001). Ptc1, a type 2C Ser/Thr phosphatase, inactivates the HOG pathway by dephosphorylating the mitogen-activated protein kinase Hog1. *Mol Cell Biol* **21**(1): 51-60.

Wellbrock, C., M. Karasarides, et al. (2004). The RAF proteins take centre stage. *Nature reviews. Molecular cell biology* **5**(11): 875-885.

Whiteway, M. S., C. Wu, et al. (1995). Association of the yeast pheromone response G protein beta gamma subunits with the MAP kinase scaffold Ste5p. *Science* **269**(5230): 1572-1575.

Widmann, C., S. Gibson, et al. (1999). Mitogen-activated protein kinase: conservation of a three-kinase module from yeast to human. *Physiological reviews* **79**(1): 143-180.

Winters, M. J., R. E. Lamson, et al. (2005). A Membrane Binding Domain in the Ste5 Scaffold Synergizes with G[beta][gamma] Binding to Control Localization and Signaling in Pheromone Response. *Molecular Cell* **20**(1): 21-32.

Zhang, S. and D. F. Klessig (2001). MAPK cascades in plant defense signaling. *Trends in plant science* **6**(11): 520-527.

Supplementary Information is linked to the online version of the paper at www.nature.com/nature.

Acknowledgements The authors would like to thank James Ferrell Jr. and members of the Michnick lab for useful discussions and comments on the manuscript; Jackie Vogel and Peter Pryciak for providing plasmids and yeast strains. This work was supported by grants from the CIHR (MOP-GMX-152556) and a Canada Research Chair in Integrative Genomics to S.W.M..

Author contributions MKM and SWM planned and designed experiments; MKM performed experiments; MKM and SWM analyzed the results wrote the manuscript.

Author Information Reprints and permissions information is available at www.npg.nature.com/reprintsandpermissions. The authors declare no competing financial interests. Correspondence should be addressed to either S.W.M. Requests for materials should be addressed to S.W.M.

3.4 Supplementary figures

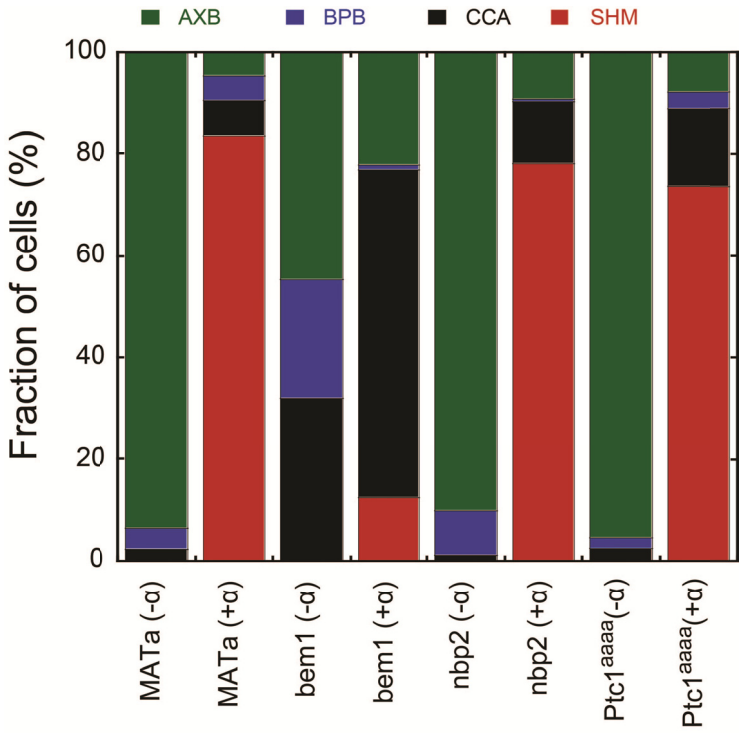

Supplementary figure 1. Portion of cells manifesting different morphologies. Morphologies in *MAT***a**, *bem1Δ*, *nbp2Δ* and *ptc1Δ* cells containing Ptc1^{AAAA}, both in the absence and presence of α-factor pheromone (1 μM). Deletion of Bem1 interfered with both budding in the absence of pheromone and shmooing in the presence of pheromone thus, indicating that it is essential for polarization. Deletion of Nbp2 did not have any effect on either budding or shmooing. Similarly Ptc1^{AAAA} mutant did not effect shmooing response indicating that this region of Ptc1 does not bind to Bem1 SH3 domain.

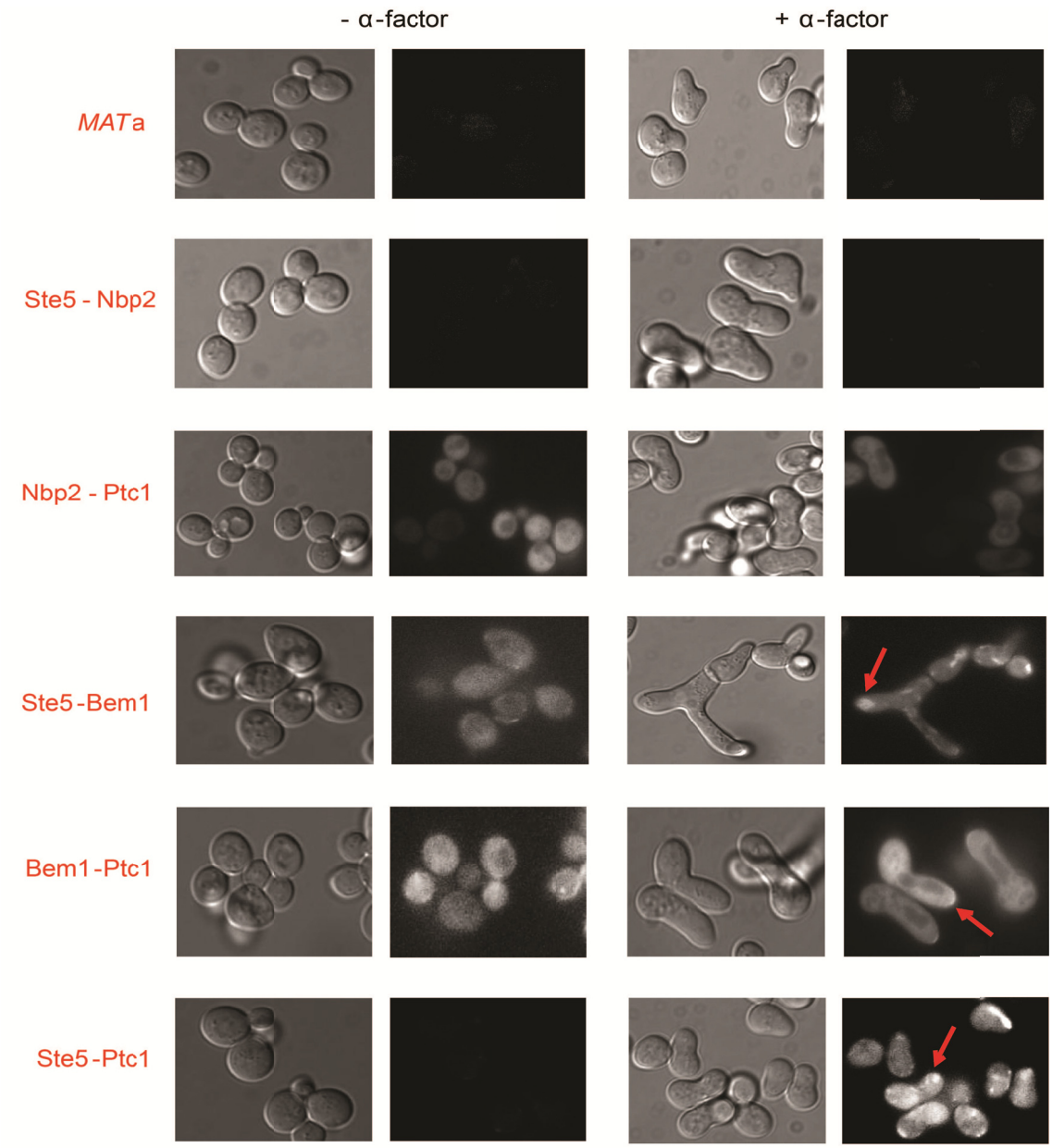

Supplementary figure 2. Visualization of interactions using Venus PCA.
Both DIC and fluorescent images are shown in the absence and presence of α-factor (1 μM). DIC images were taken with 300 ms while fluorescent images with 600 ms of exposure time. Where indicated, cells were treated with α-factor for up to 3 to 4 hours. Nbp2 does not act as an adaptor protein to recruit Ptc1 to Ste5 phosphosites. Images show Venus PCA for Nbp2 and Bem1 interaction with Ste5 and Ptc1 both in absence or presence of α-factor pheromone (1 μM). Nbp2 does not interact with Ste5. In addition the Nbp2-Ptc1 complexes show no polarization when cells are treated with α-factor.

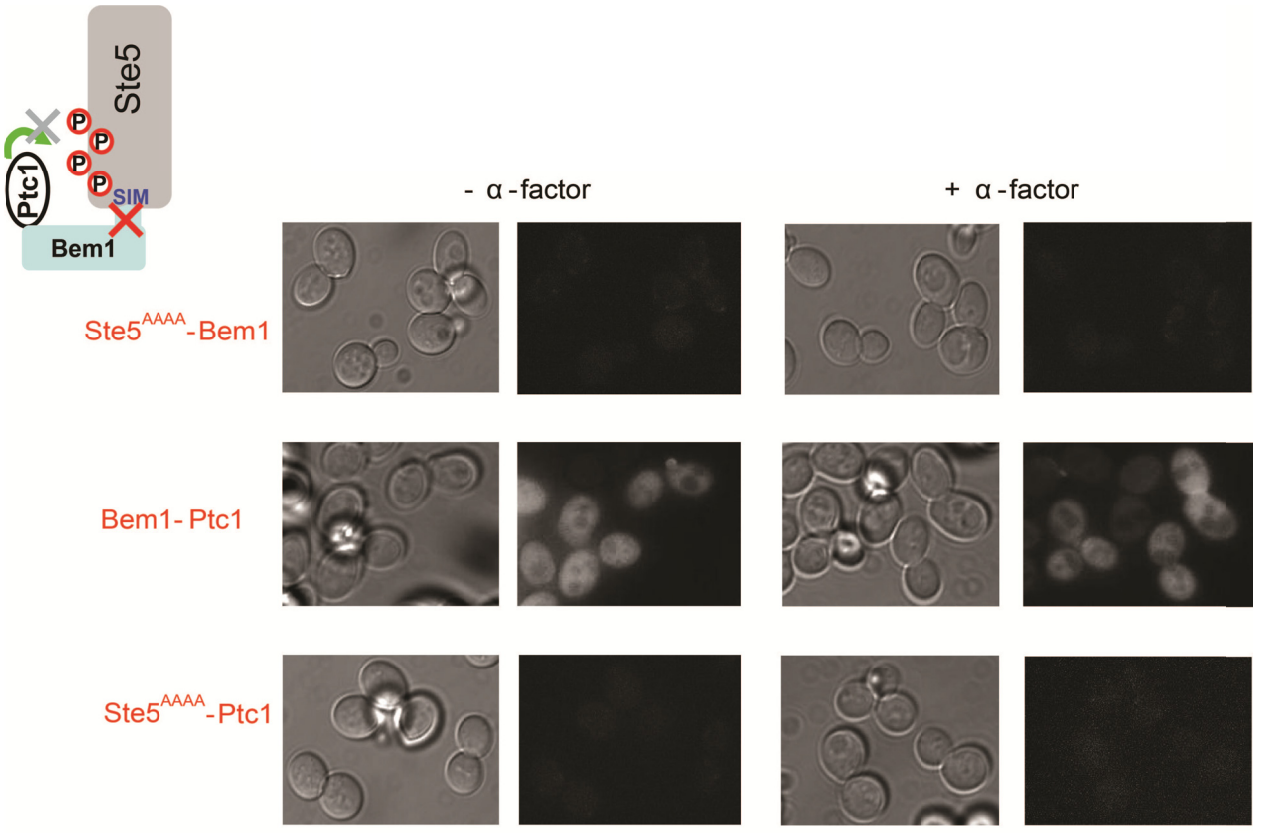

Supplementary figure 3. Disruption of Ste5-Bem1 interaction.
DIC and Venus PCA images for Ste5^{AAAA}-Bem1, Bem1-Ptc1 and Ste5^{AAAA}-Ptc1 interactions in *ste5Δ* cells. Note that strong morphological changes observed in Ste5^{WT} cells (Figure S2) are not observed in the Ste5^{AAAA} mutant. These morphogenic changes may be due to trapping of complexes by the irreversible Venus PCA.

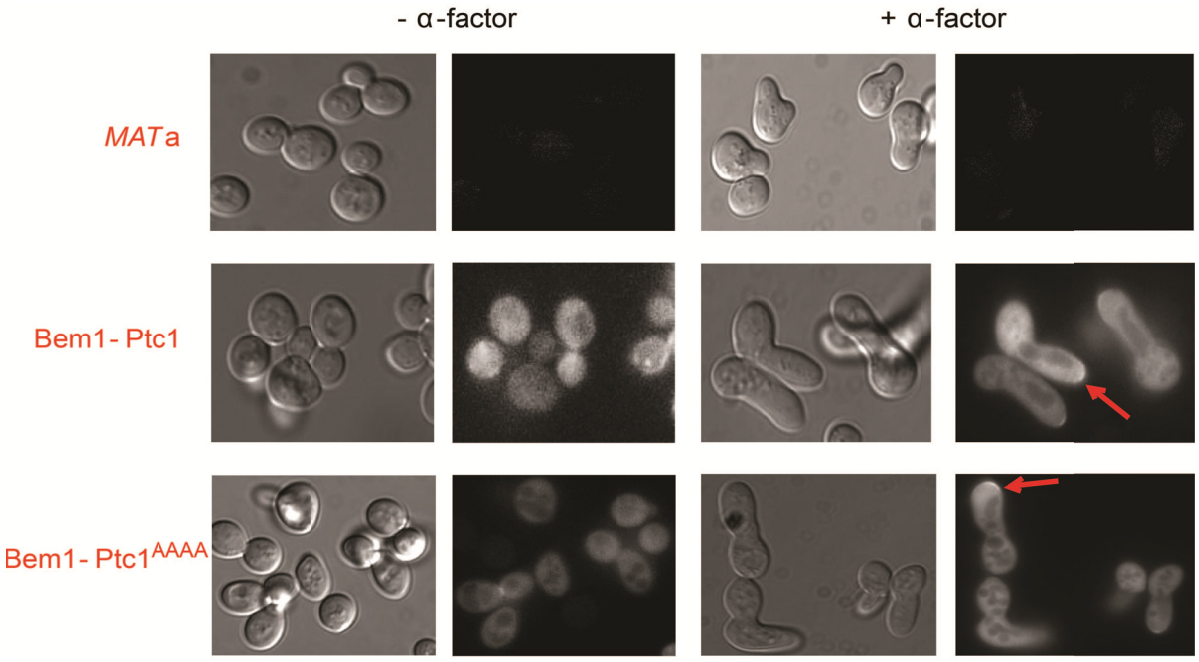

Supplementary figure 4. Venus PCA images showing Bem1 interaction with either $Ptc1^{WT}$ or $Ptc1^{AAAA}$ mutant.
There was no difference in the interaction signal and in both cases the complexes show some polarization when cells are treated with α-factor. Hence, Bem1 did not bind to Ptc1 through its SH3 domains.

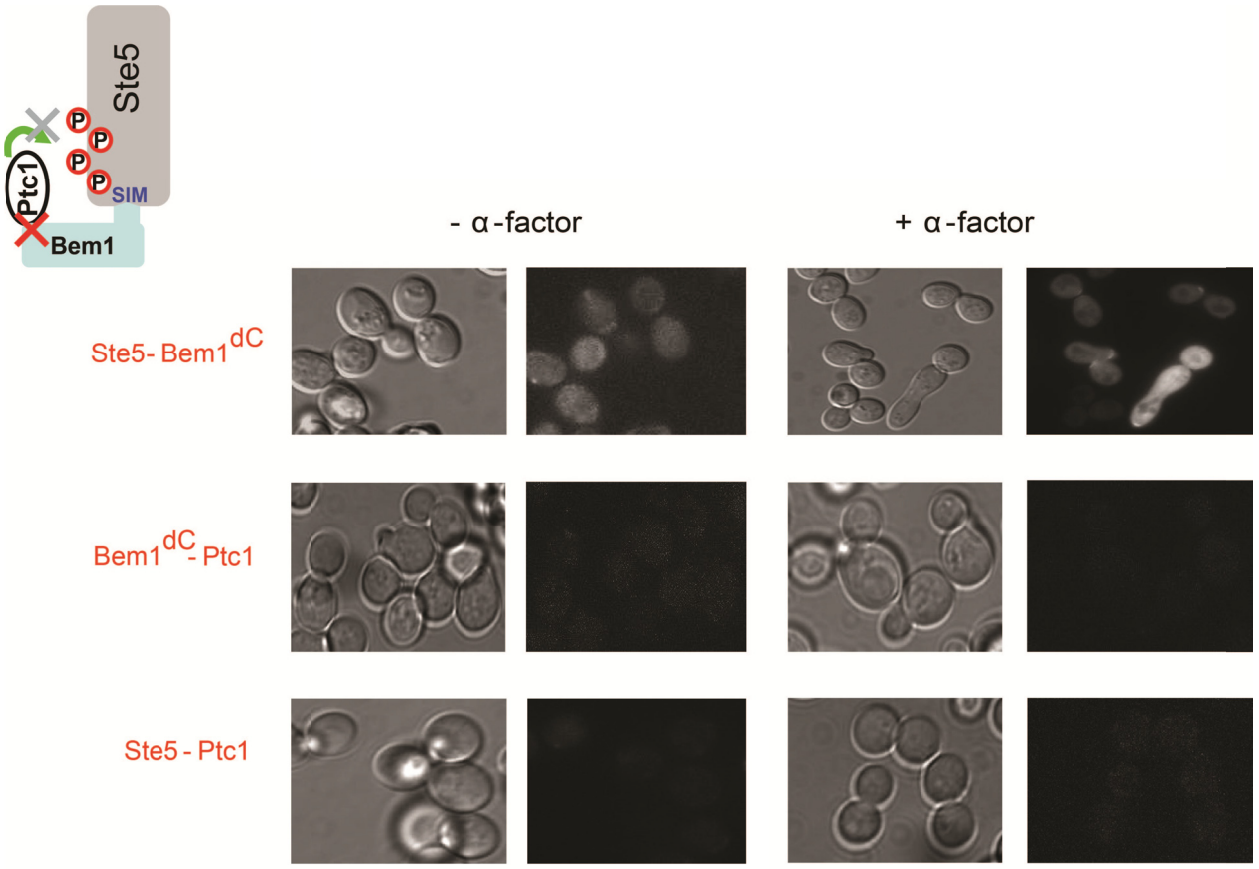

Supplementary figure 5. DIC and Venus PCA images for Ste5-Bem1$^{\Delta 417\text{-}467}$, Bem1$^{\Delta 417\text{-}467}$-Ptc1 and Ste5-Ptc1 interactions in *bem1Δ* cells.
Bem1$^{\Delta 417\text{-}467}$ mutant disrupted Bem1 interaction with Ptc1. Loss of the Ste5-Ptc1 interaction Bem1 is an adaptor essential for Ste5-Ptc1 interaction.

Interaction pair	Venus PCA signal	Mating response
$Bem1^{1-552}$ – Ptc1	+++	+++
$Bem1^{72-552}$ – Ptc1	+++	+++
$Bem1^{1-518}$ – Ptc1	+++	++
$Bem1^{1-467}$ – Ptc1	+++	++
$Bem1^{1-416}$ – Ptc1	-	-
$Bem1^{1-366}$ – Ptc1	-	-
$Bem1^{1-314}$ – Ptc1	-	-
$Bem1^{1-234}$ – Ptc1	-	-
$Bem1^{\Delta 417-467}$ – Ptc1	-	-

Supplementary figure 6. Identification of Bem1 binding region to Ptc1.
Different mutants of Bem1 (with indicated residues) were screened for their interaction with Ptc1 using Venus PCA. The same mutants were tested for their ability to restore the shmooing response in *bem1Δ* cells. A C-terminal domain (residues 417 to 467) of Bem1 is essential for interaction with Ptc1 and to restore the mating response as its deletion abolished both.

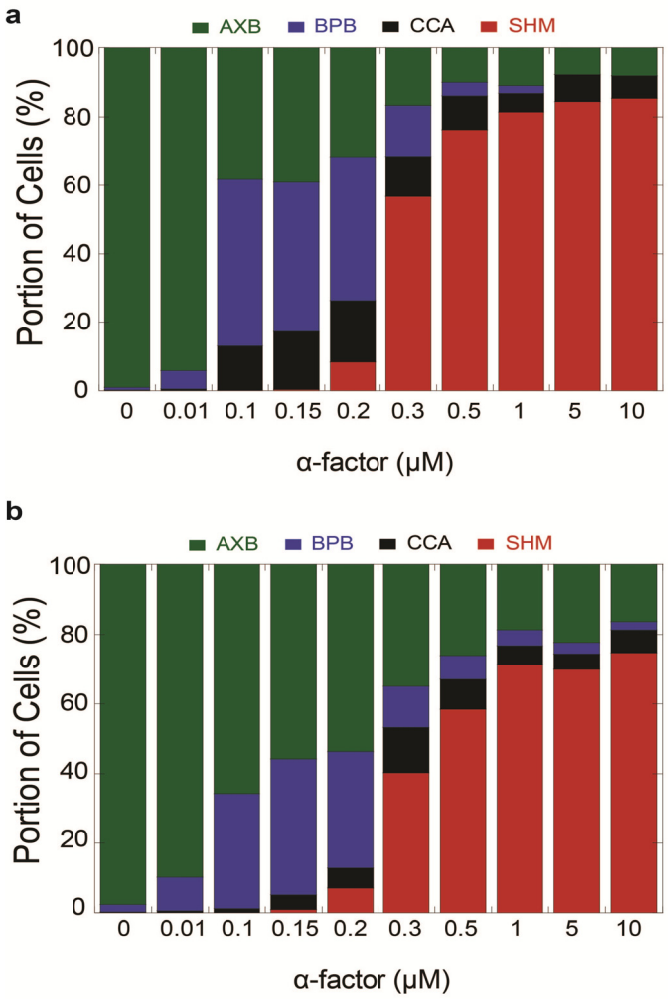

Supplementary figure 7. Morphological changes in response to α-factor in *ste5Δ* cells substituted with mutants Ste5^{8A} (a) or Ste5^{4E} (b) mutant.
Ste5^{8A} mutant did not change the response (in comparison to Ste5^{WT} (Fig 1c)) Ste5^{4E} but Ste5^{8E} (Fig 1d) reduced the sharpness and amplitude of the shmoo response.

Chapter IV: A novel and evolutionarily conserved cross-talk between protein kinase A (PKA) and MAPK signaling pathways regulate the sensitivity of yeast mating response.

Eduard Stefan[1,2], **Mohan K. Malleshaiah**[1], Po Hien Ear[1] and Stephen W Michnick[1]

In this chapter we describe a novel and conserved mechanism by which yeast cells integrate distinct signals in order to prioritize their specific response. Specifically, this mechanism shifts the threshold, but not the amplitude nor switch-like pheromone mating response when simultaneously grown in an ideal carbon source (glucose). This story illustrates an example of signal buffering, where there is a quantitative change in sensitivity of response to a stimulus, modulated by another signal, but with no qualitative effect on the nature (amplitude, sharpness) of the response. The complete study explored this mechanism in both mammalian cells and yeast. This chapter describes the yeast part of the study to maintain the relevance to other parts of the thesis. The article based on the findings from this study has been submitted to the journal *Science*.

Author contributions

Mohan Malleshaiah	Designed & performed Yeast experiments. Analyzed results & wrote the manuscript.
Eduard Stefan	Designed and performed mammalian experiments. Analyzed results and extensively wrote the manuscript. *Mammalian part of study not included in this thesis.*
Po Hien Ear	Performed YCD PCA assay in yeast. *The results included in this thesis.*
Stephen Michnick	Provided overall general supervision. Analyzed the results and wrote the manuscript.

A novel and evolutionarily conserved cross-talk between protein kinase A (PKA) and MAPK signaling pathways regulate the sensitivity of yeast mating response.

Eduard Stefan[1,3], **Mohan K. Malleshaiah**[1], Po Hien Ear[1] and Stephen W Michnick[1,2,†.]

One sentence summary: We have discovered that cAMP-bound regulatory subunits of PKA directly bind to and modulate sensitivity, amplitude and duration of receptor-triggered G-alpha-i GTPase activities and downstream MAP kinase signaling, a mechanism conserved in molecular detail from human to budding yeast.

[1]Département de Biochimie
[2]Centre Robert-Cedergren, Bio-Informatique et Génomique
Université de Montréal
C.P. 6128, Succursale centre-ville
Montréal, Québec H3C 3J7, Canada

[3]Institute of Biochemistry and Center for Molecular Biosciences,
University of Innsbruck, Austria.

† Authors for correspondence

4.1 Abstract

Living cells have evolved signal transduction pathways to distinguish and integrate extracellular signaling cues. Signals received on the cell surface by receptors are transmitted, processed and amplified *via* intracellular effectors of well-tuned and interconnected signaling cascades. G protein coupled receptors (GPCR) provide a classic example through directed signal transmission from the adenylyl cyclase 'inhibitory' G-protein-αi to the 'stimulatory' G-protein-αs coupled receptor pathway, regulating the synthesis of the second messenger cAMP. cAMP binds to regulatory subunits (Reg) of the prototypical protein kinase A (PKA), inducing dissociation and activation of the phosphotransferase activity of PKA catalytic subunits (PKAc). We have discovered that cAMP-bound Reg subunits serve an additional role in signaling through direct and specific binding to G-protein-αi. We demonstrate that cAMP-dependent formation of these complexes in mammalian cells affects conformation and activities of the trimeric G-proteins Gαi:βγ resulting in increased sensitivity, amplitude and duration of GPCR-mediated MAP kinase activation. We further show that the mechanism is conserved in the budding yeast *Saccharomyces cerevisiae* controlling the sensitivity of a mating pheromone-mediated Gαi-coupled MAP kinase cascade to nutrient availability. Similar signal integration and tuning of Gαs- and Gαi-coupled hormone responses mediated by cAMP-bound PKA Reg subunits is likely common in all eukaryotes and may cause unintended off-target effects of many drugs or suggest novel therapeutic strategies for a number of human diseases.

Key words: Cross-talk, synergism, signaling dynamics, information processing, etc.

4.2 Introduction

Inter- and intracellular communications to changes in the surrounding environment are essential to elicit specific responses in both unicellular and multi-cellular organisms. Tuned cellular responses are mediated by signal transduction pathways, which receive a primary signals at the membrane, and trigger a cascade of events that transmits the incoming signal and even amplify it in order to induce the appropriate response outputs. This signal transduction often requires the orchestrated action of enzymes (such as protein kinases, phosphatases, GTPases, etc.), which by sequential phosphorylation or other post-translational modification events enable transmission and finally translation of the signal into a cellular response (Hunter 2000; Ubersax and Ferrell Jr 2007). Two of the most well-characterized signal transduction pathways are the cAMP dependent protein kinase (PKA) and the mitogen-activated protein kinase (MAPK) pathways. Similar to other signaling cascades, the PKA and MAPK pathways do not operate independently of each other, rather they communicate with each other; through a phenomenon commonly referred to as "cross-talk" (Stork and Schmitt 2002; Houslay 2006; Gerits, Kostenko et al. 2008). Cells constantly encounter numerous stimuli from their environment and cross-talk between signalling pathways would allow the cells to regulate the distribution, duration, intensity and specificity of incoming signals and fine-tune the specific responses.

In the yeast *Saccharomyces cerevisiae*, Protein-kinase A (PKA) plays an important role in the regulation of growth, metabolism, stress resistance and filamentous differentiation in response to lack of nutrients. Yeast cells growing on a complete medium with a fermentable carbon source, such as glucose, proliferate and are ovoid in shape. However, if grown on a non-fermentable carbon source, cells accumulate high levels of storage carbohydrates (such as trehalose and glycogen), which induce the expression of stress response element-controlled genes (Gray, Petsko et al. 2004; Schneper, Duvel et al. 2004).

When nitrogen or carbon sources are limited, diploid and haploid yeast exhibit pseudohyphal or invasive growth respectively thought to represent nutrient-seeking behavior (Pan, Harashima et al. 2000). All of these characteristics are determined by the activity of PKA. Constitutively high PKA activity results in hyper-filamentation, respiration deficiency and causes growth arrest. However, if PKA activity is low, cells do not undergo filamentous growth (Cameron, Levin et al. 1988; Pan and Heitman 1999). In its inactive state, PKA is tetrameric complex composed of two regulatory and two catalytic subunits (Reg_2:Cat_2)(Zoller, Kuret et al. 1988). PKA is activated by binding of 3',5'-cyclic adenosine monophosphate (cAMP) to two unique cAMP biding domains (CBD) on the regulatory subunits, inducing dissociation of regulatory from catalytic subunits and deblocking the catalytic subunit catalytic and substrate binding sites(Thevelein and Beullens 1985; Taylor, Kim et al. 2008).

The cAMP–PKA pathway in yeast is essential for viability and is involved in nutrient dependent growth control. Inactivation of adenylate cyclase, Cdc25 or Ras (which are also required for activity of adenylate cyclase and thus synthesis of cAMP), or of PKA causes arrest at the start point in the G1 phase of the cell cycle followed by permanent exit from the growth phase into the stationary G0 phase (Thevelein and Winde 1999). Several nutrient sensors trigger rapid activation of the PKA pathway: Gpr1 for glucose and sucrose (Lemaire, Van de Velde et al. 2004), Gap1 for amino acids (Donaton, Holsbeeks et al. 2003), Pho84 for phosphate (Giots, Donaton et al. 2003) and Mep2 for ammonium (Nuland, Vandormael et al. 2006). Gpr1 is a G-protein coupled receptor (GPCR) that activates PKA through the cAMP signaling.

The budding yeast *Saccharomyces cerevisiae* has homologues of the mammalian signaling components for both PKA and MAPK pathways downstream of GPCRs (Griffioen and Thevelein 2002; Wang and Dohlman 2004; Tamaki 2007). In yeast, glucose and sucrose signals are sensed at the membrane by the GPCR Gpr1 (Yun, Tamaki et al. 1998; Lemaire, Van de Velde et al. 2004)(**Figure 1a & 2**). Gpr1 activates the trimeric G-protein Gα GTPase Gpa2, which in turn activates adenylate cyclase (AC)

to trigger the characteristic glucose-induced accumulation in cellular levels of cAMP (**Figure 2**)(Colombo, Ma et al. 1998). In yeast, the regulatory subunit of PKA is encoded by the *BCY1* gene and the partially redundant catalytic subunits by *TPK1*, *TPK2*, and *TPK3* (Toda, Cameron et al. 1987; Toda, Cameron et al. 1987).

The signaling counterpart to the Gαi:βγ-MAPK cascade in *S. cerevisiae* is the mating pheromone α-factor pathway (in *MAT***a** haploid cells) whose activation results in a number of distinct morphogenic phenotypes at different levels of pheromone stimulus, notably the coherent 'shmoo' response at a critical threshold concentration (**Figures 1a and 2**)(Malleshaiah, Shahrezaei et al. 2010). Gpa1 is a yeast homolog of mammalian Gαi while Gpa2 is of Gαs subunit of GPCRs. Both in yeast and metazoans, Gαi-coupled receptors activate MAP kinase (MAPK) signaling cascades (Dohlman 2002; Goldsmith and Dhanasekaran 2007) (**Figure 1a & 2**).

Here, we show that, the regulatory subunit of PKA (Bcy1 and Reg respectively) interact specifically with the Gα subunit of G-protein associated with MAP kinase signaling (Gpa1 and Gαi respectively). This novel interaction controls the sensitivity of Gαi-protein receptor mediated responses. Our results show that this mechanism is conserved in both yeast and mammalian cells and that it controls important cellular response decisions.

4.3 Results

We first identified, in mammalian COS7 cells, novel interactions of Reg type IIβ PKA subunits (RegIIβ), but not a Cat subunit of PKA with all three isoforms of Gαi (Gαi$_{1,2,3}$) using a 'Venus' yellow fluorescent protein (YFP) protein-fragment complementation assay (PCA) (Remy, Montmarquette et al. 2004; Stefan, Aquin et al. 2007). The Gαi:RegIIβ complexes were localized to the plasma membrane, consistent with known localization of Gαi proteins. These and other details of discovery and validation of the interactions are described in details of our full submitted manuscript.

The evolutionary conservation of regulatory PKA subunits and notably of the Gαi sequence, prompted us to evaluate whether the cAMP-bound Reg subunit mediated modulation of Gαi-signalling is also conserved in yeast. We first tested for the direct interactions of the single Gαi and Gαs homologues (Gpa1 and Gpa2) with the only yeast PKA Reg subunit Bcy1, using the Venus YFP PCA. We observed that Gpa1 but not Gpa2 interact with Bcy1 and the complex is localized at the plasma membrane (**Figure 1b upper panel; Supplementary Figure 1**) suggesting that Bcy1 is recruited to the membrane. These results are consistent with our observations in mammalian cells. Next, we made, point mutations in the homologous Reg:Gαi binding motif of Bcy1 (Bcy1* mutant) and tested for its interaction with Gpa1. We observed a decreased interaction of Bcy1 with Gpa1. The mutations did not affect the Bcy1:Bcy1 or Bcy1:Tpk2 (=Cat) complexes (**Figure 1b lower panel; Supplementary Figure 1**). These results suggest that the specific Reg:Gαi interaction has been conserved for at least 1.5 billion years since Metazoa and Fungi lineages separated (Canaves and Taylor 2002).

We next examined the role of Bcy1 on downstream pheromone signaling response, including activation of yeast Erk1/2 homologue (Fus3) phosphorylation and the shmoo response in the presence of glucose, the trigger for cAMP production. We observed an approximately three-fold decrease in sensitivity to α-factor-induced Fus3 phosphorylation and 'shmoo' response (EC_{50} right shift) in an isogenic knockout of the Bcy1 gene (*BCY1*Δ). Expression of a Reg:Gαi binding motif mutant of Bcy1 (Bcy1*) produced an intermediate (1.6 fold) decrease. Both observations are consistent with reduced MAP kinase activation indicating that; as in mammalian cells, the yeast Reg subunit Bcy1 potentiated the Gαi:βγ-mediated MAPK pathway (**Figure 1c-e; Supplementary Figures 2 & 3**). However, we observed no impact of Bcy1 over-expression on the shmooing response (four hours α-factor exposure, **Figure 1e**), suggesting that Bcy1 is already highly expressed in yeast and that the pathway is less sensitive to over-expression (**Supplementary Figure 3**). Also consistent with our model, the PKA inhibitor KT5720 had no effect on MAPK phosphorylation or the shmoo response (**Supplementary Figures 2 & 3**). Finally, using optimized yeast Cytosine deaminase (OyCD) PCA assay (Ear and Michnick 2009), we observed that mammalian

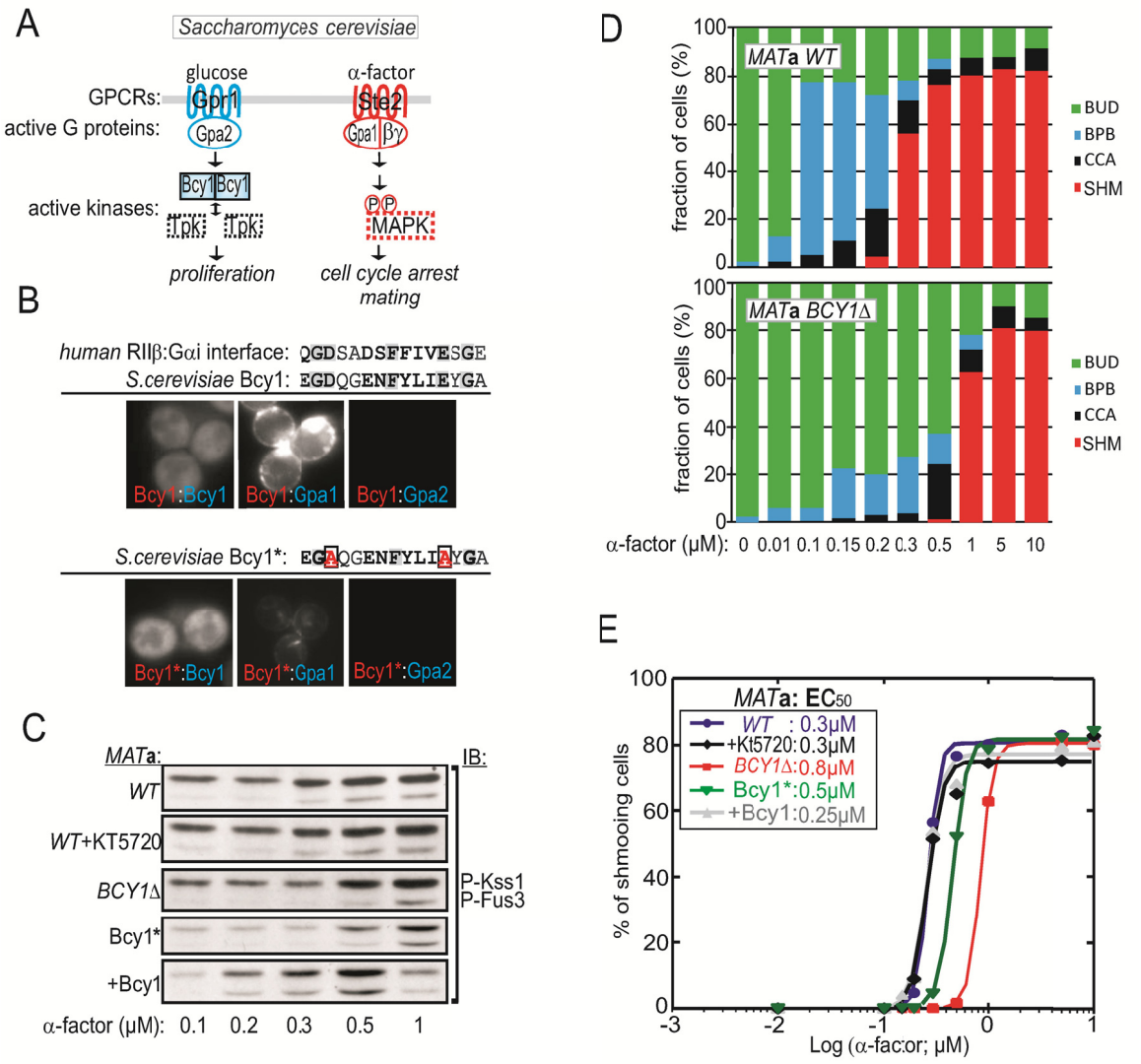

Figure 1. Conservation of cAMP-dependent modulation of MAP kinase signaling *via* R:Gαi (Bcy1:Gpa1) in yeast.

(A) Schematic of the conserved components of glucose and α-factor triggered signaling pathways in *S. cerevisiae*. (B) Fluorescence images of yeast cells expressing the indicated protein pairs fused to Venus YFP PCA F[1] and F[2] reporter protein fragments. Alignment of the human RIIβ:Gαi interface ('Reggai peptide') to yeast homologue Bcy1 (grey box = conservation, bold = conserved substitutions, grey = semi-conserved substitution). Indication of double mutations (in red) in the conserved sequence regions of Bcy1. (C) Dose-dependent effects of α-factor exposure (15 minutes) on phosphorylation of Fus3 and Kss1 (MAPKs) of indicated *MAT***a** strains in the presence of glucose detected by immunoblotting (IB) using an anti-phospho MAPK antibody. (D) Morphological changes in α-factor dose response in *wildtype* (*WT*) and *BCY1*Δ strains in the presence of glucose (BUD, budding; BPB, bipolar budding; CCA, cell cycle arrest; SHM, Shmooing). (E) Hill function curve fits for shmooing cells in α-factor dose- response.

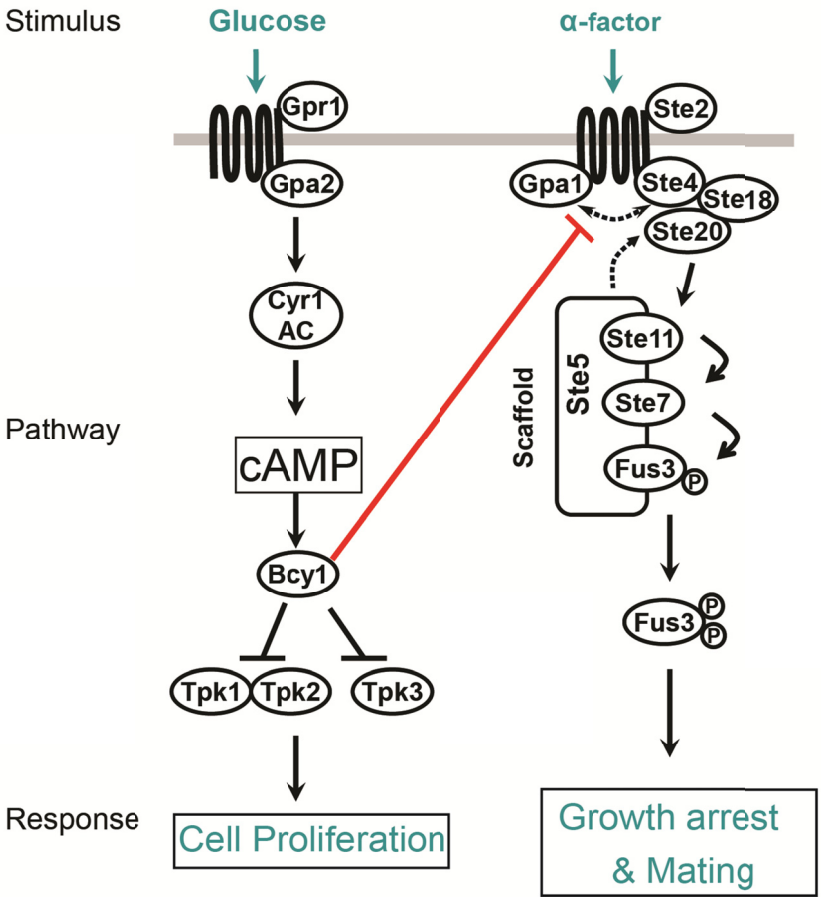

Figure 2. The conserved cross-talk among PKA and MAPK signalling pathways. Bcy1-Gpa1 protein interaction allows yeast cells to integrate pheromone information with respect to that of glucose availability. The direct binding of Bcy1 to Gpa1 inhibits the re-association dynamics of Gpa1 with Gβγ, allowing efficient pheromone information transmission towards activating MAP kinas (Fus3). The availability of glucose (through Bcy1 levels) regulates the sensitivity of cells ability to respond to pheromone concentrations. AC- adenylyl cyclase, Gβ – Ste4 and Gγ – Ste18.

proteins complemented the interactions, since the RegIIβ and Gαi3 interacted with the yeast Reg subunit Bcy1 (**Supplementary Figure 4**). These results suggest that the specific Reg:Gαi interaction has been conserved for at least 1.5 billion years since Metazoa and Fungi lineages separated (Canaves and Taylor 2002).

The biological interpretation of enhancement of pheromone pathway sensitivity by Reg subunit binding to Gαi has a simple functional interpretation: haploid yeast mates to maximize their individual fitness and would likely do so under optimum growth conditions (**Figure 2**). Indeed, budding yeast undergoes meiosis under starvation conditions and will only mate when adequate levels of nutrients become available. Glucose, as the preferred carbon source for yeast, should in part create these conditions, since it activates the Gαs-coupled receptor Gpr1 and therefore the cAMP activating signaling pathway. It follows that, based on our evidence, adequate growth conditions provided by high glucose concentrations will generate cAMP-bound free Reg subunits (Bcy1) that bind to Gαi (Tamaki 2007). Bcy1 binding inhibits the re-association dynamics of Gpa1 with Gβγ - a process that blocks the pheromone information transmission to downstream MAPK cascade. Thus, by affecting the re-association dynamics of Gpa1 with Gβγ, Bcy1 sensitizes the pheromone receptor to extracellular pheromone concentrations leading to switch-like activation of MAP kinas (Fus3) and the mating response.

These findings highlight the flexibility and versatility of signaling networks to distinctly regulate quantitative and qualitative responses to one or more stimuli simultaneously. By selectively affecting only the sensitivity of cells to pheromone concentrations and not the nature (amplitude, sharpness) of the mating response, yeast cells have evolved to meaningfully integrate nutrients and mating signal information. Similar mechanisms, as the one we have described here of distinct changes to quantitative and qualitative responses in other systems (especially metazoans), should explain cellular strategies to integrate wide variety of stimuli information.

4.4 References

Cameron, S., L. Levin, et al. (1988). cAMP-Independent control of Sporulation, Glycogen-metabolism and Heat-shock resistance in *S. cerevisiae*. *Cell* **53**(4): 555-566.

Canaves, J. M. and S. S. Taylor (2002). Classification and phylogenetic analysis of the cAMP-dependent protein kinase regulatory subunit family. *J Mol Evol* **54**(1): 17-29.

Colombo, S., P. Ma, et al. (1998). Involvement of distinct G-proteins, Gpa2 and Ras, in glucose- and intracellular acidification-induced cAMP signalling in the yeast Saccharomyces cerevisiae. *EMBO J* **17**(12): 3326-3341.

Dohlman, H. G. (2002). G-Proteins and Pheromone signaling. *Annual Review of Physiology* **64**(1): 129-152.

Donaton, M. C. V., I. Holsbeeks, et al. (2003). The Gap1 general amino acid permease acts as an amino acid sensor for activation of protein kinase A targets in the yeast (*Saccharomyces cerevisiae*). *Molecular Microbiology* **50**(3): 911-929.

Ear, P. H. and S. W. Michnick (2009). A general life-death selection strategy for dissecting protein functions. *Nat Meth* **6**(11): 813-816.

Gerits, N., S. Kostenko, et al. (2008). Relations between the mitogen-activated protein kinase and the cAMP-dependent protein kinase pathways: Comradeship and hostility. *Cellular Signalling* **20**(9): 1592-1607.

Giots, F., M. C. V. Donaton, et al. (2003). Inorganic phosphate is sensed by specific phosphate carriers and acts in concert with glucose as a nutrient signal for activation of the protein kinase A pathway in the yeast (*Saccharomyces cerevisiae*). *Molecular Microbiology* **47**(4): 1163-1181.

Goldsmith, Z. G. and D. N. Dhanasekaran (2007). G protein regulation of MAPK networks. *Oncogene* **26**(22): 3122-3142.

Gray, J. V., G. A. Petsko, et al. (2004). "Sleeping Beauty": Quiescence in Saccharomyces cerevisiae. *Microbiol. Mol. Biol. Rev.* **68**(2): 187-206.

Griffioen, G. and J. M. Thevelein (2002). Molecular mechanisms controlling the localisation of protein kinase A. *Curr Genet* **41**(4): 199-207.

Houslay, M. D. (2006). A RSK(y) Relationship with Promiscuous PKA. *Sci. STKE* **2006**(349): pe32-.

Hunter, T. (2000). Signaling--2000 and Beyond. *Cell* **100**(1): 113-127.

Lemaire, K., S. Van de Velde, et al. (2004). Glucose and Sucrose Act as Agonist and Mannose as Antagonist Ligands of the G Protein-Coupled Receptor Gpr1 in the Yeast Saccharomyces cerevisiae. *Molecular Cell* **16**(2): 293-299.

Malleshaiah, M. K., V. Shahrezaei, et al. (2010). The scaffold protein Ste5 directly controls a switch-like mating decision in yeast. *Nature* **465**(7294): 101-105.

Nuland, A. V., P. Vandormael, et al. (2006). Ammonium permease-based sensing mechanism for rapid ammonium activation of the protein kinase A pathway in yeast. *Molecular Microbiology* **59**(5): 1485-1505.

Pan, X. and J. Heitman (1999). Cyclic AMP-Dependent Protein Kinase Regulates Pseudohyphal Differentiation in Saccharomyces cerevisiae. *Mol. Cell. Biol.* **19**(7): 4874-4887.

Pan, X. W., T. Harashima, et al. (2000). Signal transduction cascades regulating pseudohyphal differentiation of Saccharomyces cerevisiae. *Current Opinion in Microbiology* **3**(6): 567-572.

Remy, I., A. Montmarquette, et al. (2004). PKB/Akt modulates TGF-beta signalling through a direct interaction with Smad3. *Nat Cell Biol* **6**(4): 358-365.

Schneper, L., K. Duvel, et al. (2004). Sense and sensibility: nutritional response and signal integration in yeast. *Current Opinion in Microbiology* **7**(6): 624-630.

Stefan, E., S. Aquin, et al. (2007). Quantification of dynamic protein complexes using Renilla luciferase fragment complementation applied to protein kinase A activities in vivo. *Proc Natl Acad Sci U S A* **104**(43): 16916-16921.

Stork, P. J. S. and J. M. Schmitt (2002). Crosstalk between cAMP and MAP kinase signaling in the regulation of cell proliferation. *Trends in Cell Biology* **12**(6): 258-266.

Tamaki, H. (2007). Glucose-Stimulated cAMP-Protein Kinase A Pathway in Yeast Saccharomyces cerevisiae. *The Society for Biotechnology, Japan* **104**(4): 245-250.

Taylor, S. S., C. Kim, et al. (2008). Signaling through cAMP and cAMP-dependent protein kinase: diverse strategies for drug design. *Biochim Biophys Acta* **1784**(1): 16-26.

THEVELEIN, J. M. and M. BEULLENS (1985). Cyclic AMP and the Stimulation of Trehalase Activity in the Yeast Saccharomyces cerevisiae by Carbon Sources, Nitrogen Sources and Inhibitors of Protein Synthesis. *J Gen Microbiol* **131**(12): 3199-3209.

Thevelein, J. M. and J. H. d. Winde (1999). Novel sensing mechanisms and targets for the cAMP & protein kinase A pathway in the yeast Saccharomyces cerevisiae. *Molecular Microbiology* **33**(5): 904-918.

Toda, T., S. Cameron, et al. (1987). Cloning and characterization of BCY1, a locus encoding a regulatory subunit of the cyclic AMP-dependent protein kinase in Saccharomyces cerevisiae. *Mol. Cell. Biol.* **7**(4): 1371-1377.

Toda, T., S. Cameron, et al. (1987). 3 Different genes in *Saccharomyces Cerevisiae* encode the catalytic subunits of the cAMP-Dependent protein kinase. *Cell* **50**(2): 277-287.

Ubersax, J. A. and J. E. Ferrell Jr (2007). Mechanisms of specificity in protein phosphorylation. *Nat Rev Mol Cell Biol* **8**(7): 530-541.

Wang, Y. and H. G. Dohlman (2004). Pheromone signaling mechanisms in yeast: a prototypical sex machine. *Science* **306**(5701): 1508-1509.

Yun, C.-W., H. Tamaki, et al. (1998). Gpr1p, a Putative G-Protein Coupled Receptor, Regulates Glucose-Dependent Cellular cAMP Level in YeastSaccharomyces cerevisiae. *Biochemical and Biophysical Research Communications* **252**(1): 29-33.

Zoller, M. J., J. Kuret, et al. (1988). Purification and characterization of C1, the catalytic subunit of Saccharomyces cerevisiae cAMP-dependent protein kinase encoded by TPK1. *Journal of Biological Chemistry* **263**(19): 9142-9148.

Acknowledgements: We thank Alfred Gilman and Henry Bourne for advice, Mel Simon and Iain Fraser for cDNAs and Elliott Ross, Klaus Bister and Antonio Feliciello for comments on the manuscript. E.S. would like to thank K. Bister for his continuous support and critical discussions. We thank Mireille Hogue for the EPAC cAMP measurements. We thank S. Geisler and F. Croze for technical assistance, J.F. Paradis for management support, and E. Klussmann for providing constructs. This work was supported by grants from the Canadian Institutes of Health Research (MOP-GMX-152556 to S.W.M.) (MOP-FRN-10501 to M.B.), the Austrian Science Fund Grant (FWF; P22608) and 'Junior Researcher Support 2009' (University of Innsbruck) to E.S, an NIGMS Glue Grant (U54 GM062114 to the Alliance for Cellular Signaling to S.W.M.) and Canada Research Chairs to S.W.M and M.B.

Author contributions: E.S. and S.W.M. conceived the project. E.S., M.M., B.B. and P.E. performed the experiments. M. Beyermann and M.B. contributed reagents. E.S, M.M, M.B. and S.W.M. analyzed the results. E.S., M.M., M.B. and S.W.M. wrote the manuscript.

*To whom correspondence should be addressed.

4.5 Supplementary figures

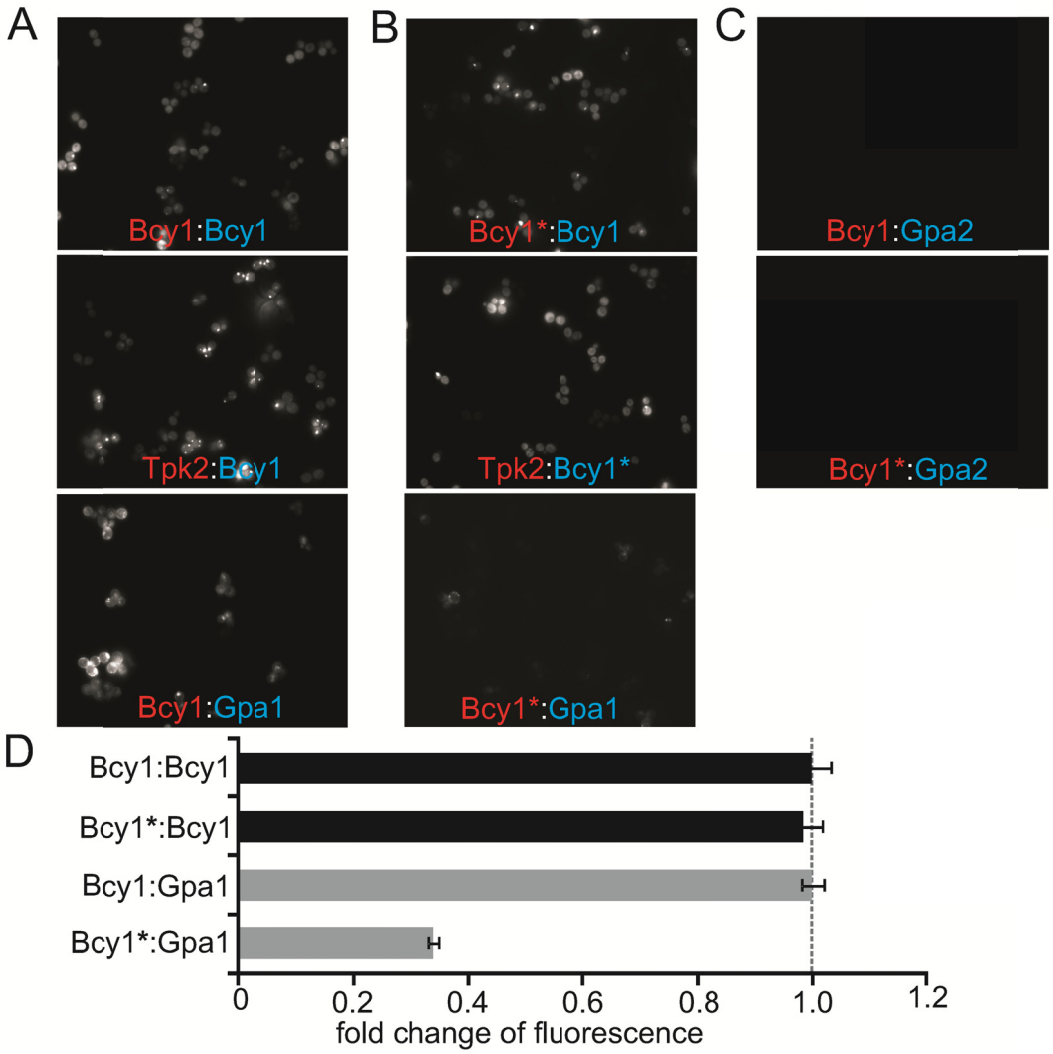

Supplementary figure 1. Detection of protein-protein interactions and visualization of their cellular locations in *S.cerevisiae* with Venus YFP PCA.
Fluorescence images were taken of yeast cells expressing the indicated proteins fused to YFP PCA F[1] (in red) or fused to F[2] (in blue). (A-C) *WT* Bcy-F[1] or F[2] was coexpressed with the indicated protein-F[1] or F[2] fusions. The double mutant Bcy1*-F[1] or F[2] was coexpressed with the indicated protein-F[1] or F[2] fusions. (D) Fluorescence images of yeast cells expressing the indicated protein couples tagged with Venus YFP PCA F[1] and F[2] have been analyzed from the individual cells after subtraction of cellular fluorescence using ImageJ (±SEM, n=3 independent experiments).

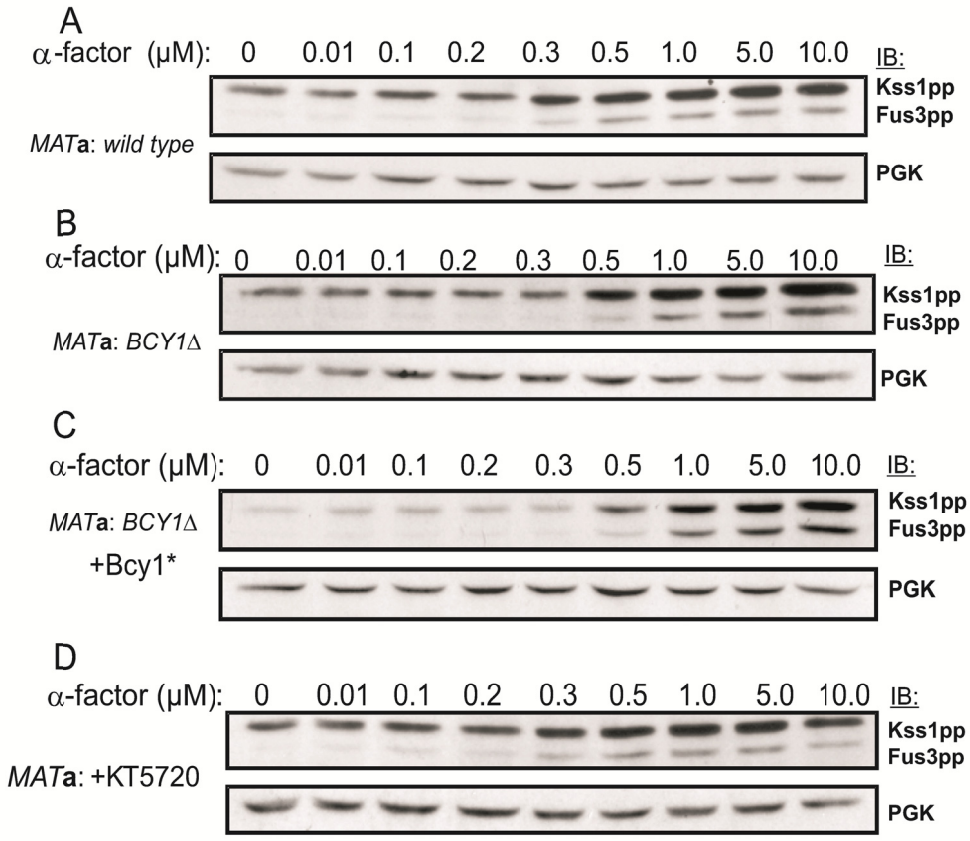

Supplementary figure 2. Phosphorylation of MAPKs Kss1 and Fus3 in α-factor treated *MAT*a cells.

Dose dependence of Fus3 and Kss1 phosphorylation in response to α-factor in indicated *MAT***a** strains detected by immunoblotting (IB) using an anti-phospho MAPK antibody. (A) Response in *MAT***a** *wild type* (*WT*) strain. (B) Response in *MAT***a** *BCY1*Δ knockout strain. (C) Response in *MAT*a *BCY1*Δ knockout strain overexpressing the mutant version of Bcy1*. (D) Response in *MAT***a** *wild type* (*WT*) strain treated with 5 μM KT5720 for 60 minutes. Phosphoglycerate kinase (PGK) expression levels were used as loading control.

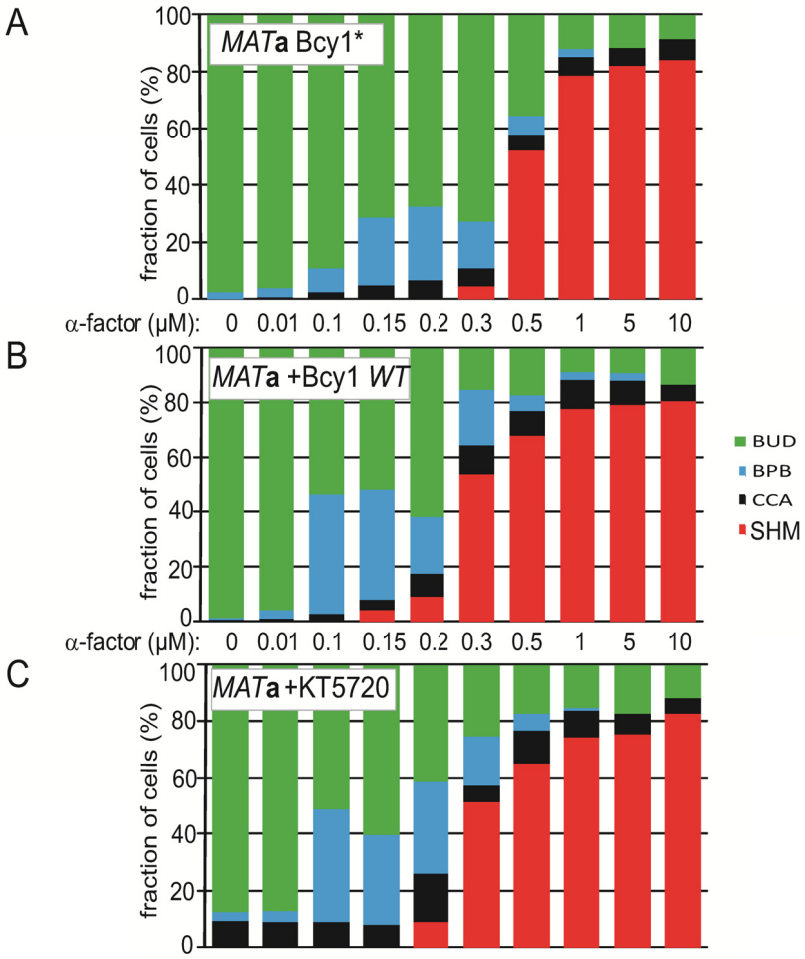

Supplementary figure 3. Morphogenic responses in response to α-factor.
Quantifications of the phenotypical consequences of dose dependent α-factor exposure in the presence of glucose (A) in *MAT***a** *BCY1*Δ knockout strain, (B) in *MAT***a** *BCY1*Δ knockout strain overexpressing the mutant version of Bcy1*, (C) in *MAT***a** *wild type* (*WT*) strain treated with 5 μM KT5720 for 60 minutes (BUD, budding; BPB, bipolar budding; CCA, cell cycle arrest; SHM, Shmooing) treated *MAT***a** cells

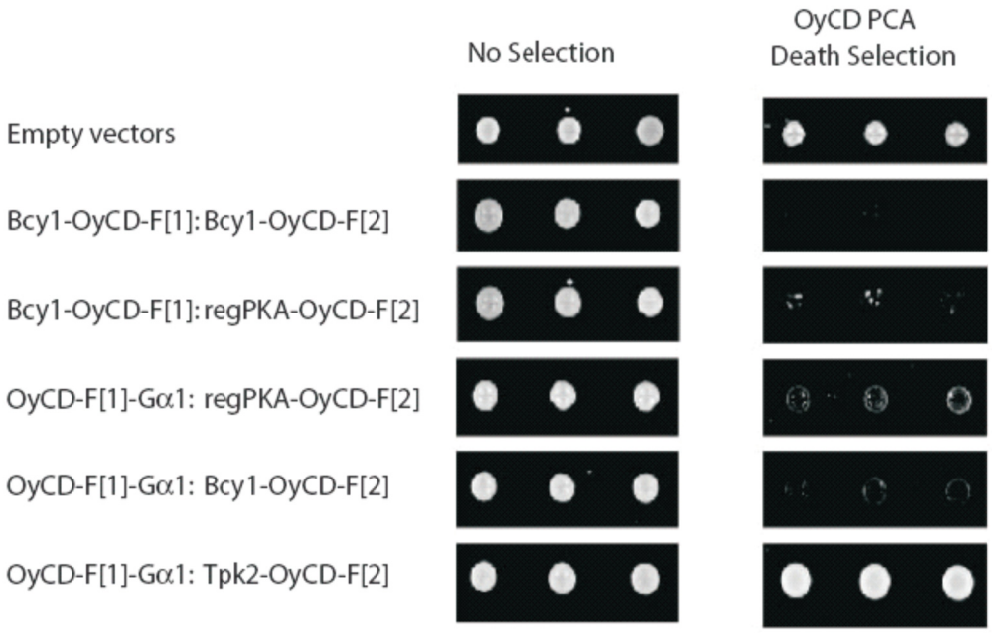

Supplementary figure 4. Interactions between human RegIIβ, Gαi3 and *S. cerevisiae* homologues.

Protein:protein interactions between mammalian or yeast PKA subunits and Gαi3 were detected using the death selection OyCD PCA. Indicated cDNAs were fused to either OyCD PCA fragments F[1] (red) or F[2] (blue). In this assay, cells that express interacting fusion proteins cannot grow in the presence of 1 μg/ml of 5-fluorocytosine (death selection medium). Three different clones of yeast expressing the indicated fusion proteins were pinned on non-selection or death selection media. The following interactions were detected: the yeast regulatory PKA subunit Bcy1 and itself, Bcy1 and the mammalian regulatory PKA subunit RegIIβ, Gαi3 and RegIIβ and Gαi3 and Bcy1. No interaction was detected between Gαi3 and the yeast catalytic PKA subunit Tpk1.

DISCUSSION

Chapter V: Discussion

In a prototypical example of the well-studied, pheromone stimulus mediated signaling in yeast, with novel discoveries, we have systematically elucidated some of the basic underlying mechanisms that regulate the 'switch-like' mating response. Thus, this work provides a dynamic model of key signaling circuits within a pathway that are attributed to achieve the overall accurate response (**Figure 1**). Further, our findings reveal how cells have evolved to measure, integrate and elicit a specific response to single and multiple stimuli.

5.1 Dynamic model for 'switch-like' yeast mating decision

Here, we have described a comprehensive mechanism to explain how yeast cells can generate 'switch-like' response to a graded pheromone stimulus (**Figure 1**). It consists of a central 'zero-order ultrasensitivity' mechanism generated by the core 'Ptc1-Ste5-Fus3' circuit. We have shown that the interactions between the Ste5 scaffold (substrate) & its four phosphorylation sites, Fus3 kinase and Ptc1 phosphatase in yeast controls the morphological switch from vegetative growth to shmooing, which occurs as pheromone levels increase. The switch is generated by Ste5 and a competition between Fus3 and the phosphatase Ptc1 to determine the levels of phosphorylated Ste5 (**Figure 1).** This basic core protein circuit of the yeast mating switch consists of the same type of elements as the ones originally described in the Goldbeter and Koshland model, i.e. a kinase and a phosphatase acting on a common substrate, but ultrasensitivity is achieved in a different way (Goldbeter and Koshland 1981; Ferrell 1996). First, enzymes are not saturated with respect to excess substrate instead, the low abundant substrate saturates the enzymes by virtue of having multiple (4) sites. Second, both the kinase and phosphatase enzymes are bound to separate sites those are distinct from their catalytic sites.

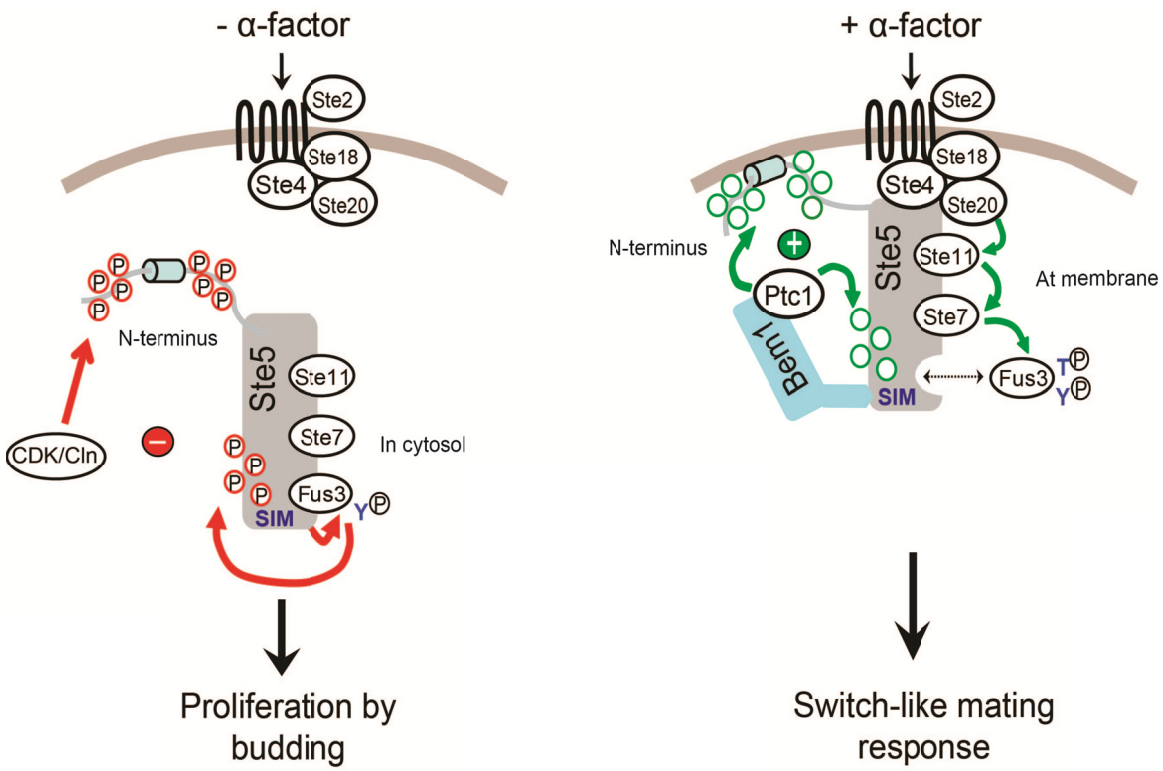

Figure 1. Schematic model of yeast mating signalling.
Multiple phosphorylations at two regions on Ste5 scaffold – four at Fus3 binding region and eight at its N-terminal membrane binding region, prevent Fus3 activation and keeps Ste5 away from membrane respectively, thus preventing any form of signalling in the absence of pheromone (left). Rapid translocation of Ste5 to membrane in the presence of pheromone (right) brings it in close proximity to Bem1 bound Ptc1, which, dephosphorylate the phosphosites at both regions on Ste5 thus simultaneously promoting both Fus3 activation and enhancement in Ste5 membrane recruitment.

Achieving the optimal conditions in the circuit in order to generate the two-stage mediated zero-order mechanism involves the combination of various signaling protein dynamics. Some of the key dynamic aspects and their combinations critical for the optimal functioning of the 'Fus3-Ste5-Ptc1' circuit include, specific protein-protein interactions of Ste5 with both Fus3 and Ptc1, their affinity and kinetics, conformational changes in Ste5, directed translocation of Ste5, Fus3 and Ptc1 towards and away from the locus of signaling. Our findings when considered with previous knowledge results in a dynamic model for switch-like response observed with yeast mating (**Figure 1**).

Achieving the phosphorylated state of Ste5 in the absence of pheromone requires Fus3 to first recognize the specific docking motif on Ste5 and bind to it with enough affinity so it can undergo conformational change to induce auto-phosphorylation on one of its activation loop phospho sites (Bhattacharyya, Remenyi et al. 2006). Interaction and partially active catalytic activity of Fus3 brings about phosphorylation of all four Ste5 sites, which further increases the affinity of Fus3 binding to Ste5. Thus, partially active molecules of Fus3 are sequestered on Ste5 away from all of its potential substrates. Since there is no contact between Ptc1 phosphatase and Ste5 phosphosites, Fus3 dominates by retaining Ste5 fully phosphorylated at steady state. Since, membrane recruitment of Ste5 is crucial to initiate the signaling into its assembled MAPK cascade, in the absence or at weaker pheromone concentrations, Ste5 also remain phosphorylated at its multiple N-terminal sites (by the CDK) (van Drogen, Stucke et al. 2001; Strickfaden, Winters et al. 2007) (**Figure 1**). Phosphorylated state of the N-terminal sites creates a bulk negative charge around the Ste5 basic membrane-binding motif resulting in its electrostatic repulsion from the acidic (negatively charged) phospholipids of the inner membrane (Serber and Ferrell 2007; Strickfaden, Winters et al. 2007). N-terminal phosphorylation of Ste5 prevents ultrasensitivity in the recruitment of Ste5 to the membrane and thus ultrasensitivity in the observed interaction of Ste5 with Bem1 and associated Ptc1. This results in a decrease of Ptc1 local concentration at Ste5 phosphosites. This decrease in Ptc1 saturation results in the sub-optimal functioning of the zero-order switch and resulting reduction in the sharpness and amplitude of the mating response (Chapter III). Treatment with pheromone results in Ste5 re-equilibration to the membrane, probably due

to interaction with the dissociated Gβγ complex of the trimeric G-protein and can associate with the Bem1-Ptc1 complex (Yu, Pesce et al. 2008; Brent 2009). Dephosphorylation of the N-terminal phosphosites by Ptc1 allowing the PM to bind to membrane, thus enhancing the equilibration of Ste5 to membrane (**Figure 1**). Ptc1, now exceeds Fus3 in its local concentration at the Ste5 phosphosites resulting in its increased capacity to dephosphorylate Ste5. The resulting reduction of phosphorylation of Ste5 (at Fus3 binding region) reduces the binding affinity of Fus3 for Ste5, allowing Fus3 to interact with and be phosphorylated and activated by the MAPKK Ste7 (Chapter II). Complete activation of Fus3 and its dissociation from Ste5 complex happens in an ultrasensitive manner. Fully active Fus3 now drives the downstream signaling events including induction of transcription, cell cycle arrest and polarization in order to mediate the switch-like mating response (Elion 2000) (**Figure 1**).

5.2 Accuracy of the yeast mating response

Cells achieve accuracy in their response to stimuli by maintaining the right sensitivity, sharpness and amplitudes of responses (**Figure 2**). The sensitivity to a stimulus sets a threshold for the level of stimulus at which a cell will respond. Sensitivity also help cells to integrate the 'range or fold of stimulus concentration' over which they switch from being non-responsive to responsive; Sharpness of a response determines the dynamic range of stimulus over which a population of cells respond; Amplitude dictates the maximal response that can be achieved, determining the fidelity with which a signal produces a deterministic response over a population of cells. The combination of sensitivity, sharpness and amplitude would thus results in an accurate stimulus/response. At a molecular level, a selection pressure for the specific and robust stimulus response have resulted in the evolution of "signaling motifs", often a kinase, phosphatase and their mutual substrate (Ma, Trusina et al. 2009). Such motifs within a signaling pathway have to function at their optimal level in order to achieve the required accuracy (Ferrell 2002). The balancing (or unbalancing) act of enzymes in such motifs dictates the stimulus-

responses (Goldbeter and Koshland 1981). In addition, such motifs must be in tune with the upstream stimulus and its variations. The optimal functioning of a motif could be regulated by various mechanisms; controlling the extent of their activation and inactivation, regulating their intracellular levels by controlling their expression and degradation, regulating their availability at the locus of signaling within the cell (by sequestering away from or by inducing the translocation to the locus), regulating their association with each other (protein-protein interactions; their affinities and kinetics) and finally, the catalytic activity of the enzymes themselves. Often it is various combinations of these basic mechanisms that are woven together to achieve the required optimal functioning of a circuit that in turn regulates the response.

5.2.1 Sharpness and amplitude in mating response

Accuracy in the mating response is achieved by various aspects of the circuit components. The multiple phosphorylation sites on a single protein and two-stage enzyme binding are essential to generate ultrasensitivity in the mating response. While the first-stage physical binding is essential to bring the enzymes closer to the substrate, the second-stage binding allows the enzymes to carry out their catalytic activity. Multiple phosphorylation sites are required to cause individual enzyme molecules to be locally saturated (Chapter II). The phosphorylated state of the sites in turn controls the affinity of the first-stage binding of enzymes (at least the kinase) to the substrate. Disruption of the two-stage binding of enzymes (Fus3 kinase via $Ste5^{ND}$ and Ptc1 phosphatase via $Ste5^{AAAA}$ mutants) completely destroys the switch in mating response. On the other hand, reducing the phosphorylated state of sites from four to one systematically reduced the sensitivity and sharpness of the mating response (**Chapter II and Figure 2**). Since the enzymes are bound in a stoichiometric complex with their substrate, the core circuit (Ptc1-Ste5-Fus3) is also robust (i.e., insensitive to changes in its individual component concentrations).

The next important contribution towards achieving the right amplitude in combination with the sharpness of mating response comes from the ultrasensitive membrane recruitment of Ste5 (**Figure 2**). In the presence of higher pheromone

concentration, Ste5 is induced to translocate to the plasma membrane where its association with Bem1 brings it into contact with the Ptc1 phosphatase (van Drogen, Stucke et al. 2001; Brent 2009). As indirectly measured through Ptc1 interaction with Ste5, the recruitment of Ste5 to membrane is ultrasensitive (with an $n_H \approx 2$). In addition to contacting Ptc1, Ste5 recruitment to membrane is one of the first events essential to efficiently transfer the stimulus induced G-protein activation information into activation of the MAPK cascade. This ultrasensitivity thus would amplify (or prime) the signaling (Ferrell 1998). The ultrasensitive Ste5 recruitment to Ptc1 (via Bem1) is dependent on its membrane recruitment (Chapter III). Thus, prevention of Ste5 binding to membrane through one branch (N-terminal multiple phosphorylations) disrupted the ultrasensitivity in Ptc1-Ste5 complex formation. Ultrasensitive Ptc1-Ste5 complex formation is essential for the two-stage binding mediated zero-order ultrasensitivity to optimally operate (Chapter II). Hence, the priming of Ste5 with Ptc1 and other signaling events at the membrane is essential to achieve the observed sharpness ($n_H \approx 9$) and amplitude (~ 80%) in the mating response (**Chapter III and Figure 2**). Prevention of priming by disruption of the multiple phosphorylations dependent Ste5 ultrasensitive membrane recruitment reduced both the sharpness and amplitude of response.

5.2.2 Sensitivity in mating response

Cells often encounter more than one stimulus in their surroundings. The simultaneous presence of multiple stimuli presents a challenge in that, now, cells have to simultaneously integrate multiple stimuli information in order to elicit a meaningful response. Under these conditions, cells might come under pressure to prioritize their response depending on the extremity of stimulus or in order to efficiently utilize intracellular resources. One way of prioritizing the multiple stimulus responses is to have different sensitivity to a stimulus under different conditions. Yeast express several modular signaling pathways that are responsible for processing specific stimuli in order to elicit a specific response (Qi and Elion 2005; Carmona-Gutierrez, Eisenberg et al. 2010).

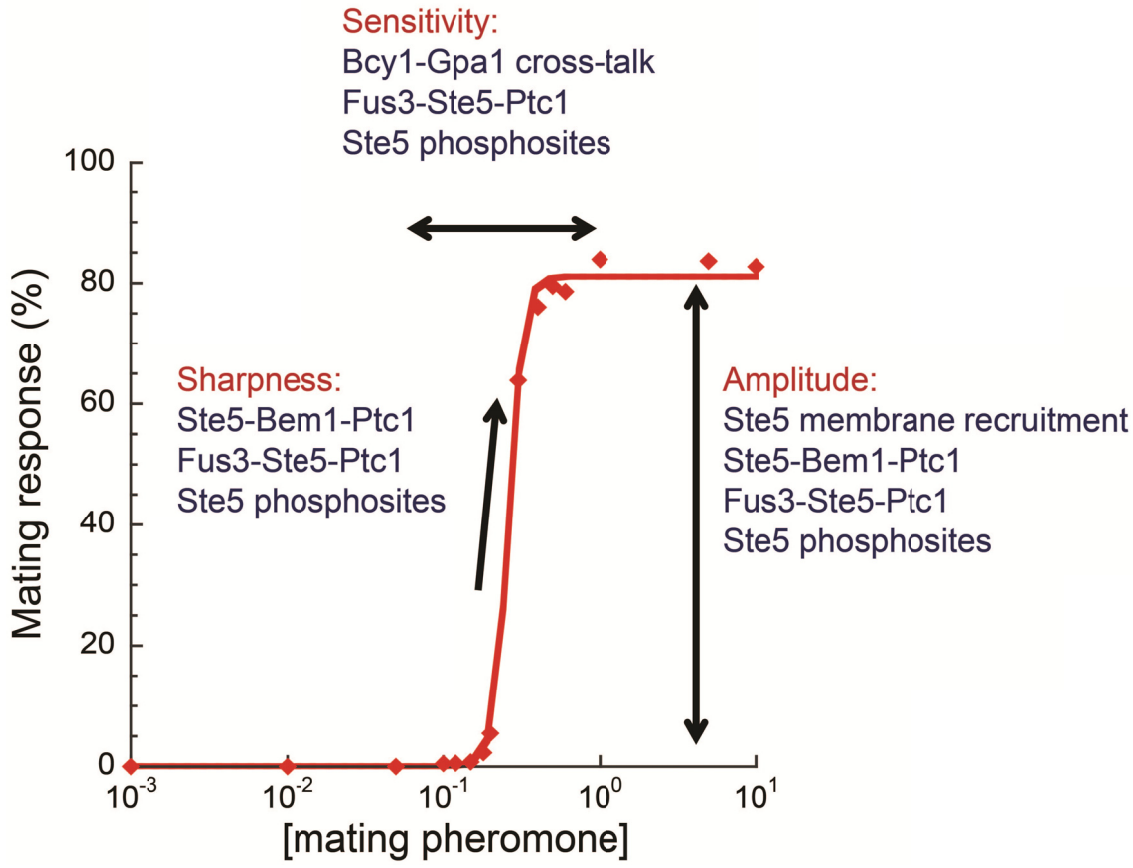

Figure 2. Schematic to show various elements of the accurate switch-like stimulus/response behavior in yeast mating system.
Sharpness (switch) is generated and maintained by the Fus3-Ste5-Ptc1 and Ste5-Bem1-Ptc1 circuits both of which are dependent on multiple phosphorylation sites of Ste5. In addition to the above circuits the maximal response (amplitude) is achieved by Ste5 membrane recruitment translocation dynamics. Sensitivity, without any influence on the steepness and amplitude, was specifically regulated by the cross pathway interaction of Bcy1 with Gpa1. All three elements of the response curve are inter-dependent and so are underlying molecular circuits. Thus, various molecular circuits within a network and their dynamic properties have to be in sync in order to generate an appropriate response to a stimulus.

Often more than one pathway shares common proteins, posing another challenge to maintain the specificity of signaling. For example; Ste11 is common to mating, filamentous and osmolar pathways; Ste7 and Kss1 are common to mating and filamentous pathways (Qi and Elion 2005).

In order to efficiently integrate and maintain the specificity to stimuli, modular signaling pathways often intersect in the form of "cross-talks". For example; mating and filamentous pathways communicate with each other through Fus3 interaction with Tec1 – a transcriptional factor of filamentous network (Bao, Schwartz et al. 2004; Chou, Zhao et al. 2008). In the presence of higher pheromone stimulus, active Fus3 phosphorylate Tec1 leading to its ubiquitination and degradation. This cross-talk allows cells to maintain their specific stimulus response to pheromone without inducing filamentous response. In a similar example, yeast cells have evolved to integrate the presence of both pheromone and osmolar stimuli and their variations through mutual inhibition cross-talk at the MAP kinase level (McClean, Mody et al. 2007). Fus3 interaction with Hog1 and their mutual inhibitions allows cells to elicit either a pheromone or osmolar specific response in a bistable manner.

Here, we have elucidated a novel and conserved cross-talk mechanism that allow cells to integrate stimulus information with respect to another in order to prioritize their response. The novel cross-talk interaction between the regulatory subunit of the PKA and the alpha subunit of the G-proteins enable cells to integrate pheromone intensity with respect the nutrients availability (Chapter IV). The same mechanism is conserved in both yeast and metazoan cells. The cross-talk allows metazoan and yeast cells to adjust their response sensitivity to the growth hormone and pheromone stimulus respectively (**Chapter IV and Figure 2**). In metazoans, higher forskolin (a general activator of PKA pathway) stimulus increases the free regulatory subunit that directly binds to the G-alpha subunit (associated with active hormone receptors) that allows cells to be optimally sensitive and respond to growth hormones by activating the MAP kinase. Conversely, if the forskolin is limiting, the strength of the cross-talk is reduced which in turn reduces the sensitivity for growth hormone stimulus response. In yeast cells, this novel cross-talk

allows cells to integrate the simultaneous presence of glucose (an essential and preferred carbon source) and pheromone stimuli. In the presence of higher glucose, due to higher cAMP, more of Bcy1 is freely available to bind to the G-alpha subunit associated with the active pheromone receptor (Chapter IV). The Bcy1 binding reduces the re-association rate of G-alpha with the G$\beta\gamma$ allowing cells to efficiently respond to pheromone. This way cells are able to optimally respond with higher sensitivity to pheromone concentrations in the presence of essential nutrients. When the glucose concentrations are limiting and cells encounter pheromone, since there is less of free Bcy1 to bind to G-alpha subunit, the later readily re-associates with Gβγ and reduces the sensitivity in response to pheromone.

The combinatorial nature of the mating switch circuit further highlights the flexibility of the basic ultrasensitivity generating mechanisms to evolve and combine various physicochemical properties of the circuit components to generate the suitable response in a signaling system. The combinatorial nature of the circuit components in addition to maintain the accuracy also renders robustness to the yeast mating response (**Figure 1**).

5.3 Regulation of Fus3-Ste5 affinity by multiple phosphorylations

We have observed that the affinity of the Fus3 binding to Ste5 is linearly dependent on the number of Ste5 phosphosites that are phosphorylated. As the phosphorylations increase the affinity of Fus3 binding to Ste5 increases and inversely as the phosphorylations decrease, the affinity reduces (Chapter II). Even though we have observed that the sudden flip in the Ste5 phosphorylated state creates the switch, the mechanism of how the phosphorylated state modulates the affinity of Fus3-Ste5 complex remains unknown (**Figure 2**). Further, in addition to switch-like release of Fus3 from Ste5, we have observed switch-like activation of Fus3 that is essential to drive the final morphological transformation for mating (shmooing) (Chapter II). Thus, Ste7, the upstream MAPK kinase that phosphorylate and activate Fus3 could be thought to be an

integral part of the switch. Then, how does the phosphorylation state of Ste5 bring about switch-like activation of Fus3 by Ste7?

The phosphorylation state dependent change in affinity of Fus3 to Ste5 might be due to the negative charge of the phosphate groups directly affecting binding (Nash, Tang et al. 2001; Serber and Ferrell 2007; Strickfaden, Winters et al. 2007) or from conformational changes on Ste5 as a result of change in phosphorylation state of its phosphosites. Understanding the exact mechanism requires further investigation. But, a clue to the mechanism comes from a recent study that described the mechanism behind essentiality of Ste5 for Ste7 mediated activation of Fus3 (Good, Tang et al. 2009). A domain in Ste5 scaffold (minimal scaffold – amino acids 593 to 786) that overlaps with its Ste7 binding site is found to catalytically unlock Fus3 for phosphorylation by Ste7. This domain selectively increases the K_{cat} of Fus3 phosphorylation by Ste7 (Good, Tang et al. 2009). Fus3's activation loop normally adopts a locked conformation with no access to the phosphosites (Remenyi, Good et al. 2005). The transient interaction of Ste5-minimal scaffold with Fus3 (only in the presence of Ste7) stabilizes the transition state of Fus3 in which its activation loop is accessible to Ste7 for phosphorylation (Good, Tang et al. 2009). Normal Fus3 interaction with Ste5 is weak but, Ste7 strongly binds to both Ste5-minimal scaffold domain and Fus3, thus tethering them together (Remenyi, Good et al. 2005; Good, Tang et al. 2009). The coactivator loop in Ste5-domain now promotes the Ste7 mediated Fus3 phosphorylation by modulating the K_{cat}. Despite this detailed mechanism, it still remains unknown - what triggers the Ste5 mediated catalytic unlocking of Fus3 and how Fus3 is switched from its inhibited state (through phosphorylated Ste5) to unlocked state in the presence of pheromone. A potential hypothesis is that in the presence of pheromone the sudden loss of multiply phosphorylated Ste5 reduces its binding affinity to Fus3 (Chapter II), Fus3 can now switch its binding from Ste5 to Ste7. In addition, a change in phosphorylated state could also trigger conformational rearrangements in Ste5 that allows it to catalytically unlock the now mostly Ste7 bound Fus3 for activation. Precise understanding of the molecular mechanisms of how the change in phosphorylated state of Ste5 brings about switch-like activation of Fus3 will require further detailed biophysical analysis.

5.4 Multiple cellular decisions to a single stimulus

Yeast adopt several morphological and cell division programs in response to pheromone, existing simultaneously in different proportions of cells at a given concentration of pheromone (**Chapter II and Figure 3**) (Paliwal, Iglesias et al. 2007). At a threshold concentration of pheromone, the proportion of cells with a particular phenotype dramatically shifts from axial and bipolar budding, elongated growth and cell cycle arrested to shmooing (**Figure 3**). In the studies described here, we have systematically elucidated the mechanisms of switch-like shmooing response. However, it is not clear what determines the bipolar budding and cell cycle arrested decisions and their stimulus/response types. A likely mechanism(s) might be driven by the small amounts of active Fus3 available just before the threshold pheromone concentration for the switch-like shmooing response. The majority of bipolar and cell cycle arrested type of cells are observed at sub-threshold pheromone concentrations (Chapter II). Bipolar budding cells resemble that of filamentous yeast cells driven by the activation of Kss1 - a Fus3 homologous MAP kinase. Deletion of Kss1 did not have any effect on the bipolar budding cells observed during pheromone stimulus/response (Chapter II). Thus, the bipolar decision like that of shmooing might be driven by Fus3 activation but at the sub-optimal levels.

The co-existence of multiple cell types at a given pheromone concentration also indicates the existence of some sort of multi-stability. Especially in case of $Ste5^{ND}$ mutant where individual cells were always found in one of the four morphological states. It is possible that there are other circuits or switches downstream of the Fus3-Ste5 switch that might have different thresholds dependent of Fus3 activation levels. One such potential downstream switch is the Fus3 activation dependent de-repression of the transcription factor Ste12 (Paliwal, Iglesias et al. 2007). Ste12 is a master transcription factor that regulates the expression of 100's of genes in response to pheromone (Roberts, Nelson et al. 2000). Ste12 normally remains inhibited directly by its inhibitors Dig1/2 and indirectly by inactive Kss1 (Paliwal, Iglesias et al. 2007). Pheromone induced active Fus3 phosphorylate Dig1/2 which removes their inhibitory function on Ste12.

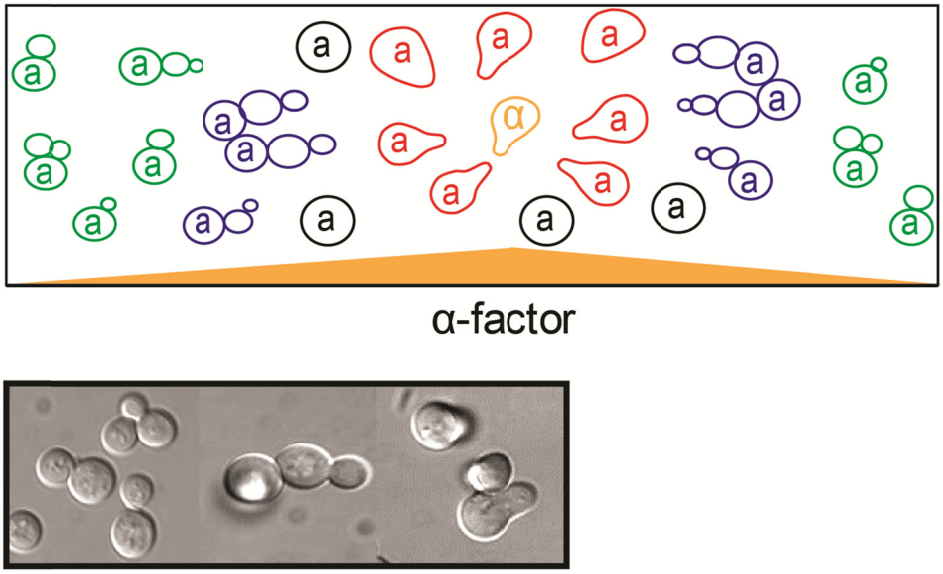

Figure 3. Multiple cellular decisions observed with varying concentrations of mating pheromone (above cartoon and its below images).
The molecular mechanisms and whether there any additional thresholds for each type of phenotype are still not understood and require detailed studies. In the cartoon, phenotypes are color coded; budding – green, bipolar budding – blue, cell cycle arrested – black and shmooing – red.

The interplay of Fus3 active levels, inhibition of Dig1/2, inactive and active levels of Kss1, directly regulates Ste12 function. This circuit functions as bimodal switch regulating the gene expression in both graded and bistable manner in different cell types (Paliwal, Iglesias et al. 2007). While the budding and arrested cells showed graded gene expression, shmooing cells exhibited bistable type of pheromone induced gene expression. Thus, different gene expression patterns in cells within a population might give rise to heterogeneity. Further, such Fus3 activation dependent downstream switches and its components might also vary stochastically across a population of cells resulting in different decisions within a single population (Elowitz, Levine et al. 2002; Shahrezaei and Swain 2008). Such variations are only revealed by the graded activation of Fus3 generated by $Ste5^{ND}$ mutant resulting in simultaneous existence of cells in any of the four morphological types.

5.5 Discrepancy of measuring mating response at transcription and the phenotype levels

Our results unambiguously show that the morphogenic shmoo response to α-factor is switch-like and caused by an equally switch-like change in Fus3-Ste5 binding (Chapter II) (**Figure 4**). However, α-factor stimulation modulates the expression of several hundred genes (Roberts, Nelson et al. 2000) and measurements of the pathway output based on a single transcriptional reporter gene, *FUS1,* can be either graded (Poritz, Malmstrom et al. 2001) (**Figure 4**) or bimodal (graded and bistable) (Paliwal, Iglesias et al. 2007). The bimodal expression of Fus1; graded in non-responding and bistable in shmooing cells, emphasizes the difference in subtle quantitative dynamics of responses in cells within a population (Elowitz, Levine et al. 2002; Paliwal, Iglesias et al. 2007). Understanding such subtle dynamics thus require the sophisticated microscopic techniques by which the gene expression can be analyzed quantitatively with respect to different phenotypes within a population (Elowitz, Levine et al. 2002). Measuring the gene expression by averaging over a population of cells or even single cell FACS analysis without correlating to their phenotypes (as have been regularly done with pheromone

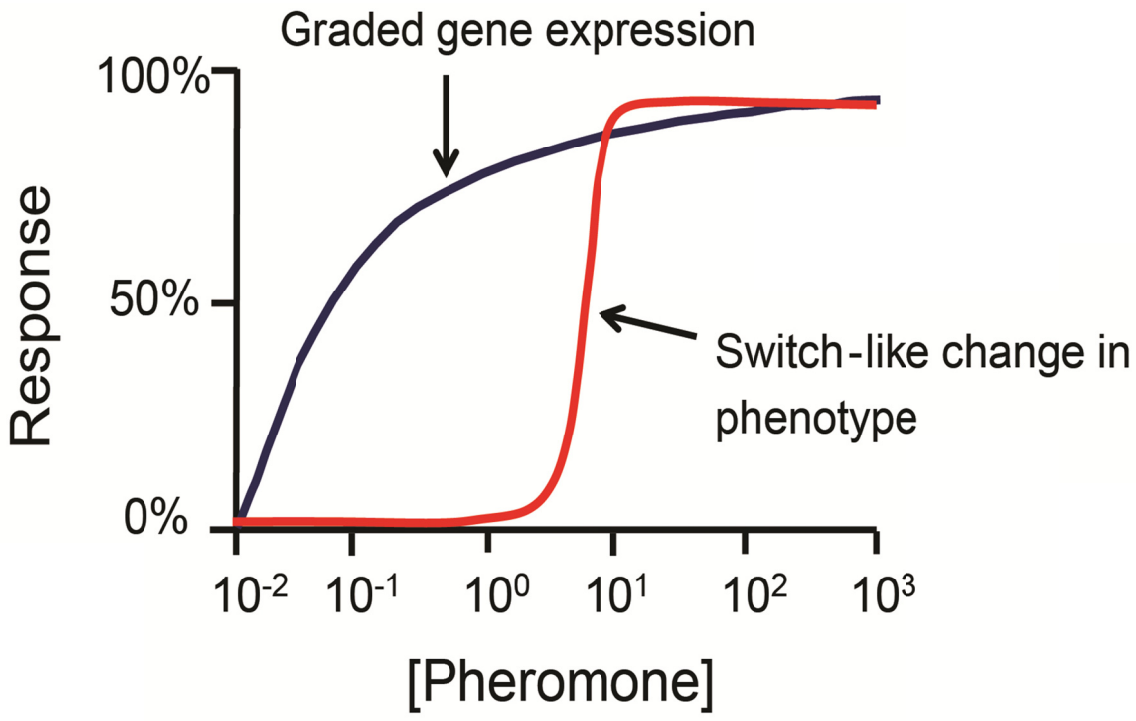

Figure 4. Schematic of pheromone response system showing the discrepancy in measuring the pathway outputs.
The less detailed (lacking phenotype information) measurements of target gene (Fus1) expression as the readout indicates mating response to be a graded. On the other hand, detailed analysis of pre-final stage of mating response (polarization or shmooing) at single cell level clearly shows the system exhibiting a switch-like response. Understanding the sources of discrepancy begs further research and debate as to which stage of the response needs to be considered to conclude the system's response type.

induced Fus1 expression), would mask their precise expression dynamics in individual cells and thus their stimulus response behaviors. Taken together with our results, these findings suggest that transcriptional readouts without precise quantitative measurements do not necessarily report on the upstream or downstream dynamics of signaling pathway in individual cells. In addition, gene expression profiles might not necessarily reflect the overall information processing in a signaling pathway but instead may reflect the regulation property of those particular genes (Paliwal, Iglesias et al. 2007). Thus, the less detailed (lacking phenotype information) measurements of target gene (Fus1) expression as the readout indicates mating response to be a graded type (Poritz, Malmstrom et al. 2001). On the other hand, detailed analysis of pre-final stage of mating response (polarization or shmooing) at single cell level clearly shows the mating response is switch-like (**Figure 4**). Resolving the sources of this discrepancy requires further research and debate as to which stage of the response needs to be considered to conclude the system's response type.

5.6 Scaffolds as flexible signaling modulator recruitment platforms

Diverse and complex phenotypes observed in nature are the result of evolution of underlying molecular networks that dictate the emergence of a phenotype and its properties. Although creation of new components is essential in the evolutionary process, the diversity and new regulatory behaviors is thought to arise by generating the new regulatory circuits through the simple mechanism of establishing novel connectivities between existing or duplicated proteins (Carroll 2005). For example, recombination of transcriptional input and output components is thought to be a major source of phenotypic variation during evolution (Carroll 2005). The strategy of producing complex behaviors through creation of networks with new combinations of proteins and/or protein domains is similar to that of electronic circuits. Wide variety of electronic circuits can be built to produce complex behaviors from a finite set of electronic components by wiring them together in different ways (Bashor, Horwitz et al. 2010; Lim 2010).

Signaling proteins that control stimulus/response behaviors are highly modular. Often signaling proteins acquire distinct properties because of their distinct modules - such as their catalytic functions and ability to bind to other proteins. Often these modules are found in different combinations with diverse catalytic functions. Insertion and recombination of modules may be a common mechanism for the evolution of new proteins and connections (Lander, Linton et al. 2001; Rubin 2001; Venter, Adams et al. 2001). Thus, increased modularity observed in signaling proteins means higher evolvability to produce diverse behaviors. In support of this hypothesis, an emerging body of work demonstrates that recombination of modular components can be used to rewire signaling pathways in nonnative ways. The modular nature of signaling proteins permits their recombination, rewiring and even build a new and novel signaling complexes (just like in electronic circuits) through synthetic biology approaches to obtain a preferable response output (Bashor, Helman et al. 2008; Bashor, Horwitz et al. 2010; Lim 2010).

Our findings demonstrate that the signaling proteins especially scaffold proteins can act as natural flexible platforms to integrate signaling through their modular nature. Ste5 scaffold has evolved distinct and independent binding sites for several of the pheromone signaling proteins (Zeke, Lukács et al. 2009). For example, Ste5 has separate binding sites to Ste11, Ste7, Fus3, Gbg, Bem1, etc. By its ability to bring together several key signaling proteins together, Ste5 acts as a central player in the mating response. Because of their highly modular nature, scaffold proteins also have the ability to recruit both positive and negative modulators of signaling; that could result in various types of stimulus/response behaviors in a system (Bashor, Helman et al. 2008). Through our studies, we elucidate and describe a similar naturally existing system which further expands the extent of scaffold protein function. We have clearly demonstrated that Ste5, in addition to recruit the negative regulator Fus3 (inactive and/or partially active form), it also recruits the positive modulator Ptc1 (Chapters II and III). The balancing and unbalancing act of Fus3 and Ptc1 through their competition generates a robust switch-like response to pheromone. The combinatory ability of Ste5 (in general of scaffolds) is further highlighted by its unique ability to form connection with other adaptor/scaffold

proteins such as Bem1 in order to have access to essential modulators and to functionally link different modules of signaling (in this case MAPK signaling to polarization modules) (Chapter III) (Pawson and Scott 1997; Bhattacharyya, Remenyi et al. 2006).

In addition to have separate recruitment sites for individual signaling modulators, Ste5 has also evolved to be their substrates - by having multiple phosphorylation sites at two distinct regions (**Figure 2**). These two sets of multiple phosphorylation sites on Ste5 are strategically placed and perform two distinct and key functions during the mating response. The first set of four sites are present amidst the modulator enzymes (Fus3 kinase and Ptc1 phosphatase (via Bem1)) binding sites (Chapters II and III). This proximity allows them to be the common substrates for both the negative and positive modulators, thus creating a zero-order competition. As we have described, the phosphorylated state of these first set of phosphorylation sites directly controls switch-like mating response (Chapter II). The second set of eight are located at the N-terminal membrane binding region of Ste5 (Strickfaden, Winters et al. 2007). The phosphorylated state of the second set of sites in addition to regulating the membrane recruitment of Ste5, also regulate the early priming of signaling by generating switch-like access to Ptc1 phosphatase (Chapter III). The priming is essential to maintain stimulus/response to mating pheromones. The combination of two sets of multiple phosphorylation sites on Ste5 thus strategically control the overall response of yeast cells to mating pheromone (**Figure 2**). In addition to highlighting the active role of scaffolds in signaling (otherwise thought of as passive assemblers) our results for the first time show a scaffold to be a flexible and easily evolvable component for generating new functional circuits within signaling networks – i.e., by acting as a common recruiting platform and as a substrate through multiple phosphorylation sites.

5.7 Robustness in signaling dynamics and diseases

As we have discussed, the circuit properties of a few key components in the MAP kinase signaling network can generate different types of responses. The switch-like

response allows cells to ignore low levels of pheromone and only respond to concentrations above a critical threshold. Such a response also indicates more sophisticated decision-making where yeast cells spatio-temporally infer the probable existence of an available mating partner from extracellular pheromone concentrations (Jackson and Hartwell 1990; Barkai, Rose et al. 1998; Libby, Perkins et al. 2007). In the case of yeast, thus, generating and maintaining a robust stimulus/response to pheromone concentrations ensures the maximum chances of mating (Jackson and Hartwell 1990). Disruption of Fus3 binding to Ste5 resulted in complete loss of ultrasensitivity in mating response (Chapter II). Cells now became super sensitive to pheromone and start to shmoo even though the chances of mating was low due to increased distance between mating partners; preventing the access to Ptc1 phosphatase at the locus of signaling completely abolished mating response (Chapter III); preventing partial membrane recruitment of Ste5 in addition to reducing the sharpness of response also reduced the proportion of cells that can achieve mating (Chapter III); disrupting the Bcy1-Gpa1 cross-talk that integrates both glucose and pheromone stimuli resulted in yeast cells being less sensitive to pheromone concentrations by increasing their threshold (Chapter IV). In general these findings clearly demonstrate that the optimal organization and functioning of the MAPK network and its components are essential to generate and maintain stimulus/response behavior in any signaling system.

Stimulus/response behaviors are universal to all living organisms. The robust ultrasensitive mechanism we have discovered is likely to occur in metazoans. Scaffold proteins are found in a number of eukaryotic signaling pathways, including those with switch-like responses and those involved in cell fate decisions. In humans, MAPK signaling cascades also play central roles in diseases including cancers, inflammatory disease, obesity and diabetes (Hirosumi, Tuncman et al. 2002; Lawrence, Jivan et al. 2008). Since the primary objective of any cellular response is to maintain the normal and healthy physiological state of cells, we could envision that in the disease state, the architecture and/or the optimal functioning of signaling mediated stimulus/response behaviors is compromised.

If similar mechanisms to those we have found in yeast do occur in mammalian signaling networks, they could prove to be important targets for therapeutic intervention towards restoring the diseased to normal state of cells. The emerging *in-vivo* technologies in quantitative microscopy, single cell analysis, protein-protein interactions in combination with computational modeling approaches promises exciting future discoveries towards understanding the mechanisms of cellular information processing. Understanding the molecular network properties and its dynamics would therefore allow us to explain the diverse and complex phenotypes observed in living organisms and nature in general.

Chapter VI: Materials and Methods

6.1 Experimental methods

6.1.1 Homologous recombination cassettes and plasmids construction

All plasmids used in this study are listed in **Supplementary Table 1**. All plasmid constructions were performed by standard molecular biology techniques.

Creation of Renilla luciferase PCA cassette templates for homologous recombination:

To construct *Renilla luciferase* Protein fragment Complementation Assay (henceforth Rluc PCA) templates, "Linker ((Gly. Gly. Gly. Gly.Ser)$_2$)-Rluc Fragments (F[1]:1-110aa; F[2]:111-310aa)" DNA sequences were PCR-amplified from yeast expression vectors that contain these sequences and subcloned into pAG25-linker-DHFR F[1,2] and pAG32-linker-DHFR F[3](Tarassov, Messier et al. 2008) plasmids between HindIII and XbaI restriction sites. This replaces linker-DHFR F[1, 2] fragment with linker-Rluc F[1] and linker-DHFR F[3] with linker-Rluc F[2] resulting in pAG25-linker-Rluc F[1] and pAG32-linker-Rluc F[2] followed by ADH gene terminator sequence (ADHter). Each of the above plasmids used to clone the linker-Rluc PCA fragments already contained unique antibiotic resistance cassettes that in the resulting constructs are 3' to the ADHter. Thus the final Rluc F[1] PCA template (pAG25-Rluc F[1]; Supplementary Table1) consists of pAG25-linker-Rluc F[1]-ADHter followed by the TEF gene promoter and the Nourseothricin N-acetyl-transferase (*NAT1*) gene that confers resistance to Clonat and finally a TEF terminator.

The final Rluc F[2] PCA template (pAG32-Rluc F[2]; Supplementary Table1) consists of pAG32-linker-Rluc[2]-ADHter followed by TEF promoter, Hygromycin-B

phosphotransferase gene (*HPH*) that confers resistance to Hygromycin-B and finally the TEF terminator. The above templates were used to PCR amplify homologous recombination cassettes to introduce Rluc PCA fragments 3' to the open reading frames-ORF, of the genes studied here.

Oligonucleotide design for PCR amplification of the Rluc PCA cassettes, their synthesis, PCR amplification and homologous recombination methods are identical to those described in our recent study(Tarassov, Messier et al. 2008).

As positive control for detection of protein-protein interaction (Ellenberg and Lippincott-Schwartz) signal using Rluc PCA and as negative control for variation in signal upon α-factor pheromone treatment, neuronal nitric oxide synthase (nNOS) and aSyntrophin (aSyn) PDZ domains that are known to form a heterodimer(Harris, Hillier et al. 2001) were used (results shown in Supplementary Figure 7). These PDZ domains are foreign to yeast. PDZ-linker-Rluc PCA fragment fusions were expressed from a plasmid under the control of the TEF promoter and by maintaining the same resistance for each fragment as on endogenously tagged proteins (i.e. Clonat for Rluc F[1] and Hygromycin for Rluc F[2]). To make these constructs, nNOS and aSyn PDZ domain DNA sequences were PCR-amplified from pCB015 and pSH71 plasmids (a kind gift from W.A. Lim, UC San Francisco) and cloned into p41NAT-linker-Rluc F[1] and p41HPH-linker-Rluc F[2] plasmids, respectively between XbaI and BspEI sites present 5' to the linker. These result in plasmids p41NAT-nNOS-linker-Rluc F[1] (pMM50; Supplementary Table1) and pHPH-aSyn-linker-Rluc F[2] (pMM51), respectively.

Rluc PCA constructions:

To measure the dynamic equilibrium of Fus3-Ste5, Bem1-Ste5 and Ptc1-Ste5 interactions by Rluc PCA and to measure active levels of Fus3 (Fus3pp) by western blotting in various mutant forms of Ste5, *STE5* was expressed from a plasmid under the control of its own endogenous promoter in a Ste5 knockout *MAT***a** strain (*ste5*Δ) where FUS3/BEM1/PTC1 genes were endogenously fused with linker-Rluc F[1] (pRS316

plasmids expressing $Ste5^{WT}$ (pSH95) and $Ste5^{ND}$ (pRB200) are gifts from Dr. W. A. Lim(Bhattacharyya, Remenyi et al. 2006)); (MM003 strain; Supplementary Table 2).

To construct Rluc PCA fusions in the above plasmids, linker-Rluc F[2] PCA fragment was fused to 3' of Ste5 variants ($Ste5^{WT}$ and $Ste5^{ND}$). For this purpose linker-Rluc F[2] along with ADHter was PCR amplified from pAG32-Rluc F[2] (Supplementary Table1). The 55 bp sequence at the 3' of *STE5* ORF (excluding the stop codon) was introduced as part of the forward oligonucleotide in order to make use of the XhoI restriction site available at 3' of *STE5* ORF. The PCR product containing 55bp of *STE5*, linker-Rluc F[2]-ADHter sequence was subcloned between XhoI and BamHI restriction sites on pSH95 and pRB200 plasmids to obtain pSH95-MM100 and pRB200-MM113, respectively (Supplementary Table 1).

In the experiments where Bem1 and Ptc1 mutants are used, they were expressed from a pRS416 based plasmid under the control of their own endogenous promoters in *bem1*Δ and *ptc1*Δ strain respectively. ORFs of $BEM1^{WT}$, $BEM1^{\Delta 417\text{-}467}$, $PTC1^{WT}$ and $PTC1^{D58N}$ were cloned in at the 5' of Linker-Rluc F[1] contained in the pRS416 plasmids.*Venus PCA plasmid construction:* To characterize and visualize the localization of protein-protein interactions in *S. cerevisiae*, we utilized the Venus YFP PCA fragments – amino acids 1-158 as fragment 1 and amino acids 159-239 as fragment 2. The original cassettes for PCA fragments consisted of p413-L-VF[1] and p415-L-VF[2] plasmids. In order to create the indicated 'gene-PCA fragment' fusions, ORFs of STE5, PTC1, BEM1, GPA1, GPA2, BCY1 and TPK2 genes were cloned in at the 5' of Linker-VF1/2 in the p413-L-VF[1] or p415-L-VF[2] plasmids. The studied candidate protein interaction pairs were constitutively over expressed under the ADH promoter from plasmids. (Supplementary Table 1).

Plasmids for localization of Ste5 mutant forms:

To test whether the phosphosite mutations on Ste5 full length protein affects its normal localization during the mating response we fused full length Venus (variant of

Yellow florescent protein) at c-terminal of Ste5. The plasmids (used for Supplementary Figure 14; listed in supplementary table 1) were created in the same way as described above for pSH95-MM100 and pRB200-MM113 but Rluc F[2] is replaced with full length Venus.

Constructs for over-expression studies:

To test the morphological pathway output and measure levels of Fus3pp under increased phosphatase (Ptc1) and the PKA regulatory subunit Bcy1 concentration in *MAT***a** cells (Chapter II: for Fig 4 & Supplementary Figures 15, 27 and Chapter IV: Fig 1and Supplementary figures 2 &3, respectively), these genes were constitutively over-expressed under control of the ADH promoter. To make these constructs, *PTC1and BCY1* ORFs sequence was PCR-amplified from Yeast genomic DNA and subcloned into a multiple cloning site (MCS) of p415 between XbaI and BamHI restriction sites.

Constructs for in vitro protein purifications:

To detect Fus3p mediated phosphorylation of individual phosphosites on Ste5_pep2 variants (for Supplementary Figure 9; see main text for description of Ste5_pep2 phosphosite mutants), *In vitro* kinase assays were performed using GST-Fus3p and GST-Ste5_pep2 (residues 214 to 334) fusion proteins purified from *E. coli* cells. N-terminal GST fusion of Fus3 was made by PCR-amplifying *FUS3* ORF sequence from Yeast genomic DNA and cloning it between BamHI and EcoRI restriction sites of MCS on pGEX-5X-3 vector (Amersham). To create N-terminal GST fusions of mutant Ste5_pep2 peptides, DNA sequence for amino acids 214 to 334 were PCR-amplified from a different plasmid template for each mutant (Supplementary Table1: $ABCD^{WT}$; pSH95-MM100, Abcd; pSH95-MM108, aBcd; pSH95-MM109, abCd; pSH95-MM110, abcD; pSH95-MM111 and abcd; pSH95-MM112). Each PCR product was separately cloned into pGEX-5X-3 plasmids between BamHI and XhoI restriction sites. Similarly, to generate plasmids with N-terminal MBP fusions of Ptc1 and Fus3, their ORF sequences were PCR-amplified from the Yeast genomic DNA and cloned in to pMAL-c2x plasmid

vector (New England Biolabs) between BamHI & HindIII and EcoRI & XbaI restriction sites respectively (pMM216 & pMM217).
All plasmid constructs were verified by standard sequencing methods.

Yeast strains:
All Yeast strains used in this study are shown in **Supplementary Table 2**.

6.1.2 Mutagenesis

The significance of each Ste5 phosphosite on Fus3-Ste5 interaction dynamics, Fus3 phosphorylation and morphological pathway output were characterized using various phosphosite mutants of Ste5. In one series, combinations of non-phosphorylatable mutants were generated for all four sites and in another two sets, combinations of pseudo-phosphorylated mutants were generated. In some cases, SH3 domain interaction motifs (SIM) were mutated to 'alanine' in order to disrupt protein-protein interactions.

To make non-phosphorylatable mutants of Ste5, Threonines (T) were mutated to Valine (V) and Serines (S) to Alanine (A), while pseudo-phosphorylated mutants were generated by mutating both Threonines and Serines to Glutamic acid (E). Mutagenesis was carried out by using standard Site-Directed mutagenesis (Quick Change Site-Directed Mutagenesis Kit- Stratagene # 200519) following the manufacturer's instructions. For both series of mutations, first single site mutations were generated using pSH95-MM100 as site-directed mutagenesis PCR template. To generate double site mutations the single site mutated plasmids were used as templates. Similarly to make triple mutations the double site mutated plasmid templates and to generate *STE5* with all four sites mutated, triple site mutated plasmids were used as PCR templates. The presence of correct mutations for all combinations was verified by sequencing.
Similarly, to disrupt the recruitment of Ptc1 to Ste5, Ste5 amino acids from 277 to 280 were mutated to Alanine.

6.1.3 Generating 3' Rluc PCA fragment fusions with endogenous genes

To study the protein-protein interaction dynamics by Rluc PCA with proteins expressed at their native levels and without over-expressing them, PCA fragments were fused to 3' of gene of interest preceded by linker sequence at their chromosomes by using standard homologous recombination methods(Ghaemmaghami, Huh et al. 2003). Design of oligos, PCR amplification of the cassette, transformation of yeast competent cells with PCR product for homologous recombination and verification of the correctly tagged genes by colony PCR were performed as described in our recent study(Tarassov, Messier et al. 2008), with the exception that instead of DHFR fragments, we amplified and created fusions with Rluc PCA fragments using Rluc PCA templates (pAG25-Rluc F[1] and pAG32-Rluc F[2]).

Since pheromone response is absent in diploid yeast cells, fusion of both Rluc F[1] & F[2] to two genes of interest was carried out in the same haploid strain (*MAT***a**; BY4741). In order to do this, we first created fusion of Rluc F[1] cassette to the first gene of interest (for example *FUS3*). Positive transformed cells were selected for Clonat antibiotic resistance and further verified by colony PCR. Verified clones were made chemically competent followed by transformation with the Rluc F[2] cassette PCR product specific for the second gene of interest (for example *STE5*). After a second transformation, clones were first selected using double antibiotic selection for both fragments (i.e., plates with Clonat and Hygromycin antibiotics) followed by further verification of correct 3' fusion of PCA fragments with specific genes by colony PCR.

In order to verify that the fusion of PCA fragments to C-terminal of Fus3 and Ste5 proteins do not interfere with their normal expression levels strains expressing fusion proteins were tested for their normal expression using Rluc fragment specific antibodies (Supplementary Figure 13). To test if expression of fusion proteins disrupts their normal physiological function in response to pheromone stimulation, morphological response was measured under non-stimulated and stimulated conditions (data not shown). No

significant change in expression or pathway responses were detected with genes expressed as fusions to PCA fragments whether they were expressed from chromosomes or from the plasmids (in the cases of $Ste5^{WT}$ and Ste5 mutants).

6.1.4 Rluc PCA luminescence detection

All protein-protein interaction signals using Rluc PCA were measured using cells equivalent to 0.1 OD_{600} (approximately $1x10^6$ cells). This was the minimal and optimal cell density required by Rluc PCA signal detection and to measure protein interaction dynamics among MAP Kinase signaling proteins (data not shown). Cells were grown in either Low Fluorescent Media (LFM) complete(Sheff and Thorn 2004) or appropriate selective medium overnight to make a pre-culture. From the pre-culture, fresh cultures were started at an OD_{600} of 0.05 or less and allowed to grow up to 0.1 OD_{600} at 30ºC with shaking. For each sample, cells equivalent to 0.1 OD_{600} were spun, supernatant was discarded and cells were resuspended in 160 µl of fresh medium. Cells were transferred to white 96-well flat bottom plates (Greiner bio-one # 655075). The Luciferase substrate Benzyl-Coelenterazine (Nanolight #301) was diluted from the stock (2 mM in absolute ethanol) using 1x phosphate-buffered saline (PBS), pH 7.2 containing 1 mM EDTA (10x PBS stock (1.4 M NaCl, 27 mM KCl, 100 mM Na_2HPO_4, 18 mM KH_2PO_4, pH 7.3) is diluted to 1x using deionized water). Pheromone α-factor (Zymo Research #Y1001) dilutions were prepared in 0.1 M sodium acetate. An LMax II^{384} Luminometer (Molecular Devices, Sunnyvale, CA, USA) was used to measure the protein-protein interaction signal.

Using the internal injectors of the Luminometer, 20 µl each of substrate (to a final concentration of 10 µM) and appropriate dilutions of α-factor or medium alone without α-factor, but with equivalent sodium acetate (to non-treated samples) were added to the cell mixture, mixed by shaking and incubated for 60 seconds. After incubation, Rluc PCA signal was integrated for 30 seconds. In a single experiment, for each sample, signal was measured in triplicates and in total, experiments were repeated independently three times.

Standard error of the mean (Fiol, Haseman et al.) were calculated from the mean values of three independent experiments and shown as error bars for all relevant results.

In order to determine Rluc PCA signal from background luminescence for all α-factor dose-response, single concentration stimulus and kinetics data, first, the luminescence signal of medium, substrate alone and the background luminescence of *MAT***a** cells were subtracted from every measured signal to obtain the net luminescence. Second, α-factor was dissolved in 0.1 M sodium acetate and dilution of acetate resulted in a small linear decrease in substrate stability, resulting in an apparent 8.157% decrease in signal. In order to account for this, we applied a correction of 8.157 % to net PCA luminescence signal.

6.1.5 Venus PCA fluorescence detection

In order to detect and characterize the protein-protein interactions using Venus PCA, using standard yeast molecular biology methods, we co-transformed *MAT***a** (*S. cerevisiae* strain BY4741) with plasmid p413 (for F[1]; ADH promotor) and plasmid p415 (for F[2]; ADH promotor) encoding the indicated Venus YFP PCA fusions. Positive clones were selected on the synthetic complete media lacking the amino acids Histidine (His) and Leucine (Zhao, Leung et al.). To acquire fluorescent cell images, cells were grown in low fluorescent media (LFM) and images were taken using a Nikon Eclipse TE2000U inverted microscope with 60× objective and YFP filter cube (41028, Chroma Technologies). Images were captured with a CoolSnap CCD camera (Photometrics) using Metamorph software (Molecular Devices). Quantification of fluorescence intensities from individual cells was done using the Image J software.

6.1.6 OyCD PCA analysis of complementary mammalian-yeast protein:protein interactions.

The *BCY1* and *TPK2* genes and the mouse cDNA for the *RegIIβ* subunit of PKA were amplified by PCR and subcloned in p413Gal1-Linker-OyCD-F[1] or p415Gal1-Linker-OyCD-F[2] using SpeI and BamHI restriction sites. The human *Gαi3* gene was subcloned in p413Gal-F[1]-OyCD-Ras by substituting the *Ras* gene via BspEI / XhoI. The respective plasmid pairs were co-transformed in BY4741 *FCY1*Δ *S. cerevisiae* strains and transformed clones wers selected on synthetic complete medium (SC) without Lysine, Histidine and Leucine in the presence of 2% glucose and 2% agar (SC –Lys, –His, –Leu, +2% glucose, +2% agar). Three different colonies were picked from each transformation and inoculated in 1 ml of SC medium (–Lys, –His, –Leu, +2% raffinose) overnight. Protein expression was induced by adding 2% galactose to the overnight culture for additional shaking for 3 hours at 30 °C. 1µl of each yeast culture was transferred to SC medium (–Lys, –His, –Leu, +2% raffinose, +2% galactose, +2% agar) without 5-fluorocytosine or with 1 mg/ml of 5-fluorocytosine for the OyCD PCA death selection assay. The plates were incubated at 30°C for 3 days.

6.1.7 Western analysis to detect Fus3 phosphorylation

Cells were grown overnight to saturation in YPD or appropriate selective medium. Overnight cultures were used to start fresh 250 ml culture starting at cell density of 0.05 OD_{600} or less and grown to 0.1 OD_{600}. Cells were stimulated with α-factor for 15 minutes, spun for 5 minutes at 500xg, supernatant was discarded, the pellet washed with sterile water, spun again and frozen at -80ºC. Frozen pellets were thawed on ice, resuspended in 500 µl of Yeast protein extract buffer containing protease inhibitors. Buffer composition was adopted from Andersson et.al.(Andersson, Simpson et al. 2004) with some modifications; 10% Glycerol v/v, 15 mM EDTA, 15 mM $MgCl_2$, 1 mM DTT, 0.1% Triton X-100 v/v, 250 mM NaCl, 1 mM NaN_3 in 25 mM Tris-Cl pH=7.4. In addition, phosphatase inhibitor: 0.25 mM Sodium ortho-vanadate and protease inhibitors (PMSF-1

mM, Pepstatin A 5 µg/ml, Leupeptin 5 µg/ml and protease inhibitor cocktail (Roche Diagnostics # 11873580001)

To the above cell suspension 250 µl of glass beads were added and the mix was vortexed for 1 minute, 5-6 times with 1 minute intervals of incubation on ice. Vortexed cell mix was spun at 10,000xg for 10 min at 4ºC, cell lysate (supernatant) was aspirated into a new vial. An aliquot of lysate was used for SDS-PAGE and the rest was stored at -80ºC. Standard methods were used for the SDS-PAGE and western blotting experiments. Samples were run on 12% SDS-PAGE gel. Proteins from the gel were transferred to PVDF membranes using semi-dry transfer method. After the transfer, the membrane was blocked with 5% milk solution in Tris buffered saline and 0.2% Triton X-100 (TBST) for one hour at room temperature (RT). Following this, blots were probed with primary anti-phospho MAPK antibody (Cell signaling; Phospho-p44/42 MAP Kinase antibody #9101) in 5% w/v bovine serum albumin (BSA) solution at 4ºC overnight with gentle shaking. Blots were then washed three times with TBST, each wash for 10 minutes at RT on a rocker. Following the wash, blots were incubated with a secondary antibody (Cell signaling #7074) in 5% milk solution in TBST for one hour at RT. Then the blots were washed three times with TBST. Electrochemiluminescent reagent (PerkinElmer, # NEL 104 and NEL 105) was added to the blots and allowed for 60 seconds on bench. Excess ECL reagent was removed and blots were then exposed to film (GE Healthcare #28906838) and the films were developed on a KODAK M35A X-OMAT processor.

Stripping the blots and probing for loading control:

In order to strip the antibodies from blots, they were incubated in stripping buffer (62.5 mM Tris-Cl pH=6.8, 2% SDS w/v and 100 mM β-Mercaptoethanol) at 60-65ºC for 45 minutes with occasional shaking. Then blots were washed 4-5 times with TBST. Stripped blots were blocked with 5% milk in TBST for 1 hour at room temperature followed by probing the common and abundant protein in yeast, 3-Phosphoglecerate Kinase (PGK) using anti-PGK antibody (Molecular Probes # A6457).

6.1.8 Analysis of different morphological phenotypes

Cells were grown overnight in Low Fluorescence Medium (LFM) either complete or containing selective antibiotics to make a pre-culture. From the pre-culture fresh 3 ml cultures were started beginning at 0.05 OD_{600} or less cell density and grown at 30ºC with shaking up to 0.1 OD_{600}. Cultures were treated with indicated concentrations of α-factor pheromone and continued to incubate at 30ºC with shaking. To avoid heterogeneities from different stages of the cell cycle, α-factor treated cells were incubated for 3 to 4 hours before taking the images.

Preparation of microscopy plates:

For image acquisition by microscopy, 96-well optical quality clear bottom plates (NUNC #164588) were used. In order to attach the cells to the bottom of wells, lectin Concanavalin A (ConA; Sigma # C-2631) was used as a cell binding agent. Each well was coated with 0.1 % ConA w/v at room temperature for 15 min. Then, the ConA solution was aspirated and wells were washed once with deionized sterile water. In order to activate the ConA, a solution of 20 mM $CaCl_2$ and 20 mM $MnSO_4$ was added to each well and incubated for another 15 minutes at room temperature followed by a wash with deionized sterile water. Cell suspension was added to wells and allowed to attach for 10 min. Differential Interference Contrast-DIC, images were acquired on a NIKON eclipse TE2000-U inverted microscope connected to a CoolSNAP-fx CCD camera (Photometrics, Pleasanton, CA, USA) using a 60X DIC H Plan APO Oil objective. Image acquisition was done with Metamorph software (Molecular Devices, Downingtown, PA, USA).

Image Analysis and classification of phenotypes:

Before we did any morphological response analysis, we observed under the microscope for 'over-time development or change in morphologies' after treating the cells with different concentrations of alpha-factor. We took images every 15 minutes starting 30 minutes after stimulation until 6 to 8 hours. In addition to determining the optimal time for imaging, over-time development of morphologies also helped us to

clearly classify the morphologies into different categories (i.e. axial budding, bipolar budding, cell-cycle arrested and shmooing). Movie files generated from the time series images are included in Supplementary Figure 2 (requires the latest version of Adobe reader (9 and above) to view the movies).

As seen in the movies, after 4 hours of stimulation with 0.1 μM alpha-factor, cells rapidly recover from the Bipolar budding state and start to re-bud normally (i.e. axially). When stimulated with 1.0 μM α-factor, shmooing state is maintained until 5 hours, after which cells slowly start to re-bud. For all the morphology analysis in the paper, images were taken between 3 to 4 hours of time after stimulation, which was also the optimal time to distinguish morphologies. No re-budding phenotype was observed within this time period.

We have performed all the experiments in *BAR1* intact cells (BY4741 strain). Since we focused on the final cell fates of pheromone response, it was very important that we do not make the strains more sensitive (by deleting *BAR1* gene) to α-factor than normal wild type cells. In order to avoid the heterogeneity that might be caused by Bar1 mediated degradation of α-factor in the medium and to keep the results consistent, we undertook the following precautions:

1. As seen with the over-time development of morphologies, cells start to recover from the pheromone response after 4 to 5 hours of stimulation (Supplementary Figure 2). Since Bar1 is mainly shown to help cells recover from pheromone arrest which could affect the rate of recovery of different morphologies, we avoided taking images after 4 hours of stimulation.

2. We optimized and reduced the cell-density to the minimum that would result in large dilution of the available Bar1 in the medium. For both morphology and Rluc PCA assays, fresh cultures were made the next day from the overnight cultures and allowed to grow till very minimal cell-density (OD_{600} 0.05 to 0.1) that was optimal for both the assays. In case of Rluc assays, cells were again resuspended in fresh medium thus further removing the Bar1, if any present in the medium.

3. Whenever possible aliquots from the same fresh stock of α-factor was used for related experiments in order to avoid any was irregularities from batch to batch of α-factor.

During image analysis cells were manually classified in to 4 different phenotypes; axial budding, bipolar budding, cell cycle arrested and shmooing. The phenotypes were distinguished in the following manner: axial budding; normal round cells (3-5 μM diameter) with daughter cells (buds) appearing axial to previous budding site. Bipolar budding; round cells with daughter cells appearing in the opposite direction to the previous budding site resulting in a chain of cells attached together. Cell cycle arrested; enlarged cells with larger average size (5-8 μM) compared to budding cells and Shmooing; pear shaped cells that are elongated and with active extension called shmoo. Anywhere from 500 to 1,500 individual cells were counted from 10 to 15 images taken per sample and sorted into either of the above four categories. Fractions of different phenotypes (percentage) were calculated from the total number of cells.

6.1.9 Protein purifications

GST-fusions of Fus3, mutant variants of Ste5_pep2 (WT, Abcd, aBcd, abCd, abcD and abcd) and MBP fusions of Fus3 and Ptc1 were purified from Rosetta (DE3) strain of *E.coli*. Cells transformed with appropriate plasmid were grown overnight to make a pre-culture from which fresh 500 ml cultures were started. Cells were grown up to 0.6 OD_{600} at 37ºC with shaking. To induce over-expression of fusion proteins, cells were treated with 1 mM Isopropyl-β-D-thiogalactoside (IPTG) and allowed to grow at 18ºC with shaking for 12 to 14 hours. Then, cells were harvested by centrifugation, resuspended in PBS containing protease inhibitors, lysed by sonication, spun and cell-lysate was aspirated. From cell-lysates, GST-fusion proteins were purified using Glutathione Sepharose 4B (GE Healthcare #17-0756-01) column and MBP-fusion proteins using the Amylose Resin (New England Biolabs #E8021S) following the

manufacturer's instructions. Purified proteins were buffer exchanged with 20 mM Tris-Cl. pH=8.0, 150 mM NaCl and 2 mM $MgCl_2$ overnight at 4ºC. Buffer exchanged proteins were either directly used for the kinase assay or aliquoted and frozen at -80ºC.

6.1.10 In-vitro Kinase assay

In order to detect partially active Fus3 (Fus3p) mediated phosphorylation on all four individual phosphosites present on Ste5, various mutant forms of Ste5_pep2 were used; for each site a peptide was generated wherein all but one phosphosites were mutated to non-phosphorylatable form (Supplementary Table 1). In wild type peptide, no sites were mutated while in "abcd" peptide all four sites were mutated to the non-phosphorylatable form (Ser or Thr->Ala). These peptides were used as positive and negative controls respectively in the *in vitro* kinase assay.

Fus3 purified from *E.coli* has been shown to be phosphorylated on Tyrosine (Y182) of its activation loop (Remenyi, Good et al. 2005). The tyrosine phosphorylated form of Fus3 has also previously been shown to possess partial kinase activity (Bhattacharyya, Remenyi et al. 2006). Hence, to detect Fus3p mediated phosphorylation of individual phosphosites of Ste5, purified GST-Fus3p was used without any modifications. In *in vitro* kinase assays, purified GST-fusions of individual mutants (all from 214-334 amino acids) of Ste5_pep2 (1.0 µM) were incubated with GST-Fus3p (0.5 µM) in 100 µl of kinase reaction buffer (20 mM Tris-Cl, pH=8.0, 150 mM NaCl, 2 mM $MgCl_2$, 0.1% IGEPAL (tert-Octylphenoxy poly(oxyethylene)ethanol), 2mM TCEP (Tris[2-carboxyethyl] phosphine)) containing 0.5 mM ATP and 10 µCi of γ^{32}P-ATP (PerkinElmer # BLU002Z). As controls, one mix with Ste5_pep2^{WT} peptide was made in the absence of kinase (GST-Fus3p) and another without γ^{32}P-ATP. Reaction mixes were incubated at 30ºC and an aliquote was taken for different time points (10, 30 and 120 minutes). To test for phosphatase Ptc1 competition with Fus3 for the Ste5 phosphosites, Mbp-Ptc1 was included in equal concentration (0.5 µM) and twice (1.0 µM) the concentration of GST-Fus3 in two different assays. Reaction was stopped by adding 6X

protein loading buffer (350 mM Tris-Cl (pH 6.8), 10.28% (w/v) SDS, 36% (v/v) glycerol, 0.6 M dithiothreitol, 0.012% (w/v) bromophenol blue. Samples were boiled for 10 minutes and run on 12% SDS-PAGE gels after which the gels were dried, exposed to Amersham Hyperfilm (GE Healthcare) and films were developed on a KODAK M35A X-OMAT processor.

6.2 Computational modeling

6.2.1 Assumptions of the model

To explain the switch-like behavior observed in the mating MAPK pathway we constructed a model based on the following assumptions (Fig. 3a and Supplementary Figure 23):

i. Only Ste5, Fus3, and Ptc1 contribute to the switch.
ii. Fus3 phosphorylates identically the 4 phosphosites on Ste5, which surround the Fus3 docking motif (FDM).
iii. In the absence of α-factor, cytosolic Fus3 is not active and cannot phosphorylate Ste5, unless it first binds to the FDM.
iv. The association rate of Fus3 to the FDM on Ste5 is constant, and denoted $f_1^{(K)}$, but its dissociation rate can depend on the number of phosphorylated sites on Ste5, and will be denoted $b_1^{(K)}$ to $b_5^{(K)}$.
v. When Fus3 is bound to the FDM, it is partially active and can bind equally to any of the unphosphorylated phosphosites of Ste5. The kinase activity of Fus3 obeys a Michaelis-Menten type enzymatic reactions (rates denoted $f_2^{(K)}$, $b_6^{(K)}$ and $k^{(K)}$). We also assume that phosphorylation is distributive. Fus3 needs to dissociate from the FDM after one phosphorylation in order to phosphorylate other sites on Ste5. This assumption is critical to observe zero-order ultrasensitivity.
vi. The amount of Ptc1 available is a function of α-factor. We use a Hill equation with a Hill number of greater than 1 (based on PCA data of Fig. 2e). We assume a small

level of Ptc1 even in the absence of α-factor. Mathematically, we have

$$Ptc1 = [Ptc1]_0 + [Ptc1]_{\max} \frac{\alpha^{n_H^{(P)}}}{\alpha^{n_H^{(P)}} + EC_{50}^{(P)n_H^{(P)}}},$$

where $[Ptc1]_0$, $[Ptc1]_{max}$, $n_H^{(P)}$, and $EC_{50}^{(P)}$ are all parameters we fit and α specifies the level of α-factor.

vii. Ptc1 like Fus3 must be first recruited to Ste5 before it can dephosphorylate any phosphosites (rates denoted $f_1^{(P)}$ and $b_1^{(P)}$).

viii. Ptc1 can bind equally to any of the phosphorylated phosphosites of Ste5. Its phosphatase activity obeys a Michaelis-Menten type enzymatic reactions (rates denoted $f_2^{(K)}$, $b_2^{(P)}$ and $k^{(P)}$). We assume that dephosphorylation is also distributive.

ix. At saturating concentrations of α-factor, a small fraction of fully active cytosolic Fus3 called $Fus3_{active}$ can phosphorylate Ste5 without binding to the FDM. The level of active Fus3 is related to α-factor through a Hill function:

$$Fus3_{active} = [Fus3_{active}]_{\max} \frac{\alpha^{n_H^{(K)}}}{\alpha^{n_H^{(K)}} + EC_{50}^{(K)n_H^{(K)}}},$$

where $[Fus3_{active}]_{max}$, $n_H^{(K)}$, and $EC_{50}^{(K)}$ are all parameters that we fit. This assumption is only necessary to explain the slight increase in the levels of the Ste5-Fus3 complex at high α-factor and it is not essential for the switch.

x. The PCA signal we measure for the Fus3-Ste5 complex reflects the total amount of Fus3 interacting with Ste5 either through the FDM, the phosphosites, or both. Equally, the PCA signal for the Ptc1-Ste5 complex reflects the total amount of Ptc1 interacting with Ste5 either through the Ptc1 binding site, the phosphosites, or both.

6.2.2 Generating sufficient ultrasensitivity

We constructed and tested two different versions of the model. The first assumes that Fus3 or Ptc1 cannot dissociate from their docking motifs when acting at the phosphosites (Fig. 3a and Supplementary Figure 23a). Although this model can produce sharp responses, it cannot explain all the Ste5 mutant data. The second model assumes

that the enzymes can dissociate from their docking motifs while acting on the phosphosites (Supplementary Figure 23b). The model of Supplementary Figure 23b fits the data more accurately, although it has two extra parameters ($f_3^{(K)}$ and $f_3^{(P)}$). For clarity, we have shown the first model in Supplementary Figure 23a, but we carry out all our fits with the model of Supplementary Figure 23b. Both models produce sharp responses through a combination of zero-order ultrasensitivity and steric hinderance.

Ultrasensitivity does not occur if the enzymes remain sequestered to the substrate after modification(Salazar and Hofer 2006). A distributive enzyme dissociates from the substrate after each modification and needs to be rebound for further modifications. A distributive kinase or phosphatase acting on a substrate with multiple phosphorylation sites can generate ultrasensitive behavior because the rate at which product is formed is determined not just by the concentration of available enzyme, but by the available concentration raised to a power because the substrate "sees" the concentration of the enzyme once for each enzymatic reaction that occurs(Ferrell 1996; Gunawardena 2005). In our model a distributive mechanism alone produces a Hill coefficient of about 3 and is not enough to explain the sharp switch. The model of Supplementary Figure 23a assumes distributivity by allowing the enzymes to dissociate from the substrate after modification. The model of Supplementary Figure 23b is more flexible and can accommodate either processive or distributive mechanisms. However, the parameter fit to the data resulted in parameter values that resemble a distributive mechanism.

To understand the roles of steric hinderance and the zero-order mechanism, we tested two modifications of the model in Supplementary Figure 25. If we remove two-stage binding, we will lose enzyme saturation so the switch only works through steric hinderance. This model produces less sharp and less robust switches (Supplementary Figure 25b). The second modification is to keep two-stage binding, but make the affinity of Fus3 to the Ste5 docking site independent of phosphorylation state of Ste5 The model then solely works through zero-order ultrasensitivity because this modification prevents steric hinderance. The sharpness of the switch is lower but robustness to changes in concentration of the enzyme and substrate does not change (Supplementary Figure 25c).

Robustness is therefore a property of the two-stage zero-order mechanism. Finally, if we assume Fus3 and Ptc1 bind simultaneously to Ste5, steric hinderance, which relies on competitive binding of Fus3 and Ptc1 to Ste5, would not generate a sharp switch. However, the zero-order mechanism still works.

Another variation of the model that assumes non-identical phosphosites can produce bistability (Markevich, Hoek et al. 2004; Salazar and Hofer 2007). Since the data for the Ste5 mutants in Supplementary Figures 10-12 suggest that all phosphosites have similar effects, however, we worked with a model with identical phosphosites.

6.2.3 Local saturation generates a robust ultrasensitivity

To understand how two-stage binding generates a highly ultrasensitive response that is robust to the ratio of the concentration of the enzymes to the concentration of the substrate Ste5, let us first consider classic zero-order ultrasensitivity with one-stage binding and with Ste5 having only one phosphosite. For ease of explanation, we will discuss the completely symmetric case, with equal concentrations of kinase and phosphatase and with the kinetic rates for the action of the kinase identical to the corresponding rates for the action of the phosphatase. At steady-state then half of all Ste5 molecules will be phosphorylated, and both the kinase and the phosphatase will be saturated if there is a sufficiently high concentration of Ste5. Any increase in the concentration of phosphatase will increase the number of unphosphorylated substrates and therefore maintain the saturation of the kinase. A small increase in the phosphatase concentration therefore generates a large decrease in the concentration of phosphorylated Ste5 because any additional phosphatase has no competition from the kinase. Similarly, for a large increase in the concentration of phosphorylated Ste5 for a small decrease in the concentration of the phosphatase, we require that the phosphatase remains saturated.

Two-stage binding allows local saturation of the enzymes. With two-stage binding, the initial binding of an enzyme to the substrate occurs at a rate independent of the state

of phosphorylation of the substrate because the enzyme binds only to its docking site on the substrate. Once bound, an enzyme can either dissociate or bind to one of the substrate's phosphosites, either unphosphorylated sites for the kinase Fus3 or phosphorylated sites for the phosphatase Ptc1. We say that an enzyme is locally saturated when the probability of an enzyme binding to a phosphosite rather than dissociating from Ste5 is close to unity. This probability is determined by the rate of dissociation of the enzyme from its docking site and the rate of associating with a single phosphosite multiplied by the number of available phosphosites. Therefore increasing the number of phosphosites on Ste5 increases the potential degree of local saturation of the enzymes.

Ultrasensitivity generated through two-stage binding of both enzymes to the substrate is analogous to classic zero-order ultrasensitivity. Consider again the completely symmetric case, but now with two stage-binding and multiple phosphosites on Ste5. For equal concentrations of enzymes, half of these phosphosites on all Ste5 molecules will be phosphorylated. With a sufficient number of phosphorylation sites, both enzymes will therefore be locally saturated regardless of the ratio of their concentration to the concentration of Ste5 or whether they have their own docking sites on Ste5 or compete for a single docking site. If we increase the concentration of the phosphatase at this steady-state, then the local saturation of the kinase is maintained. More phosphatase will increase the number of unphosphorylated phosphosites on Ste5 increasing the probability that a kinase once bound to Ste5 will bind a phosphosite rather than dissociate. If the kinase and phosphatase have their own docking sites on Ste5 then the rate of binding of the kinase to Ste5 will remain unchanged; if they compete for the same docking site, the rate of binding of the kinase will decrease. Analogous to classic zero-order ultrasensitivity, any small increase in the concentration of the phosphatase will therefore be unopposed by the kinase and generate a large decrease in the level of phosphorylation of Ste5. We emphasize that this ultrasensitive decrease will occur regardless of the ratio of the concentration of the enzymes to the substrate providing the enzymes are locally saturated. For example, ultrasensitivity will be undermined with just one phosphorylation site on Ste5 or with processive enzymes because then increasing the concentration of phosphatase will increase the concentration of completely unphosphorylated substrates

and so allow the total rate of phosphorylation to also increase. With many phosphosites on Ste5 and distributive enzymes, however, a phosphatase dephosphorylates at most one phosphosite each time it binds to Ste5, and multiple phosphorylated phosphosites on Ste5 are maintained. All kinases consequently remain locally saturated when bound to a substrate, and the rate of phosphorylation does not increase.

6.2.4 Mathematical details

Our model has 27 parameters **(Supplementary Table 3)**. For the kinetic rates in Supplementary Figure 23b, the concentrations of the enzymes Fus3 and Ptc1 and of Ste5, we assume that;

i. The concentration of Ste5 is 0.052 μM and Fus3 is 0.197 μM by averaging published data(Maeder, Hink et al. 2007).
ii. The level of the PCA signal for the Fus3-Ste5 interaction in wild type cells in the absence of pheromone (F) corresponds to 20% of the Ste5 concentration (~0.01 μM) from Maeder *et al.(Maeder, Hink et al. 2007)*. This choice scales the values of the dissociation constants we fit.
iii. We fit all the other parameters and kinetic rates to the Fus3-Ste5 (Fig. 2a) and the Ptc1-Ste5 (Fig. 2e) PCA data of the dose-response to α-factor and to the PCA data for the Fus3-Ste5 interaction with the pseudo-phosphorylated mutants of Ste5 (Fig. 2d).

The model was constructed using the *Facile* network compiler(Siso-Nadal, Ollivier et al. 2007) with Allosteric Network Compiler a rule-based modeling scheme, courtesy of Julien Ollivier, to generate a description of the model as a set of differential equations. We integrated the model in Matlab (The Mathworks, Nattick, Massachusetts). To fit the data, we optimized the parameters using an efficient Markov chain Monte Carlo method(H. Haario 2006), which uses an adaptive Metropolis sampler and delayed rejection.

We give the differential equations for the model below. Here $Ste5^n$ denotes Ste5 with n phosphorylated sites where n is an integer between 0 and 4. We have 3 distinct forms of Ste5-Fus3 complexes: $Fus3\_Ste5^n\_0$ denotes a complex where Fus3 is only bound to the FDM, shown by (0) (Supplementary Figure 23b); $Fus3\_Ste5^n\_1$ denotes a complex where Fus3 is bound to the FDM and to a phosphosite, shown by (1); and $Fus3\_Ste5^n\_2$ denotes a complex where Fus3 is bound only to a phosphosite, shown by (2). Similarly, Ste5-Ptc1 complexes have the same three forms denoted by $Ptc1\_Ste5^n\_0$, $Ptc1\_Ste5^n\_1$ and $Ptc1\_Ste5^n\_2$ (Supplementary Figure 23b).

The concentration of each species in Supplementary Figure 23b changes with time and is described by a differential equation:

$$\frac{dFus3}{dt} = \sum_{n=0}^{4} b_n^{(K)}.Fus3\_Ste5^n\_0 - f_1^{(K)}.Fus3.\sum_{n=0}^{4} Ste5^n + \sum_{n=0}^{3} k^{(K)}.Fus3\_Ste5^n\_2 + \sum_{n=0}^{3} b_6^{(K)}.Fus3\_Ste5^n\_2.$$

$$\frac{dPtc1}{dt} = \sum_{n=0}^{4} b_1^{(P)}.Ptc1\_Ste5^n\_0 - f_1^{(P)}.Ptc1.\sum_{n=0}^{4} Ste5^n + \sum_{n=1}^{4} k^{(P)}.Ptc1\_Ste5^n\_2 + \sum_{n=1}^{4} b_2^{(P)}.Ptc1\_Ste5^n\_2.$$

For n= 0 to 4, we have (For n=0 and n=4, we ignore any terms that result in $Ste5^{-1}$ and $Ste5^5$.):

$$\frac{dSte5^n}{dt} = b_n^{(K)}.Fus3\_Ste5^n\_0 - f_1^{(K)}.Fus3.Ste5^n + b_1^{(P)}.Ptc1\_Ste5^n\_0 - f_1^{(P)}.Ptc1.Ste5^n + k^{(K)}.Fus3\_Ste5^{n-1}\_2 + k^{(P)}.Ptc1\_Ste5^{n+1}\_2 + b_6^{(K)}.Fus3\_Ste5^n\_2 + b_2^{(P)}.Ptc1\_Ste5^n\_2.$$

$$\frac{dFus3\_Ste5^n\_0}{dt} = f_1^{(K)}.Fus3.Ste5^n - b_n^{(K)}.Fus3\_Ste5^n - (4-n).f_2^{(K)}.Fus3\_Ste5^n\_0 + b_6^{(K)}.Fus3\_Ste5^n\_1 + k^{(K)}.Fus3\_Ste5^{n-1}\_1.$$

$$\frac{dPtc1\_Ste5^n\_0}{dt} = f_1^{(P)}.Ptc1.Ste5^n - b_1^{(P)}.Ptc1\_Ste5^n - n.f_2^{(P)}.Ptc1\_Ste5^n\_0 + b_2^{(P)}.Ptc1\_Ste5^n\_1 + k^{(P)}.Ptc1\_Ste5^{n+1}\_1.$$

For n=0 to 3, we have:

$$\frac{dFus3\_Ste5^n\_1}{dt} = (4-n).f_2^{(K)}.Fus3\_Ste5^n\_0 - b_6^{(K)}.Fus3\_Ste5^n\_1 - k^{(K)}.Fus3\_Ste5^n\_1 - b_n^{(K)}.Fus3\_Ste5^n\_1 + f_3^{(K)}.Fus3\_Ste5^n\_2.$$

$$\frac{dFus3\_Ste5^n\_2}{dt} = b_n^{(K)}.Fus3\_Ste5^n\_1 - k^{(P)}.Fus3\_Ste5^n\_2 - b_6^{(K)}.Fus3\_Ste5^n\_2 - f_3^{(K)}.Fus3\_Ste5^n\_2.$$

For n=1 to 4, we have:

$$\frac{dPtc1\_Ste5^n\_1}{dt} = n.f_2^{(P)}.Ptc1\_Ste5^n\_0 - b_2^{(P)}.Ptc1\_Ste5^n\_1 - k^{(P)}.Ptc1\_Ste5^n\_1 - b_1^{(P)}.Ptc1\_Ste5^n\_1 + f_3^{(P)}.Ptc1\_Ste5^n\_2.$$

$$\frac{dPtc1\_Ste5^n\_2}{dt} = b_1^{(P)}.Ptc1\_Ste5^n\_1 - k^{(P)}.Ptc1\_Ste5^n\_2 - b_2^{(P)}.Ptc1\_Ste5^n\_2 - f_3^{(P)}.Ptc1\_Ste5^n\_2.$$

In total, there are 33 equations. In addition, if we assume some level of $Fus3_{active}$ we have an additional 5 equations:

$$\frac{dFus3_{active}}{dt} = \sum_{n=0}^{4} b_6^{(K)}.Fus3_{active}\_Ste5^n - (4-n).f_4^{(K)}.Fus3_{active}.\sum_{n=0}^{4} Ste5^n + \sum_{n=0}^{3} k^{(K)}.Fus3_{active}\_Ste5^n\_2.$$

For n =0 to 3, we have:

$$\frac{dFus3_{active}\_Ste5^n}{dt} = (n-4).f_4^{(K)}.Fus3_{active}.Ste5^n - b_6^{(K)}.Fus3_{active}\_Ste5^n - k^{(K)}.Fus3_{active}\_Ste5^n.$$

We also need to add terms to the $Ste5^n$ equations to describe the phosphorylation carried out by $Fus3_{active}$.

We investigated the sensitivity of the switch to variation in the parameters of the model. Changes in concentrations of Ste5, Fus3, and Ptc1 can all influence the EC_{50} and n_H (Supplementary Figure 26). We observe, however, a high Hill number in the population data (Figure 2a), which suggests that the EC_{50} and n_H of the switch in single cells should not be very variable between cells. This robust behavior could result from correlated fluctuations in the concentrations of Fus3, Ste5 and Ptc1, as suggested recently in other systems(Feinerman, Veiga et al. 2008; Shahrezaei, Ollivier et al. 2008).

Figure 3c is generated using a classic model of zero-order ultrasensitivity with only one phosphosite. The kinetic parameters for the Michaelis-Menten reactions we use are:

$f^{(K)} = f^{(P)} = 500\ nM^{-1}s^{-1}$,
$b^{(K)} = b^{(P)} = 1\ s^{-1}$,
$k^{(K)} = k^{(P)} = 1\ s^{-1}$.

6.3 Supplementary tables

Supplementary table 1: List of plasmids used in this study

VF[1]-Venus fragment 1, VF[2]-Venus fragment 2 and VFL-Venus full length

Plasmid	Parent Vector	Promoter	Description
pAG25-RlucF[1]	pAG25		RlucF[1] cassette
pAG32-RlucF[2]	pAG32		RlucF[2] cassette
pMM50 p413	TEF	nNOS-RlucF[1]	
pMM51 p415	TEF	aSyn-RlucF[2]	
pSH95	pRS316	Ste5 native	$Ste5^{WT}$ (Bhattacharyya et.al., 2006)
pRB200	pRS316	Ste5 native	$Ste5^{ND}$ (Bhattacharyya et.al., 2006)
pRB200-MM300	pRS316	Ste5 native	$Ste5^{ND}$ – RlucF[2]
pSH95-MM100	pRS316	Ste5 native	ABCD ($Ste5^{WT}$ – RlucF[2])
pSH95-MM101	pRS316	Ste5 native	aBCD ($Ste5^{T267V}$ – RlucF[2])
pSH95-MM102	pRS316	Ste5 native	AbCD ($Ste5^{S276A}$ - Rluc[F])
pSH95-MM103	pRS316	Ste5 native	ABcD ($Ste5^{T287V}$ - RlucF[2])
pSH95-MM104	pRS316	Ste5 native	ABCd ($Ste5^{S329A}$ – RlucF[2])
pSH95-MM105	pRS316	Ste5 native	abCD ($Ste5^{T267V,S276A}$ – RlucF[2])
pSH95-MM106	pRS316	Ste5 native	AbcD ($Ste5^{S276A,T287V}$ – RlucF[2])
pSH95-MM107	pRS316	Ste5 native	ABcd ($Ste5^{T287V,S329A}$ – RlucF[2])
pSH95-MM108	pRS316	Ste5 native	aBcD ($Ste5^{T267V,T287V}$ – RlucF[2])
pSH95-MM109	pRS316	Ste5 native	aBCd ($Ste5^{T267V,S329A}$ – RlucF[2])
pSH95-MM110	pRS316	Ste5 native	AbCd ($Ste5^{S276A,S329A}$ – RlucF[2])
pSH95-MM111	pRS316	Ste5 native	Abcd ($Ste5^{S276A,T287V,S329A}$ – RlucF[2])
pSH95-MM112	pRS316	Ste5 native	aBcd ($Ste5^{T267V,T287V,S329A}$ – RlucF[2])
pSH95-MM113	pRS316	Ste5 native	abCd ($Ste5^{T267V,S276A,S329A}$ – RlucF[2])
pSH95-MM114	pRS316	Ste5 native	abcD ($Ste5^{T267V,S276A,T287V}$ – RlucF[2])
pSH95-MM115	pRS316	Ste5 native	abcd ($Ste5^{T267V,S276A,T287V,S329A}$ – RlucF[2])
pSH95-MM116	pRS316	Ste5 native	Ebcd ($Ste5^{T267E,S276A,T287V,S329A}$ – RlucF[2])
pSH95-MM117	pRS316	Ste5 native	aFcd ($Ste5^{T267V,S276E,T287V,S329A}$ – RlucF[2])
pSH95-MM118	pRS316	Ste5 native	abGd ($Ste5^{T267V,S276A,T287E,S329A}$ – RlucF[2])
pSH95-MM119	pRS316	Ste5 native	abcH ($Ste5^{T267V,S276A,T287V,S329E}$ – RlucF[2])
pSH95-MM120	pRS316	Ste5 native	EFcd ($Ste5^{T267E,S276E,T287V,S329A}$ – RlucF[2])
pSH95-MM121	pRS316	Ste5 native	EbGd ($Ste5^{T267E,S276A,T287E,S329A}$ – RlucF[2])
pSH95-MM122	pRS316	Ste5 native	EbcH ($Ste5^{T267E,S276A,T287V,S329H}$ – RlucF[2])
pSH95-MM123	pRS316	Ste5 native	aFGd ($Ste5^{T267V,S276E,T287E,S329A}$ – RlucF[2])
pSH95-MM124	pRS316	Ste5 native	aFcH ($Ste5^{T267V,S276E,T287V,S329H}$– RlucF[2])
pSH95-MM125	pRS316	Ste5 native	abGH ($Ste5^{T267V,S276A,T287E,S329E}$ – RlucF[2])
pSH95-MM126	pRS316	Ste5 native	EFGd ($Ste5^{T267E,S276E,T287E,S329A}$ – RlucF[2])
pSH95-MM127	pRS316	Ste5 native	EbGH ($Ste5^{T267E,S276A,T287E,S329E}$ – RlucF[2])
pSH95-MM128	pRS316	Ste5 native	aFGH ($Ste5^{T267V,S276E,T287E,S329E}$ – RlucF[2])
pSH95-MM129	pRS316	Ste5 native	EFcH ($Ste5^{T267E,S276E,T287V,S329E}$ – RlucF[2])
pSH95-MM130	pRS316	Ste5 native	EFGH ($Ste5^{T267E,S276E,T287E,S329E}$ – RlucF[2])
pSH95-MM131	pRS316	Ste5 native	EBCD ($Ste5^{T267E,S276,T287,S329}$ – RlucF[2])
pSH95-MM132	pRS316	Ste5 native	AFCD ($Ste5^{T267,S276E,T287,S329}$ – RlucF[2])
pSH95-MM133	pRS316	Ste5 native	ABGD ($Ste5^{T267,S276,T287E,S329}$ – RlucF[2])
pSH95-MM134	pRS316	Ste5 native	ABCH ($Ste5^{T267,S276,T287,S329E}$ – RlucF[2])
pSH95-MM135	pRS316	Ste5 native	$Ste5^{*AAAA}$ ($Ste5^{P277A,L278A,L279A,P280A}$)

Plasmid		Parent Vector	Promoter	Description
pSH95-MM136		pRS316	Ste5 native	ABCD (Ste5^{WT} – VFL)
pSH95-MM137		pRS316	Ste5 native	aBCD (Ste5^{T267V} – VFL)
pSH95-MM138		pRS316	Ste5 native	AbCD (Ste5^{S276A} - VFL)
pSH95-MM139		pRS316	Ste5 native	ABcD (Ste5^{T287V} - VFL)
pSH95-MM140		pRS316	Ste5 native	ABCd (Ste5^{S329A} – VFL)
pSH95-MM141		pRS316	Ste5 native	abCD (Ste5^{T267V,S276A} – VFL)
pSH95-MM142		pRS316	Ste5 native	ABcd (Ste5^{T287V,S329A} – VFL)
pSH95-MM143		pRS316	Ste5 native	Abcd (Ste5^{S276A,T287V,S329A} – VFL)
pSH95-MM144		pRS316	Ste5 native	abcD (Ste5^{T267V,S276A,T287V} – VFL)
pSH95-MM145		pRS316	Ste5 native	abcd (Ste5^{T267V,S276A,T287V,S329A} – VFL)
pRB200-MM146		pRS316	Ste5 native	Ste5ND – VFL
pMM60	p415	ADH	Ptc1	
pMM61	p413	ADH	Ste5-L-VF [1]	
pMM62	p413	ADH	Ste5*(Ste5^{P277A,L278A,L279A,P280A})-L-VF [1]	
pMM63	p415	ADH	Ptc1-L-VF [2]	
pMM200		pGEX-5X-3		GST-Fus3
pMM210		pGEX-5X-3		GST-Ste5_pep2 $^{(214-334)}$ (ABCD-WT)
pMM211		pGEX-5X-3		GST-Ste5_pep2 $^{(214-334)}$ (Abcd)
pMM212		pGEX-5X-3		GST-Ste5_pep2 $^{(214-334)}$ (aBcd)
pMM213		pGEX-5X-3		GST-Ste5_pep2 $^{(214-334)}$ (abCd)
pMM214		pGEX-5X-3		GST-Ste5_pep2 $^{(214-334)}$ (abcD)
pMM215		pGEX-5X-3		GST-Ste5_pep2 $^{(214-334)}$ (abcd)
pMM216		pMAL-c2x		MBP-Ptc1
pMM217		pMAL-c2x		MBP-Fus3
pMM250		pRS316	Ste5 native	Ste5^{AAAA} (Ste5^{P277A,L278A,L279A,P280A})-RlucF[2]
pRS416-BEM1^{WT}-L-RlucF[1]				
pRS416-BEM1$^{\Delta 417-467}$-L-RlucF[1]				
pRS416-PTC1^{WT}-L-RlucF[1]				
pRS416-PTC1^{D58N}-L-RlucF[1]				
p413-BEM1-L-VF[1]				
p413-NBP2-L-VF[1]				
p413-BCY1-L-VF[1]				
p413-BCY1*-L-VF[1]				
p413-TPK2-L-VF[1]				
p415-BEM1-L-VF[2]				
p415-BEM1 $^{\Delta 417-467}$-L-VF[2]				
p415-NBP2-L-VF[2]				
p415-PTC1^{AAAA}-L-VF[2]				
p415-BCY1-L-VF[2]				
p415-GPA1-L-VF[2]				
p415-GPA2-L-VF[2]				

Supplementary table 2: List of yeast strains

Strain	Description
BY4741	*MATa his3*Δ *leu2*Δ *met15*Δ *ura3*Δ
MM001	BY4741 *FUS3* - L- RlucF[1]
MM002	BY4741 *FUS3*-L-RlucF[1] *STE5*-L-RlucF[2]
MM003	BY4741 *ste5*Δ *FUS3* - L- RlucF[1]
MM004	BY4741 *ptc1*Δ *FUS3* - L- RlucF[1]
MM005	BY4741 *ptc1*Δ *FUS3* - L- RlucF[1] *STE5*-L-RlucF[2]
MM006	BY4741 *FUS3(K42R)*-L-RlucF[1] *STE5*-L-RlucF[2]
MM007	BY4741 *STE5*-L-RlucF[1] *PTC1*-L-RlucF[2]
MM008	BY4741 *STE5*-L-RlucF[1] *STE11*-L-RlucF[2]
MM007	BY4741 *STE5*-L-RlucF[1] *STE7*-L-RlucF[2]
MM010	BY4741 *ste5*Δ *ptc1*Δ *FUS3* - L- RlucF[1]
MM011	BY4741 *BEM1* - L- RlucF[1]
MM012	BY4741 *PTC1* - L- RlucF[1]
MM013	BY4741 *ste5*Δ BEM1 - L- RlucF[1] *PTC1*-L-RlucF[2]
MM014	BY4741 bem1Δ STE5 - L- RlucF[1] *PTC1*-L-RlucF[2]
MM015	BY4741 *bem1*Δ FUS3 - L- RlucF[1] *STE5*-L-RlucF[2]BY4741 *fus3*Δ
BY4741 *kss1*Δ	
BY4741 *hog1*Δ	
BY4741 *ptc1*Δ	
BY4741 *ptc1*Δ *kss1*Δ	
BY4741 *ppz1*Δ	
BY4741 *ppz2*Δ	
BY4741 *sal6*Δ	
BY4741 *pph21*Δ	
BY4741 *pph22*Δ	
BY4741 *ppg1*Δ	
BY4741 *cna1*Δ	
BY4741 *cna2*Δ	
BY4741 *ppt1*Δ	
BY4741 *ptc3*Δ	
BY4741 *ptc4*Δ	
BY4741 *ptc6*Δ	
BY4741 *ptc5*Δ	
BY4741 *ptp1*Δ	
BY4741 *ptp3*Δ	
BY4741 *mih1*Δ	
BY4741 *ltp1*Δ	
BY4741 *pps1*Δ	
BY4741 *tep1*Δ	
BY4741 *sdp1*Δ	
BY4741 *ymr1*Δ	
BY4741 *msg5*Δ	
BY4741 *ptp2*Δ	
BY4741 *pph3*Δ	
BY4741 *ptc2*Δ	

Supplementary table 3: List of all parameters used in the model

Parameter	Value	Error (%)
F	0.2	not fitted
$[Ste5]_{tot}$	52 nM	not fitted
$[Fus3]_{tot}$	197 nM	not fitted
$[Ptc1]_{max}$	39 nM	33
$EC_{50}^{(P)}$	240 n m	17
$n_H^{(P)}$	2.3	18
$[Ptc1]_0$	1.2 nM	25
$[Fus3_{active}]_{max}$	5.8 nM	21
$EC_{50}^{(K)}$	1680 nM	26
$n_H^{(K)}$	1.3	23
$f_1^{(P)}$	186000 $nM^{-1}s^{-1}$	35
$f_2^{(P)}$	327 s^{-1}	34
$f_3^{(P)}$	0.3 s^{-1}	31
$b_1^{(P)}$	22 s^{-1}	18
$b_2^{(P)}$	0.12 s^{-1}	35
$k^{(P)}$	0.5 s^{-1}	30
$f_1^{(K)}$	12000 $nM^{-1}s^{-1}$	24
$f_2^{(K)}$	850 s^{-1}	35
$f_3^{(K)}$	0.1 s^{-1}	31
$f_4^{(K)}$	109000 $nM^{-1}s^{-1}$	28
$b_1^{(K)}$	99 s^{-1}	25
$b_2^{(K)}$	42 s^{-1}	25
$b_3^{(K)}$	21 s^{-1}	25
$b_4^{(K)}$	13 s^{-1}	25
$b_5^{(K)}$	10 s^{-1}	25
$b_6^{(K)}$	24 s^{-1}	28
$k^{(K)}$	1.13 s^{-1}	28

Except for the first three parameters, all others were obtained by fitting the model predictions to the experimental data using a Markov chain Monte Carlo method. The best-fit parameters were found through extensive fitting of the data by a combination of trial-and-error and Monte Carlo methods. The errors shown as the standard deviation as a percentage of the mean represent the standard deviation of the parameters over a Monte Carlo run, where the parameters were restricted to vary only within a factor of 2 from their best-fit values.

6.4 References

Andersson, J., D. M. Simpson, et al. (2004). Differential input by Ste5 scaffold and Msg5 phosphatase route a MAPK cascade to multiple outcomes. *Embo J* **23**(13): 2564-2576.

Bhattacharyya, R. P., A. Remenyi, et al. (2006). The Ste5 scaffold allosterically modulates signaling output of the yeast mating pathway. *Science* **311**(5762): 822-826.

Dohlmanm, H. and J. Thorner (2001). Regulation of G protein-initiated signal transduction in yeast: paradigms and principles. *Annu. Rev. Biochem.* **70**: 703-754.

Ellenberg, J. and J. Lippincott-Schwartz (1998). in Cells: A Laboratory Manual, Nature Publishing Group**:** 79.71-79.23.

Feinerman, O., J. Veiga, et al. (2008). Variability and robustness in T cell activation from regulated heterogeneity in protein levels. *Science* **321**(5892): 1081-1084.

Ferrell, J. E., Jr. (1996). Tripping the switch fantastic: how a protein kinase cascade can convert graded inputs into switch-like outputs. *Trends Biochem Sci* **21**(12): 460-466.

Fiol, C. J., J. H. Haseman, et al. (1988). Phosphoserine as a recognition determinant for Glycogen-synthase kinase-3 - Phosphorylation of a synthetic peptide based on the G-component of protein phosphatase-1. *Archives of Biochemistry and Biophysics* **267**(2): 797-802.

Ghaemmaghami, S., W. K. Huh, et al. (2003). Global analysis of protein expression in yeast. *Nature* **425**(6959): 737-741.

Gunawardena, J. (2005). Multisite protein phosphorylation makes a good threshold but can be a poor switch. *Proc Natl Acad Sci U S A* **102**(41): 14617-14622.

H. Haario, M. L., A. Mira & E.Saksman. (2006). DRAM: Efficient adaptive MCMC. *Stat Comput* **16**: 339–354.

Harris, B. Z., B. J. Hillier, et al. (2001). Energetic determinants of internal motif recognition by PDZ domains. *Biochemistry* **40**(20): 5921-5930.

Maeder, C. I., M. A. Hink, et al. (2007). Spatial regulation of Fus3 MAP kinase activity through a reaction-diffusion mechanism in yeast pheromone signalling. *Nat Cell Biol* **9**(11): 1319-1326.

Markevich, N. I., J. B. Hoek, et al. (2004). Signaling switches and bistability arising from multisite phosphorylation in protein kinase cascades. *J Cell Biol* **164**(3): 353-359.

Remenyi, A., M. C. Good, et al. (2005). The role of docking interactions in mediating signaling input, output, and discrimination in the yeast MAPK network. *Mol Cell* **20**(6): 951-962.

Salazar, C. and T. Hofer (2006). Kinetic models of phosphorylation cycles: a systematic approach using the rapid-equilibrium approximation for protein-protein interactions. *Biosystems* **83**(2-3): 195-206.

Salazar, C. and T. Hofer (2007). Versatile regulation of multisite protein phosphorylation by the order of phosphate processing and protein-protein interactions. *FEBS J* **274**(4): 1046-1061.

Shahrezaei, V., J. F. Ollivier, et al. (2008). Colored extrinsic fluctuations and stochastic gene expression. *Mol Syst Biol* **4**: 196.

Sheff, M. A. and K. S. Thorn (2004). Optimized cassettes for fluorescent protein tagging in Saccharomyces cerevisiae. *Yeast* **21**(8): 661-670.

Siso-Nadal, F., J. F. Ollivier, et al. (2007). Facile: a command-line network compiler for systems biology. *BMC Syst Biol* **1**: 36.

Tarassov, K., V. Messier, et al. (2008). An in Vivo Map of the Yeast Protein Interactome. *Science*.

Zhao, Z. S., T. Leung, et al. (1995). Pheromone signalling in Saccharomyces cerevisiae requires the small GTP- binding protein Cdc42p and its activator CDC24. *Mol. Cell. Biol.* **15**(10): 5246-5257.

BIBLIOGRAPHY

References

Angeli, D., J. E. Ferrell, Jr., et al. (2004). Detection of multistability, bifurcations, and hysteresis in a large class of biological positive-feedback systems. *Proc Natl Acad Sci U S A* 101(7): 1822-1827.

Arkowitz, R. A. (1999). Responding to attraction: chemotaxis and chemotropism in Dictyostelium and yeast. *Trends in Cell Biology* 9(1): 20-27.

Artyukhin, A. B., L. F. Wu, et al. (2009). Only Two Ways to Achieve Perfection. *Cell* 138(4): 619-621.

Ayscough, K. R. and D. G. Drubin (1998). A role for the yeast actin cytoskeleton in pheromone receptor clustering and signalling. *Current biology : CB* 8(16): 927-930.

Ballensiefen, W. and H. D. Schmitt (1997). Periplasmic Barl Protease of Saccharomyces Cerevisiae is Active Before Reaching its Extracellular Destination. *European Journal of Biochemistry* 247(1): 142-147.

Bao, M. Z., M. A. Schwartz, et al. (2004). Pheromone-Dependent Destruction of the Tec1 Transcription Factor Is Required for MAP Kinase Signaling Specificity in Yeast. *Cell* 119(7): 991-1000.

Bardwell, A. J., L. J. Flatauer, et al. (2001). A conserved docking site in MEKs mediates high-affinity binding to MAP kinases and cooperates with a scaffold protein to enhance signal transmission. *Journal of Biological Chemistry* 276(13): 10374-10386.

Bardwell, L. (2005). A walk-through of the yeast mating pheromone response pathway. *Peptides* 26(2): 339-350.

Bardwell, L., J. G. Cook, et al. (1996). Signaling in the yeast pheromone response pathway: Specific and high-affinity interaction of the mitogen-activated protein (MAP) kinases Kss1 and Fus3 with the upstream MAP kinase kinase Ste7. *Molecular and Cellular Biology* 16(7): 3637-3650.

Bardwell, L., J. G. Cook, et al. (1998). Differential regulation of transcription: Repression by unactivated mitogen-activated protein kinase Kss1 requires the Dig1 and Dig2 proteins. *Proceedings of the National Academy of Sciences* 95(26): 15400-15405.

Bardwell, L. and J. Thorner (1996). A conserved motif at the amino termini of MEKs might mediate high-affinity interaction with the cognate MAPKs. *Trends Biochem Sci* 21(10): 373-374.

Barkai, N., M. D. Rose, et al. (1998). Protease helps yeast find mating partners. *Nature* 396(6710): 422-423.

Barsyte-Lovejoy, D., A. Galanis, et al. (2002). Specificity determinants in MAPK signaling to transcription factors. *J Biol Chem* 277(12): 9896-9903.

Bashor, C. J., N. C. Helman, et al. (2008). Using engineered scaffold interactions to reshape MAP kinase pathway signaling dynamics. *Science* 319(5869): 1539-1543.

Bashor, C. J., A. A. Horwitz, et al. (2010). Rewiring cells: synthetic biology as a tool to interrogate the organizational principles of living systems. *Annu Rev Biophys* 39: 515-537.

Batchelor, E., A. Loewer, et al. (2009). The ups and downs of p53: understanding protein dynamics in single cells. *Nat Rev Cancer* 9(5): 371-377.

Berthet, J., T. W. Rall, et al. (1957). The relationship of epinephrine and glucagon to liver phosphorylase. IV. Effect of epinephrine and glucagon on the reactivation of phosphorylase in liver homogenates. *The Journal of biological chemistry* 224(1): 463-475.

Bhattacharyya, R. P., A. Remenyi, et al. (2006). The Ste5 scaffold allosterically modulates signaling output of the yeast mating pathway. *Science* 311(5762): 822-826.

Bhattacharyya, R. P., A. Remenyi, et al. (2006). Domains, motifs, and scaffolds: the role of modular interactions in the evolution and wiring of cell signaling circuits. *Annu Rev Biochem* 75: 655-680.

Biondi, R. M. and A. R. Nebreda (2003). Signalling specificity of Ser/Thr protein kinases through docking-site-mediated interactions. *Biochem J* 372(Pt 1): 1-13.

Blumer, K. J. and J. Thorner (1990). Beta and gamma subunits of a yeast guanine nucleotide-binding protein are not essential for membrane association of the alpha subunit but are required for receptor coupling. *Proceedings of the National Academy of Sciences of the United States of America* 87(11): 4363-4367.

Botstein, D., S. A. Chervitz, et al. (1997). Yeast as a model organism. *Science* 277(5330): 1259-1260.

Botstein, D. and G. R. Fink (1988). Yeast: an experimental organism for modern biology. *Science* 240(4858): 1439-1443.

Brandman, O., J. E. Ferrell, Jr., et al. (2005). Interlinked fast and slow positive feedback loops drive reliable cell decisions. *Science* 310(5747): 496-498.

Breitkreutz, A., L. Boucher, et al. (2001). MAPK specificity in the yeast pheromone response independent of transcriptional activation. *Current Biology* 11(16): 1266-+.

Breitkreutz, A. and M. Tyers (2002). MAPK signaling specificity: it takes two to tango. *Trends in Cell Biology* 12(6): 254-257.

Brent, R. (2009). Cell signaling: What is the signal and what information does it carry? *FEBS Letters* 583(24): 4019-4024.

Brewster, J. L., T. de Valoir, et al. (1993). An osmosensing signal transduction pathway in yeast. *Science* 259(5102): 1760-1763.

Burack, W. R. and A. S. Shaw (2000). Signal transduction: hanging on a scaffold. *Curr Opin Cell Biol* 12(2): 211-216.

Burnett, G. and E. P. Kennedy (1954). The enzymatic phosphorylation of proteins. *Journal of Biological Chemistry* 211(2): 969-980.

Butty, A.-C., P. M. Pryciak, et al. (1998). The Role of Far1p in Linking the Heterotrimeric G Protein to Polarity Establishment Proteins During Yeast Mating. *Science* 282(5393): 1511-1516.

Campbell-Valois, F. X. and S. Michnick (2005). Chemical biology on PINs and NeeDLes. *Current opinion in chemical biology* 9(1): 31-37.

Carmona-Gutierrez, D., T. Eisenberg, et al. (2010). Apoptosis in yeast: triggers, pathways, subroutines. *Cell Death Differ* 17(5): 763-773.

Carroll, S. B. (2005). Evolution at two levels: on genes and form. *PLoS Biol* 3(7): e245.

Chang, C. I., B. E. Xu, et al. (2002). Crystal structures of MAP kinase p38 complexed to the docking sites on its nuclear substrate MEF2A and activator MKK3b. *Mol Cell* 9(6): 1241-1249.

Chang, F. and I. Herskowitz (1990). Identification of a gene necessary for cell cycle arrest by a negative growth factor of yeast: FAR1 is an inhibitor of a G1 cyclin, CLN2. *Cell* 63(5): 999-1011.

Chant, J. (1999). CELL POLARITY IN YEAST. *Annual Review of Cell and Developmental Biology* 15(1): 365-391.

Charvin, G., C. Oikonomou, et al. (2010). Origin of Irreversibility of Cell Cycle Start in Budding Yeast. *PLoS Biol* 8(1): e1000284.

Chen, Z., T. B. Gibson, et al. (2001). MAP kinases. *Chem Rev* 101(8): 2449-2476.

Choi, K. Y., J. E. Kranz, et al. (1999). Characterization of Fus3 localization: active Fus3 localizes in complexes of varying size and specific activity. *Mol. Biol. Cell* 10: 1553-1568.

Choi, K. Y., B. Satterberg, et al. (1994). Ste5 tethers multiple protein kinases in the MAP kinase cascade required for mating in S. cerevisiae. *Cell* 78(3): 499-512.

Chou, S., S. Zhao, et al. (2008). Fus3-triggered Tec1 degradation modulates mating transcriptional output during the pheromone response. *Mol Syst Biol* 4.

Ciejek, E. and J. Thorner (1979). Recovery of S. cerevisiae a cells from G1 arrest by alpha factor pheromone requires endopeptidase action. *Cell* 18(3): 623-635.

Conklin, B. R. and H. R. Bourne (1993). Structural elements of G[alpha] subunits that interact with G[beta][gamma], receptors, and effectors. *Cell* 73(4): 631-641.

Cross, F., L. H. Hartwell, et al. (1988). Conjugation in Saccharomyces cerevisiae. *Annual review of cell biology* 4: 429-457.

Dan, I., N. M. Watanabe, et al. (2001). The Ste20 group kinases as regulators of MAP kinase cascades. *Trends in Cell Biology* 11(5): 220-230.

Darwin, C. (1859). On the Origin of Species by Means of Natural Selection, or the Preservation of Favoured Races in the Struggle for Life. London, John Murray.

Darwin, C. (1871). The Descent of Man and Selection in Relation to Sex. London, John Murray.

Deribe, Y. L., T. Pawson, et al. (2010). Post-translational modifications in signal integration. *Nature structural & molecular biology* 17(6): 666-672.

Dohlman, H. G. (2002). G PROTEINS AND PHEROMONE SIGNALING. *Annual Review of Physiology* 64(1): 129-152.

Dohlman, H. G. and J. Thorner (1997). RGS Proteins and Signaling by Heterotrimeric G Proteins. *Journal of Biological Chemistry* 272(7): 3871-3874.

Drapkin, B. J., Y. Lu, et al. (2009). Analysis of the mitotic exit control system using locked levels of stable mitotic cyclin. *Mol Syst Biol* 5.

Dubnau, D. and R. Losick (2006). Bistability in bacteria. *Molecular Microbiology* 61(3): 564-572.

Dueber, J. E., B. J. Yeh, et al. (2004). Rewiring cell signaling: the logic and plasticity of eukaryotic protein circuitry. *Curr Opin Struct Biol* 14(6): 690-699.

Elion, E. A. (2000). Pheromone response, mating and cell biology. *Curr Opin Microbiol* 3(6): 573-581.

Elion, E. A. (2001). The Ste5p scaffold. *J Cell Sci* 114(Pt 22): 3967-3978.

Elion, E. A., M. Qi, et al. (2005). Signal transduction. Signaling specificity in yeast. *Science* 307(5710): 687-688.

Elowitz, M. B., A. J. Levine, et al. (2002). Stochastic Gene Expression in a Single Cell. *Science* 297(5584): 1183-1186.

Erdman, S. and M. Snyder (2001). A filamentous growth response mediated by the yeast mating pathway. *Genetics* 159(3): 919-928.

Farley, F. W., B. Satterberg, et al. (1999). Relative dependence of different outputs of the Saccharomyces cerevisiae pheromone response pathway on the MAP kinase Fus3p. *Genetics* 151(4): 1425-1444.

Ferrell, J. E., Jr. (1996). Tripping the switch fantastic: how a protein kinase cascade can convert graded inputs into switch-like outputs. *Trends Biochem Sci* 21(12): 460-466.

Ferrell, J. E., Jr. (1998). How regulated protein translocation can produce switch-like responses. *Trends in Biochemical Sciences* 23(12): 461-465.

Ferrell, J. E., Jr. (1999). Building a cellular switch: more lessons from a good egg. *Bioessays* 21(10): 866-870.

Ferrell, J. E., Jr. (2002). Self-perpetuating states in signal transduction: positive feedback, double-negative feedback and bistability. *Current opinion in cell biology* 14(2): 140-148.

Ferrell, J. E., Jr. and E. M. Machleder (1998). The biochemical basis of an all-or-none cell fate switch in Xenopus oocytes. *Science* 280(5365): 895-898.

Ferrell, J. E. and W. Xiong (2001). Bistability in cell signaling: How to make continuous processes discontinuous, and reversible processes irreversible. *Chaos* 11(1): 227-236.

Ferrigno, P., F. Posas, et al. (1998). Regulated nucleo/cytoplasmic exchange of HOG1 MAPK requires the importin beta homologs NMD5 and XPO1. *EMBO J.* 17: 5606-5614.

Fischer, E. H. (2009). Phosphorylase and the origin of reversible protein phosphorylation. *Biological Chemistry* 391(2/3): 131-137.

Fischer, E. H. and E. G. Krebs (1955). Conversion og Phosphorylase-b to Phosphorylase-a in muscle extracts. *Journal of Biological Chemistry* 216(1): 121-132.

Ford, C. E., N. P. Skiba, et al. (1998). Molecular Basis for Interactions of G Protein βγ Subunits with Effectors. *Science* 280(5367): 1271-1274.

Freese, E. B., M. I. Chu, et al. (1982). Initiation of yeast sporulation of partial carbon, nitrogen, or phosphate deprivation. *J Bacteriol* 149(3): 840-851.

Galarneau, A., M. Primeau, et al. (2002). [beta]-Lactamase protein fragment complementation assays as in vivo and in vitro sensors of protein protein interactions. *Nature Biotech.* 20: 619-622.

Garrenton, L. S., A. Braunwarth, et al. (2009). Nucleus-specific and cell cycle-regulated degradation of mitogen-activated protein kinase scaffold protein Ste5 contributes to the control of signaling competence. *Molecular and cellular biology* 29(2): 582-601.

Garrenton, L. S., C. J. Stefan, et al. (2010). Pheromone-induced anisotropy in yeast plasma membrane phosphatidylinositol-4,5-bisphosphate distribution is required for MAPK signaling. *Proceedings of the National Academy of Sciences of the United States of America* 107(26): 11805-11810.

Garrenton, L. S., S. L. Young, et al. (2006). Function of the MAPK scaffold protein, Ste5, requires a cryptic PH domain. *Genes & Development* 20(14): 1946-1958.

Gartner, A., D.-I. Jeoung, et al. (1998). Pheromone-Dependent G1 Cell Cycle Arrest Requires Far1 Phosphorylation, but May Not Involve Inhibition of Cdc28-Cln2 Kinase, In Vivo. *Mol. Cell. Biol.* 18(7): 3681-3691.

Ghosh, I., A. D. Hamilton, et al. (2000). Antiparallel leucine zipper-directed protein reassembly: application to the green fluorescent protein. *J. Am. Chem. Soc.* 122: 5658-5659.

Goldbeter, A. and D. E. Koshland, Jr. (1981). An amplified sensitivity arising from covalent modification in biological systems. *Proc Natl Acad Sci U S A* 78(11): 6840-6844.

Goldbeter, A. and D. E. Koshland, Jr. (1982). Sensitivity amplification in biochemical systems. *Quarterly reviews of biophysics* 15(3): 555-591.

Goldbeter, A. and D. E. Koshland, Jr. (1984). Ultrasensitivity in biochemical systems controlled by covalent modification. Interplay between zero-order and multistep effects. *The Journal of biological chemistry* 259(23): 14441-14447.

Good, M., G. Tang, et al. (2009). The Ste5 scaffold directs mating signaling by catalytically unlocking the Fus3 MAP kinase for activation. *Cell* 136(6): 1085-1097.

Grewal, S., D. M. Molina, et al. (2006). Mitogen-activated protein kinase (MAPK)-docking sites in MAPK kinases function as tethers that are crucial for MAPK regulation in vivo. *Cell Signal* 18(1): 123-134.

Han, J., J. D. Lee, et al. (1994). A MAP kinase targeted by endotoxin and hyperosmolarity in mammalian cells. *Science* 265(5173): 808-811.

Hao, N., S. Nayak, et al. (2008). Regulation of cell signaling dynamics by the protein kinase-scaffold Ste5. *Mol Cell* 30(5): 649-656.

Harrison, J. C., T. R. Zyla, et al. (2004). Stress-specific activation mechanisms for the "cell integrity" MAPK pathway. *J Biol Chem* 279(4): 2616-2622.

Hartwell, L. H. (2004). Yeast and cancer. *Bioscience reports* 24(4-5): 523-544.

Henchoz, S., Y. Chi, et al. (1997). Phosphorylation- and ubiquitin-dependent degradation of the cyclin-dependent kinase inhibitor Far1p in budding yeast. *Genes & Development* 11(22): 3046-3060.

Hirosumi, J., G. Tuncman, et al. (2002). A central role for JNK in obesity and insulin resistance. *Nature* 420(6913): 333-336.

Hirschman, J. E., G. S. De Zutter, et al. (1997). The Gβγ Complex of the Yeast Pheromone Response Pathway. *Journal of Biological Chemistry* 272(1): 240-248.

Ho, D. T., A. J. Bardwell, et al. (2003). A docking site in MKK4 mediates high affinity binding to JNK MAPKs and competes with similar docking sites in JNK substrates. *J Biol Chem* 278(35): 32662-32672.

Holland, P. M. and J. A. Cooper (1999). Protein modification: docking sites for kinases. *Curr Biol* 9(9): R329-331.

Holt, L. J., A. N. Krutchinsky, et al. (2008). Positive feedback sharpens the anaphase switch. *Nature* 454(7202): 353-357.

Hu, C. D., Y. Chinenov, et al. (2002). Visualization of interactions among bZIP and Rel family proteins in living cells using bimolecular fluorescence complementation. *Mol. Cell* 9: 789-798.

Huang, C. Y. and J. E. Ferrell, Jr. (1996). Ultrasensitivity in the mitogen-activated protein kinase cascade. *Proceedings of the National Academy of Sciences of the United States of America* 93(19): 10078-10083.

Huang, L. S., H. K. Doherty, et al. (2005). The Smk1p MAP kinase negatively regulates Gsc2p, a 1,3-beta-glucan synthase, during spore wall morphogenesis in Saccharomyces cerevisiae. *Proc Natl Acad Sci U S A* 102(35): 12431-12436.

Inouye, C., N. Dhillon, et al. (1997). Ste5 RING-H2 Domain: Role in Ste4-Promoted Oligomerization for Yeast Pheromone Signaling. *Science* 278(5335): 103-106.

Jackson, C. L. and L. H. Hartwell (1990). Courtship in S. cerevisiae: both cell types choose mating partners by responding to the strongest pheromone signal. *Cell* 63(5): 1039-1051.

Jackson, C. L. and L. H. Hartwell (1990). Courtship in Saccharomyces cerevisiae: an early cell-cell interaction during mating. *Mol Cell Biol* 10(5): 2202-2213.

Jacobs, D., D. Glossip, et al. (1999). Multiple docking sites on substrate proteins form a modular system that mediates recognition by ERK MAP kinase. *Genes Dev* 13(2): 163-175.

Johnsson, N. and A. Varshavsky (1994). Split ubiquitin as a sensor of protein interactions in vivo. *Proc. Natl Acad. Sci. USA* 91: 10340-10344.

Kaihara, A., Y. Kawai, et al. (2003). Locating a protein-protein interaction in living cells via split Renilla luciferase complementation. *Anal. Chem.* 75: 4176-4181.

Kataoka, T., S. Powers, et al. (1985). Functional homology of mammalian and yeast RAS genes. *Cell* 40(1): 19-26.

Keyse, S. M. (2000). Protein phosphatases and the regulation of mitogen-activated protein kinase signalling. *Curr Opin Cell Biol* 12(2): 186-192.

Koshland, D. E., Jr., A. Goldbeter, et al. (1982). Amplification and adaptation in regulatory and sensory systems. *Science* 217(4556): 220-225.

Kranz, J. E., B. Satterberg, et al. (1994). The MAP kinase Fus3 associates with and phosphorylates the upstream signalling component Ste5. *Genes Dev.* 8: 313-327.

Krebs, E. G. and E. H. Fischer (1956). The phosphorylase b to a converting enzyme of rabbit skeletal muscle. *Biochimica et biophysica acta* 20(1): 150-157.

Krebs, E. G., D. J. Graves, et al. (1959). Factors Affecting the Activity of Muscle Phosphorylase b Kinase. *Journal of Biological Chemistry* 234(11): 2867-2873.

Kusari, A. B., D. M. Molina, et al. (2004). A conserved protein interaction network involving the yeast MAP kinases Fus3 and Kss1. *J Cell Biol* 164(2): 267-277.

Lahav, G., N. Rosenfeld, et al. (2004). Dynamics of the p53-Mdm2 feedback loop in individual cells. *Nature genetics* 36(2): 147-150.

Lamson, R. E., S. Takahashi, et al. (2006). Dual Role for Membrane Localization in Yeast MAP Kinase Cascade Activation and Its Contribution to Signaling Fidelity. *Current Biology* 16(6): 618-623.

Lan, K.-L., H. Zhong, et al. (2000). Rapid Kinetics of Regulator of G-protein Signaling (RGS)-mediated Gαi and Gαo Deactivation. *Journal of Biological Chemistry* 275(43): 33497-33503.

Lander, E. S., L. M. Linton, et al. (2001). Initial sequencing and analysis of the human genome. *Nature* 409(6822): 860-921.

Laub, M. T. and M. Goulian (2007). Specificity in two-component signal transduction pathways. *Annual review of genetics* 41: 121-145.

Lawrence, M. C., A. Jivan, et al. (2008). The roles of MAPKs in disease. *Cell Res* 18(4): 436-442.

Leberer, E. (1997). Functional characterization of the Cdc42p-binding domain of yeast Ste20p protein kinase. *EMBO J.* 16: 83-97.

Leberer, E., D. Y. Thomas, et al. (1997). Pheromone signalling and polarized morphogenesis in yeast. *Current Opinion in Genetics & Development* 7(1): 59-66.

Leeuw, T., C. Wu, et al. (1998). Interaction of a G-protein [beta]-subunit with a conserved sequence in Ste20/PAK family protein kinases. *Nature* 391(6663): 191-195.

Lemmon, M. A. and J. Schlessinger (2010). Cell signaling by receptor tyrosine kinases. *Cell* 141(7): 1117-1134.

Levin, D. E. (2005). Cell wall integrity signaling in Saccharomyces cerevisiae. *Microbiol Mol Biol Rev* 69(2): 262-291.

Libby, E., T. J. Perkins, et al. (2007). Noisy information processing through transcriptional regulation. *Proc Natl Acad Sci U S A* 104(17): 7151-7156.

Lim, W. A. (2010). Designing customized cell signalling circuits. *Nat Rev Mol Cell Biol* 11(6): 393-403.

Locke, J. C. and M. B. Elowitz (2009). Using movies to analyse gene circuit dynamics in single cells. *Nature reviews. Microbiology* 7(5): 383-392.

Luker, K. E. (2004). Kinetics of regulated protein-protein interactions revealed with firefly luciferase complementation imaging in cells and living animals. *Proc. Natl Acad. Sci. USA* 101: 12288-12293.

Ma, W., A. Trusina, et al. (2009). Defining Network Topologies that Can Achieve Biochemical Adaptation. *Cell* 138(4): 760-773.

Madden, K. and M. Snyder (1998). Cell polarity and morphogenesis in budding yeast. *Annual review of microbiology* 52: 687-744.

Madhani, H. D. and G. R. Fink (1998). The riddle of MAP kinase signalling specificity. *Trends Genet.* 14: 151-155.

Maeder, C. I., M. A. Hink, et al. (2007). Spatial regulation of Fus3 MAP kinase activity through a reaction-diffusion mechanism in yeast pheromone signalling. *Nat Cell Biol* 9(11): 1319-1326.

Mahanty, S. K., Y. Wang, et al. (1999). Nuclear shuttling of yeast scaffold Ste5 is required for its recruitment to the plasma membrane and activation of the mating MAPK cascade. *Cell* 98(4): 501-512.

Manahan, C. L., M. Patnana, et al. (2000). Dual lipid modification motifs in G(alpha) and G(gamma) subunits are required for full activity of the pheromone response pathway in Saccharomyces cerevisiae. *Molecular biology of the cell* 11(3): 957-968.

Manderson, E. N., M. Malleshaiah, et al. (2008). A Novel Genetic Screen Implicates Elm1 in the Inactivation of the Yeast Transcription Factor SBF. *PLoS ONE* 3(1): e1500.

Marcus, S., A. Polverino, et al. (1994). Complexes between STE5 and components of the pheromone-responsive mitogen-activated protein kinase module. *Proc. Natl Acad. Sci. USA* 91: 7762-7766.

McClean, M. N., A. Mody, et al. (2007). Cross-talk and decision making in MAP kinase pathways. *Nat Genet* 39(3): 409-414.

Meinke, M. H. and R. D. Edstrom (1991). Muscle glycogenolysis. Regulation of the cyclic interconversion of phosphorylase a and phosphorylase b. *The Journal of biological chemistry* 266(4): 2259-2266.

Melen, G. J., S. Levy, et al. (2005). Threshold responses to morphogen gradients by zero-order ultrasensitivity. *Mol Syst Biol* 1: 2005 0028.

Metodiev, M. V., D. Matheos, et al. (2002). Regulation of MAPK Function by Direct Interaction with the Mating-Specific Gα in Yeast. *Science* 296(5572): 1483-1486.

Michnick, S. W., I. Remy, et al. (2000). Detection of protein-protein interactions by protein fragment complementation strategies. *Methods Enzymol.* 328: 208-230.

Mishra, P., M. Socolich, et al. (2007). Dynamic scaffolding in a G protein-coupled signaling system. *Cell* 131(1): 80-92.

Nachman, I., A. Regev, et al. (2007). Dissecting timing variability in yeast meiosis. *Cell* 131(3): 544-556.

Nash, P., X. Tang, et al. (2001). Multisite phosphorylation of a CDK inhibitor sets a threshold for the onset of DNA replication. *Nature* 414(6863): 514-521.

Neiman, A. M. (2005). Ascospore formation in the yeast Saccharomyces cerevisiae. *Microbiol Mol Biol Rev* 69(4): 565-584.

Neiman, A. M. and I. Herskowitz (1994). Reconstitution of a yeast protein kinase cascade in vitro: activation of the yeast MEK homologue STE7 by STE11. *Proceedings of the National Academy of Sciences of the United States of America* 91(8): 3398-3402.

Nern, A. and R. A. Arkowitz (1998). A GTP-exchange factor required for cell orientation. *Nature* 391(6663): 195-198.

Nern, A. and R. A. Arkowitz (1999). A Cdc24p-Far1p-Gβγ Protein Complex Required for Yeast Orientation during Mating. *The Journal of Cell Biology* 144(6): 1187-1202.

Nern, A. and R. A. Arkowitz (2000). G Proteins Mediate Changes in Cell Shape by Stabilizing the Axis of Polarity. *Molecular Cell* 5(5): 853-864.

Nern, A. and R. A. Arkowitz (2000). Nucleocytoplasmic Shuttling of the Cdc42p Exchange Factor Cdc24p. *The Journal of Cell Biology* 148(6): 1115-1122.

Nguyen, A. N., A. D. Ikner, et al. (2002). Cytoplasmic localization of Wis1 MAPKK by nuclear export signal is important for nuclear targeting of Spc1/Sty1 MAPK in fission yeast. *Mol Biol Cell* 13(8): 2651-2663.

Nurse, P. (2008). Life, logic and information. *Nature* 454(7203): 424-426.

Oehlen, L. J., J. D. McKinney, et al. (1996). Ste12 and Mcm1 regulate cell cycle-dependent transcription of FAR1. *Mol. Cell. Biol.* 16(6): 2830-2837.

Palecek, S. P., A. S. Parikh, et al. (2002). Sensing, signalling and integrating physical processes during Saccharomyces cerevisiae invasive and filamentous growth. *Microbiology* 148(4): 893-907.

Paliwal, S., P. A. Iglesias, et al. (2007). MAPK-mediated bimodal gene expression and adaptive gradient sensing in yeast. *Nature* 446(7131): 46-51.

Paulmurugan, R. and S. S. Gambhir (2003). Monitoring protein-protein interactions using split synthetic Renilla luciferase protein-fragment-assisted complementation. *Anal. Chem.* 75: 1584-1589.

Pawson, T. (1995). Protein modules and signalling networks. *Nature* 373(6515): 573-580.

Pawson, T. and P. Nash (2003). Assembly of cell regulatory systems through protein interaction domains. *Science* 300(5618): 445-452.

Pawson, T. and J. D. Scott (1997). Signaling through scaffold, anchoring, and adaptor proteins. *Science* 278(5346): 2075-2080.

Payne, D. M., A. J. Rossomando, et al. (1991). Identification of the regulatory phosphorylation sites in pp42/mitogen-activated protein kinase (MAP kinase). *The EMBO journal* 10(4): 885-892.

Peisajovich, S. G., J. E. Garbarino, et al. (2010). Rapid diversification of cell signaling phenotypes by modular domain recombination. *Science* 328(5976): 368-372.

Pelletier, J. N., F. Campbell-Valois, et al. (1998). Oligomerization domain-directed reassembly of active dihydrofolate reductase from rationally designed fragments. *Proc. Natl Acad. Sci. USA* 95: 12141-12146.

Pelletier, J. N. and S. W. Michnick (1997). A protein complementation assay for detection of protein-protein interactions in vivo. *Protein Eng.* 10: 89.

Perez, P. and S. A. Rincon (2010). Rho GTPases: regulation of cell polarity and growth in yeasts. *The Biochemical journal* 426(3): 243-253.

Peter, M., A. Gartner, et al. (1993). FAR1 links the signal transduction pathway to the cell cycle machinery in yeast. *Cell* 73(4): 747-760.

Peter, M., A. M. Neiman, et al. (1996). Functional Analysis of the interaction between the small GTP-binding protein Cdc42 and the Ste20 protein kinase in yeast. *EMBO J.* 15: 7046-7059.

Pi, H., C. T. Chien, et al. (1997). Transcriptional activation upon pheromone stimulation mediated by a small domain of Saccharomyces cerevisiae Ste12p. *Mol. Cell. Biol.* 17(11): 6410-6418.

Poritz, M. A., S. Malmstrom, et al. (2001). Graded mode of transcriptional induction in yeast pheromone signalling revealed by single-cell analysis. *Yeast* 18(14): 1331-1338.

Printen, J. A. and G. F. Sprague, Jr. (1994). Protein-protein interactions in the yeast pheromone response pathway: Ste5p interacts with all members of the MAP kinase cascade. *Genetics* 138(3): 609-619.

Pryciak, P. M. and F. A. Huntress (1998). Membrane recruitment of the kinase cascade scaffold protein Ste5 by the Gβγ complex underlies activation of the yeast pheromone response pathway. *Genes & Development* 12(17): 2684-2697.

Qi, M. and E. A. Elion (2005). Formin-induced actin cables are required for polarized recruitment of the Ste5 scaffold and high level activation of MAPK Fus3. *J Cell Sci* 118(13): 2837-2848.

Qi, M. and E. A. Elion (2005). MAP kinase pathways. *J Cell Sci* 118(Pt 16): 3569-3572.

Remenyi, A., M. C. Good, et al. (2005). The role of docking interactions in mediating signaling input, output, and discrimination in the yeast MAPK network. *Mol Cell* 20(6): 951-962.

Remy, I. and S. Michnick (2004). A cDNA library functional screening strategy based on fluorescent protein complementation assays to identify novel components of signaling pathways. *Methods* 32: 381-388.

Remy, I. and S. W. Michnick (1999). Clonal selection and in vivo quantitation of protein interactions with protein fragment complementation assays. *Proc. Natl Acad. Sci. USA* 96: 5394-5399.

Remy, I. and S. W. Michnick (2001). Visualization of biochemical networks in living cells. *Proc. Natl Acad. Sci. USA* 98: 7678-7683.

Remy, I. and S. W. Michnick (2004). Regulation of apoptosis by the Ft1 protein, a new modulator of protein kinase B/Akt. *Mol. Cell. Biol.* 24: 1493-1504.

Remy, I. and S. W. Michnick (2006). A highly sensitive protein-protein interaction assay based on Gaussia luciferase. *Nature Methods* 3: 977-979.

Remy, I., I. A. Wilson, et al. (1999). Erythropoietin receptor activation by a ligand-induced conformation change. *Science* 283: 990-993.

Robbins, D. J., E. Zhen, et al. (1993). Regulation and properties of extracellular signal-regulated protein kinases 1 and 2 in vitro. *The Journal of biological chemistry* 268(7): 5097-5106.

Roberts, C. J., B. Nelson, et al. (2000). Signaling and circuitry of multiple MAPK pathways revealed by a matrix of global gene expression profiles. *Science* 287(5454): 873-880.

Rodbell, M. (1980). The role of hormone receptors and GTP-regulatory proteins in membrane transduction. *Nature* 284(5751): 17-22.

Rosenfeld, N., J. W. Young, et al. (2005). Gene Regulation at the Single-Cell Level. *Science* 307(5717): 1962-1965.

Rubin, G. M. (2001). The draft sequences - Comparing species. *Nature* 409(6822): 820-821.

Serber, Z. and J. E. Ferrell, Jr. (2007). Tuning bulk electrostatics to regulate protein function. *Cell* 128(3): 441-444.

Shahrezaei, V. and P. S. Swain (2008). The stochastic nature of biochemical networks. *Current Opinion in Biotechnology* 19(4): 369-374.

Sharrocks, A. D., S. H. Yang, et al. (2000). Docking domains and substrate-specificity determination for MAP kinases. *Trends Biochem Sci* 25(9): 448-453.

Shimada, Y., M.-P. Gulli, et al. (2000). Nuclear sequestration of the exchange factor Cdc24 by Far1 regulates cell polarity during yeast mating. *Nat Cell Biol* 2(2): 117-124.

Skotheim, J. M., S. Di Talia, et al. (2008). Positive feedback of G1 cyclins ensures coherent cell cycle entry. *Nature* 454(7202): 291-296.

Slaughter, B. D., J. W. Schwartz, et al. (2007). Mapping dynamic protein interactions in MAP kinase signaling using live-cell fluorescence fluctuation spectroscopy and imaging. *Proceedings of the National Academy of Sciences of the United States of America* 104(51): 20320-20325.

Song, J., Z. Chen, et al. (2001). Molecular Interactions of the Gβ Binding Domain of the Ste20p/PAK Family of Protein Kinases. *Journal of Biological Chemistry* 276(44): 41205-41212.

Spotts, J. M., R. E. Dolmetsch, et al. (2002). Time-lapse imaging of a dynamic phosphorylation-dependent protein-protein interaction in mammalian cells. *Proc. Natl Acad. Sci. USA* 99: 15142-15147.

Springer, M. S., M. F. Goy, et al. (1979). Protein methylation in behavioural control mechanisms and in signal transduction. *Nature* 280(5720): 279-284.

Stefan, E., S. Aquin, et al. (2007). Quantification of dynamic protein complexes using Renilla luciferase fragment complementation applied to protein kinase A activities in vivo. *Proc Natl Acad Sci U S A* 104(43): 16916-16921.

Strickfaden, S. C., M. J. Winters, et al. (2007). A mechanism for cell-cycle regulation of MAP kinase signaling in a yeast differentiation pathway. *Cell* 128(3): 519-531.

Tamaki, H. (2007). Glucose-Stimulated cAMP-Protein Kinase A Pathway in Yeast Saccharomyces cerevisiae. *The Society for Biotechnology, Japan* 104(4): 245-250.

Tanoue, T., M. Adachi, et al. (2000). A conserved docking motif in MAP kinases common to substrates, activators and regulators. *Nat Cell Biol* 2(2): 110-116.

Tanoue, T., R. Maeda, et al. (2001). Identification of a docking groove on ERK and p38 MAP kinases that regulates the specificity of docking interactions. *EMBO J* 20(3): 466-479.

Tedford, K., S. Kim, et al. (1997). Regulation of the mating pheromone and invasive growth responses in yeast by two MAP kinase substrates. *Current Biology* 7(4): 228-238.

Tsai, T. Y., Y. S. Choi, et al. (2008). Robust, tunable biological oscillations from interlinked positive and negative feedback loops. *Science* 321(5885): 126-129.

Tyers, M. and B. Futcher (1993). Far1 and Fus3 link the mating pheromone signal transduction pathway to three G1-phase Cdc28 kinase complexes. *Mol. Cell. Biol.* 13(9): 5659-5669.

Tyson, J. J., K. C. Chen, et al. (2003). Sniffers, buzzers, toggles and blinkers: dynamics of regulatory and signaling pathways in the cell. *Curr Opin Cell Biol* 15(2): 221-231.

van Drogen, F., S. M. O'Rourke, et al. (2000). Phosphorylation of the MEKK Ste11p by the PAK-like kinase Ste20p is required for MAP kinase signaling in vivo. *Current Biology* 10(11): 630-639.

van Drogen, F. and M. Peter (2001). MAP kinase dynamics in yeast. *Biol. Cell* 93(1-2): 63-70.

van Drogen, F., V. M. Stucke, et al. (2001). MAP kinase dynamics in response to pheromones in budding yeast. *Nat Cell Biol* 3(12): 1051-1059.

Veening, J.-W., W. K. Smits, et al. (2008). Bistability, Epigenetics, and Bet-Hedging in Bacteria. *Annual review of microbiology* 62(1): 193-210.

Venter, J. C., M. D. Adams, et al. (2001). The sequence of the human genome. *Science* 291(5507): 1304-1351.

Wehrman, T., B. Kleaveland, et al. (2002). Protein-protein interactions monitored in mammalian cells via complementation of [beta]-lactamase enzyme fragments. *Proc. Natl Acad. Sci. USA* 99: 3469-3474.

Whiteway, M. S., C. Wu, et al. (1995). Association of the yeast pheromone response G protein beta gamma subunits with the MAP kinase scaffold Ste5p. *Science* 269(5230): 1572-1575.

Widmann, C., S. Gibson, et al. (1999). Mitogen-activated protein kinase: conservation of a three-kinase module from yeast to human. *Physiological reviews* 79(1): 143-180.

Winters, M. J., R. E. Lamson, et al. (2005). A Membrane Binding Domain in the Ste5 Scaffold Synergizes with G[beta][gamma] Binding to Control Localization and Signaling in Pheromone Response. *Molecular Cell* 20(1): 21-32.

Yablonski, D., I. Marbach, et al. (1996). Dimerization of Ste5, a mitogen-activated protein kinase cascade scaffold protein, is required for signal transduction. *Proceedings of the National Academy of Sciences* 93(24): 13864-13869.

Yao, G., T. J. Lee, et al. (2008). A bistable Rb-E2F switch underlies the restriction point. *Nat Cell Biol* 10(4): 476-482.

Yu, R. C., C. G. Pesce, et al. (2008). Negative feedback that improves information transmission in yeast signalling. *Nature* 456(7223): 755-761.

Zeke, A., M. Lukács, et al. (2009). Scaffolds: interaction platforms for cellular signalling circuits. *Trends in Cell Biology* 19(8): 364-374.

Zhan, X. L., R. J. Deschenes, et al. (1997). Differential regulation of FUS3 MAP kinase by tyrosine-specific phosphatases PTP2/PTP3 and dual-specificity phosphatase MSG5 in Saccharomyces cerevisiae. *Genes Dev* 11(13): 1690-1702.

Zhang, S. and D. F. Klessig (2001). MAPK cascades in plant defense signaling. *Trends in plant science* 6(11): 520-527.

Zhao, Z. S., T. Leung, et al. (1995). Pheromone signalling in Saccharomyces cerevisiae requires the small GTP- binding protein Cdc42p and its activator CDC24. *Mol. Cell. Biol.* 15(10): 5246-5257.